

# New developments in the treatment of corneal ectatic disorders

Citation for published version (APA):

Brekelmans, J. (2023). *New developments in the treatment of corneal ectatic disorders*. [Doctoral Thesis, Maastricht University]. Maastricht University. <https://doi.org/10.26481/dis.20231006jb>

## Document status and date:

Published: 01/01/2023

## DOI:

[10.26481/dis.20231006jb](https://doi.org/10.26481/dis.20231006jb)

## Document Version:

Publisher's PDF, also known as Version of record

## Please check the document version of this publication:

- A submitted manuscript is the version of the article upon submission and before peer-review. There can be important differences between the submitted version and the official published version of record. People interested in the research are advised to contact the author for the final version of the publication, or visit the DOI to the publisher's website.
- The final author version and the galley proof are versions of the publication after peer review.
- The final published version features the final layout of the paper including the volume, issue and page numbers.

[Link to publication](#)

## General rights

Copyright and moral rights for the publications made accessible in the public portal are retained by the authors and/or other copyright owners and it is a condition of accessing publications that users recognise and abide by the legal requirements associated with these rights.

- Users may download and print one copy of any publication from the public portal for the purpose of private study or research.
- You may not further distribute the material or use it for any profit-making activity or commercial gain
- You may freely distribute the URL identifying the publication in the public portal.

If the publication is distributed under the terms of Article 25fa of the Dutch Copyright Act, indicated by the "Taverne" license above, please follow below link for the End User Agreement:

[www.umlib.nl/taverne-license](http://www.umlib.nl/taverne-license)

## Take down policy

If you believe that this document breaches copyright please contact us at:

[repository@maastrichtuniversity.nl](mailto:repository@maastrichtuniversity.nl)

providing details and we will investigate your claim.

# **NEW DEVELOPMENTS IN THE TREATMENT OF CORNEAL ECTATIC DISORDERS**



**Jurriaan Brekelmans**

# **NEW DEVELOPMENTS IN THE TREATMENT OF CORNEAL ECTATIC DISORDERS**

**Jurriaan Brekelmans**

ISBN: 978-94-6469-467-3

Printing: Gildeprint

Cover design: Luke Sky ([artgallerysky.com](http://artgallerysky.com))

Layout: Mariska Offerman ([www.mikka-art.nl](http://www.mikka-art.nl))

Medical illustrations: Chapter 1 (Figure 1, 2, and 4), Rogier Trompert Medical Arts

©2023 Jurriaan Brekelmans



# **NEW DEVELOPMENTS IN THE TREATMENT OF CORNEAL ECTATIC DISORDERS**

Proefschrift

ter verkrijging van de graad van doctor aan de Universiteit Maastricht,  
op gezag van de Rector Magnificus, Prof.dr. Pamela Habibović  
volgens het besluit van het College van Decanen,  
in het openbaar te verdedigen  
op vrijdag 6 oktober 2023 om 10:00 uur

door

Jurriaan Brekelmans

**Promotor**

Prof. dr. Rudy M.M.A. Nuijts

**Copromotoren**

Dr. Mor M. Dickman

Prof. dr. Arie L. Marcovich (Kaplan Medical Center, Israel)

**Beoordelingscommissie**

Prof. dr. Tilman M. Hackeng (voorzitter)

Prof. dr. Anders Behndig (Umeå University, Sweden)

Prof. dr. René R.J.W. van der Hulst

Dr. Ruth Lapid-Gortzak (Amsterdam UMC)

Prof. dr. Chris P.M. Reutelingsperger

De studies in dit proefschrift werden financieel gesteund door het Academic Incentive Fund azM/MUMC+ en de volgende organisaties die hebben bijgedragen via UitZicht: Algemene Nederlandse Vereniging ter Voorkoming van Blindheid, Landelijke Stichting voor Blinden en Slechtzienenden en Stichting Steunfonds UitZicht.

## Table of contents

List of abbreviations	7
<b>Chapter 1</b> General introduction	9
<b>Chapter 2</b> Five years outcomes after corneal cross-linking for keratoconus	35
<b>Chapter 3</b> Decreased riboflavin impregnation time does not increase the risk for endothelial phototoxicity during corneal cross-linking	53
<b>Chapter 4</b> Excimer laser assisted corneal epithelial pattern ablation for corneal cross-linking	81
<b>Chapter 5</b> Corneal stiffening by a bacteriochlorophyll derivative with Dextran and near-infrared light: effect of shortening irradiation time up to 1 minute	107
<b>Chapter 6</b> Long-term Biomechanical and histologic results of WST-D/NIR corneal stiffening in rabbits, up to 8 months follow-up	123
<b>Chapter 7</b> Enzymatic digestion of porcine corneas cross-linked by hypo- and hyperosmolar formulations of riboflavin/ultraviolet A or WST11/NIR	143
<b>Chapter 8</b> General discussion	161
<b>Addendum</b> Summary	193
Samenvatting (Dutch)	199
Impact paragraph	205
Acknowledgements	211
Curriculum vitae	217
List of publications	221



## LIST OF ABBREVIATIONS

A-CXL	Accelerated collagen cross-linking
ARVO	Association for Research in Vision and Ophthalmology
BL	Bowman's Layer
CXL	Collagen cross-linking
DALK	Deep anterior lamellar keratoplasty
DM	Descemet's membrane
DUCK	Dutch Cross-linking for keratoconus score
ECD	Endothelial cell density
Epi-off	Epithelium-off
Epi-on	Epithelium-on
EY	Eosin Y
FDA	U.S. Food and Drug Administration
GL	Green light
ICRS	Intracorneal ring segments
IK	Infectious keratitis
IOL	Intraocular lens
KC	Keratoconus
NIR	Near-infrared
NLO	Nonlinear optical
PACK-CXL	Photoactivated chromophore for infectious keratitis
pIOL	Phakic intraocular lens
PKP	Penetrating keratoplasty
PRK	Photorefractive keratectomy
RB	Rose Bengal
RF	Riboflavin
RL	Red light
ROS	Reactive oxygen species
UVA	Ultra-violet A
VP	Verteporfin
WST11	Water-soluble-taurine
WST-D	Dextran enriched WST11





# Chapter 1

## General introduction





# ANATOMY OF THE EYE

The eye derives its structure and shape from a fibrous outer layer consisting of the sclera, the 'white of the eye', and the cornea, the 'window to the eye'. Light can enter the eye through the cornea, pass the crystalline lens, and project a sharp and crystal-clear image onto the retina. The optic nerve, consisting of over a million individual nerve fibers, transports the induced signal from the retina to the visual cortex, where it is processed into an interpretable image. Even micrometer-scale alterations within this elaborate optical system can alter the final image perceived, showcasing the tight relationship between structure and function within the eye. While alterations may occur at any of the aforementioned levels, this thesis will focus on the cornea and its pathologies.

## Corneal structure

### *Corneal macrostructure – five layers*

The approximately 550  $\mu\text{m}$  thick (increasing towards the periphery) convex and aspheric cornea constitutes five distinctive layers: epithelium, Bowman's layer, stroma, Descemet's membrane, and endothelium (Figure 1).

- Epithelium: the outer 53  $\mu\text{m}$  thick epithelium consist of several layers of tightly joined epithelial cells. The epithelium forms a barrier that protects the inner layers of the cornea and deeper structures of the eye from the external environment.<sup>1</sup>
- Bowman's Layer (BL): BL is an approximately 18  $\mu\text{m}$  thick acellular membrane-like layer of randomly-oriented collagen fibrils. It's suggested BL functions as a physical barrier between the subepithelial nerve plexus and the epithelium.<sup>2</sup>
- Stroma: the stroma comprises the bulk part of the cornea, with a variable thickness of approximately 500  $\mu\text{m}$ . Over three quarters of the stromal weight is accounted for by (bound or unbound) water, with approximately only one quarter attributed to structural components (15% to collagen, and 7% to non-collagenous proteins, proteoglycans and salts).<sup>3,4</sup> The stroma provides most of the corneal strength and stability, and is composed of uniquely organized collagen fibrils in approximately 240 parallel running lamellae.<sup>5</sup> Keratocytes can be found diffusely spread within the stroma, and are activated upon injury to maintain and repair the structural organization. In regards to this thesis, the stroma will be the area of greatest interest.
- Descemet's membrane (DM): DM can be distinguished as an acellular fibrous layer of mere 3  $\mu\text{m}$  thick. It serves as a basement membrane to the next layer, the endothelium.
- Endothelium: the inner endothelium is a monolayer of endothelial cells. Although reorganization does occur when endothelial cells are damaged, they lack the ability to regenerate and are therefore vulnerable to (surgically induced) trauma. Endothelial cells regulate corneal hydration and are thus vital in maintaining corneal transparency.

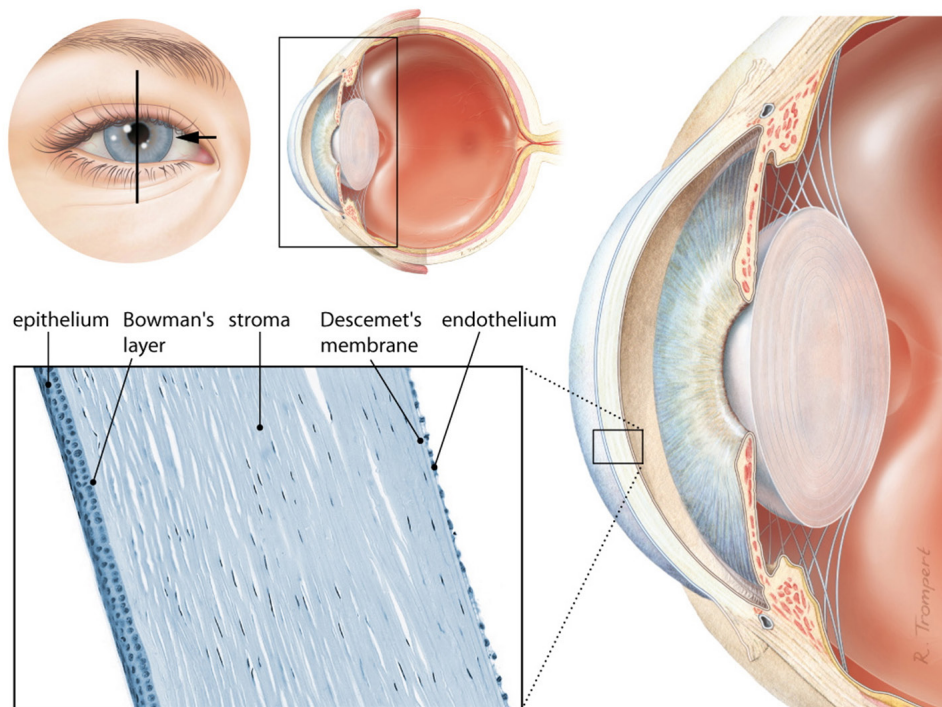


Figure 1. Schematic overview of the eye's anatomy, focusing on the anterior segment. The inset shows a magnified image of the cornea, with its five distinctive layers (outwards in: epithelium, Bowman's layer, stroma, Descemet's membrane, and endothelium).

### *Corneal microstructure – Collagen*

The importance of microstructural organization can be seen in a glance when sclera and cornea are compared. While they form a continuous layer and consist of roughly the same proteins, they show opposite optical properties (i.e., opaque versus transparent). Corneal transparency is a result of highly regular packing of proteins, whereas the heterogenic organization of proteins found in the sclera causes a high degree of light scattering, and thus an opaque appearance. The main protein found within the cornea and sclera is collagen, surrounded by a proteoglycan rich matrix.

Collagen is the most abundant protein in animals, with 28 subtypes identified in vertebrates of which at least 12 have been identified in the eye.<sup>6</sup> These subtypes serve different functions, and may be broadly classified into fibrous and non-fibrous. Regardless of its function, the basic unit of each collagen protein complex is a polymer of amino acids (Figure 2A), with glycine at every third position, forming a polypeptide (Figure 2B). Three polypeptides together, form a left-handed helix configuration (Figure 2C). These units, known as procollagen, undergo different post-translational modifications to form

tropocollagen. Differences in the polypeptide amino acid sequences, polypeptide composition within each helix, and post-translational modifications determine the final subtype. Extra-cellular, tropocollagen units of fibrous collagen undergo further assembly into microfibrils: the tropocollagen units are staggered lengthwise and lateral associations occur by hydrophobic interaction and cross-link formation of lysine and hydroxylysine (Figure 2D). Multiple microfibrils together form a collagen fibril, with diameters ranging from 10 nm to 300 nm, depending on the tissue location (Figure 2E). Also depending on the tissue, e.g., in cornea or tendon, but not in the sclera, several collagen fibrils associate further to form a collagen fiber.<sup>7</sup> Non-fibrous collagens participate in the formation of fibrils of other collagen types (e.g., type II), form sheet-like structures (e.g. types IV and VIII), or serve as anchors between cells and tissues.

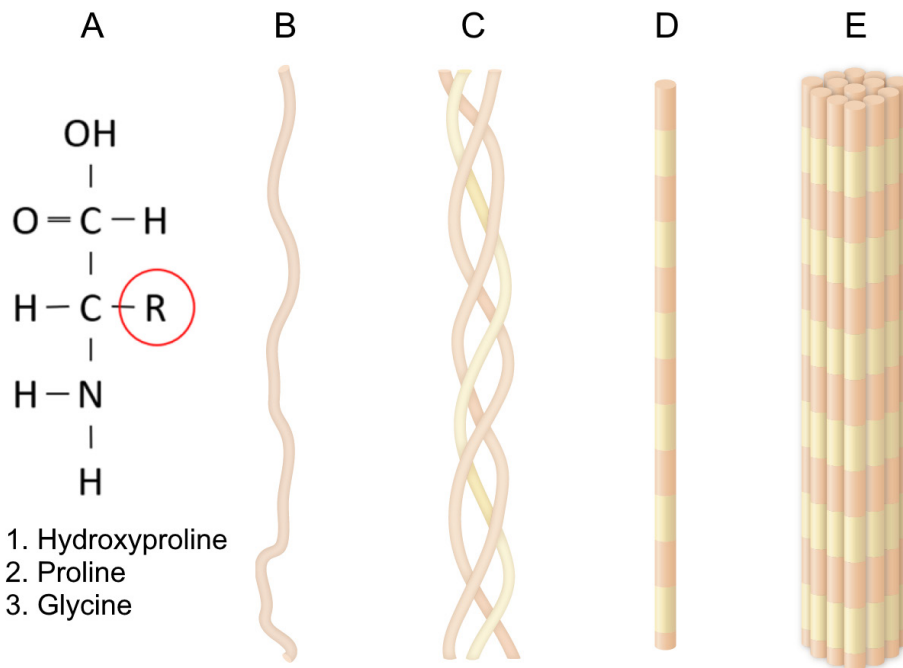


Figure 2. Schematic representation of collagen structure: (A) amino acid, (B) peptide, (C) triple helix, (D) microfibril, and (E) fibril.

### Corneal function

In broad lines, the cornea serves three functions: (1) provide an optically clear window for light to enter the eye, (2) refract entering light, and (3) maintain ocular shape and integrity. In healthy corneas, over 80% of the visible light between 400 nm to 700 nm is transmitted.<sup>8</sup> Alterations, such as scarring, haze formation, or corneal decompensation,

can drastically reduce light transmission. In regards to light refraction, i.e., focusing of the light, the cornea (in particular the anterior surface) accounts for approximately 42 diopters, which is about two-thirds of the total refractive power of the eye, with the lens responsible for the remaining third.<sup>9</sup> The cornea derives this strong refractive power from the change in refractive index as light passes from air into the cornea, and through its curvature. Changes in corneal shape, either intentionally (e.g., refractive surgery) or pathologically (e.g., keratoconus), can thus have a great impact on the perceived image. Despite constant changing forces, both internal (e.g., intra-ocular pressure, osmotic changes) and external (e.g., gravity, eye rubbing, muscle contractions/eye movement), a healthy cornea is able to maintain and restore its shape and function through a delicate balance between stiffness, strength, extensibility, and toughness. The field of corneal biomechanics describes and quantifies such tissue characteristics, and plays an important role as outcome measure in **Chapters 4, 5, and 6** of this thesis.

### *Corneal biomechanics*

The cornea is a complex viscoelastic tissue, meaning it exhibits characteristics of both elasticity and viscosity. Elasticity describes the ability of a substance to deform reversibly under stress, whereas viscosity describes the resistance to flow. The combination of both characteristics results in a non-linear response to external stress (see **Chapter 5**, Figure 2). The stroma provides most of the biomechanical stability to the cornea, thus deemed the area of greatest interest to this thesis before. Corneal tissue is highly heterogenic, both in anterior to posterior, and central to peripheral direction. The anterior stroma contributes more than the posterior stroma; the posterior 60% is at least 50% weaker as compared to the anterior 40%. This is important to note for understanding the treatment effect later on in this thesis, which primarily aims at the anterior cornea. Bowman's layer and DM do provide some tensile strength, but their contribution to the total cornea's strength is negligible, and they are believed mainly to prevent transmission of stresses to the cellular layers (epithelium and endothelium) rather than providing structural support.<sup>4</sup> The epithelium and endothelium provide little to no tensile strength.<sup>10</sup> Quantifying corneal biomechanics has been a topic of interest, as it can provide valuable diagnostic and prognostic information.

Several methods are available for in vivo assessing corneal biomechanical parameters, applying techniques such as air puff deformation ('Ocular Response Analyzer' and 'CorVis ST' devices), or more recently Brillouin microscopy. Each device produces its own parameters, of which clinical relevance is currently under debate and subject to investigation. Ex vivo testing, allows for more direct testing as tissue destruction is possible. Given the high heterogenic nature of corneal tissue, reduction to linear and isotropic measures is common. A common quantifiable biomechanical measure



in ophthalmologic research is the elastic modulus, also known as Young's modulus, which describes the force needed to inflict a change in length.<sup>11-13</sup> For research purpose, a well-established method to obtain the cornea's elastic modulus is to submit strips of corneal tissue to extensimetry testing, as is applied in **Chapters 4, 5, and 6** (illustrated in **Chapter 5**, Figure 1). A higher elastic modulus means greater tissue's stiffness, and in regards to corneal pathology, as described below, a higher elastic modulus after treatment is believed to result in reduced progression of corneal ectasias. Assessing corneal biomechanics is covered in more detail in **Chapter 8**.

## CORNEAL PATHOPHYSIOLOGY

Pathologies affecting corneal integrity, either by reducing corneal transparency or altering the corneal shape, have a tremendous impact on corneal function. Corneal shape may be altered as a result of corneal ectatic disorders, in which corneal thinning and thus weakening occurs. Depending on the etiology, thinning of the central or peripheral cornea occurs, and vision progressively deteriorates. Disease such as keratoconus (KC), keratoglobus, pellucid marginal degeneration, Terrien's marginal degeneration, and post-LASIK ectasia all belong to the spectrum of corneal ectatic disorders. Keratoconus is the most prevalent and studied corneal ectatic disorder, and is discussed in further detail below.

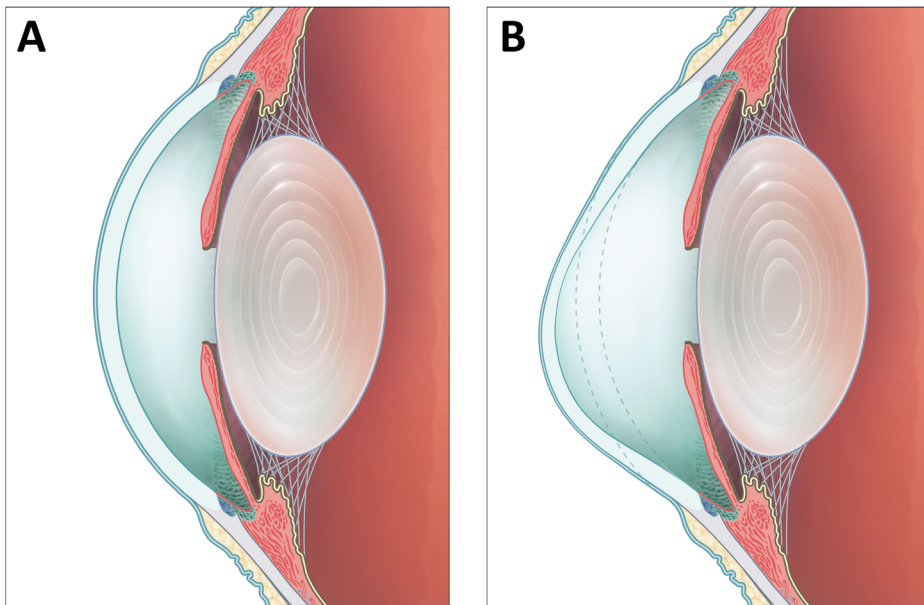


Figure 3. Schematic cross-section of (A) a normal cornea and (B) a cornea affected by keratoconus.

### Keratoconus

Anecdotal reports did exist, but Nottingham was the first to extensively publish on KC in 1854, naming it 'conical cornea'.<sup>14,15</sup> While he contemporary lacked understanding of the disease and was technically limited in diagnostic capabilities, he was able to describe an accurate image by mere macroscopic observation.<sup>16</sup> It's the distinctive cone shaped appearance of (modern-day highly progressed) KC (Figure 3) that eventually led to the denomination keratoconus (*kéras* = cornea, *conus* = cone).

### *Pathophysiology*

Keratoconus often presents asymmetrical, but is a bilateral condition, with the less affected eye showing eventual progression in 50% of the patients.<sup>17</sup> Histologically, KC is characterized by stromal thinning, interruption in BL, and iron deposits in the basal cell layer.<sup>18,19</sup> The cornea thins, loses strength, steepens, and protrudes, resulting in an irregular ocular surface, sometimes scars, and severe vision loss uncorrectable with spectacles. Onset is often between the second and fourth decade, with a younger age of onset believed to be associated with faster progression.<sup>20,21</sup> Given the young age of onset, the chronic aspect of the corneal deformation, and induced optical distortion, the lifetime burden of KC is high.<sup>22,23</sup>

### *Etiology*

The exact etiology of KC still remains an enigma, but both environmental and genetic factors appear to underly the disease, with a family history of KC found in 5% to 23%.<sup>24</sup> Keratoconus is associated with multiple comorbidities, many of which are connective tissue diseases, such as Ehlers-Danlos, Marfan syndrome, floppy eyelid syndrome, and mitral valve prolapse.<sup>25–29</sup> Given the pathological biomechanical changes in corneas affected by KC, this association may speak to mind. Physical external forces, i.e., eye rubbing, was shown to be one of the most important risk factors in developing manifest KC.<sup>30</sup> Daily eye rubbing increases the odds ratio to develop KC by threefold, and Tourette's syndrome, often associated with obsessive-compulsive eye rubbing, has a strong association with KC.<sup>30,31</sup> Similarly, sleep position and associated nocturnal pressure to the cornea is also hypothesized to play a role.<sup>32</sup> Patients with Down syndrome, obesity, and sleep apnea have been reported to be affected more frequent by KC.<sup>33–37</sup> No clear significant correlation of sex and KC could be found, although some studies report a higher prevalence amongst men.<sup>30,38,39</sup> In contrast to the risk factors above, diabetes type II may have a protective effect on developing KC.<sup>30,40–43</sup>

### *Epidemiology*

While Nottingham considered KC to be a rare disease, evolving diagnostic capabilities and more frequent screening, have increased reported incidence numbers of KC over time. Prevalence varies widely in the literature, from less than 1 per 100.000 to almost 5000 per 100.000, depending on the sampled population. A global average was calculated at 138 per 100.000, and 265 per 100.000 in the Netherlands.<sup>30,44–46</sup> Thus, in modern ophthalmological practice, KC certainly is not a rare disease anymore.

### *Diagnosis and classification*

Back in 1854, diagnosis of 'conical cornea' (i.e., KC) was done based on the patient's history of reduced visual acuity, and on the observation of corneal deformations.<sup>14,15</sup> Progressed cases would have shown a Fleischer ring, Vogt's striae, a scissoring reflex on

retinoscopy, or even corneal scarring. In the late 19<sup>th</sup> century, objectification of the corneal curvature became possible by invention of a keratoscope by Antonio Placido and a keratometer by Louis-Émile Javal. While much more refined nowadays, these techniques still retain, and diagnostic parameters for KC still greatly rely on measurements of corneal shape (i.e., corneal tomography). Technological progress has led to increasingly accurate measurements of corneal topography, pachymetry, and posterior corneal surface. To determine clinical relevance of these changing measures, scoring systems have been developed. While nowadays obsolete, the Amsler-Krumeich classification, based on corneal topography, thickness, and refraction, has long been a widely applied grading scale.<sup>47</sup> Newer scoring systems, like the ABCD grading system, and the Dutch Cross-linking for KC (DUCK) score provide greater sensitivity in disease diagnosis and assessing risk of progression.<sup>48,49</sup> While these scoring systems still greatly rely on corneal tomography, other diagnostical test have been investigated. High-resolution optical coherence tomography and in vivo confocal microscopy can provide insights in morphological changes. In vivo corneal biomechanical measurements, as mentioned earlier, may detect pathological corneal weakening. While all these techniques are based on measuring structural changes, most recent and promising developments look at biochemical markers.<sup>50</sup> Biochemical markers have the potential to allow KC diagnosis, before vision affecting structural changes occur, strongly reducing the disease's burden.

## KERATOCONUS MANAGEMENT

Management strategies for KC depend on the disease severity, progression, and visual impairment, and include both invasive and non-invasive options. While clinicians will aim at arresting disease progression based on objective measurements, most notably to the patient will be the decrease in vision, and adequate correction will be their primary objective.

### Refractive aids

#### *Spectacles and contact lenses*

Spectacles generally only suffice in early stages of KC, as they are unable to correct the irregular astigmatism occurring with disease progression. For mild to moderate and non-progressive cases of KC, several contact lens systems are available, which was the mainstay of therapy in approximately 90% of the patient up to about 20 years ago.<sup>18,39</sup> Types of contact lenses include rigid gas permeable contact lenses, piggyback systems, soft contact lenses, and hybrid lenses.<sup>51</sup> Rigid contact lenses provide the best optical correction, as they allow correction of the irregular corneal astigmatism through neutralization of the tear lens. They may be corneal, corneoscleral, scleral, or as part of a piggyback system (in which a soft contact lens underlies a rigid corneal contact lens for comfort and improved stability).<sup>52</sup> Soft contact lenses offer improved comfort compared to rigid lenses, but conform to the irregular cone shape and thus provide less optimal correction. In early disease stages, soft contact lenses may however provide sufficient correction through small design adaptations, (partly) masking the irregular corneal shape.<sup>53,54</sup> Hybrid lenses combine rigid and soft materials, with a rigid corneal lens surrounded by a soft skirt for enhanced comfort.<sup>55</sup> Each design offers different advantages in regards to centration, stability, and comfort, and should be fitted by a specialist.

### Refractive surgery

Several refractive surgery interventions have been used in KC management. While some have been abandoned due to poor results (such as thermal therapy and radial keratectomy), intracorneal ring segments (ICRS), laser refractive surgery, and intraocular lens (IOL) implantation may provide visual relief.<sup>56–62</sup> None of these procedures however arrest disease progression, and can thus only be performed after the disease has stabilized.

#### *Intracorneal ring segments*

Originally, ICRS were designed in the 90's to treat low grade myopia, but have since been employed in mild to moderate KC.<sup>62</sup> One or two polymethacrylate rings, with their length and radius tailored to the specific patient's corneal topography, are surgically

placed within the corneal stroma at approximately 75% depth. They effectively reduce corneal steepening and irregular astigmatism, sometimes even to an extent that additional correction by contact lenses or spectacles is obsolete. One advantage of ICRS lies in the reversibility of the procedure in cases of insufficient or unpredicted effect.

#### *Laser refractive surgery*

Photorefractive keratectomy (PRK) is a well-studied surgical refractive procedure in KC. An excimer laser is applied to ablate corneal stromal tissue, often topography or wavefront-guided, in order to permanently reshape the cornea. While used as a standalone procedure in general ophthalmology clinic, PRK in KC management is usually performed in combination with corneal collagen cross-linking (CXL; discussed below).<sup>63</sup>

#### *Phakic lens implantation*

If corneal procedures cannot be performed or if a patient is intolerant to contact lenses, a phakic intraocular lens (pIOL) may be surgically implanted into the anterior chamber of the eye.<sup>52</sup> Astigmatism, may be (partly) corrected by the implant of a toric lens, or pIOL implantation may be combined with one of the aforementioned corneal procedures.<sup>64</sup> Thorough pre-operative imaging of the anterior segment should be undertaken to assess the patient's suitability for pIOL implantation.

### **Corneal transplantation**

Advanced KC, particularly if corneal scarring has occurred, may be managed by corneal transplantation. Initially, penetrating keratoplasty (PKP) was performed, replacing the entire thickness (from epithelium to endothelium) of the affected cornea by donor tissue. Before alternative treatment options became available, as discussed below, 12% to 22% of the patients at some point in life required a PKP, and 18% of the PKP procedures performed was due to KC.<sup>21,39,65,66</sup> Although PKP is still routinely performed nowadays, surgical advancement and insights led to the development of deep anterior lamellar keratoplasty (DALK), in which only the anterior cornea is transplanted (from epithelium up to DM). Of the DALK procedures, approximately 40% is performed for KC patients.<sup>66</sup> An advantage of DALK over PKP is the lower graft rejection rate and preferable post-operative spherical equivalent.<sup>67</sup> However, DALK procedures are technically more challenging, especially in the case of extensive corneal scarring, which frequently leads to per-operative converting from a DALK to PKP procedure. Both PKP and DALK offer improved vision and arrestment of KC progression, but are highly invasive treatment options, and a large number of KC patients still require contact lenses for optimal vision post-operatively. Recent innovations in the field of KC treatment thus aim to arrest KC by a minimally invasive procedure: corneal CXL.<sup>68</sup>



## Corneal collagen cross-linking

Corneal CXL was introduced to ophthalmology in the 90's of the previous century by Spoerl, Seiler, Wollensak, and colleagues.<sup>69,70</sup> It relies on the principle that new bonds, referred to as cross-links, are formed between collagen fibrils and surrounding proteoglycans within the corneal stroma.<sup>71,72</sup> As a result, corneal stiffness and resistance against enzymatic digestion increases, both considered to underly the mechanism of action in KC progression.<sup>73-75</sup> The clinical introduction of CXL has caused a paradigm shift towards less invasive treatment procedures for KC, and an exponential growing number of studies on the matter have been published since. Although studied to a much lesser extent than KC, RF/UVA CXL for pellucid marginal degeneration, post-refractive surgery ectasia, and Terrien's marginal degeneration has been applied clinically as well.<sup>76-89</sup> While other CXL modalities do exist, the original and most applied protocol involves the instillation of Riboflavin (RF) and consecutive irradiation by ultra-violet A (UVA) light.

### *Riboflavin and ultra-violet A*

Wollensak *et al.* published their seminal clinical protocol on RF/UVA CXL in 2003, which became known as the 'Dresden protocol'. In brief, the Dresden protocol comprises debridement of the corneal epithelium over the central 8 to 9 mm, instillation of RF (vitamin B2) drops for 30 minutes, and consecutive irradiation by long wavelength UVA light (wavelength of 370 nm) for another 30 minutes (Figure 4). Riboflavin with UVA CXL was shown to be able to arrest KC progression in over 90% of patients in multiple long-term clinical studies and meta-analysis, with our own long-term results presented in **Chapter 2** of this thesis.<sup>90-94</sup> This high success rate has resulted in a significant reduction of patients needing invasive cornea transplantation (i.e., PKP or DALK), and makes CXL a very cost-effective procedure.<sup>95,96</sup> While RF/UVA CXL has certainly revolutionized the treatment of KC, it too knows several limitations.

A major limitation of RF/UVA CXL is the application of intrinsically toxic UVA light, which in particular together with RF, can cause damage to deeper ocular structures such as the lens and corneal endothelium. To warrant CXL safety, a minimal amount of UVA attenuation has to occur before the light reaches the endothelial level.<sup>97-99</sup> This has resulted in a minimal required corneal thickness of 400  $\mu\text{m}$  to allow safe RF/UVA CXL.<sup>100-102</sup> While debated, and lesser corneal thicknesses may most-likely suffice, this minimal thickness is still maintained in many clinical protocols, excluding a significant number of patients from receiving RF/UVA CXL. Several protocol adaptations, such as application of a RF-soaked contact lens, and reduced UVA intensities, have been suggested to overcome this shortcoming, with varying results.<sup>103-105</sup> **Chapters 3 and 8** provide a more in-depth discussion on this subject. A second limitation of CXL lies in the removal of the epithelium to allow stromal RF penetration. Epithelial removal is related to several possible post-operative complications,

including both sterile and infectious keratitis, corneal opacity, striae, pain and discomfort, and reduced visual acuity.<sup>106–108</sup> Several authors have tried to overcome this by various methods, including addition of ‘enhancers’, ‘trans-epithelial’ cross-linking, injection of RF into a stromal pocket, iontophoresis-assisted cross-linking, partial de-epithelialization, and even oral administration of RF.<sup>109–118</sup> In **Chapters 4 and 8** of this thesis, the role of the epithelium in corneal CXL is further addressed. In **Chapter 4**, we introduce a proof-of-concept for a new corneal de-epithelialization method using an excimer laser.

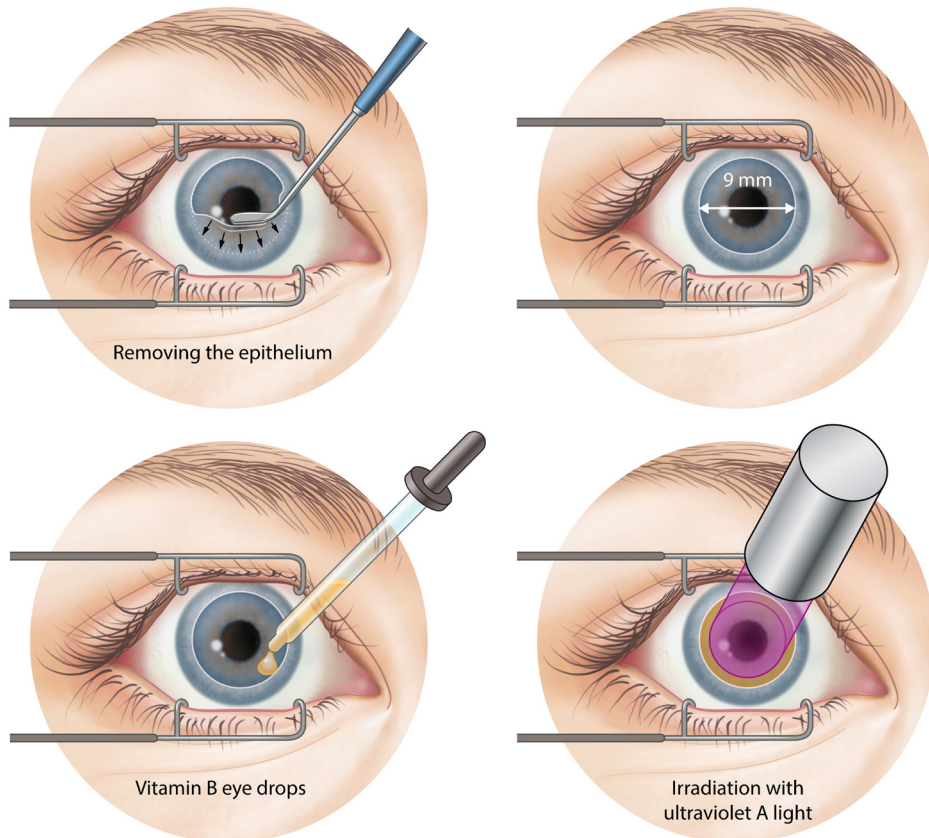


Figure 4. Schematic representation of surgical steps during corneal cross-linking treatment. The epithelium is removed, a photosensitizer applied, and the cornea irradiated.

### Alternative cross-linking modalities

While RF/UVA CXL dominates the treatment of corneal ectasias, CXL can be achieved by many more modalities. It is therefore that several groups have sought to overcome the limitations of RF/UVA CXL by investigating alternatives rather than by adapting treatment protocols. In broad lines, two methods of CXL exist: chemical (direct) and photochemical (indirect) cross-linking. Chemical CXL utilizes a pharmacological compound to induce cross-links without the need for light excitation. Hypothesized benefits lie in the ease of application, but control of which areas are cross-linked is lower compared to photochemical CXL. Photochemical CXL, alike RF/UVA CXL, applies a photosensitizer that is activated by light at a specific wavelength. While it allows a more targeted approach of CXL, the applied light has to be able to reach the area of interest and may pose a hazard to ocular structures. Multiple chemical and photochemical CXL modalities have been studied in pre-clinical set-ups, and were shown to induce similar corneal stiffening compared to RF/UVA CXL (Table 1), but none of which have yet reached a clinical phase.<sup>119–124</sup> One of these alternative photochemical cross-linkers is WST11, which plays an important role in this thesis, and is addressed in more detail in **Chapters 4 to 8**.<sup>119</sup>

Table 1. Cross-linking modalities applied to the cornea.

Photochemical Compound	Light source	Chemical Compound
Eosin Y	Green light (525 nm) <sup>125</sup>	Acai extract <sup>124,126</sup>
Riboflavin	Ultra-violet A (365 nm) <sup>68</sup> Blue light (460 nm) <sup>69,70</sup> Non-linear optical (760 nm) <sup>127,128</sup>	Aldehydes <sup>69,70,129–133</sup> Carbohydrates <sup>70</sup> Chondroitin sulfate <sup>145</sup> Decorin <sup>123</sup>
Rose Bengal	Green light (560 nm) <sup>73,120,134–144</sup>	Genipin <sup>122,131,133,150–154</sup>
Verteporfin	Red light (689 nm) <sup>121</sup>	Nitro-alcohols <sup>131,155–157</sup>
Water-soluble-aurine	Near-infrared (755 nm) <sup>119,146–149</sup>	Transglutaminase <sup>158,159</sup>

## AIM AND OUTLINE OF THIS THESIS

Corneal CXL provided a new and very welcome treatment modality to arrest KC progression, filling the gap between symptomatic treatment and invasive transplantation surgery. The aim of this thesis was to investigate the current state of corneal CXL for ectasia, and advance a new alternative CXL modality: WST11/NIR.

**Chapters 2 and 3** focus on current clinically applied RF/UVA CXL. Our personal long-term results on CXL to stabilize KC progression are presented in **Chapter 2**, endorsing the high success rate of RF/UVA CXL and determining pre-operative measures predictive of post-operative outcomes. In **Chapter 3** we show that reduction of the treatment duration of the current widespread applied RF/UVA CXL protocol (the 'Dresden protocol') actually increases treatment safety. After 10 minutes, sufficient RF is present in the corneal stroma to safely attenuate the applied UVA light. **Chapter 4** reports the experimental outcomes of a new approach for chromophore application in corneal CXL, in which an excimer laser is applied to only partially ablate the epithelium prior to CXL treatment.

In **Chapter 5** we show in both an in vivo and ex vivo model, that WST11/NIR CXL can provide significant corneal stiffening, while reducing the total treatment procedure duration by more than half. This increased corneal stiffening is shown to be a long-term effect in **Chapter 6**. Increased resistance against enzymatic digestion is believed to be part of the mechanism of action of CXL, which is assessed for both RF/UVA and WST11/NIR CXL in **Chapter 7**.

## REFERENCES

1. Reinstein DZ, Archer TJ, Gobbe M, Silverman RH, Coleman DJ. Epithelial thickness in the normal cornea: Three-dimensional display with artemis very high-frequency digital ultrasound. *J Refract Surg*. 2008;24(6):571-581.
2. Schmoll T, Unterhuber A, Kolbitsch C, Le T, Stingl A, Leitgeb R. Precise thickness measurements of bowman's layer, epithelium, and tear film. *Optom Vis Sci*. 2012;89(5):795-802.
3. Cheng X, Petsche SJ, Pinsky PM. A structural model for the in vivo human cornea including collagen-swelling interaction. *J R Soc Interface*. 2015;12(109).
4. Dupps WJ, Wilson SE. Biomechanics and wound healing in the cornea. *Exp Eye Res*. 2006;83(4):709-720.
5. Bergmanson JPG, Horne J, Doughty MJ, Garcia M, Gondo M. Assessment of the number of lamellae in the central region of the normal human corneal stroma at the resolution of the transmission electron microscope. *Eye Contact Lens*. 2005;31(6):281-287.
6. Fink BA. *Biochemistry of the Eye, 2nd Ed*. Vol 81. Butterworth-Heinemann; 2004.
7. Boote C, Sigal IA, Grytz R, Hua Y, Nguyen TD, Girard MJA. Scleral structure and biomechanics. *Prog Retin Eye Res*. 2020;74(June 2019):100773.
8. Boettner EA, Wolter JR. Transmission of the Ocular Media. *Invest Ophthalmol Vis Sci*. 1962;1(6):776-783.
9. Sridhar MS. Anatomy of cornea and ocular surface. *Indian J Ophthalmol*. 2018;66(2):190-194.
10. Thomasy SM, Raghunathan VK, Winkler M, et al. Elastic modulus and collagen organization of the rabbit cornea: Epithelium to endothelium. *Acta Biomater*. 2014;10(2):785-791.
11. Hatami-Marbini H, Rahimi A. Stiffening effects of riboflavin/UVA corneal collagen cross-linking is hydration dependent. *J Biomech*. 2015;48(6):1052-1057.
12. Zhang Y, Li Z, Liu L, Han X, Zhao X, Mu G. Comparison of riboflavin/ultraviolet-A cross-linking in porcine, rabbit, and human sclera. *Biomed Res Int*. 2014;2014:194204.
13. Liu X, Wang L, Ji J, et al. A Mechanical model of the cornea considering the crimping morphology of collagen fibrils. *Investig Ophthalmol Vis Sci*. 2014;55(4):2739-2746.
14. Grzybowski A, McGhee CNJ. The early history of keratoconus prior to Nottingham's landmark 1854 treatise on conical cornea: A review. *Clin Exp Optom*. 2013;96(2):140-145.
15. Nottingham J. *Practical Observations on Conical Cornea, and on the Short Sight, and Other Defects of Vision Connected with It* /. J. Churchill ; 2019.
16. Gokul A, Patel D V., McGhee CNJ. Dr John Nottingham's 1854 Landmark Treatise on Conical Cornea Considered in the Context of the Current Knowledge of Keratoconus. *Cornea*. 2016;35(5):673-678.
17. Li X, Rabinowitz YS, Rasheed K, Yang H. Longitudinal study of the normal eyes in unilateral keratoconus patients. *Ophthalmology*. 2004;111(3):440-446.
18. Rabinowitz YS. Keratoconus. *Surv Ophthalmol*. 1998;42(4):297-319.
19. Krachmer JH, Feder RS, Belin MW. Keratoconus and related noninflammatory corneal thinning disorders. *Surv Ophthalmol*. 1984;28(4):293-322.
20. Barr JT, Wilson BS, Gordon MO, et al. Estimation of the incidence and factors predictive of corneal scarring in the Collaborative Longitudinal Evaluation of Keratoconus (CLEK) study. *Cornea*. 2006;25(1):16-25.
21. Gordon MO, Steger-May K, Szczotka-Flynn L, et al. Baseline Factors Predictive of Incident Penetrating Keratoplasty in Keratoconus. *Am J Ophthalmol*. 2006;142(6):923-930.

22. Chan E, Baird PN, Vogrin S, Sundararajan V, Daniell MD, Sahebjada S. Economic impact of keratoconus using a health expenditure questionnaire: A patient perspective. *Clin Exp Ophthalmol*. 2020;48(3):287-300.
23. Balparda K, Herrera-Chalarca T, Silva-Quintero LA, Torres-Soto SA, Segura-Muñoz L, Vanegas-Ramirez CM. Both subjective emotional distress and visual handicap correlate with belin abcd classification in the worse eye as measured with the "keratoconus end-points assessment questionnaire" (Kepaq). *Clin Ophthalmol*. 2020;14:1839-1845.
24. Loukovitis E, Sfakianakis K, Syrmakesi P, et al. Genetic Aspects of Keratoconus: A Literature Review Exploring Potential Genetic Contributions and Possible Genetic Relationships with Comorbidities. *Ophthalmol Ther*. 2018;7(2):263-292.
25. Robertson I. Keratoconus and the Ehlers Danlos syndrome: a new aspect of keratoconus. *Med J Aust*. 1975;1(18):571-573.
26. Kalkan Akcay E, Akcay M, Uysal BS, et al. Impaired corneal biomechanical properties and the prevalence of keratoconus in mitral valve prolapse. *J Ophthalmol*. 2014;2014:402193.
27. Naderan M, Jahanrad A, Farjadnia M. Prevalence of eyelid laxity and its association with ophthalmic findings and disease severity in patients with keratoconus. *Eur J Ophthalmol*. 2017;27(6):670-674.
28. Ezra DG, Beaconsfield M, Sira M, Bunce C, Wormald R, Collin R. The Associations of Floppy Eyelid Syndrome: A Case Control Study. *Ophthalmology*. 2010;117(4):831-838.
29. Sharif KW, Casey TA, Coltart J. Prevalence of mitral valve prolapse in keratoconus patients. *J R Soc Med*. 1992;85(8):446-448.
30. Hashemi H, Heydarian S, Hooshmand E, et al. The Prevalence and Risk Factors for Keratoconus: A Systematic Review and Meta-Analysis. *Cornea*. 2020;39(2):263-270.
31. Mashor RS, Kumar NL, Ritenour RJ, Rootman DS. Keratoconus caused by eye rubbing in patients with Tourette Syndrome. *Can J Ophthalmol*. 2011;46(1):83-86.
32. Gatinel D, Galvis V, Tello A, et al. Obstructive Sleep Apnea-Hypopnea Syndrome and Keratoconus: An Epiphenomenon Related to Sleep Position? *Cornea*. 2020;39(4):e11.
33. Pihlblad MS, Schaefer DP. Eyelid laxity, obesity, and obstructive sleep apnea in keratoconus. *Cornea*. 2013;32(9):1232-1236.
34. Slater JA, Misra SL, Braatvedt G, McGhee CNJ. Keratoconus and obesity: can high body mass alter the shape of the cornea? *Clin Exp Ophthalmol*. 2018;46(9):1091-1093.
35. Pedrotti E, Demasi CL, Fasolo A, et al. Obstructive Sleep Apnea Assessed by Overnight Polysomnography in Patients With Keratoconus. *Cornea*. 2018;37(4):470-473.
36. Alio JL, Vega-Estrada A, Sanz P, et al. Corneal morphologic characteristics in patients with down syndrome. *JAMA Ophthalmol*. 2018;136(9):971-978.
37. Real De Asua D, Quero M, Moldenhauer F, Suarez C. Clinical profile and main comorbidities of Spanish adults with Down syndrome. *Eur J Intern Med*. 2015;26(6):385-391.
38. Millodot M, Shneur E, Albou S, Atlani E, Gordon-Shaag A. Prevalence and associated factors of keratoconus in jerusalem: A cross-sectional study. *Ophthalmic Epidemiol*. 2011;18(2):91-97.
39. Romero-Jiménez M, Santodomingo-Rubido J, Wolffsohn JS. Keratoconus: A review. *Contact Lens Anterior Eye*. 2010;33(4):157-166.
40. Seiler T, Huhle S, Spoerl H, Kunath H. Manifest diabetes and keratoconus: A retrospective case-control study. *Graefes Arch Clin Exp Ophthalmol*. 2000;238(10):822-825.
41. Naderan M, Naderan M, Rezagholizadeh F, Zolfaghari M, Pahlevani R, Rajabi MT. Association between diabetes and keratoconus: A case-control study. *Cornea*. 2014;33(12):1271-1273.



42. Kuo IC, Broman A, Pirouzmanesh A, Melia M. Is there an association between diabetes and keratoconus? *Ophthalmology*. 2006;113(2):184-190.
43. Kosker M, Suri K, Hammersmith KM, Nassef AH, Nagra PK, Rapuano CJ. Another look at the association between diabetes and keratoconus. *Cornea*. 2014;33(8):774-779.
44. Torres Netto EA, Al-Otaibi WM, Hafezi NL, et al. Prevalence of keratoconus in paediatric patients in Riyadh, Saudi Arabia. *Br J Ophthalmol*. 2018;102(10):1436-1441.
45. Ferrari G, Rama P. The keratoconus enigma: A review with emphasis on pathogenesis. *Ocul Surf*. 2020;18(3):363-373.
46. Godefrooij DA, de Wit GA, Uiterwaal CS, Imhof SM, Wisse RPL. Age-specific Incidence and Prevalence of Keratoconus: A Nationwide Registration Study. *Am J Ophthalmol*. 2017;175:169-172.
47. Krumeich JH, Daniel J, Knalle A. Live-epikeratophakia for keratoconus. *J Cataract Refract Surg*. 1998;24(4):456-463.
48. Belin MW, Duncan JK. Keratoconus: The ABCD Grading System. *Klin Monbl Augenheilkd*. 2016;233(6):701-707.
49. Wisse RPL, Simons RWP, Van Der Vossen MJB, et al. Clinical Evaluation and Validation of the Dutch Crosslinking for Keratoconus Score. *JAMA Ophthalmol*. 2019;137(6):610-616.
50. Shetty R, D'Souza S, Khamar P, Ghosh A, Nuijts RMMA, Sethu S. Biochemical markers and alterations in keratoconus. *Asia-Pacific J Ophthalmol*. 2020;9(6):533-540.
51. Şengör T, Kurna SA. Update on contact lens treatment of keratoconus. *Turkish J Ophthalmol*. 2020;50(4):234-244.
52. Santodomingo-Rubido J, Carracedo G, Suzaki A, Villa-Collar C, Vincent SJ, Wolffsohn JS. Keratoconus: An updated review. *Contact Lens Anterior Eye*. 2022;(November 2021):101559.
53. Sultan P, Dogan C, Iskeleli G. A retrospective analysis of vision correction and safety in keratoconus patients wearing Toris K soft contact lenses. *Int Ophthalmol*. 2016;36(6):799-805.
54. Gumus K, Kahraman N. A New Fitting Approach for Providing Adequate Comfort and Visual Performance in Keratoconus: Soft HydroCone (Toris K) Lenses. *Eye Contact Lens*. 2016;42(4):225-230.
55. Kloeck D, Koppen C, Kreps EO. Clinical Outcome of Hybrid Contact Lenses in Keratoconus. *Eye Contact Lens*. 2021;47(5):283-287.
56. Leccisotti A. Effect of circular keratotomy on keratoconus. *J Cataract Refract Surg*. 2006;32(12):2139-2141.
57. Alpíns N, Stamatelatos G. Customized photoastigmatic refractive keratectomy using combined topographic and refractive data for myopia and astigmatism in eyes with forme fruste and mild keratoconus. *J Cataract Refract Surg*. 2007;33(4):591-602.
58. Bilgihan K, Özdek SC, Sari A, Hasanreisoglu B. Microkeratome-assisted lamellar keratoplasty for keratoconus: Stromal sandwich. *J Cataract Refract Surg*. 2003;29(7):1267-1272.
59. Colin J, Cochener B, Savary G, Malet F. Correcting keratoconus with intracorneal rings. *J Cataract Refract Surg*. 2000;26(8):1117-1122.
60. Tomalla M, Cagnolati W. Modern treatment options for the therapy of keratoconus. *Contact Lens Anterior Eye*. 2007;30(1):61-66.
61. Zare MA, Hashemi H, Salari MR. Intracorneal ring segment implantation for the management of keratoconus: Safety and efficacy. *J Cataract Refract Surg*. 2007;33(11):1886-1891.
62. Coskunseven E, Kymionis GD, Tsiklis NS, et al. One-Year Results of Intrastromal Corneal Ring Segment Implantation (KeraRing) using Femtosecond Laser in Patients with Keratoconus. *Am J Ophthalmol*. 2008;145(5):775-780.

63. Russo A, Faria-Correia F, Rechichi M, Festa G, Morescalchi F, Semeraro F. Topography/wavefront-guided photorefractive keratectomy combined with crosslinking for the treatment of keratoconus: preliminary results. *J Cataract Refract Surg.* 2021;47(1):11-17.
64. Coskunseven E, Onder M, Kymionis GD, et al. Combined Intacs and Posterior Chamber Toric Implantable Collamer Lens Implantation for Keratoconic Patients with Extreme Myopia. *Am J Ophthalmol.* 2007;144(3).
65. Kennedy RH, Bourne WM, Dyer JA. A 48-year clinical and epidemiologic study of keratoconus. *Am J Ophthalmol.* 1986;101(3):267-273.
66. Arnalich-Montiel F, Alió del Barrio JL, Alió JL. Corneal surgery in keratoconus: which type, which technique, which outcomes? *Eye Vis.* 2016;3(1):1-14.
67. Song Y, Zhang J, Pan Z. Systematic review and meta-analysis of clinical outcomes of penetrating keratoplasty versus deep anterior lamellar keratoplasty for keratoconus. *Exp Clin Transplant.* 2020;18(4):417-428.
68. Wollensak G, Spoerl E, Seiler T. Riboflavin/ultraviolet-A-induced collagen crosslinking for the treatment of keratoconus. *Am J Ophthalmol.* 2003;135(5):620-627.
69. Spoerl E, Huhle M, Seiler T. Induction of cross-links in corneal tissue. *Exp Eye Res.* 1998;66(1):97-103.
70. Spoerl E, Seiler T. Techniques for stiffening the cornea. *J Refract Surg.* 1999;15(6):711-713.
71. Hayes S, Kamma-Lorger CS, Boote C, et al. The Effect of Riboflavin/UVA Collagen Cross-linking Therapy on the Structure and Hydrodynamic Behaviour of the Ungulate and Rabbit Corneal Stroma. *PLoS One.* 2013;8(1):e52860.
72. Zhang Y, Conrad AH, Conrad GW. Effects of ultraviolet-A and riboflavin on the interaction of collagen and proteoglycans during corneal cross-linking. *J Biol Chem.* 2011;286(15):13011-13022.
73. Wang T, Peng Y, Shen N, Yu Y, Yao M, Zhu J. Photochemical activation increases the porcine corneal stiffness and resistance to collagenase digestion. *Exp Eye Res.* 2014;123:97-104.
74. Aldahlawi NH, Hayes S, O'Bart DPS, Meek KM. Standard versus accelerated riboflavin-ultraviolet corneal collagen crosslinking: Resistance against enzymatic digestion. *J Cataract Refract Surg.* 2015;41(9):1989-1996.
75. Spoerl E, Wollensak G, Seiler T. Increased resistance of crosslinked cornea against enzymatic digestion. *Curr Eye Res.* 2004;29(1):35-40.
76. Kymionis G, Voulgari N, Samutelela E, Kontadakis G, Tabibian D. Combined corneal wedge resection and corneal cross-linking for pellucid marginal degeneration: A first report. *Ther Clin Risk Manag.* 2019;15:1319-1324.
77. Pircher N, Lammer J, Holzer S, Gschließer A, Schmidinger G. Corneal crosslinking for pellucid marginal degeneration. *J Cataract Refract Surg.* 2019;45(8):1163-1167.
78. Kymionis GD, Grentzelos MA, Plaka AD, et al. Simultaneous conventional photorefractive keratectomy and corneal collagen cross-linking for pellucid marginal corneal degeneration. *J Refract Surg.* 2014;30(4):272-276.
79. Spadea L, Maraone G, Cagini C. Sliding keratoplasty followed by transepithelial iontophoresis collagen cross-linking for pellucid marginal degeneration. *J Refract Surg.* 2016;32(1):47-50.
80. Cagil N, Sarac O, Yesilirmak N, Caglayan M, Uysal BS, Tanriverdi B. Transepithelial Phototherapeutic Keratectomy Followed by Corneal Collagen Crosslinking for the Treatment of Pellucid Marginal Degeneration: Long-term Results. *Cornea.* 2019;38(8):980-985.
81. Mamoosa B, Razmjoo H, Peyman A, Ashtari A, Ghafouri I, Moghaddam A. Short-term result of collagen crosslinking in pellucid marginal degeneration. *Adv Biomed Res.* 2016;5(1):194.

82. de Almeida Ferreira G, Coral Ghanem V, Coral Ghanem R. Late progressive corneal flattening, haze and visual loss after eccentric crosslinking for Pellucid marginal degeneration. *Am J Ophthalmol Case Reports*. 2020;18(June 2019):100621.
83. Fuentes-Páez G, Castanera F, Salazar-Martínez RG De, Salas JF, Izquierdo E, Pinalla B. Corneal cross-linking in patients with radial keratotomy: Short-term follow-up. *Cornea*. 2012;31(3):232-235.
84. Elbaz U, Yeung SN, Ziai S, et al. Collagen crosslinking after radial keratotomy. *Cornea*. 2014;33(2):131-136.
85. Hafezi F, Gatziofias Z, Seiler TG, Seiler T. Corneal collagen cross-linking for Terrien marginal degeneration. *J Refract Surg*. 2014;30(7):498-500.
86. Kymionis GD, Karavitaki AE, Kounis GA, Portaliou DM, Yoo SH, Pallikaris IG. Management of pellucid marginal corneal degeneration with simultaneous customized photorefractive keratectomy and collagen crosslinking. *J Cataract Refract Surg*. 2009;35(7):1298-1301.
87. Lamarca J, Salvador-Culla B, Fernández-Vega C, Barraquer RI. Long-term results of corneal cross-linking for terrien's marginal degeneration. *J Refract Surg*. 2018;34(6):424-429.
88. Spadea L. Corneal collagen cross-linking with riboflavin and UVA irradiation in pellucid marginal degeneration. *J Refract Surg*. 2010;26(5):375-377.
89. Hassan Z, Nemeth G, Modis L, Szalai E, Berta A. Collagen cross-linking in the treatment of pellucid marginal degeneration. *Indian J Ophthalmol*. 2014;62(3):367-370.
90. Marafon SB, Kwitko S, Marinho DR. Long-term results of accelerated and conventional corneal cross-linking. *Int Ophthalmol*. 2020;40(10):2751-2761.
91. Or L, Rozenberg A, Abulafia A, Avni I, Zadok D. Corneal cross-linking in pediatric patients: Evaluating treated and untreated eyes—5-year follow-up results. *Cornea*. 2018;37(8):1013-1017.
92. Sykakis E, Karim R, Evans JR, et al. Corneal collagen cross-linking for treating keratoconus. Hamada S, ed. *Cochrane Database Syst Rev*. 2015;2015(3):CD010621.
93. Raiskup F, Theuring A, Pillunat LE, Spoerl E. Corneal collagen crosslinking with riboflavin and ultraviolet-A light in progressive keratoconus: Ten-year results. *J Cataract Refract Surg*. 2015;41(1):41-46.
94. Poli M, Lefevre A, Auxenfans C, Burillon C. Corneal Collagen Cross-linking for the Treatment of Progressive Corneal Ectasia: 6-Year Prospective Outcome in a French Population. *Am J Ophthalmol*. 2015;160(4):654-662.e1.
95. Godefrooij DA, Gans R, Imhof SM, Wisse RPL. Nationwide reduction in the number of corneal transplantations for keratoconus following the implementation of cross-linking. *Acta Ophthalmol*. 2016;94(7):675-678.
96. Godefrooij DA, Mangen MJJ, Chan E, et al. Cost-Effectiveness Analysis of Corneal Collagen Crosslinking for Progressive Keratoconus. *Ophthalmology*. 2017;124(10):1485-1495.
97. Spoerl E, Mrochen M, Sliney D, Trokel S, Seiler T. Safety of UVA-riboflavin cross-linking of the cornea. *Cornea*. 2007;26(4):385-389.
98. Koller T, Mrochen M, Seiler T. Complication and failure rates after corneal crosslinking. *J Cataract Refract Surg*. 2009;35(8):1358-1362.
99. Dhawan S, Rao K, Natrajan S. Complications of Corneal Collagen Cross-Linking. *J Ophthalmol*. 2011;2011:1-5.
100. Wollensak G, Spörl E, Reber F, Pillunat L, Funk R. Corneal endothelial cytotoxicity of riboflavin/ UVA treatment in vitro. *Ophthalmic Res*. 2003;35(6):324-328.
101. Wollensak G, Spoerl E, Wilsch M, Seiler T. Endothelial cell damage after riboflavin-ultraviolet-A treatment in the rabbit. *J Cataract Refract Surg*. 2003;29(9):1786-1790.

102. Wollensak G, Spoerl E, Wilsch M, Seiler T. Keratocyte Apoptosis after Corneal Collagen Cross-linking Using Riboflavin/UVA Treatment. *Cornea*. 2004;23(1):43-49.
103. Wollensak G, Aurich H, Wirbelauer C, Sel S. Significance of the riboflavin film in corneal collagen crosslinking. *J Cataract Refract Surg*. 2010;36(1):114-120.
104. Hafezi F, Kling S, Gilardoni F, et al. Individualized Corneal Cross-linking With Riboflavin and UV-A in Ultrathin Corneas: The Sub400 Protocol. *Am J Ophthalmol*. 2021;224(December):133-142.
105. Knyazer B, Kormas RM, Chorny A, Lifshitz T, Achiron A, Mimouni M. Corneal cross-linking in thin corneas: 1-year results of accelerated contact lens-assisted treatment of keratoconus. *J Refract Surg*. 2019;35(10):642-648.
106. Evangelista CB, Hatch KM. Corneal Collagen Cross-Linking Complications. *Semin Ophthalmol*. 2018;33(1):29-35.
107. Maharana PK, Sahay P, Sujeeth M, et al. Microbial keratitis after accelerated corneal collagen cross-linking in keratoconus. *Cornea*. 2018;37(2):162-167.
108. Abbouda A, Abicca I, Alió JL. Infectious Keratitis Following Corneal Crosslinking: A Systematic Review of Reported Cases: Management, Visual Outcome, and Treatment Proposed. *Semin Ophthalmol*. 2016;31(5):485-491.
109. Kissner A, Spoerl E, Jung R, Spekl K, Pillunat LE, Raiskup F. Pharmacological modification of the epithelial permeability by benzalkonium chloride in UVA/Riboflavin corneal collagen cross-linking. *Curr Eye Res*. 2010;35(8):715-721.
110. Caporossi A, Mazzotta C, Paradiso AL, Baiocchi S, Marigliani D, Caporossi T. Transepithelial corneal collagen crosslinking for progressive keratoconus: 24-month clinical results. *J Cataract Refract Surg*. 2013;39(8):1157-1163.
111. Soeters N, Wisse RPL, Godefröoij DA, Imhof SM, Tahzib NG. Transepithelial versus epithelium-off corneal cross-linking for the treatment of progressive keratoconus: A randomized controlled trial. *Am J Ophthalmol*. 2015;159(5):821-828.e3.
112. Wollensak G, Hammer CM, Spörl E, et al. Biomechanical efficacy of collagen crosslinking in porcine cornea using a femtosecond laser pocket. *Cornea*. 2014;33(3):300-305.
113. Kaya V, Utine CA, Yilmaz OF. Efficacy of corneal collagen cross-linking using a custom epithelial debridement technique in thin corneas: A confocal microscopy study. *J Refract Surg*. 2011;27(6):444-450.
114. Hashemi H, Mirafteb M, Hafezi F, Asgari S. Matched comparison study of total and partial epithelium removal in corneal cross-linking. *J Refract Surg*. 2015;31(2):110-115.
115. Rechichi M, Daya S, Scorcia V, Meduri A, Scorcia G. Epithelial-disruption collagen crosslinking for keratoconus: One-year results. *J Cataract Refract Surg*. 2013;39(8):1171-1178.
116. Stulting RD, Trattler WB, Woolfson JM, Rubinfeld RS. Corneal crosslinking without epithelial removal. *J Cataract Refract Surg*. 2018;44(11):1363-1370.
117. Jia HZ, Pang X, Fan ZJ, Li N, Li G, Peng XJ. Iontophoresis-assisted corneal crosslinking using 0.1% riboflavin for progressive keratoconus. *Int J Ophthalmol*. 2017;10(5):717-722.
118. Vinciguerra P, Romano V, Rosetta P, et al. Iontophoresis-Assisted Corneal Collagen Cross-Linking with Epithelial Debridement: Preliminary Results. *Biomed Res Int*. 2016;2016:1-5.
119. Marcovich AL, Brandis A, Daphna O, et al. Stiffening of rabbit corneas by the bacteriochlorophyll derivative WST11 using near infrared light. *Investig Ophthalmol Vis Sci*. 2012;53(10):6378-6388.
120. Cherfan D, Verter EE, Melki S, et al. Collagen cross-linking using rose bengal and green light to increase corneal stiffness. *Investig Ophthalmol Vis Sci*. 2013;54(5):3426-3433.
121. Alageel SA, Arafat SN, Salvador-Culla B, et al. Corneal Cross-Linking with Verteporfin and Nonthermal Laser Therapy. *Cornea*. 2018;37(3):362-368.

122. Avila MY, Narvaez M, Castañeda JP. Effects of genipin corneal crosslinking in rabbit corneas. *J Cataract Refract Surg*. 2016;42(7):1073-1077.
123. Metzler KM, Roberts CJ, Mahmoud AM, Agarwal G, Liu J. Ex vivo transepithelial collagen cross-linking in porcine and human corneas using human decorin core protein. *J Refract Surg*. 2016;32(6):410-417.
124. Bersanetti PA, Bueno TLN, Morandim-Giannetti A de A, Nogueira RF, Matos JR, Schor P. Characterization of Rabbit Corneas Subjected to Stromal Stiffening by the Açai Extract (*Euterpe oleracea*). *Curr Eye Res*. 2017;42(4):528-533.
125. Yildiz E, Anwaar Nazeer M, Bayraktutar B, Zibandeh N, Kizilel S, Sahin A. Novel corneal crosslinking technique with eosin-Y and visible light. *Acta Ophthalmol*. 2019;97(S263):j.1755-3768.2019.5148.
126. Zeitoune AA, Bersanetti PA, Schor P, Erbes LA, Cesar CL, Adur J. Comparison of morphological changes of corneal collagen fibers treated with collagen crosslinking agents using second harmonic generation images. *Int J Biol Macromol*. 2020;165(Pt A):346-353.
127. Bradford SM, Mikula ER, Chai D, Brown DJ, Juhasz T, Jester J V. Custom built nonlinear optical crosslinking (NLO CXL) device capable of producing mechanical stiffening in ex vivo rabbit corneas. *Biomed Opt Express*. 2017;8(10):4788.
128. Bradford SM, Brown DJ, Juhasz T, Mikula E, Jester J V. Nonlinear optical corneal collagen crosslinking of ex vivo rabbit eyes. *J Cataract Refract Surg*. 2016;42(11):1660-1665.
129. Spoerl E, Wollensak G, Dittert DD, Seiler T. Thermomechanical behavior of collagen-cross-linked porcine cornea. *Ophthalmologica*. 2004;218(2):136-140.
130. Labate C, De Santo MP, Lombardo G, Lombardo M. Understanding of the viscoelastic response of the human corneal stroma induced by riboflavin/UV-A cross-linking at the nano level. *PLoS One*. 2015;10(4):e0122868.
131. Kim MJ, Takaoka A, Hoang Q V., Trokel SL, Paik DC. Pharmacologic alternatives to riboflavin photochemical corneal cross-linking: A comparison study of cell toxicity thresholds. *Investig Ophthalmol Vis Sci*. 2014;55(5):3247-3257.
132. Tang J, Pan X, Weber PA, Liu J. Effect of corneal stiffening on goldmann applanation tonometry and Tono-Pen measurements in canine eyes. *Investig Ophthalmol Vis Sci*. 2012;53(3):1397-1405.
133. Avila MY, Gerena VA, Navia JL. Corneal crosslinking with genipin, comparison with UV-riboflavin in ex-vivo model. *Mol Vis*. 2012;18(April):1068-1073.
134. Germann JA, Martinez-Enriquez E, Carmen Martinez-García M, Kochevar IE, Marcos S. Corneal collagen ordering after in vivo Rose Bengal and riboflavin cross-linking. *Investig Ophthalmol Vis Sci*. 2020;61(3):28.
135. Wertheimer CM, Elhardt C, Kaminsky SM, et al. Enhancing rose bengal-photosensitized protein crosslinking in the cornea. *Investig Ophthalmol Vis Sci*. 2019;60(6):1845-1852.
136. Gallego-Muñoz P, Ibares-Frías L, Lorenzo E, et al. Corneal wound repair after rose bengal and green light crosslinking: Clinical and histologic study. *Investig Ophthalmol Vis Sci*. 2017;58(9):3471-3480.
137. Wertheimer CM, Mendes B, Pei Q, Brandt K, Kochevar IE. Arginine as an enhancer in rose bengal photosensitized corneal crosslinking. *Transl Vis Sci Technol*. 2020;9(8):24.
138. Bekesi N, Gallego-Muñoz P, Ibarés-Frías L, et al. Biomechanical changes after in vivo collagen cross-linking with rose bengal-green light and riboflavin-UVA. *Investig Ophthalmol Vis Sci*. 2017;58(3):1612-1620.
139. Bekesi N, Kochevar IE, Marcos S. Corneal biomechanical response following collagen cross-linking with Rose Bengal-green light and riboflavin-UVA. *Investig Ophthalmol Vis Sci*. 2016;57(3):992-1001.

140. Singh M, Li J, Han Z, et al. Evaluating the effects of riboflavin/UV-a and rose-bengal/green light cross-linking of the rabbit cornea by noncontact optical coherence elastography. *Investig Ophthalmol Vis Sci*. 2016;57(9):OCT112-OCT120.
141. Zhu H, Alt C, Webb RH, Melki S, Kochevar IE. Corneal crosslinking with rose bengal and green light: Efficacy and safety evaluation. *Cornea*. 2016;35(9):1234-1241.
142. Fadlallah A, Zhu H, Arafat S, Kochevar I, Melki S, Ciolino JB. Corneal resistance to keratolysis after collagen crosslinking with rose bengal and green light. *Investig Ophthalmol Vis Sci*. 2016;57(15):6610-6614.
143. Lorenzo-Martin E, Gallego-Muñoz P, Ibares-Frías L, et al. Rose bengal and green light versus riboflavin-UVA cross-linking: Corneal wound repair response. *Investig Ophthalmol Vis Sci*. 2018;59(12):4821-4830.
144. Wang T, Zhu L, Zhu J, et al. Subacute effects of rose Bengal/Green light cross linking on rabbit thin corneal stability and safety. *Lasers Surg Med*. 2018;50(4):324-332.
145. Wang X, Majumdar S, Ma G, et al. Chondroitin sulfate-based biocompatible crosslinker restores corneal mechanics and collagen alignment. *Investig Ophthalmol Vis Sci*. 2017;58(10):3887-3895.
146. Hayes S, Aldahlawi N, Marcovich AL, et al. The effect of bacteriochlorophyll derivative WST-D and near infrared light on the molecular and fibrillar architecture of the corneal stroma. *Sci Rep*. 2020;10(1):9836.
147. Brekelmans J, Veugen J, Rieff K, et al. Enzymatic digestion of porcine corneas cross-linked by hypo- and hyperosmolar formulations of riboflavin/ultraviolet A or WST11/near-infrared light. *Transl Vis Sci Technol*. 2020;9(10):1-9.
148. Brekelmans J, Goz A, Dickman MM, et al. Corneal Stiffening by a Bacteriochlorophyll Derivative with Dextran and Near-Infrared Light: Effect of Shortening Irradiation Time up to 1 Minute. *Cornea*. 2017;36(11):1395-1401.
149. Brekelmans J, Goz A, Dickman MM, et al. Long-term biomechanical and histologic results of WST-D/NIR corneal stiffening in rabbits, up to 8 months follow-up. *Investig Ophthalmol Vis Sci*. 2017;58(10):4089-4095.
150. Song W, Tang Y, Qiao J, et al. The Short-Term Safety Evaluation of Corneal Crosslinking Agent-Genipin. *Ophthalmic Res*. 2019;62(3):141-149.
151. Tang Y, Song W, Qiao J, Rong B, Wu Y, Yan X. A study of corneal structure and biomechanical properties after collagen crosslinking with genipin in rabbit corneas. *Mol Vis*. 2019;25(8):574-582.
152. Gharaibeh AM, Saez V, Garcia N, Bataille L, Alió JL. Optimizing genipin concentration for corneal collagen cross-linking: An ex vivo study. *Ophthalmic Res*. 2018;60(2):100-108.
153. Song W, Tang Y, Qiao J, et al. The comparative safety of genipin versus UVA-riboflavin crosslinking of rabbit corneas. *Mol Vis*. 2017;23:504-513.
154. Avila MY, Navia JL. Effect of genipin collagen crosslinking on porcine corneas. *J Cataract Refract Surg*. 2010;36(4):659-664.
155. Paik DC, Wen Q, Braunstein RE, Trokel SL. Short chain aliphatic  $\beta$ -nitro alcohols for corneoscleral cross-linking: Corneal endothelial toxicity studies. *J Refract Surg*. 2008;24(7):S741-7.
156. Wen Q, Trokel SL, Kim MJ, Paik DC. Aliphatic  $\beta$ -nitroalcohols for therapeutic corneoscleral cross-linking: Corneal permeability considerations. *Cornea*. 2013;32(2):179-184.
157. Paik DC, Wen Q, Braunstein RE, Airiani S, Trokel SL. Initial studies using aliphatic  $\beta$ -nitro alcohols for therapeutic corneal cross-linking. *Investig Ophthalmol Vis Sci*. 2009;50(3):1098-1105.

158. Wu Y, Song W, Tang Y, Yan X. Biomechanical Changes after in vivo Enzyme-Induced Corneal Crosslinking in Rabbits. *Ophthalmic Res.* 2020;63(5):501-506.
159. Wu Y, Song W, Tang Y, Elsheikh A, Shao Y, Yan X. Efficacy and safety of transglutaminase-induced corneal stiffening in rabbits. *Transl Vis Sci Technol.* 2019;8(6):27.







# Chapter 2

## **Five years outcomes after corneal cross-linking for keratoconus**

Asli Ayvaz, Jurriaan Brekelmans, Tos T.J.M. Berendschot, Mor M. Dickman,  
Nienke Visser, Rudy M.M.A. Nuijts, Isabelle E.Y. Saelens.

*Journal of EuCornea*, December 2019; 6:9–12



# ABSTRACT

Purpose: To evaluate five-year outcomes of riboflavin (RF) and ultra-violet A (UVA) corneal collagen crosslinking (CXL) and determine pre-operative predictive parameters.

Methods: This retrospective clinical study included 265 eyes of 206 patients, undergoing RF/UVA CXL for progressive keratoconus (KC) between 2007 and 2014. Assessment pre-operatively, and post-operatively after one week, one, three, six, twelve months, and yearly thereafter, included Snellen corrected distance visual acuity (CDVA), Goldmann applanation tonometry, endothelial cell density (ECD), and corneal topography. The CXL procedure was performed following the Dresden protocol, applying hyperosmolar 0.1% RF for 30 minutes with consecutive UVA irradiance at a 3 mW/cm<sup>2</sup> for 30 minutes, and corneal pachymetry measured throughout the procedure to be at least 400 µm.

Results: Mean age was 29 ± 11 years, and 146 males and 60 females were included. Steep, mean, and maximum keratometry values (K-values) and corneal astigmatism were significantly decreased after one and five years, with an average annual decrease of 0.18 D, 0.20 D, 0.25 D, and 0.19 D, respectively. Mean CDVA was significantly improved by 0.11 LogMAR after one year, and remained stable thereafter. Higher pre-operative K-values resulted in a stronger topographic decrease, whereas a lower pre-operative CDVA resulted in greater visual improvement after CXL. Mean ECD and intra-ocular pressure did not significantly change after one and five years. Progression of ≥1 D was seen in 19 of 205 eyes (9.3%) after one year.

Conclusions: RF/UVA CXL significantly arrests KC in over 90% of patients. Patients with higher pre-operative keratometric astigmatism and lower CDVA are more likely to have improvement after CXL.

## INTRODUCTION

Keratoconus (KC) is a multifactorial eye disorder with progressive protrusion and thinning of the cornea which results in irregular astigmatism, greatly impairing visual acuity and quality of life.<sup>1,2</sup> Conventional treatment of KC varies depending on the state of progression of the disease. In early cases spectacles and contact lenses can be used to achieve a good visual acuity, where rigid contact lenses are the most commonly used for visual rehabilitation. Intracorneal ring segments implantation and lamellar or penetrating keratoplasty are often applied in more advanced stages of the disease.<sup>3</sup> In 2003, corneal crosslinking (CXL) was introduced as a new and more conservative treatment.<sup>4</sup>

Corneal CXL using riboflavin (RF) and ultra-violet A (UVA) irradiation is the first, and currently the only, clinically approved treatment capable of effectively arresting ectatic corneal disorders such as KC, pellucid marginal corneal degeneration and post-laser in situ keratomileusis (LASIK) ectasia.<sup>5-7</sup> Alternative CXL methods, applying different photosensitizers or inducing crosslinks chemically, are currently studied.<sup>8-10</sup> Several short- and long-term clinical studies showed that CXL is effective in arresting progression of KC and hence delays or prevents the need for corneal transplantation.<sup>11,12</sup> However, long-term clinical data are still sparse and only small study cohorts have been reported. In addition, little is known about pre-operative predictors for effectiveness of RF/UVA CXL in the treatment of KC. Therefore, the aim of this large prospective study was to evaluate the five year outcomes of CXL and to extract possible pre-operative parameters to predict the outcome of the treatment.

## METHODS

### Patient population and study design

In this retrospective study, 265 eyes of 206 patients with progressive KC were enrolled that visited the University Eye Clinic Maastricht from 2007 to 2014. Inclusion criteria were a documented progression of KC and pachymetry (Pentacam HR; OCULUS Optikgeräte GmbH, Wetzlar, Germany)  $\geq 400 \mu\text{m}$  at the thinnest location. Patients with other ocular pathology (e.g., herpes simplex keratitis) or corneal scarring were excluded. Progression of KC was defined either as an increase in keratometry value (K-value) on the corneal topography by  $\geq 1.0 \text{ D}$ , an increase  $\geq 1.0 \text{ D}$  in spherical equivalent, or a  $\geq 10\%$  decrease in central corneal thickness (CCT) in the previous 12 months.<sup>4,13</sup> After receiving a detailed description, all patients provided informed consent for CXL.

### Preoperative and postoperative examinations

Patients were assessed preoperatively, and postoperatively after one week, one, three, six and twelve months, and yearly thereafter up to five years. At each examination, Snellen CDVA, Goldmann applanation tonometry (Haag-Streit AG, Koeniz, Switzerland), endothelial cell count (SP 2000 Specular Microscope; Topcon Corp., Tokyo, Japan) and corneal topography (Pentacam HR; OCULUS Optikgeräte GmbH, Wetzlar, Germany) were performed. If possible, hard contact lenses were removed two days prior to examination. For the additional analysis of progression, the stromal demarcation line depth was measured preoperatively and postoperatively after one and three months with an ocular coherence tomographer (CASIA SS-1000; Tomey, Nishi-Ku, Japan).

### CXL procedure

All CXL treatments were performed according to the Dresden protocol.<sup>4</sup> Before the treatment, the irradiance of the UVA light source (VEGA CBM X-linker; SOOFT Italia SpA, Italy) was confirmed with a power meter (LaserMate-Q; Coherent, California, USA) to measure  $3 \text{ mW/cm}^2$  at the corneal surface.

A nine-millimeter epithelial abrasion was performed under topical anesthesia (tetracaine 1%; Bausch&Lomb, New York, USA) using a blunt hockey-stick blade. A hyperosmolar 0.1% Riboflavin (RF) (Ricrolin; SOOFT Italia SpA, Italy), containing 20% Dextran 500 kDa solution was applied on the cornea every two minutes for 30 minutes. Before starting UVA irradiation, CCT was measured by ultrasound pachymetry (POCKET II; Quantel-Medical, Clermont-Ferrand, France). If stromal thickness was less than  $400 \mu\text{m}$ , corneal swelling was induced by application of hypo-osmolar RF solution (INNOCROSS-R; IROC, Switzerland). Subsequently, the eye was irradiated for 30 min with UVA light of 370 nm. RF drops were instilled on the cornea every five minutes during the UVA exposure.

to maintain a sufficient level of corneal RF and to guarantee a safe CXL treatment. At the end of the CXL procedure, 0.3% ofloxacin (Trafloxal E.D.O.; Bausch&Lomb, Berlin, Germany) and 0.5% tropicamide (Bausch& Lomb, New York, USA) eye drops were administered, and a soft bandage contact lens (Bausch& Lomb, New York, USA) was placed until corneal epithelial healing was completed. Postoperatively, the patient received preservative-free artificial tears (Duratears Free; Alcon, Puurs, Belgium) eight times daily and 0.3% ofloxacin eye drops (Bausch&Lomb, Berlin, Germany) three times daily, for three weeks. The bandage contact lens was removed as soon as re-epithelialization had occurred, which was evaluated by slit lamp examination. When corneal haze was observed, topical corticosteroids (FML Liquifilm; Allergan, Ireland) were applied twice a day for three weeks.

### **Statistical analysis**

All collected data was exported from a Microsoft Excel-spreadsheet to SPSS (SPSS for Windows, version 22.0; SPSS Inc., Illinois, USA) for statistical analysis.

A Linear Mixed Model (LMM) analysis was used to analyze changes over time and to explore possible predictive factors of treatment effect such as age, gender, and pre-operative K-values. Snellen visual acuity was converted to logarithm of the minimal angle of resolution (LogMAR) for statistical comparison. Results are expressed as mean  $\pm$  standard deviation (SD). A  $p$ -value of  $<0.05$  was considered significant.

# RESULTS

## Demographics

The study group consisted of 146 males (187 eyes) and 60 females (78 eyes) with a mean age of  $29 \pm 11$  years and a mean follow-up of  $32 \pm 19$  months. Pre-operative characteristics are shown in Table 1.

Table 1. Preoperative patient characteristics.

	Mean $\pm$ SD	Range
Number of eyes	265	
Number of females	60 (78 eyes)	
Number of males	146 (187 eyes)	
Age (years)	$29 \pm 11$	12 - 76
Spherical equivalent (D)	$-4.2 \pm 3.9$	-21 - 4.3
CDVA (LogMAR)	$0.32 \pm 0.28$	-0.10 - 1.30
Intraocular pressure (mmHg)	$11.8 \pm 2.9$	5 - 21
Steep K-value (D)	$50.4 \pm 5.0$	40.3 - 69.6
Mean K-value (D)	$48.5 \pm 4.8$	39.6 - 67.3
Maximum K-value (D)	$57.2 \pm 6.6$	43.0 - 84.9
Astigmatism K-value (D)	$4.3 \pm 2.7$	0.10 - 18.8
Preoperative ECD (cells/mm <sup>2</sup> )	$2717 \pm 333$	2020 - 3803

SD = standard deviation, CDVA = corrected distance visual acuity, D = diopters, ECD = endothelial cell density.

## Keratometry and corneal astigmatism

Steep, mean and maximum K-values decreased significantly ( $p < 0.001$ ) over one to five years follow-up compared to pre-operative values (Table 2 and Figure 1). Corneal (topographic) astigmatism showed a significant ( $p = 0.001$ ) gradual decrease over time (Table 2 and Figure 2).

LMM analysis including all post-operative data yielded a significant average annual decrease of 0.18 D, 0.20 D, 0.25 D, and 0.19 D for steep, mean and maximal K-values, and corneal astigmatism respectively (all  $p < 0.001$ ). Furthermore, LMM analysis indicated that a higher preoperative mean K-value resulted in a stronger decrease in the mean K-value over time. For example, preoperative mean K-values of 44 D and 53 D resulted in yearly decreases of 0.06 D and 0.37 D respectively. Similarly, higher preoperative corneal astigmatism was associated with a stronger decrease in corneal astigmatism

over time. Here, preoperative corneal astigmatism of 4.0 D and 4.6 D resulted in yearly decreases of 0.17 D and 0.20 D respectively. Furthermore, the influence of age was assessed by dividing the cohort in three groups: <18, 18–26, and >26 years of age. Age was not correlated to a change in mean or astigmatism K-values. However, patients above 26 years of age showed a slower decrease in maximum K-value, compared to patients in both age groups below 26 years ( $p = 0.037$ ). No gender effect was found.

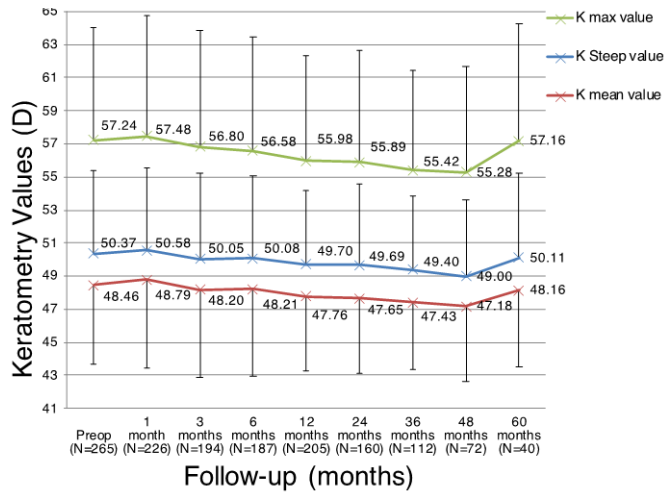


Figure 1. Postoperative keratometry (mean  $\pm$  standard deviation, in diopters [D]). A significant annual decrease of 0.20 D, 0.18 D, and 0.25 D was found for mean, steep, and maximal K-value respectively. Linear mixed modeling showed a correlation between preoperative mean K-value and its postoperative decrease.

Table 2. Postoperative change in keratometry.

Follow-up	Steep K-value	Mean K-value	Maximum K-value	Astigmatism K-value
Preop (n = 265)	50.4 $\pm$ 5.0	48.5 $\pm$ 4.8	57.2 $\pm$ 6.8	4.3 $\pm$ 2.7
12 months (n = 205)	49.7 $\pm$ 4.5	47.8 $\pm$ 4.5	56.0 $\pm$ 6.4	3.9 $\pm$ 2.3
24 months (n = 160)	49.7 $\pm$ 4.9	47.7 $\pm$ 4.5	55.9 $\pm$ 6.7	3.9 $\pm$ 2.8
36 months (n = 112)	49.4 $\pm$ 4.5	47.4 $\pm$ 4.1	55.4 $\pm$ 6.1	3.7 $\pm$ 2.6
48 months (n = 72)	49.0 $\pm$ 4.6	47.2 $\pm$ 4.5	55.3 $\pm$ 6.4	3.5 $\pm$ 1.9
60 months (n = 40)	50.1 $\pm$ 5.1	48.2 $\pm$ 4.6	57.2 $\pm$ 7.1	3.7 $\pm$ 2.2

Mean  $\pm$  standard deviation. In diopters.

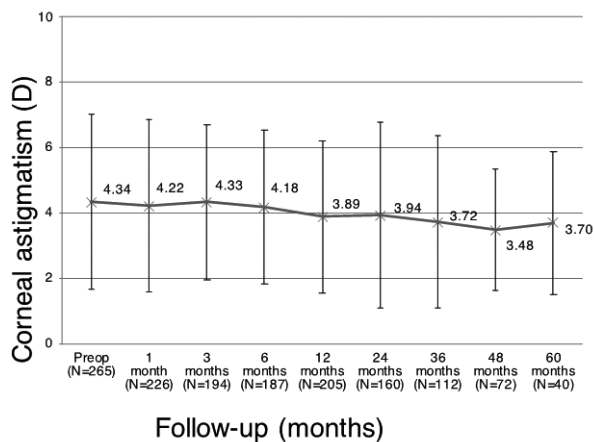


Figure 2. Postoperative corneal astigmatism (mean  $\pm$  standard deviation, in diopters [D]). An average annual decrease of 0.19 D was found. Furthermore, linear mixed model analysis showed a significant correlation between preoperative corneal astigmatism and its decrease after RF/UVA CXL.

### Refraction

Mean preoperative spherical equivalent (SE) was  $-4.2 \pm 3.9$  D. One year postop, SE was  $-4.6 \pm 4.7$  D ( $n = 149$ ,  $p = 0.41$ ) and after five years SE was  $-5.2 \pm 5.8$  D ( $n = 29$ ,  $p = 0.14$ ). Using all postoperative data, LMM analysis showed a yearly decrease in SE of 0.22 D ( $p = 0.051$ ). Postoperative values are shown in Table 2.

### Visual acuity

Mean CDVA improved by 0.11 LogMAR after one year ( $0.32 \pm 0.28$  vs.  $0.21 \pm 0.22$  LogMAR,  $n = 204$ ,  $p < 0.001$ ), and remained stable thereafter (Figure 3). After one year, 91 out of 204 eyes (44.6%) gained one line or more, while 15 eyes (7.3%) lost two lines or more. LMM analysis showed that a lower preoperative CDVA resulted in greater visual improvement after CXL. Using the LMM parameter estimates as input, a preoperative CDVA of 0.04 LogMAR led to an improvement after one year of 0.05 LogMAR, whereas a preoperative CDVA of 0.60 LogMAR led to an improvement of 0.24 LogMAR.

### Endothelial cell density

Mean preoperative endothelial cell density (ECD) was  $2717 \pm 333$  cells/mm<sup>2</sup>, which decreased to  $2662 \pm 296$  cells/mm<sup>2</sup> ( $n = 124$ ,  $p = 0.14$ ) and  $2625 \pm 306$  cells/mm<sup>2</sup> ( $n = 22$ ,  $p = 0.53$ ), after one and five years respectively (Figure 4). However, LMM analysis yielded a yearly decrease of 0.6% ( $p = 0.001$ ). ECD data of two patients was excluded from statistical analysis due to erroneous measurements caused by either the presence of an anterior chamber phakic intraocular lens, or a contact lens related corneal scar.



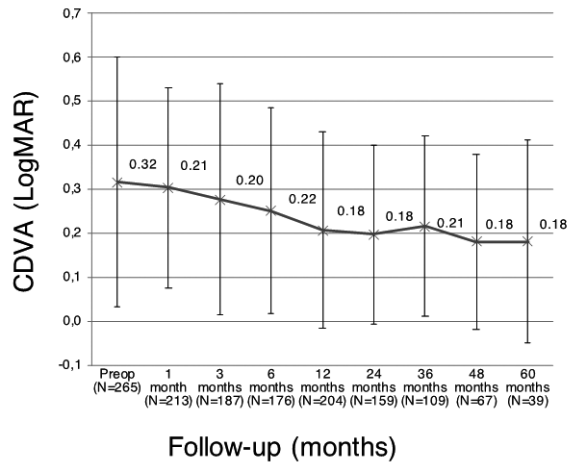


Figure 3. Change in the corrected distance visual acuity (CDVA, mean  $\pm$  standard deviation, in LogMAR). CDVA improved significantly after treatment. The largest improvement was seen within one year after treatment, whereafter CDVA stabilized.

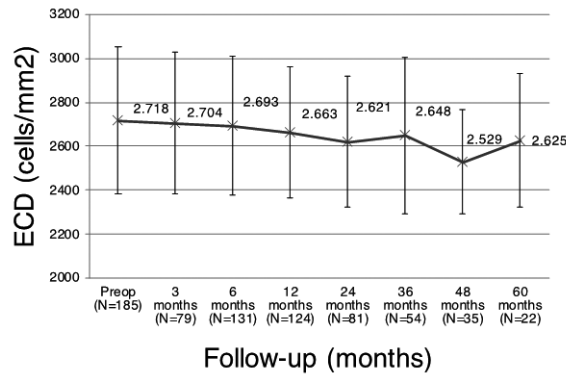


Figure 4. Change of the endothelial cell density (ECD, mean  $\pm$  standard deviation, in cells/mm²). An annual decrease in ECD of 0.6% was found, in line with age-related ECD changes in healthy subjects.

### Complications and treatment failure

Seven of 265 patients (2.6%) showed sterile stromal infiltrates one week after CXL. After one year, a progression of 1 D or more in mean K-value was seen in 19 of 205 eyes (9.3%). There was no correlation between the depth of the stromal demarcation line and progression after CXL. Our data also proved that after CXL there is no correlation between progression and bilaterality of KC. Postoperative values of the mean depth of the demarcation line are shown in Table 3. The intraocular pressure showed no significant changes in time during the follow-up. Postoperative values are shown in Table 4.

Table 3. Mean demarcation line depth, one and three months after corneal collagen cross-linking, in patients with postoperative stable and progressive keratoconus (KC).

Follow-up	Stable KC	Progressive KC
1 month	293 ± 50	294 ± 70
3 months	218 ± 71	208 ± 5

Mean ± standard deviation, in micrometers.

Table 3. Mean demarcation line depth, one and three months after corneal collagen cross-linking, in patients with postoperative stable and progressive keratoconus (KC).

Follow-up	Spherical equivalent	Intraocular pressure
Preop	-4.2 ± 3.9	11.8 ± 2.9
1 month	-4.6 ± 4.5	12.4 ± 2.7
3 months	-4.2 ± 4.3	11.7 ± 2.9
6 months	-4.5 ± 4.2	12.1 ± 3.2
12 months	-4.6 ± 4.8	11.8 ± 2.8
24 months	-5.0 ± 4.3	11.6 ± 3.3
36 months	-5.2 ± 4.1	12.7 ± 3.8
48 months	-6.2 ± 5.7	11.0 ± 2.9
60 months	-5.2 ± 5.8	10.3 ± 2.8

Mean ± standard deviation, in micrometers.

## DISCUSSION

Corneal CXL is now the standard of care for the treatment of progressive KC, thereby postponing or preventing the need for corneal transplantation.<sup>12,14</sup> RF/UVA CXL has been well shown to arrest KC progression on the short term, but long-term clinical data are still sparse and only small cohort studies have been published.<sup>15–21</sup> Given the young age of KC patients, a better understanding of the long-term RF/UVA CXL effect is important. Furthermore, RF/UVA CXL is reported to only halt KC progression in approximately 90% of adult patients, and risk factors for treatment failure are poorly understood.<sup>22</sup> The aim of this study was therefore to determine the long-term keratometric and visual acuity results of corneal CXL and identify predictive factors for RF/UVA CXL efficacy.

Our keratometric results show the largest decrease within the first year after treatment, remaining stable thereafter, whereas results of corneal astigmatism show a more gradual decrease over time. When compared to the literature, the changes in K-values found in this study up to five years of follow-up are in line with that of other long-term studies, ranging between  $-0.7$  D and  $-1.2$  D.<sup>19,23,24</sup> Hashemi *et al.* reported a decrease of  $0.44$  D and  $0.86$  D in maximum K-values, after one and five years respectively.<sup>19</sup> After ten years, Raiskup *et al.* reported a decrease in maximum K-value of  $-3.6$  D.<sup>16</sup> Four and five years after treatment, our results show an unexpected increase and subsequent decrease, compared to the measurements at three years. We do not have a clear explanation for these findings, rather than a difference in number of subjects in these longest follow-up groups. In our study we used a LMM analysis to exclude the impact of varying number of subjects on the results and found a significant annual decrease of approximately  $0.2$  D for all K-values. More interestingly, our analysis also indicated that higher preoperative mean K-values result in a greater decrease after treatment. Although studies have previously described such relationship between preoperative and postoperative keratometry, we were not able to identify steep and maximal K-values as predictive factors.<sup>5,25–28</sup> Similar to preoperative mean K-values, a higher preoperative corneal astigmatism was found to be associated with a greater decrease after RF/UVA CXL. Contrary to other studies, our study shows no evidence for age and sex to be predictive factors for cone flattening.<sup>13,28,29</sup> We believe that patient specific preoperative parameters can help health-care professionals to better predict treatment effect and perhaps even allow for a certain degree of refractive correction, as is aimed for in some novel customized CXL protocols.

CDVA improved significantly after treatment, with one line or more gained in 44.6% of the patients. Our results furthermore indicate that a lower preoperative CDVA was associated with a greater postoperative improvement. This association has been described previously, however only up to one year follow-up, while this study shows the treatment effect persists beyond one year after treatment.<sup>26–28,30</sup> In 15 eyes (7.3%), CDVA decreased by two lines or more over time after RF/UVA CXL. Overall, the current study shows similar findings regarding visual acuity, when compared to other long-term studies.<sup>16,17,31</sup> Furthermore, our results endorse the previously shown trend of stabilizing CDVA after six to 12 months. Thus, RF/UVA CXL provides long-term stabilization and improvement of the visual acuity after CXL.

Endothelial cell density measurements in patients with more severe KC, high K-values, high irregularities and stromal scars are often difficult to obtain. This might be reflected in this study by a relatively low number of patients in which it was possible to quantify ECD (approximately 60% at one year). This is supported by a significant correlation between the number of missing ECD data and both Kmax ( $r = 0.27$ ,  $p < 0.001$ ), and Kmean at baseline ( $r = 0.21$ ,  $p = 0.001$ ). It should however be noted that no clinical signs of endothelial decompensation were seen throughout the study, indicating a functional endothelium after CXL. The yearly decrease of 0.6% found in this study is in line with the age-related decrease in healthy subjects, reported in the literature (0.3% to 1%).<sup>32–35</sup> Thus, based on the available literature and our data, RF/UVA CXL appears not to have an adverse effect on the corneal endothelium.

Although RF/UVA CXL evolved greatly over the years, the treatment success rate is still reported to be around 90% in adults, only reaching to 100% in several smaller studies.<sup>16,17,22,36</sup> This is in line with the 90.7% success rate seen in this study at one-year follow-up. One year after treatment, further KC progression had occurred in 19 out of 205 patients. Closer examination of these specific patients revealed no further insight in predictive risk factors, and while age has been described as a factor for RF/UVA CXL success, we did not see such a relationship in this study.<sup>36</sup> Doors *et al.*, Yam *et al.* and some others assumed the demarcation line depth after CXL as representative of CXL effectiveness.<sup>36–39</sup> Our data showed that there is no difference in depth of demarcation line between patients with or without progression. We also found that bilaterality of KC was not correlated with progression after CXL.

Limitations of our study were a small number of patients at five-year follow up. Limited follow-up is a well-known problem of cohort studies after CXL and has been reported by Hashemi *et al.* where a loss to follow up of 96% in year 4 was reported and by Raiskup *et al.* where a 98% loss to follow up was reported.<sup>19,20</sup>

In conclusion, this prospective long-term follow up study confirms the efficacy of RF/UVA CXL for arresting KC progression, reducing the K-values and improving visual acuity. Linear mixed model analysis indicates preoperative mean keratometry, corneal astigmatism, and CDVA are predictive factors for their change in time after CXL treatment. The stromal demarcation line depth is not a prognostic factor for treatment efficacy.

## REFERENCES

1. Vazirani J, Basu S. Keratoconus: Current perspectives. *Clin Ophthalmol*. 2013;7:2019-2030.
2. Rebenitsch RL, Kymes SM, Walline JJ, Gordon MO. The lifetime economic burden of keratoconus: A decision analysis using a markov model. *Am J Ophthalmol*. 2011;151(5):768-773.e2.
3. Bromley JG, Randleman JB. Treatment strategies for corneal ectasia. *Curr Opin Ophthalmol*. 2010;21(4):255-258.
4. Wollensak G, Spoerl E, Seiler T. Riboflavin/ultraviolet-A-induced collagen crosslinking for the treatment of keratoconus. *Am J Ophthalmol*. 2003;135(5):620-627.
5. Greenstein SA, Hersh PS. Characteristics influencing outcomes of corneal collagen crosslinking for keratoconus and ectasia: Implications for patient selection. *J Cataract Refract Surg*. 2013;39(8):1133-1140.
6. Kymionis GD, Mikropoulos DG, Portaliou DM, Voudouragaki IC, Kozobolis VP, Konstas AGP. An overview of corneal collagen cross-linking (CXL). *Adv Ther*. 2013;30(10):858-869.
7. Wollensak G. Crosslinking treatment of progressive keratoconus: New hope. *Curr Opin Ophthalmol*. 2006;17(4):356-360.
8. Cherfan D, Verter EE, Melki S, et al. Collagen cross-linking using rose bengal and green light to increase corneal stiffness. *Investig Ophthalmol Vis Sci*. 2013;54(5):3426-3433.
9. Metzler KM, Roberts CJ, Mahmoud AM, Agarwal G, Liu J. Ex vivo transepithelial collagen cross-linking in porcine and human corneas using human decorin core protein. *J Refract Surg*. 2016;32(6):410-417.
10. Brekelmans J, Goz A, Dickman MM, et al. Long-term biomechanical and histologic results of WST-D/NIR corneal stiffening in rabbits, up to 8 months follow-up. *Investig Ophthalmol Vis Sci*. 2017;58(10):4089-4095.
11. Snibson GR. Collagen cross-linking: A new treatment paradigm in corneal disease - a review. *Clin Exp Ophthalmol*. 2010;38(2):141-153.
12. Sandvik GF, Thorsrud A, Råen M, Østern AE, Sæthre M, Drolsum L. Does Corneal Collagen Cross-linking Reduce the Need for Keratoplasties in Patients with Keratoconus? *Cornea*. 2015;34(9):991-995.
13. Maguire LJ, Lowry JC. Identifying progression of subclinical keratoconus by serial topography analysis. *Am J Ophthalmol*. 1991;112(1):41-45.
14. Godefrooij DA, Gans R, Imhof SM, Wisse RPL. Nationwide reduction in the number of corneal transplantations for keratoconus following the implementation of cross-linking. *Acta Ophthalmol*. 2016;94(7):675-678.
15. Meiri Z, Keren S, Rosenblatt A, Sarig T, Shenhav L, Varssano D. Efficacy of corneal collagen cross-linking for the treatment of keratoconus: A systematic review and meta-analysis. *Cornea*. 2016;35(3):417-428.
16. Raiskup F, Theuring A, Pillunat LE, Spoerl E. Corneal collagen crosslinking with riboflavin and ultraviolet-A light in progressive keratoconus: Ten-year results. *J Cataract Refract Surg*. 2015;41(1):41-46.
17. Poli M, Lefevre A, Auxenfans C, Burillon C. Corneal Collagen Cross-linking for the Treatment of Progressive Corneal Ectasia: 6-Year Prospective Outcome in a French Population. *Am J Ophthalmol*. 2015;160(4):654-662.e1.

18. O'Brart DPS, Patel P, Lascaratos G, et al. Corneal Cross-linking to Halt the Progression of Keratoconus and Corneal Ectasia: Seven-Year Follow-up. *Am J Ophthalmol.* 2015;160(6):1154-1163.
19. Hashemi H, Seyedian MA, Mirafteb M, Fotouhi A, Asgari S. Corneal collagen cross-linking with riboflavin and ultraviolet A irradiation for keratoconus: Long-term results. *Ophthalmology.* 2013;120(8):1515-1520.
20. Raiskup-Wolf F, Hoyer A, Spoerl E, Pillunat LE. Collagen crosslinking with riboflavin and ultraviolet-A light in keratoconus: Long-term results. *J Cataract Refract Surg.* 2008;34(5):796-801.
21. Asri D, Touboul D, Fournié P, et al. Corneal collagen crosslinking in progressive keratoconus: Multicenter results from the French National Reference Center for Keratoconus. *J Cataract Refract Surg.* 2011;37(12):2137-2143.
22. O'Brart DPS. Riboflavin for corneal cross-linking. *Drugs Today (Barc).* 2016;52(6):331-346.
23. Wittig-Silva C, Chan E, Islam FMA, Wu T, Whiting M, Snibson GR. A randomized, controlled trial of corneal collagen cross-linking in progressive keratoconus: Three-year results. *Ophthalmology.* 2014;121(4):812-821.
24. Goldich Y, Barkana Y, Lior OW, et al. Corneal collagen cross-linking for the treatment of progressive keratoconus: 3-year prospective outcome. *Can J Ophthalmol.* 2014;49(1):54-59.
25. Godefrooij DA, Boom K, Soeters N, Imhof SM, Wisse RPL. Predictors for treatment outcomes after corneal crosslinking for keratoconus: a validation study. *Int Ophthalmol.* 2017;37(2):341-348.
26. Wisse RPL, Godefrooij DA, Soeters N, Imhof SM, Van Der Lelij A. A multivariate analysis and statistical model for predicting visual acuity and keratometry one year after cross-linking for keratoconus. *Am J Ophthalmol.* 2014;157(3):519.
27. Badawi AE, Abou Samra WA, El Ghafar AA. Predictive Factors of the Standard Cross-linking Outcomes in Adult Keratoconus: One-Year Follow-Up. *J Ophthalmol.* 2017;2017:4109208.
28. Koller T, Mrochen M, Seiler T. Complication and failure rates after corneal crosslinking. *J Cataract Refract Surg.* 2009;35(8):1358-1362.
29. Toprak I, Yaylali V, Yildirim C. Factors affecting outcomes of corneal collagen crosslinking treatment. *Eye.* 2014;28(1):41-46.
30. Kymionis GD, Grentzelos MA, Liakopoulos DA, et al. Long-term follow-up of corneal collagen cross-linking for keratoconus-the cretan study. *Cornea.* 2014;33(10):1071-1079.
31. Islam QU, Saeed MK, Mehboob MA. Age related changes in corneal morphological characteristics of healthy Pakistani eyes. *Saudi J Ophthalmol.* 2017;31(2):86-90.
32. Niederer RL, Perumal D, Sherwin T, McGhee CNJ. Age-related differences in the normal human cornea: A laser scanning in vivo confocal microscopy study. *Br J Ophthalmol.* 2007;91(9):1165-1169.
33. Møller-Pedersen T. A comparative study of human corneal keratocyte and endothelial cell density during aging. *Cornea.* 1997;16(3):333-338.
34. Galgauskas S, Norvydaite D, Krasauskaite D, Stech S, Ašoklis RS. Age-related changes in corneal thickness and endothelial characteristics. *Clin Interv Aging.* 2013;8:1445-1450.
35. Caporossi A, Mazzotta C, Baiocchi S, Caporossi T, Denaro R. Age-Related Long-Term Functional Results after Riboflavin UV A Corneal Cross-Linking. *J Ophthalmol.* 2011;2011(44):1-6.
36. Doors M, Tahzib NG, Eggink FA, Berendschot TTJM, Webers CAB, Nuijts RMMA. Use of Anterior Segment Optical Coherence Tomography to Study Corneal Changes After Collagen Cross-linking. *Am J Ophthalmol.* 2009;148(6):844-851.e2.

37. Yam JCS, Chan CWN, Cheng ACK. Corneal collagen cross-linking demarcation line depth assessed by Visante OCT after CXL for keratoconus and corneal ectasia. *J Refract Surg.* 2012;28(7):475-481.
38. Spadea L, Tonti E, Vingolo EM. Corneal stromal demarcation line after collagen cross-linking in corneal ectatic diseases: A review of the literature. *Clin Ophthalmol.* 2016;10:1803-1810.
39. Spadea L, Di Genova L, Tonti E. Corneal stromal demarcation line after 4 protocols of corneal crosslinking in keratoconus determined with anterior segment optical coherence tomography. *J Cataract Refract Surg.* 2018;44(5):596-602.







# Chapter 3

## **Decreased riboflavin impregnation time does not increase the risk for endothelial phototoxicity during corneal cross-linking**

Arie L. Marcovich, Jurriaan Brekelmans, Alexander Brandis, Ilan Samish,  
Iddo Pinkas, Dina Preise, Keren Sasson, Ilan Feine, Alexandra Goz,  
Mor M. Dickman, Rudy M.M.A. Nuijts, Avigdor Scherz

*Transl. Vis. Sci. Technol.* 2020 May 11;9(6):4



# ABSTRACT

Purpose: To evaluate the riboflavin (RF) concentration and distribution in the corneal stroma and the risk for endothelial photodamage during corneal crosslinking (CXL) following 10- and 30-minute impregnation.

Methods: De-epithelialized rabbit corneas were subjected to impregnation for 10 and 30 minutes with different RF formulations. Human corneal endothelial cells (HCECs) were subjected to different RF concentrations and ultra-violet A (UVA) dosages. Assays included fluorescence imaging, absorption spectroscopy of corneal buttons and anterior chamber humor, and cell viability staining.

Results: After 10 and 30 minutes of impregnation, respectively, anterior chamber fluid showed an RF concentration of  $(1.6 \pm 0.21) \cdot 10^{-4}\%$  and  $(5.4 \pm 0.21) \cdot 10^{-4}\%$ , and transcorneal absorption reported an average corneal RF concentration of 0.0266% and 0.0345%. This results in a decrease in endothelial RF concentration from 0.019% to 0.0056%, whereas endothelial UVA irradiance increases by 1.3-fold when changing from 30 to 10 minutes of impregnation. HCEC viability in cultures exposed to UVA illumination and RF concentrations as concluded for the endothelium after 10- and 30-minute impregnation was non-statistically different at  $51.0 \pm 3.9\%$  and  $41.3 \pm 5.0\%$ , respectively.

Conclusions: The risk for endothelial damage in CXL by RF/UVA treatment does not increase by shortened impregnation because the 30% increase in light intensity is accompanied by a 3.4-fold decrease of the RF concentration in the posterior stroma. This is substantiated by similar endothelial cell toxicity seen in vitro, which in fact appears to favor 10-minute impregnation.

## INTRODUCTION

Keratoconus (KC) is a common degenerative corneal disorder that has been reported in 0.05% to 2.3% of the population depending on diagnosis criteria and country studied.<sup>1,2</sup> Symptoms include irregular astigmatism, myopia, corneal scarring and structural changes of the cornea including thinning, protrusion, and bulging forward to a more conical shape. The disorder is proposed to be affected by family history, eye rubbing, sex, race, atopy, allergy, and other conditions, such as connective tissue disease.<sup>2-4</sup> Up to 1998, treatment was symptomatic using contact lenses, or in severe cases, invasive by penetrating keratoplasty. In 1998, corneal collagen crosslinking (CXL) with riboflavin (RF) and ultra-violet A (UVA) light was introduced, allowing to stabilize progressing keratoconus by stiffening the collagenous corneal tissue. To overcome practical hurdles, increase safety, and reduce patient's discomfort, multiple protocols of RF/UVA CXL have been studied, varying in RF formulation and impregnation times, UVA intensity and duration, and epithelial debridement (Supplementary Table S1).

In the first reported clinical treatment with epithelial removal, dextran enriched RF (RF-D500) was applied for 5 minutes before consecutive UVA irradiation was applied.<sup>5</sup> Later, the RF-D500 impregnation was prolonged to 20 to 30 minutes.<sup>6-10</sup> Currently, a prolonged 30-minute presoaking of the cornea with RF-D500 is regularly applied (Dresden protocol).<sup>11</sup> This impregnation time was chosen to assure sufficient corneal and RF UVA absorption, thereby preventing toxic photodynamic activity at the endothelial level. Based on in vitro studies Wollensak *et al.*<sup>12,13</sup> determined an endothelial phototoxic level of 0.35 mW/cm<sup>2</sup>, and determined a minimal corneal thickness of 400 µm are needed to assure safe RF/UVA CXL. Despite these precautions, postoperative corneal edema suggestive of endothelial damage has been reported also in thicker corneas.<sup>14</sup> Although shorter impregnation times are emerging to reduce the discomforting procedure duration and operating theater time, established protocols along with safety justifications are still lacking.

Here we address the correlations between RF impregnation time and RF concentration, distribution, and subsequent UVA/RF phototoxicity to the endothelium based on an in vitro study using human corneal endothelial cells (HCECs). We follow 10 and 30 minutes of impregnation durations because these two periods were found effective in CXL treatment of de-epithelialized cornea with RF and RF-D500, and the 30-minute impregnation has been assumed safer as providing better UVA attenuation.<sup>11,15-19</sup> We hypothesize that, although the attenuated UVA is lower after a 30-minute impregnation period, the overall risk for photodynamic

damage at the endothelium is actually higher because of the increased endothelial RF concentration. To test this hypothesis, we applied RF/UVA combinations using the experimentally based calculated RF concentrations and light intensities for the two CXL protocols to in vitro grown HCECs.

## METHODS

### Sample preparation riboflavin formulations

Two formulations of RF were used: (1) hypo-osmolar riboflavin-5'-phosphate (F6750; Sigma- Aldrich, St. Louis, MO) in saline solution, adjusted to pH 7.3 (RF); and (2) hyper-osmolar commercial riboflavin-5'-phosphate in 20% dextran 500 kDa (RF-D500), (MedioCross, Kiel, Germany; pH 6.8). For the in vivo and ex vivo experiments a concentration of 0.1% was applied, whereas for the in vitro studies a range of RF concentrations was used.

### Animal models

Both ex vivo (n = 17) and in vivo (n = 14) experiments were performed with New Zealand White (NZW) rabbits of 12 to 25 weeks old (2.5-3.7 kg weight), respectively, either obtained from a local abattoir, or housed with ad libitum access to food and water at the animal facility of the Weizmann Institute of Science (Rehovot, Israel). All experimental procedures were approved by the Institutional Animal Care and Use Committee, and in adherence to the Association for Research in Vision and Ophthalmology Statement for the Use of Animals in Ophthalmic and Visual Research.

For the ex vivo experiments, eyes were obtained within several hours after enucleation, deepithelialized, and left unimpregnated (n = 3), or impregnated with RF for 10 (n = 5) or 30 (n = 9) minutes. For the in vivo experiments the rabbits were anesthetized by intramuscular injection of 35 mg/kg ketamine (Rhone Merieux, Lyon, France) and 5 mg/kg xylazine (Vitamed, Binyamina, Israel). After treatment, rabbits were euthanized by intravenous injection of pentobarbital sodium (CTS Chemical Industries Ltd, Kiryat Malachi, Israel). As negative controls for stromal RF distribution measurements by fluorescent microscopy, this experiment included two corneas in the in vivo group, in which the epithelium was left intact prior to RF impregnation. All other eyes were de-epithelialized, after which the cornea was incubated with either RF or RF-D500 using an eye cap (12 mm in diameter) for 10 (n = 2 and n = 2, respectively) or 30 (n = 3 and n = 4, respectively) minutes, or with saline solution for 30 minutes (n = 1), as previously described.<sup>9</sup> The corneas were then briefly rinsed with saline solution, and a central 8 mm corneal button was trephined for further processing.

### Stromal riboflavin distribution

Immediately after euthanization and corneal button trephination, buttons were frozen on dry ice until further processing. Twenty-micrometer thick sagittal slices were cut using a cryotome from both RF and RF-D500 in vivo treated corneas, and mounted on a microscope glass slide, stored frozen and in the dark until consecutive fluorescence

readings. Fluorescence intensity from three serial slices per cornea was recorded using a fluorescence microscope (BX61 Olympus, Tokyo, Japan) equipped with a CCD camera (Cascade 512B, Roper Scientific, Inc., Tucson, AZ). An excitation wavelength of 488 nm was used, and fluorescence intensity above 530 nm was recorded using a filter. Intensity of 50 lines within each image of a cross section were averaged using ImageJ software (National Institutes of Health, Bethesda, MD). To avoid bias, the analysis was done blinded with respect to sample treatment.

### Absorption measurements riboflavin calibration curve

A calibration curve was prepared for deriving the RF concentration from the 446 nm optical absorption. The stock solution used included the same RF used for the impregnation, that is, RF-D500 (0.1% RF, 20% dextran, MedioCross), in a mixture of 2.4:1 methanol and water to provide optimal RF solubility, which was adjusted to pH 7.3 and used to prepare 5, 10, 15, and 20 µg/mL solutions for calibration. Optical absorption of the four solutions was measured through a 1-cm path quartz cuvette using a spectrophotometer (V750; Jasco, Oklahoma City, OK).

### Anterior chamber humor measurements

After corneal impregnation in vivo, as described earlier, corneal paracentesis was performed, and anterior chamber humor was drawn and frozen on dry ice until further analysis. The humor (100 µL) was diluted with methanol (240 µL) and centrifuged (21,000g x 5 minutes) to remove large particles. Optical absorption of a filled 1 cm path cuvette was measured (V750; Jasco), the diluting mixture's baseline spectrum was removed, and zero absorption was set at 600 nm.

### Trans-corneal absorption

Ex vivo treated corneal buttons were placed on a specially designed 1 mm light pass cuvette (Figure 1). Recorded trans-corneal absorption spectra (Evolution 220 spectrophotometer; Thermo Scientific, Waltham, MA) were normalized to the deviation from the average thickness after de-epithelialization. The trans-corneal spectrum of untreated de-epithelialized eyes (average of three eyes) was considered baseline and subtracted from each measured spectrum. In addition, the optical absorption was set to zero at 600 nm. The obtained corneal absorption at 446 nm ( $A_{446}$ ) was used to calculate the average RF concentration in the stroma according to the Beer Lambert law:

1.  $A_{446} = \epsilon_{RF}^{446} \cdot \bar{C} \cdot \ell$ , where  $\epsilon_{RF}^{446} = 12,550 \text{ M}^{-1}\text{cm}^{-1}$ ,  $\ell = 0.045 \text{ cm}$ , and  $\bar{C}$  is the average concentration of the RF-5'-phosphate (molecular weight: 456 lg/mol) in the corneal stroma.



To estimate the RF concentration in the posterior stroma (i.e., endothelial layer) after 30 minutes of impregnation, we follow the near-linear cross-corneal fluorescence decay and assume that  $\bar{C}$  is roughly given by:

2.  $\bar{C} = \frac{(\bar{C}_{ant} + \bar{C}_{post})}{2}$ , where  $\bar{C}_{ant}$  and  $\bar{C}_{post}$  are the RF concentrations in the anterior (0-200  $\mu\text{m}$ ) and posterior (200-400  $\mu\text{m}$ ) corneal stroma.  $\bar{C}_{ant}$  is known from the literature to range between 0.05-0.09%, the lowest value was chosen in order not to underestimate the posterior RF concentration.<sup>20-23</sup>

As stromal diffusion after 10 minutes of RF impregnation is known not to be linear, posterior RF concentration after 10 minutes impregnation was estimated by dividing the obtained value after 30 minutes by the ratio between aqueous humor concentration after 10 and 30 minutes of RF impregnation.

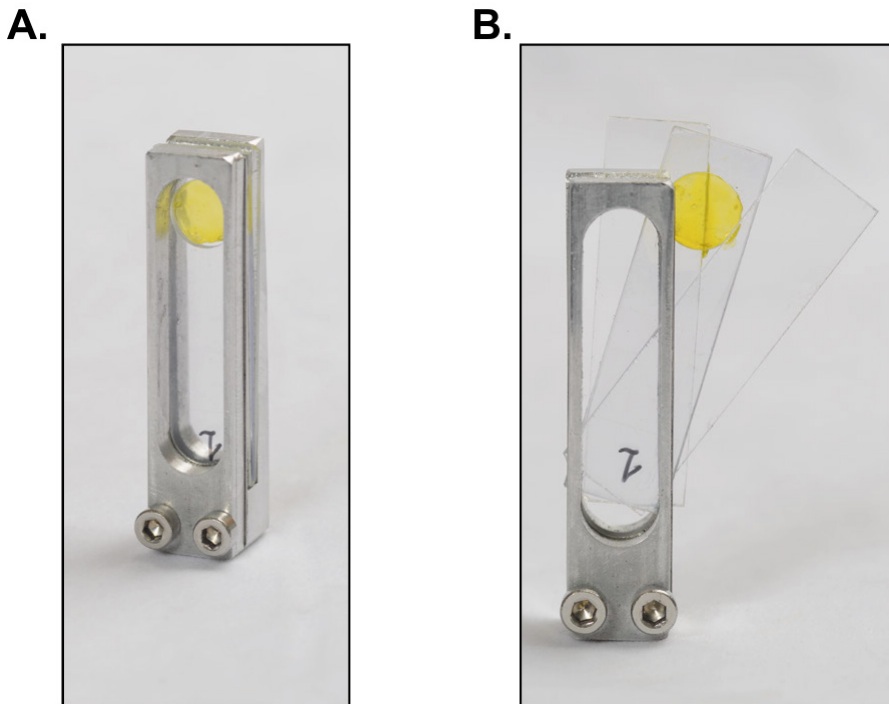


Figure 1. Assembled (A) and disassembled (B) views of the specially designed cuvette for measuring trans-corneal absorption spectra of a corneal button with a corneal button impregnated with RF in the cuvette spacer between two glass holders.

### **In vitro endothelial toxicity measurements**

Immortalized HCECs (HCEC-12; DSMZ, Braunschweig, Germany) were grown in culture medium consisting of 95% Dulbecco's Modified Eagle Medium, supplemented with 5% fetal bovine serum, 1/100 penicillin-streptomycin, and 1/125 amphotericin B in an incubator at 37°C, according previously published protocol.<sup>24,25</sup> Cells were plated at  $2.5 \cdot 10^4$  cells per well in a flat-bottomed transparent 96-well plate. After 24 hours, the culture medium in three wells per plate was replaced with 200  $\mu$ L culture medium containing 0.04%, 0.02%, 0.01%, 0.005%, 0.0025%, or no RF (F6750; Sigma-Aldrich) and kept in the dark for 10 minutes. Consecutively, irradiation was performed from below, accounting for the plate's UVA absorption (measured at 18.6% by spectrophotometry), with environmental temperature and oxygen concentration at 25°C and 20%, respectively. UVA intensity (365 nm) was set to deliver either no UVA or ranging between 0.3 and 1.3 mW/cm<sup>2</sup> at 0.2 mW/cm<sup>2</sup> intervals. After irradiation, the solution in all wells was replaced by fresh culture medium. Twenty-four hours later, the medium was replaced by a 9:1 mixture of culture medium and WST1 viability staining (Sigma-Aldrich) and kept for 1 hour, per manufacturer's protocol. Per plate, three empty wells were filled with the same culture medium and WST1 mixture for baseline determination. Luminescence of each well was measured (Infinite m200pro; Tecan, Mannedorf, Switzerland) and baseline corrected. A total of nine plates (three plates per irradiation group each) were seeded and treated as described earlier, resulting in nine readings per combination of RF concentration and UVA irradiation (three plates x three wells). Cell survival was calculated by dividing each well's baseline corrected luminescence reading by the average luminescence reading of the wells that did not contain any RF and did not receive UVA irradiation. Significance was determined using a linear regression model (IBM SPSS Statistics for Windows, Version 23, IBM Corp., Armonk, NY).

## RESULTS

### Baseline characteristics

Corneal thickness measured before epithelium debridement was  $497 \pm 48 \mu\text{m}$ . On average  $50 \mu\text{m}$  were removed on epithelium debridement.

### Stromal riboflavin distribution

Negligible fluorescence was detected from deepithelialized corneas incubated in vivo for 30 minutes with saline solution (one eye), or with RF without de-epithelialization (two eyes) (Figure 2A and 2B). In contrast, after 10 minutes of impregnation to deepithelialized eyes (two eyes), RF penetrated the corneal stroma entirely. Stromal fluorescence peaked at the anterior cornea and decayed by approximately 50% at a depth of  $\sim 200 \mu\text{m}$  in which it leveled off and remained so until reaching the posterior stroma. After 30 minutes of RF incubation (three eyes), the fluorescence intensity at the anterior cornea decayed only by 20% at  $200 \mu\text{m}$  and remained so until reaching the Descemet membrane (Figure 2C and 2D). Application of the clinically applied RF-D500 resulted in significant changes in the photosensitizer distribution within the cornea, compared with the dextran-free solution (Figure 3A and 3B). The cornea impregnated for 10 minutes (two eyes) presented a gradient decline in RF concentration reaching a minimum at a depth of  $209 \mu\text{m}$ . In contrast, the 30-minute impregnation (four eyes) showed a mild gradient across the entire cornea with a measured minimum at  $366 \mu\text{m}$ .

### Absorption measurements

#### *RF calibration curve*

All spectra displayed a flat absorption from approximately 520 to 600 nm. The background noise level was negligible with  $R^2 = 0.994$ , and a low error for the lowest measured RF concentration ( $0.09 \pm 0.0007 \mu\text{g RF/mL}$ ; Figure 4A and 4B). Using Equation 1, this calibration curve provides value of  $\epsilon_{RF}^{446} = 12,550 \text{ M}^{-1}\text{cm}^{-1}$ , similar to literature value of  $\epsilon_{RF}^{446} = 12,500 \text{ M}^{-1}\text{cm}^{-1}$  for RF.<sup>26</sup>

#### *Anterior chamber humor measurements*

Using equation (1) with  $l = 1 \text{ cm}$  and  $\epsilon_{RF}^{446} = 12,550 \text{ M}^{-1}\text{cm}^{-1}$ , the obtained concentrations of RF in the anterior chamber were found to be  $(1.6 \pm 0.21) \cdot 10^{-4}$  and  $(5.4 \pm 0.59) \cdot 10^{-4}\%$  ( $p < 0.01$ ) for 10- and 30-minutes impregnation, respectively (Figure 4D).

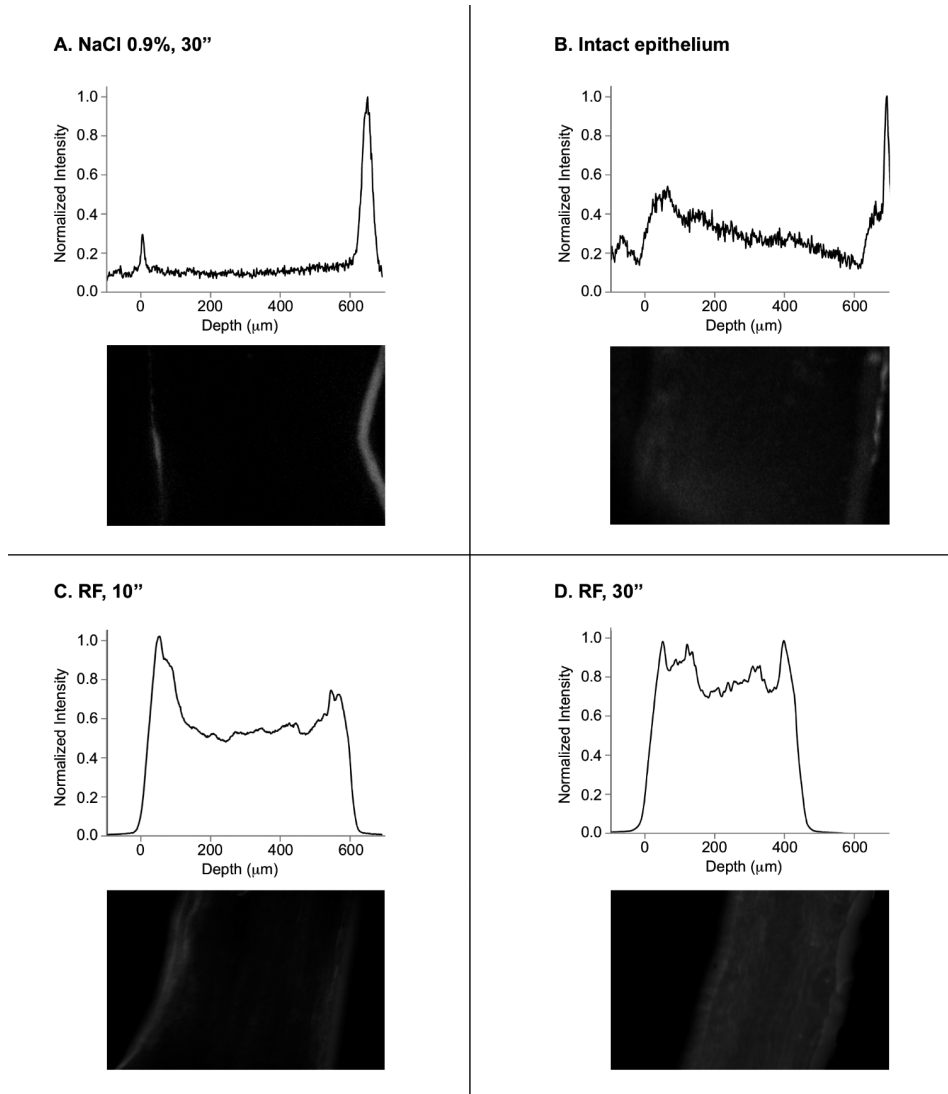
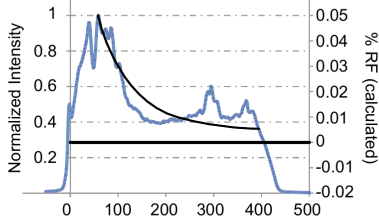
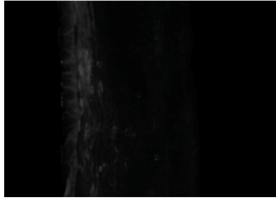
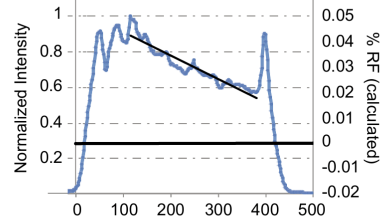


Figure 2. In vivo cross-corneal penetration of RF in saline solution across rabbit corneas. No signal was detected from a de-epithelialized cornea incubated with saline solution for 30 minutes (A). Likewise, no signal was detected from the intact cornea with the epithelium on (B). Rabbit corneas were exposed to RF in saline solution for (C) 10 minutes and (D) 30 minutes. The graphs represent the trans-corneal fluorescence signal as averaged over 50 lines of the fluorescence image.

**A. RF-D500, 10"**

Depth (μm)

**B. RF-D500, 30"**

Depth (μm)

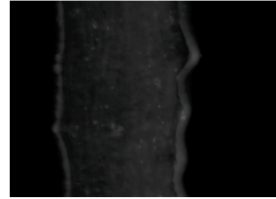


Figure 3. In vivo corneal penetration of RF-D500 after impregnation for (A) 10 and (B) 30 minutes. The normalized intensity graphs depict the distribution of RF-D500 concentration across the corneal sagittal slice. The graph was normalized to give the same thickness (400 μm) in the two panels. The exponential trend line for panel (A) is  $y = 0.045 \cdot e^{-0.11 \cdot X555} + 0.005$ .

### Trans-corneal absorption

Trans-corneal spectra clustered tightly according to the impregnation duration, except for two outliers in the 30-minute group ( $n = 9$ ) that were excluded. The trans-corneal optical absorption at 446 nm ( $A_{446}$ ) measured  $0.398 \pm 0.021$  and  $0.496 \pm 0.033$  for the 10 (five eyes) and 30 (seven eyes) minutes of RF impregnation, respectively (Figure 5A). For nonimpregnated corneas,  $A_{446}$  was  $0.069 \pm 0.005$  (three eyes). After removing this contribution to the light absorption by the corneal stroma, the RF absorption was 0.329 and 0.427 after 10- and 30-minute impregnation, respectively (Figure 5B).

### Stromal riboflavin concentrations

Applied to Equation 1 and multiplied by the molecular weight (456 g/mol), the measured  $A_{446}$  values as mentioned earlier, result in an average stromal concentration of 0.0266% and 0.0345% after 10- and 30-minute RF impregnation, respectively. Thus, already after 10 minutes of RF impregnation, there is 77% of the RF concentration across the stroma relative to 30-minute impregnation. The average RF concentration in the posterior stroma for the 30-minute impregnation ( $\bar{C}_{post\ 30min}$ ) is then 0.019%. After 10-minute RF impregnation, the average posterior stromal concentration ( $\bar{C}_{post\ 10min}$ ) equals 0.0056% (0.019% divided by the ratio found in anterior chamber RF concentrations: 3.4).

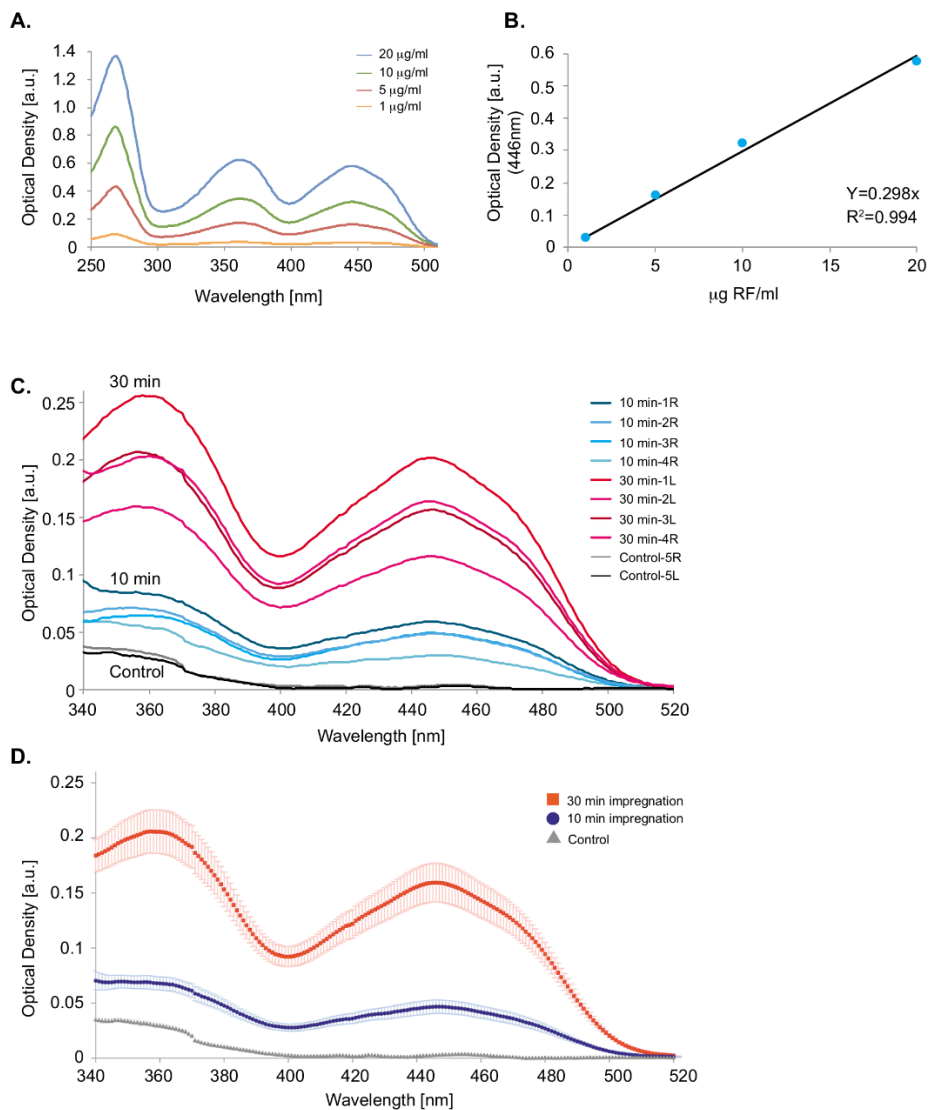


Figure 4. Anterior chamber concentrations of RF following 10 and 30 minutes of RF-D500 impregnation. (A) Different concentrations of RF in solution were used to construct a calibration curve (B) using the spectrum peak at 446 nm. The equation was set to pass at (0,0). (C) Spectra of the anterior chamber humor drawn from rabbits after the de-epithelialized cornea was incubated, under anesthesia, for 10 (right eye, denoted "R") and 30 minutes (left eye, denoted "L") of impregnation with RF-D500. The numbers in the inset legend refer to the rabbit number to enable comparison of the spectra between the two eyes. Eyes of an untreated rabbit served as a control. (D) Averages for the data presented in panel (C). Error bars represent the standard error.

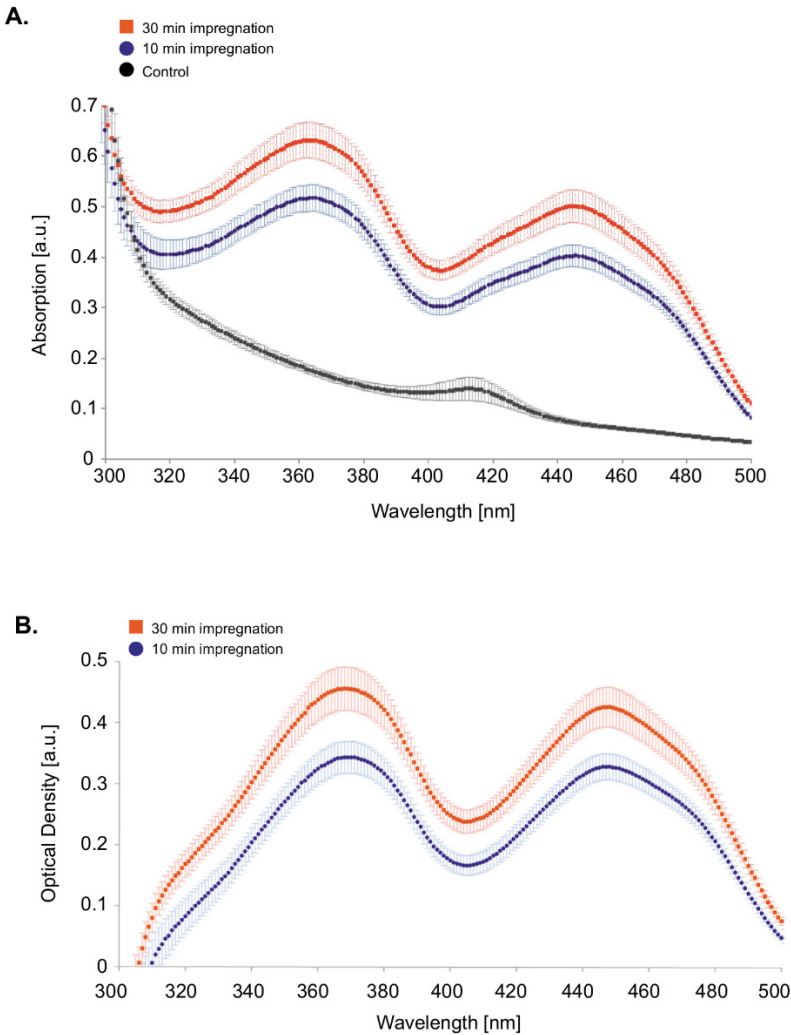


Figure 5. (A) Trans-corneal absorption spectra. Ex vivo de-epithelialized trans-corneal absorption spectrum following 10 (blue) and 30 (red) minutes of RF impregnation and the absorption of the cornea without impregnation (gray). (B) The absorption spectra of the two impregnation durations after deducting the contribution of the native cornea. Averaging was conducted for five and seven eyes for the two spectra, respectively. Error bars represent the standard error.

### Expected light fluency at the endothelium

Considering both the optical density due to RF absorption and the absorption and scattering of the untreated cornea (control, Figure 5A), the absorption at 370 nm is 0.5116 and 0.6255, for the 10- and 30-minute impregnated corneas, respectively. Calculated

transmitted light intensity at 370 nm, by substituting the relevant values in  $T = 10^{-A}$ , was then 30.08% and 23.7%, respectively. Thus, with a fluency of 3 mW/cm<sup>2</sup> at the corneal anterior surface, the endothelium is subjected to 0.9 and 0.7 mW/cm<sup>2</sup>, after 10 and 30 minutes of RF impregnation, respectively.

### In vitro corneal endothelial toxicity measurements

Cell survival of HCECs for a range of RF concentrations and UVA intensities, including the parameters we found after 10 minutes (0.005% RF and 0.9 mW/cm<sup>2</sup> UVA) and 30 minutes (0.02% RF and 0.7 mW/cm<sup>2</sup> UVA) of RF impregnation, are shown in Figure 6 and Supplementary Table S2. We found no significant difference in cell survival between the 10- and 30-minute impregnation protocols ( $p = 0.056$ ). In fact, there appears to be a slightly lower photodynamic toxicity for the shorter impregnation, with a mean cell survival of  $51.0 \pm 3.9\%$  and  $41.3 \pm 5.0\%$ , for the 10- and 30-minute impregnation protocol, respectively. UVA alone, RF alone, and the combination of RF and consecutive UVA irradiation show a highly significant trend toward reduced cell viability (all  $p < 0.001$ ).  $\beta$ -Coefficients for UVA irradiation, RF concentration, and their interaction term are  $-29.3\%$  per mW/cm<sup>2</sup> UVA,  $-605.2\%$  per % RF, and  $-1206.9\%$  per mW/cm<sup>2</sup> UVA \* % RF, respectively.

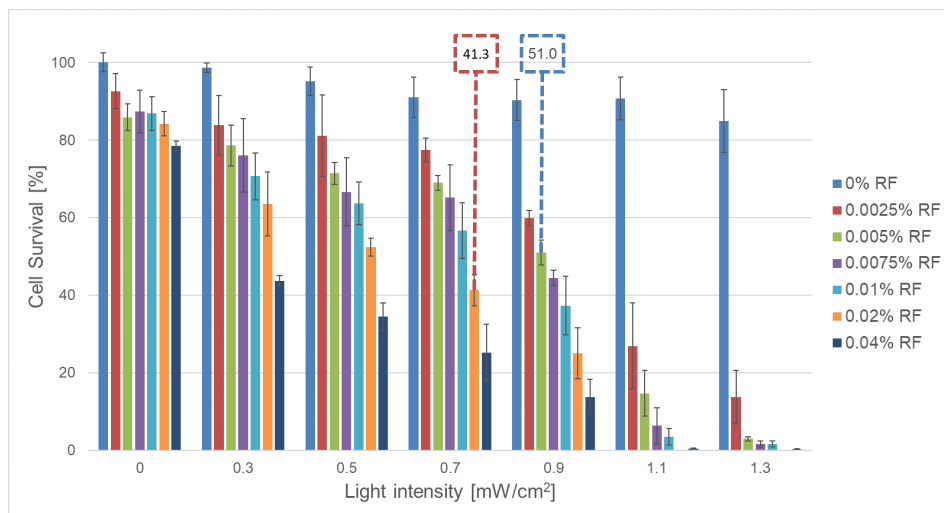


Figure 6. Cell survival of in vitro RF/UVA treated HCEC-12. Bars were normalized to the average luminescence reading of nine wells containing no RF and receiving no UVA irradiation. Error bars represent the standard deviation. Mean endothelial cell survival corresponding to the 10 minutes (blue dashed box) and 30 minutes (red dashed box) are highlighted.



## DISCUSSION

The main goal of CXL is to arrest progression of KC and corneal ectasia with minimal side effects and risk.<sup>3–6,8,27–30</sup> An established benchmark protocol (Dresden) includes RF impregnation of the corneal stroma for 30 minutes and subsequent irradiation with UVA light.<sup>11</sup> The RF impregnation time is guided by the minimal RF concentration to allow for sufficient CXL, and the minimal RF concentration across the cornea needed to sufficiently attenuate the UVA light, minimizing the photodamage to the corneal endothelium.<sup>11,31–33</sup> Following the apparent conflict of the risk/benefit of shorter impregnation times, we explored the time-dependent distribution of RF across the corneal stroma and the corresponding endothelial cell survival. Although RF distribution has been shown before by several authors, to the best of our knowledge, little attention has been paid to the safety implication of reduced RF impregnation times.

On the ground of theoretical and experimental considerations, 30 minutes of impregnation followed by 30 minutes of illumination at 3 mW/cm<sup>2</sup> have been recommended for safe and effective treatment.<sup>11,13,32</sup> Yet, to reduce patient burden and adverse effects, numerous reports demonstrated efficient stiffening without compromising clinical safety following shorter times of RF impregnation (Supplementary Table S1). Not less important, Supplementary Table S1 shows that there is currently no established protocol as to RF impregnation duration. Previous studies show deep stromal RF penetration already occurs after 8 to 10 minutes of impregnation, with a further moderate rise to a plateau after 30 minutes.<sup>31,34,35</sup> Although Baiocchi *et al.* measured a ratio of 75% for the average total RF concentration, Spoerl *et al.* showed that in the range of 0 to 180 µm there is no difference between the RF concentration after 10 and 30 minutes of impregnation.<sup>31,36</sup> However, when looking at the endothelium (360–540 µm), after 10 minutes of impregnation the RF concentration is 30% to 40% of that achieved after 30 minutes of impregnation. The overall distribution demonstrated therein is in agreement with the change of RF fluorescence across the cornea as presented in this study (Figure 3A and 3B). The data from our study, as displayed in Figure 5, shows the 30-minute incubation decreases the transmitted light intensity by merely a factor of ~1.3 compared with the transmitted intensity after 10 minutes (23.7% and 30.8% for the long and short impregnation durations, respectively). Thus, although RF concentration at the endothelial level increases over three-fold after 30 minutes compared with 10 minutes of impregnation, the attenuation of UVA light only decreases by a factor of ~1.3 in the longer 30-minute incubation protocol.

Photodynamic toxicity is usually achieved when the product of a photosensitizing agent concentration by the light energy overcomes a threshold value given by Equation 3:

3.  $PDT_{PS} = [PS] \cdot E_I$  where  $PDT_{PS}$ ,  $[PS]$  and  $E_I$  denote photodynamic therapy, photosensitizer concentration (in percent, defined as g/100mL) and light intensity energy (in Joules), respectively that show initiation of photodynamic damage.

Wollensak *et al.* found out that for endothelial cells in culture a cytotoxic threshold was set at  $PDT_{RF} = 0.024 \cdot 0.63 = 0.0151$  where 0.024% and 0.63 J/cm<sup>2</sup> are the RF concentration and UVA light energy, respectively.<sup>12</sup> Our data demonstrates that the UVA light intensity of 3 mW/cm<sup>2</sup> at the anterior stroma will be attenuated to 0.9 and 0.7 mW/cm<sup>2</sup> at the posterior stroma after 10 and 30 minutes of RF impregnation, respectively. The total delivered energy at the endothelium will thus be 1.62 and 1.26 J/cm<sup>2</sup> for the 10- and 30-minute impregnation protocols, respectively, neglecting the additional attenuation by the RF film, after the standard 30 minutes of UVA irradiation. Applying these numbers and the corresponding RF concentrations at the posterior stroma as found in this study in Equation 3, results in a respective  $PDT_{RF}$  value of 0.00903 and 0.0239. Thus, the probability for photodamage actually increases by over a two-fold and above the 0.0151 threshold determined by Wollensak *et al.*, for the prolonged incubation time, whereas that of the short time stays below.<sup>12</sup>

Current methods to assess corneal stromal RF concentration lack the ability to directly measure concentrations and are subjected to some degree of variability due to factors, such as light attenuation, physiological state of the measured tissue (e.g., hydration, de-epithelialization, and others), or resolution of confocal sectioning. The lack of a gold standard is clear from the variety of methods applied in the literature.<sup>21,37</sup> Our study suffers from similar limitations. First, although corneal hydration was monitored and in vivo pachymetry was performed in physiological state, our cohort of NZW rabbits had thicker pachymetry measurements than what was to be expected.<sup>38</sup> Second, our calculations rely on previously published data on anterior stromal RF concentrations.<sup>20–23</sup> Although these values correspond well, this does allow for variation. Nevertheless, our data are in line with recent reported literature.<sup>39</sup> Notably, our data also agrees with reports in which 30 minutes of RF impregnation cannot bring the corneal absorption to sufficiently attenuate the UVA below the putative threshold of 0.63 J/cm<sup>2</sup> suggested by Wollensak *et al.* for 0.024% RF.<sup>13</sup> Only on considering the precorneal RF film, the attained UVA light intensity is lower than this threshold.<sup>32</sup> Thus, when considering the RF concentration in the posterior stroma for 10- and 30-minute impregnation, the shorter time of incubation appears to be the safer regimen, as shown earlier. The first series of successful CXL treatments applied 5 minutes of impregnation without expressing endothelial damage.<sup>5</sup> Recent practices of reduced

impregnation times (Supplementary Table S1) further substantiate the notion that a long impregnation duration is not required. When applying RF during the CXL, the resulting 70  $\mu\text{m}$  RF film can further attenuate the irradiance in a significant manner.<sup>32</sup> As the film breaks up only after 20 minutes, it will remain during CXL, let alone during accelerated CXL even without more frequent RF drops as commonly applied.<sup>32</sup>

Several studies have investigated the effect of RF/UVA CXL on the corneal endothelium, applying different models and cell lines (Supplementary Table S3). Wollensak *et al.* provided data on CXL endothelial toxicity that led to a threshold corneal thickness of 400  $\mu\text{m}$  to allow for safe CXL.<sup>13</sup> In vitro studies with corneal endothelium derived from different animal species showed toxicity at 100  $\mu\text{M}$  (Cho *et al.*) or 50  $\mu\text{M}$  (Wollensak *et al.*).<sup>12,40</sup> A study by Mooren *et al.* using human donor corneas has, however, demonstrated that HCECs may be more resistant than what is suggested by the earlier mentioned in vitro studies using animal cell lines.<sup>41</sup> Notably, in this ex vivo setup, it is not clear what the final RF concentration is at the endothelium at the time of irradiation. It is unlikely that a difference between the biology of human and animal endothelial cells accounts for the observed difference in toxicity. Most probably, this difference is related to differences in the experimental conditions used.

To our knowledge, our study is the first to use HCECs grown in vitro to assess toxicity. Our results indicate endothelial toxicity is related to RF concentration and applied UVA intensity, both parameters influenced by altering RF impregnation time. Furthermore, we show toxicity of UVA irradiation alone for both intensities applied, which was seen in vitro using porcine corneal endothelial cells only at much higher intensities.<sup>12</sup> Although the in vitro setup and immortalization of the HCECs may not exactly mimic the in vivo situation, it does allow for comparison between treatment protocols with accurate control over applied RF concentrations. Greater oxygen availability in vitro will most likely overestimate the corresponding in vivo endothelial toxicity. However, when comparing RF concentration and UVA intensity as applicable during CXL after 10- or 30-minute RF impregnation, we find a similar toxicity of 50% to 60%, in favor of the 10-minute impregnation protocol. This indicates that lowering RF impregnation time from 30 to 10 minutes does not increase corneal endothelial toxicity and may in fact even be safer.

Our study suggests that 30-minute RF impregnation does not increase the CXL safety compared with 10 minutes of impregnation, as confirmed by our in vitro endothelial toxicity study. Rather, theoretically the increased posterior stromal RF concentration may enhance the risk for photodynamic damage of the endothelium. When combined with other preclinical and clinical data, this supports the current trends of shortening the impregnation time (Supplementary Table S1), thus decreasing associated corneal thinning and drying, and overall treatment duration along with patient discomfort.

## REFERENCES

1. Millodot M, Shneor E, Albou S, Atlani E, Gordon-Shaag A. Prevalence and associated factors of keratoconus in jerusalem: A cross-sectional study. *Ophthalmic Epidemiol.* 2011;18(2):91-97.
2. Kennedy RH, Bourne WM, Dyer JA. A 48-year clinical and epidemiologic study of keratoconus. *Am J Ophthalmol.* 1986;101(3):267-273.
3. Chunyu T, Xiujun P, Zhengjun F, Xia Z, Feihu Z. Corneal collagen cross-linking in keratoconus: A systematic review and meta-analysis. *Sci Rep.* 2014;4(1):5652.
4. Sorkin N, Varssano D. Corneal collagen crosslinking: A systematic review. *Ophthalmologica.* 2014;232(1):10-27.
5. Wollensak G, Spoerl E, Seiler T. Riboflavin/ultraviolet-A-induced collagen crosslinking for the treatment of keratoconus. *Am J Ophthalmol.* 2003;135(5):620-627.
6. Caporossi A, Mazzotta C, Baiocchi S, Caporossi T. Long-term Results of Riboflavin Ultraviolet A Corneal Collagen Cross-linking for Keratoconus in Italy: The Siena Eye Cross Study. *Am J Ophthalmol.* 2010;149(4):585-593.
7. Raiskup F, Theuring A, Pillunat LE, Spoerl E. Corneal collagen crosslinking with riboflavin and ultraviolet-A light in progressive keratoconus: Ten-year results. *J Cataract Refract Surg.* 2015;41(1):41-46.
8. Hafezi F, Kanellopoulos J, Wiltfang R, Seiler T. Corneal collagen crosslinking with riboflavin and ultraviolet A to treat induced keratectasia after laser in situ keratomileusis. *J Cataract Refract Surg.* 2007;33(12):2035-2040.
9. Asri D, Touboul D, Fournié P, et al. Corneal collagen crosslinking in progressive keratoconus: Multicenter results from the French National Reference Center for Keratoconus. *J Cataract Refract Surg.* 2011;37(12):2137-2143.
10. Goldich Y, Marcovich AL, Barkana Y, Avni I, Zadok D. Safety of corneal collagen cross-linking with UV-A and riboflavin in progressive keratoconus. *Cornea.* 2010;29(4):409-411.
11. Spoerl E, Mrochen M, Sliney D, Trokel S, Seiler T. Safety of UVA-riboflavin cross-linking of the cornea. *Cornea.* 2007;26(4):385-389.
12. Wollensak G, Spörl E, Reber F, Pillunat L, Funk R. Corneal endothelial cytotoxicity of riboflavin/UVA treatment in vitro. *Ophthalmic Res.* 2003;35(6):324-328.
13. Wollensak G, Spoerl E, Wilsch M, Seiler T. Endothelial cell damage after riboflavin-ultraviolet-A treatment in the rabbit. *J Cataract Refract Surg.* 2003;29(9):1786-1790.
14. Gokhale NS. Corneal endothelial damage after collagen cross-linking treatment. *Cornea.* 2011;30(12):1495-1498.
15. Bouheraoua N, Jouve L, El Sanharawi M, et al. Optical coherence tomography and confocal microscopy following three different protocols of corneal collagen-crosslinking in keratoconus. *Investig Ophthalmol Vis Sci.* 2014;55(11):7601-7609.
16. Mazzotta C, Traversi C, Caragiuli S, Rechichi M. Pulsed vs continuous light accelerated corneal collagen crosslinking: In vivo qualitative investigation by confocal microscopy and corneal OCT. *Eye.* 2014;28(10):1179-1183.
17. Mita M, Waring IV GO, Tomita M. High-irradiance accelerated collagen crosslinking for the treatment of keratoconus: Six-month results. *J Cataract Refract Surg.* 2014;40(6):1032-1040.
18. O'Bart DPS, Kwong TQ, Patel P, McDonald RJ, O'Bart NA. Long-term follow-up of riboflavin/ultraviolet A (370 nm) corneal collagen cross-linking to halt the progression of keratoconus. *Br J Ophthalmol.* 2013;97(4):433-437.

19. Mazzotta C, Traversi C, Paradiso AL, Latronico ME, Rechichi M. Pulsed Light Accelerated Crosslinking versus Continuous Light Accelerated Crosslinking: One-Year Results. *J Ophthalmol*. 2014;2014:1-6.
20. Cui L, Huxlin KR, Xu L, MacRae S, Knox WH. High-resolution, noninvasive, two-photon fluorescence measurement of molecular concentrations in corneal tissue. *Investig Ophthalmol Vis Sci*. 2011;52(5):2556-2564.
21. Seiler TG, Ehmke T, Fischinger I, et al. Two-photon fluorescence microscopy for determination of the riboflavin concentration in the anterior corneal stroma when using the dresden protocol. *Investig Ophthalmol Vis Sci*. 2015;56(11):6740-6746.
22. Gore DM, Margineanu A, French P, O'Bart D, Dunsby C, Allan BD. Two-photon fluorescence microscopy of corneal riboflavin absorption. *Investig Ophthalmol Vis Sci*. 2014;55(4):2476-2481.
23. Ehmke T, Seiler TG, Fischinger I, Ripken T, Heisterkamp A, Frueh BE. Comparison of corneal riboflavin gradients using dextran and HPMC solutions. *J Refract Surg*. 2016;32(12):798-802.
24. Bednarz J, Teifel M, Friedl P, Engelmann K. Immortalization of human corneal endothelial cells using electroporation protocol optimized for human corneal endothelial and human retinal pigment epithelial cells. *Acta Ophthalmol Scand*. 2000;78(2):130-136.
25. Hesse M, Kuerten D, Walter P, Plange N, Johnen S, Fuest M. The effect of air, SF6 and C3F8 on immortalized human corneal endothelial cells. *Acta Ophthalmol*. 2017;95(4):e284-e290.
26. Otto MK, Jayaram M, Hamilton RM, Delbruck M. Replacement of riboflavin by an analogue in the blue-light photoreceptor of *Phycomyces*. *Proc Natl Acad Sci U S A*. 1981;78(1 II):266-269.
27. Meek KM, Hayes S. Corneal cross-linking - a review. *Ophthalmic Physiol Opt*. 2013;33(2):78-93.
28. Caporossi A, Mazzotta C, Paradiso AL, Baiocchi S, Marigliani D, Caporossi T. Transepithelial corneal collagen crosslinking for progressive keratoconus: 24-month clinical results. *J Cataract Refract Surg*. 2013;39(8):1157-1163.
29. Raiskup-Wolf F, Hoyer A, Spoerl E, Pillunat LE. Collagen crosslinking with riboflavin and ultraviolet-A light in keratoconus: Long-term results. *J Cataract Refract Surg*. 2008;34(5):796-801.
30. Shalchi Z, Wang X, Nanavaty MA. Safety and efficacy of epithelium removal and transepithelial corneal collagen crosslinking for keratoconus. *Eye*. 2015;29(1):15-29.
31. Spoerl E, Raiskup F, Kampik D, Geerling G. Correlation between UV absorption and riboflavin concentration in different depths of the cornea in CXL. *Curr Eye Res*. 2010;35(11):1040-1041.
32. Wollensak G, Aurich H, Wirbelauer C, Sel S. Significance of the riboflavin film in corneal collagen crosslinking. *J Cataract Refract Surg*. 2010;36(1):114-120.
33. Lombardo M, Micali N, Villari V, et al. Ultraviolet A: Visible spectral absorbance of the human cornea after transepithelial soaking with dextran-enriched and dextran-free riboflavin 0.1% ophthalmic solutions. *J Cataract Refract Surg*. 2015;41(10):2283-2290.
34. Kampik D, Ralla B, Keller S, Hirschberg M, Friedl P, Geerling G. Influence of corneal collagen crosslinking with riboflavin and ultraviolet-a irradiation on excimer laser surgery. *Investig Ophthalmol Vis Sci*. 2010;51(8):3929-3934.
35. Wang M, Zhang F, Zhao X, Song Y, Zhang M. Riboflavin Concentration Analysis in Rabbit Corneas Before and After Corneal Collagen Cross-Linking Using Confocal Laser Scanning Microscopy. *Asia-Pacific J Ophthalmol*. 2014;3(6):388-394.
36. Baiocchi S, Mazzotta C, Cerretani D, Caporossi T, Caporossi A. Corneal crosslinking: Riboflavin concentration in corneal stroma exposed with and without epithelium. *J Cataract Refract Surg*. 2009;35(5):893-899.

37. Lombardo M, Lombardo G. Noninvasive real-time assessment of riboflavin consumption in standard and accelerated corneal crosslinking. *J Cataract Refract Surg*. 2019;45(1):80-86.
38. Riau AK, Tan NYS, Angunawela RI, Htoon HM, Chaurasia SS, Mehta JS. Reproducibility and age-related changes of ocular parametric measurements in rabbits. *BMC Vet Res*. 2012;8(1):138.
39. Seiler TG, Batista A, Frueh BE, Koenig K. Riboflavin concentrations at the endothelium during corneal cross-linking in humans. *Investig Ophthalmol Vis Sci*. 2019;60(6):2140-2145.
40. Cho KS, Lee EH, Choi JS, Joo CK. Reactive oxygen species-induced apoptosis and necrosis in bovine corneal endothelial cells. *Investig Ophthalmol Vis Sci*. 1999;40(5):911-919.
41. Mooren P, Gobin L, Bostan N, et al. Evaluation of UVA cytotoxicity for human endothelium in an ex vivo corneal crosslinking experimental setting. *J Refract Surg*. 2016;32(1):41-46

## SUPPLEMENTARY MATERIAL

Supplemental Table S1. Reported cross-linking (CXL) protocols demonstrating different times of RF incubation, ultra-violet A (UVA) intensity and duration and very few side-effects.

Year	Impregnation time (min)	UVA intensity (mW/cm <sup>2</sup> )	Irradiation duration (min)	Reported side-effects	References
2003	5'	3	30	None	Wollensak <i>et al</i> <sup>1</sup>
2006	20'	3	30	None	Seiler <i>et al</i> <sup>2</sup>
2007	30'	3	30	None	Spoerl <i>et al</i> <sup>3</sup>
2008	20'	3	30	None	Raiskup-Wolf <i>et al</i> <sup>4</sup>
2010	15'	3	30	9.8% transient haze disappearing progressively after topical preservative-free steroid therapy	Caprossi <i>et al</i> <sup>5</sup>
2011	20'	3	30	7% complications: 3.5% of eyes – loss of > 2 Snellen lines of CDVA. 1.4% haze (at 3 months), 0.7% corneal burn (1 month), 0.7% corneal edema (1 month), 3.5% transient haze, 0.7% central opacity (1 month)	Asri <i>et al</i> <sup>6</sup>
2013	5-10'	3	30	None	O'Brart <i>et al</i> <sup>7</sup>
2014	30'	9	10	12.5% transient subepithelial haze in early postoperative period	Elbaz <i>et al</i> <sup>8</sup>
2014	30'	9	10	Mild haze in majority of patients that was subsided by eight weeks postoperation	Shetty <i>et al</i> <sup>9</sup>
2014	20 <sup>†</sup>	9	10	None	Jain <i>et al</i> <sup>10</sup>
2014	2 <sup>†</sup>	30	4	None	Pahuja <i>et al</i>
2014	15 <sup>†</sup>	30	3	None	Tomita <i>et al</i> <sup>11</sup>
2014	10'	30	3	None	Bouheraoua <i>et al</i> <sup>12</sup>
2014	10 <sup>†</sup>	30	3	5% lost one line of corrected distance visual acuity. Transient haze and edema detected by confocal microscopy	Mita <i>et al</i> <sup>13</sup>
2014	10 <sup>†</sup>	30	8 <sup>d</sup>	None	Mazzotta <i>et al</i> <sup>14,15</sup>
2014	10 <sup>†</sup>	30	4	None	Mazzotta <i>et al</i> <sup>14,15</sup>
2015	30'	3	30	15.8% transient haze	Chow <i>et al</i> <sup>16</sup>

Supplemental Table S1. Continued.

Year	Impregnation time (min)	UVA intensity (mW/cm <sup>2</sup> )	Irradiation duration (min)	Reported side-effects	References
2015	5'	18	5	15.8% transient haze	Chow <i>et al</i> <sup>16</sup>
2015	30'	3	30	ECD reduction similar to accelerated protocol	Hashemi <i>et al</i> <sup>17</sup>
2015	30'	18	5	ECD reduction similar to regular protocol	Hashemi <i>et al</i> <sup>17</sup>
2016	20-30 <sup>§</sup>	3	30	None	Cummings <i>et al</i> <sup>18</sup>
2016	20-30 <sup>§</sup>	9	10	None	Cummings <i>et al</i> <sup>18</sup>
2016	30'	3	30	None	Kymionis <i>et al</i> <sup>19</sup>
2016	30'	18	7	None	Kymionis <i>et al</i> <sup>19</sup>

Riboflavin (RF) with dextran T500 (D500), <sup>1</sup>RF with hydroxypropyl methycellulose (HPMC), <sup>4</sup>RF only (dextran free), <sup>§</sup>RF with or without dextran, depending on corneal thickness. ECD = endothelial cell density.



Supplemental Table S2. Studies experimentally investigating corneal endothelial toxicity in RF/UVA CXL.

Year	Model	Species	Parameters evaluated	Results	References
1999	In vitro	Bovine	Range of RF concentrations	Toxicity at RF concentrations of 50 $\mu$ M or more.	Cho <i>et al</i> <sup>20</sup>
2003	In vitro	Porcine	Range of UVA intensities	Toxicity at UVA intensity of 0.35 mW/cm <sup>2</sup> with RF concentrations of 100 $\mu$ M	Wollensak <i>et al</i> <sup>21</sup>
2003	In vivo	Lapine	Range of UVA intensities	Toxicity at UVA intensity of 0.36 mW/cm <sup>2</sup> or higher	Wollensak <i>et al</i> <sup>22</sup>
2009	Ex vivo	Human	UVA and RF according to Dresden protocol <sup>a</sup>	Histologically normal appearing endothelium	Dhaliwal <i>et al</i> <sup>23</sup>
2012	Ex vivo	Porcine	UVA and RF according to Dresden protocol <sup>a</sup>	Endothelial cell damage of 10.35 $\pm$ 1.7%	Avila <i>et al</i> <sup>24</sup>
2015	Ex vivo	Human	UVA and RF according to Dresden protocol <sup>a</sup> , and iontophoresis assisted or accelerated CXL	Histologically normal appearing endothelium after CXL according to Dresden protocol <sup>a</sup>	Menucci <i>et al</i> <sup>25</sup>
2016	Ex vivo	Human	UVA applied as accelerated protocol	No toxicity seen	Mooren <i>et al</i> <sup>26</sup>

<sup>a</sup>Topically applied 0.1% RF for 30 minutes followed by UVA irradiation at 3 mW/cm<sup>2</sup> for 30 minutes<sup>3</sup>

Supplementary Table S3. Cell survival of Human corneal endothelial cells, after RF/UVA CXL at different irradiances and concentrations.

UVA intensity (mW/cm <sup>2</sup> )	RF concentration (%)	Cell survival (%; mean $\pm$ SD)
0.0	0.0000	100.0 $\pm$ 3.0
	0.0025	92.6 $\pm$ 5.5
	0.0050	85.9 $\pm$ 4.2
	0.0075	87.4 $\pm$ 6.8
	0.0100	86.9 $\pm$ 5.3
	0.0200	84.2 $\pm$ 3.9
	0.0400	78.5 $\pm$ 1.5
0.3	0.0000	98.7 $\pm$ 1.5
	0.0025	83.9 $\pm$ 9.3
	0.0050	78.6 $\pm$ 6.5
	0.0075	76.0 $\pm$ 11.6
	0.0100	70.6 $\pm$ 7.5
	0.0200	63.5 $\pm$ 10.2
	0.0400	43.7 $\pm$ 1.6
0.5	0.0000	95.2 $\pm$ 4.5
	0.0025	81.1 $\pm$ 13.0
	0.0050	71.4 $\pm$ 3.5
	0.0075	66.7 $\pm$ 12.4
	0.0100	63.7 $\pm$ 6.7
	0.0200	52.4 $\pm$ 2.9
	0.0400	34.5 $\pm$ 4.3
0.7	0.0000	91.1 $\pm$ 6.4
	0.0025	77.5 $\pm$ 3.8
	0.0050	69.0 $\pm$ 2.3
	0.0075	65.2 $\pm$ 10.4
	0.0100	56.7 $\pm$ 8.8
	0.0200	41.3 $\pm$ 5.0
	0.0400	25.2 $\pm$ 8.9

Supplementary Table S3. Continued.

UVA intensity (mW/cm <sup>2</sup> )	RF concentration (%)	Cell survival (%; mean ± SD)
0.9	0.0000	90.3 ± 6.5
	0.0025	59.9 ± 2.4
	0.0050	51.0 ± 3.9
	0.0075	44.5 ± 2.5
	0.0100	37.3 ± 9.3
	0.0200	25.0 ± 8.1
	0.0400	13.7 ± 5.5
1.1	0.0000	90.8 ± 6.8
	0.0025	26.9 ± 13.6
	0.0050	14.6 ± 7.2
	0.0075	6.3 ± 5.7
	0.0100	3.5 ± 2.6
	0.0200	0.9 ± 1.3
	0.0400	0.3 ± 0.3
1.3	0.0000	84.9 ± 9.9
	0.0025	13.7 ± 8.4
	0.0050	2.9 ± 0.6
	0.0075	1.6 ± 1.0
	0.0100	1.6 ± 0.9
	0.0200	0.4 ± 0.6
	0.0400	0.2 ± 0.3

In vitro endothelial cell viability (mean ± standard deviation, in %) after RF/UVA CXL, at different UVA intensities and RF concentrations.

## REFERENCES SUPPLEMENTARY MATERIAL

1. Wollensak G, Spoerl E, Seiler T. Riboflavin/ultraviolet-A-induced collagen crosslinking for the treatment of keratoconus. *Am J Ophthalmol*. 2003;135(5):620-627.
2. Seiler T, Hafezi F. Corneal cross-linking-induced stromal demarcation line. *Cornea*. 2006;25(9):1057-1059.
3. Spoerl E, Mrochen M, Sliney D, Trokel S, Seiler T. Safety of UVA-riboflavin cross-linking of the cornea. *Cornea*. 2007;26(4):385-389.
4. Raiskup-Wolf F, Hoyer A, Spoerl E, Pillunat LE. Collagen crosslinking with riboflavin and ultraviolet-A light in keratoconus: Long-term results. *J Cataract Refract Surg*. 2008;34(5):796-801.
5. Caporossi A, Mazzotta C, Baiocchi S, Caporossi T. Long-term Results of Riboflavin Ultraviolet A Corneal Collagen Cross-linking for Keratoconus in Italy: The Siena Eye Cross Study. *Am J Ophthalmol*. 2010;149(4):585-593.
6. Asri D, Touboul D, Fournié P, et al. Corneal collagen crosslinking in progressive keratoconus: Multicenter results from the French National Reference Center for Keratoconus. *J Cataract Refract Surg*. 2011;37(12):2137-2143.
7. O'Bart DPS, Kwong TQ, Patel P, McDonald RJ, O'Bart NA. Long-term follow-up of riboflavin/ultraviolet A (370 nm) corneal collagen cross-linking to halt the progression of keratoconus. *Br J Ophthalmol*. 2013;97(4):433-437.
8. Elbaz U, Shen C, Lichtinger A, et al. Accelerated (9-mW/cm<sup>2</sup>) corneal collagen crosslinking for keratoconus - A 1-year follow-up. *Cornea*. 2014;33(8):763-773.
9. Shetty R, Nagaraja H, Jayadev C, Pahuja NK, Kurian Kummelil M, Nuijts RMMA. Accelerated Corneal Collagen Cross-Linking in Pediatric Patients: Two-Year Follow-Up Results. *Biomed Res Int*. 2014;2014:894095.
10. Jain V, Gazali Z, Bidayi R. Isotonic riboflavin and HPMC with accelerated cross-linking protocol. *Cornea*. 2014;33(9):910-913.
11. Tomita M, Mita M, Huseynova T. Accelerated versus conventional corneal collagen crosslinking. *J Cataract Refract Surg*. 2014;40(6):1013-1020.
12. Bouheraoua N, Jouve L, El Sanharawi M, et al. Optical coherence tomography and confocal microscopy following three different protocols of corneal collagen-crosslinking in keratoconus. *Investig Ophthalmol Vis Sci*. 2014;55(11):7601-7609.
13. Mita M, Waring IV GO, Tomita M. High-irradiance accelerated collagen crosslinking for the treatment of keratoconus: Six-month results. *J Cataract Refract Surg*. 2014;40(6):1032-1040.
14. Mazzotta C, Traversi C, Caragiuli S, Rechichi M. Pulsed vs continuous light accelerated corneal collagen crosslinking: In vivo qualitative investigation by confocal microscopy and corneal OCT. *Eye*. 2014;28(10):1179-1183.
15. Mazzotta C, Traversi C, Paradiso AL, Latronico ME, Rechichi M. Pulsed Light Accelerated Crosslinking versus Continuous Light Accelerated Crosslinking: One-Year Results. *J Ophthalmol*. 2014;2014:1-6.
16. Chow VWS, Chan TCY, Yu M, Wong VWY, Jhanji V. One-year outcomes of conventional and accelerated collagen crosslinking in progressive keratoconus. *Sci Rep*. 2015;5(August):14425.
17. Hashemi H, MirafTAB M, Seyedian MA, et al. Long-term Results of an Accelerated Corneal Cross-linking Protocol (18 mW/cm<sup>2</sup>) for the Treatment of Progressive Keratoconus. *Am J Ophthalmol*. 2015;160(6):1164-1170.e1.

18. Cummings AB, McQuaid R, Naughton S, Brennan E, Mrochen M. Optimizing corneal cross-linking in the treatment of keratoconus: A comparison of outcomes after standard-and high-intensity protocols. *Cornea*. 2016;35(6):814-822.
19. Kymionis GD, Tsoulnaras KI, Liakopoulos DA, Skatharoudi CA, Grentzelos MA, Tsakalis NG. Corneal stromal demarcation line depth following standard and a modified high intensity corneal cross-linking protocol. *J Refract Surg*. 2016;32(4):218-222.
20. Cho KS, Lee EH, Choi JS, Joo CK. Reactive oxygen species-induced apoptosis and necrosis in bovine corneal endothelial cells. *Investig Ophthalmol Vis Sci*. 1999;40(5):911-919.
21. Wollensak G, Spoerl E, Wilsch M, Seiler T. Endothelial cell damage after riboflavin-ultraviolet-A treatment in the rabbit. *J Cataract Refract Surg*. 2003;29(9):1786-1790.
22. Wollensak G, Spörl E, Reber F, Pillunat L, Funk R. Corneal endothelial cytotoxicity of riboflavin/UVA treatment in vitro. *Ophthalmic Res*. 2003;35(6):324-328.
23. Dhaliwal JS, Kaufman SC. Corneal collagen cross-linking: A confocal, electron, and light microscopy study of eye bank corneas. *Cornea*. 2009;28(1):62-67.
24. Avila MY, Gerena VA, Navia JL. Corneal crosslinking with genipin, comparison with UV-riboflavin in ex-vivo model. *Mol Vis*. 2012;18(April):1068-1073.
25. Mencucci R, Ambrosini S, Paladini I, et al. Early effects of corneal collagen cross-linking by iontophoresis in ex vivo human corneas. *Graefes Arch Clin Exp Ophthalmol*. 2015;253(2):277-286.
26. Mooren P, Gobin L, Bostan N, et al. Evaluation of UVA cytotoxicity for human endothelium in an ex vivo corneal crosslinking experimental setting. *J Refract Surg*. 2016;32(1):41-46.



# Chapter 4

## **Excimer laser-assisted corneal epithelial pattern ablation for corneal cross-linking**

Jurriaan Brekelmans, Mor M. Dickman, Shwetabh Verma, Samuel Arba-Mosquera,  
Ruth Goldschmidt, Alexandra Goz, Alexander Brandis, Tos T.J.M. Berendschot,  
Isabelle E.Y. Saelens, Arie L. Marcovich, Avigdor Scherz, Rudy M.M.A. Nuijts

*Acta Ophthalmol.* 2022 Jun;100(4):422-430



# ABSTRACT

Purpose: To determine corneal cross-linking (CXL) efficacy and chromophore penetration after excimer laser-assisted patterned de-epithelialization.

Methods: Two-hundred-twenty porcine eyes were de-epithelialized ex vivo, either fully (mechanical;  $n = 88$ ) or patterned (excimer laser;  $n = 132$ ). Consecutively, corneas were impregnated with hypo- or hyperosmolar riboflavin (RF;  $n = 20$ , RF-D;  $n = 40$ , respectively) or water-soluble taurine (WST11;  $n = 40$ , and WST-D;  $n = 40$ , respectively), or kept unimpregnated ( $n = 80$ ). Sixty corneas were subsequently irradiated, inducing CXL, with paired contralateral eyes serving as controls. Outcome measurements included strip extensimetry to assess CXL efficacy, and spectrophotometry and fluorescence microscopy to determine stromal chromophore penetration.

Results: All tested chromophores induced significant CXL ( $p < 0.001$ ), ranging from 7.6% to 14.6%, with similar stiffening for all formulations ( $p = 0.60$ ) and both de-epithelialization methods ( $p = 0.56$ ). Light transmittance was significantly lower ( $p < 0.001$ ) after full compared with patterned de-epithelialization. Stromal chromophore penetration was comparable between fully and patterned de-epithelialized samples, with full penetration in RF and RF-D samples and penetration depths measuring  $591.7 \pm 42.8 \mu\text{m}$  and  $592.9 \pm 63.5 \mu\text{m}$  for WST11 ( $p = 0.963$ ) and  $504.2 \pm 43.2 \mu\text{m}$  and  $488.8 \pm 93.1 \mu\text{m}$  for WST-D ( $p = 0.669$ ), respectively.

Conclusions: Excimer laser-assisted patterned de-epithelialization allows for effective CXL. Stromal chromophore concentration is, however, reduced, which may have safety implications given the need for sufficient ultra-violet A (UVA) attenuation in RF/UVA CXL. The different safety profile of near-infrared (NIR) may allow safe WST11/NIR CXL even with reduced stromal chromophore concentration values. In vivo studies are needed to evaluate the benefits and further assess safety of excimer laser-assisted patterned de-epithelialization for corneal CXL.



## INTRODUCTION

Corneal collagen cross-linking (CXL) is applied to arrest thinning and destabilization associated with keratoconus (KC) progression. CXL using riboflavin (RF) and ultra-violet A (UVA) light is currently the only clinically approved treatment modality. Although good clinical results showing stabilization of disease for up to 10 years, the procedure has several downsides.<sup>1-3</sup> One major disadvantage is related to epithelial debridement, which is associated with discomfort and postoperative complications, such as haze formation, delayed healing and infection.<sup>4-6</sup> Various approaches have been suggested to overcome the need for full epithelial debridement, including epithelium-on CXL, chemical modification of RF and mechanical removal of only part of the epithelium.<sup>7-11</sup> Thus far, most reports show reduced RF penetration and reduced efficacy for epithelium-on procedures.<sup>12-14</sup>

Besides RF/UVA CXL, several other light-activated chromophores have been investigated, providing corneal stiffening with different drug and treatment characteristics.<sup>15-17</sup> One alternative is water-soluble taurine (WST11).<sup>15</sup> In contrast to RF, which uses potentially toxic UVA light, WST11 can be activated by near-infrared (NIR) light at 755 nm, which is safe to the eye at intensities beyond what is needed for effective CXL.<sup>18</sup> Due to their different characteristics, both chromophores rely on different stromal diffusion patterns to assure safety. Alternative CXL modalities offer a perspective to patients non-responsive to or unsuitable for RF/UVA CXL, such as patients with thin corneas.

In this study, we use a clinically approved excimer laser platform to selectively ablate the corneal epithelium in a patterned fashion, creating 350  $\mu\text{m}$  wide and 375  $\mu\text{m}$  spaced epithelial channels to allow for chromophore diffusion while leaving up to 60% of the epithelium in the treated area in situ. We hypothesize this may promote faster epithelial healing, reduce patient discomfort and increase treatment safety. In an ex vivo porcine model, we evaluated stromal penetration, light attenuation and biomechanical stiffening of the two chromophores WST11 and RF, in hypo- and hyperosmotic formulations, after full mechanical or patterned excimer laser-assisted de-epithelialization.

## MATERIALS AND METHODS

### Sample preparation

#### *Ex vivo porcine model*

We included 220 paired porcine eyes, freshly obtained from a local abattoir and macroscopically inspected for damage, haze, oedema or surface irregularities. Porcine corneas provide a well-established ex vivo animal model for preclinical research on corneal procedures, with reported central corneal thickness (CCT) ex vivo of approximately 920  $\mu\text{m}$ , shown to remain stable for up to 24 hours after enucleation.<sup>19–21</sup>

#### *Manual and excimer laser-assisted de-epithelialization*

All 220 corneas were de-epithelialized, either manually ( $n = 88$ ) or excimer laser-assisted ( $n = 132$ ). Full manual de-epithelialization of the central epithelium with a 9 mm diameter was performed using a blunt hockey knife, following the Dresden protocol similar to clinical practice without the application of alcohol.<sup>22</sup> Selective patterned de-epithelialization was performed over the central 9 mm using the SCHWIND Amaris excimer laser (SCHWIND Eye-Tech-Solutions, Kleinostheim, Germany). Epithelial channels with a radius of 350  $\mu\text{m}$ , the minimal radius possible for this excimer laser apparatus, were created in a hexagonal pattern with equal distance between channels (Figure 1 and 2, Supplementary Figure S1). Pilot studies showed chromophore diffusion became heterogenous if the spacing between channels was greater than 375  $\mu\text{m}$ . Thus, the distance between channels was set at 375  $\mu\text{m}$ , resulting in approximately 40% total surface ablation of the treated area (Supplementary Equation S1). Ablation depth was determined for each cornea individually and set to penetrate the full epithelial thickness, measured by ocular coherence tomography (OCT), as described below.

#### *Chromophore preparation*

Four different formulations of photosensitizer were prepared: RF, RF with 20% dextran T500 (RF-D), WST11 and WST11 with 20% dextran T500 (WST-D). RF solutions (Sigma-Aldrich, St. Louis, Missouri, USA) were prepared at a concentration of 0.1% WST11 (Steba Laboratories Ltd., Rehovot, Israel) solutions at 2.5%. All solutions were prepared in saline and corrected to a pH between 7.2 and 7.3.

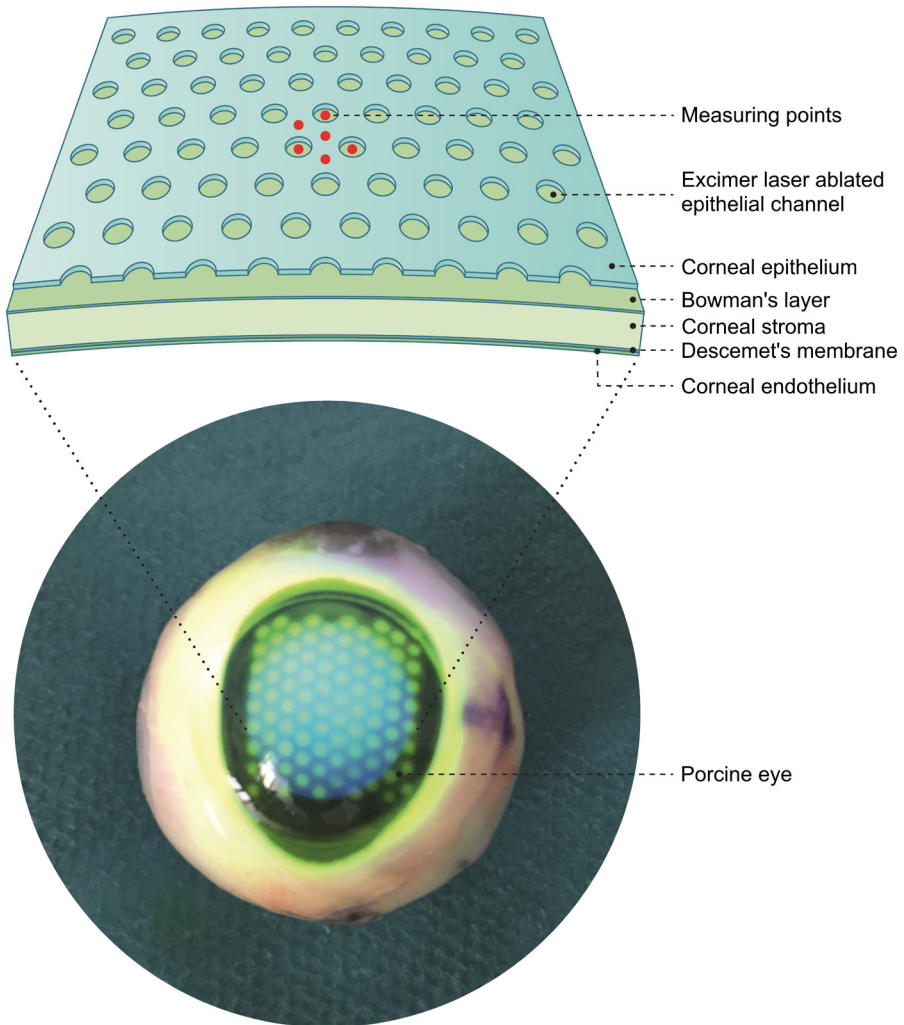


Figure 1. Porcine cornea, after excimer laser-patterned de-epithelialization and riboflavin (RF) impregnation (bottom), and schematic representation of hexagonal pattern of ablated epithelium (top). Radius of the channels measured  $350\text{ }\mu\text{m}$ , with a distance between the channels of  $375\text{ }\mu\text{m}$ . This corresponds to approximately 60% of the epithelium remaining (following Supplementary Equation S1). Fluorescence was imaged confocally in three, centered at an epithelial channel or at unablated epithelium (red marks).

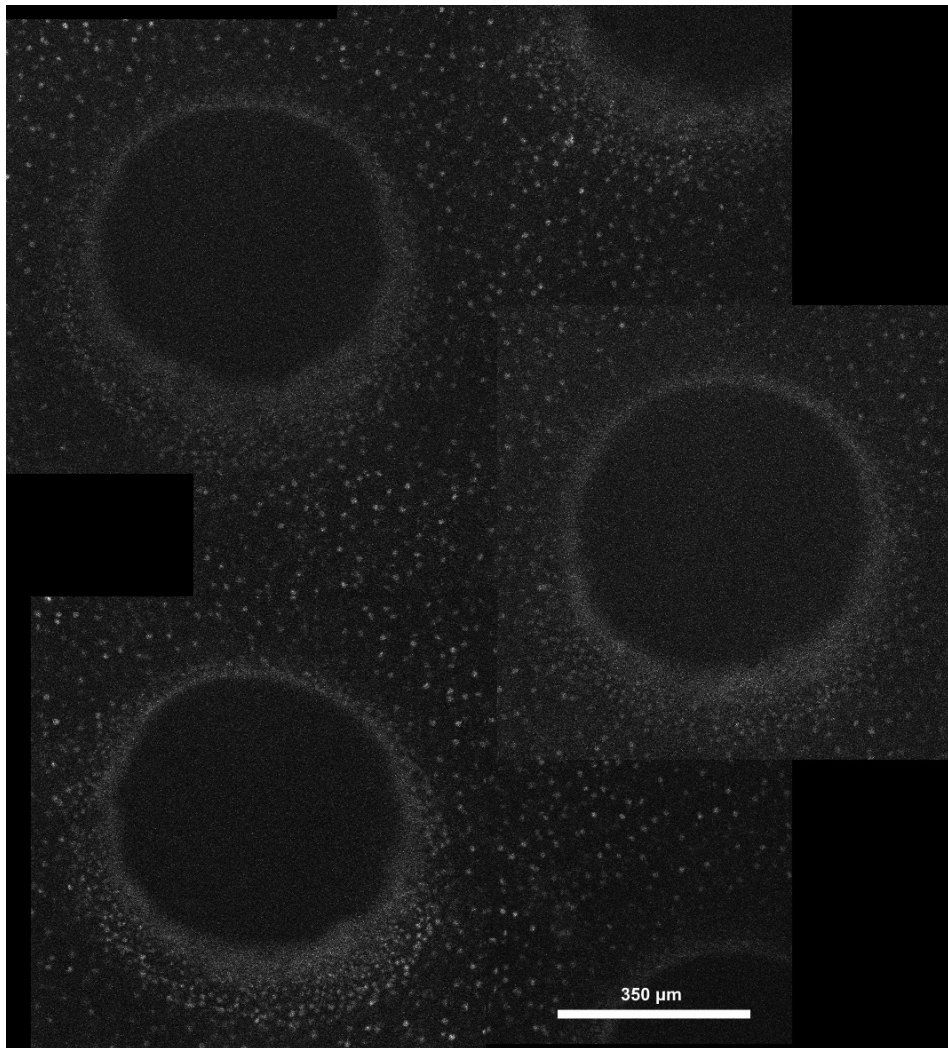


Figure 2. Stitched image derived by fluorescence microscopy showing several epithelial channels, and intermediate remaining epithelium, with cell nuclei stained by propidium iodide.

### Sample allocation

Samples were divided into two groups: 100 eyes were used to assess safety (i.e., stromal chromophore diffusion; Figure 3A) and 120 eyes were used to determine CXL efficacy (Figure 3B). In the first group (i.e., safety group), allocation of paired eyes to each chromophore was done in a layered design (Supplementary Table S1). In the second group (i.e., efficacy group), a paired setup was used with one eye of each pair receiving full CXL treatment, with the contralateral eye serving as control (de-epithelialized only).

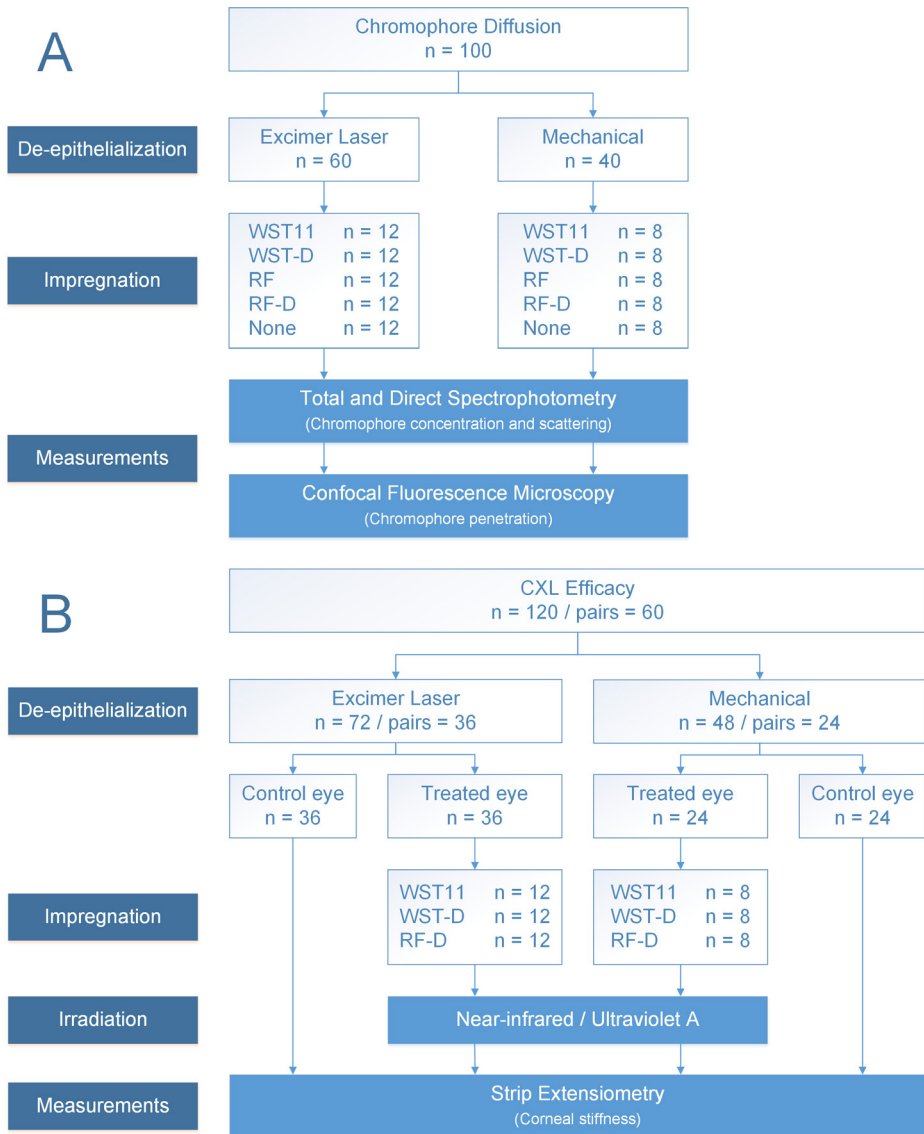


Figure 3. Study flowchart of cornea allocated to (A) assess chromophore diffusion and penetration and (B) corneal cross-linking (CXL) efficacy.

### Sample treatment

After de-epithelialization, a self-manufactured plastic well, 12 mm in diameter with round edges, was placed on top of corneas allocated to receive chromophore impregnation. The well was filled with 1 mL of the respective photosensitizer, providing a constant supply of chromophore, alike the chromophore film existing during frequent topical

chromophore application.<sup>23</sup> Control corneas were left unimpregnated. After 30 or 20 minutes of impregnation, for RF and RF-D, and WST and WST-D, respectively, the remaining photosensitizer was removed and the cornea was briefly rinsed with 2 mL of distilled water to remove excess photosensitizer.

In addition to the above, in the CXL efficacy group, 60 eyes of 60 pairs received additional irradiation treatment to achieve full CXL treatment (Figure 3B). CXL efficacy was assessed for RF-D, WST11 and WST-D-based CXL. After either RF-D or WST11/WST-D impregnation, corneas were irradiated for 30 minutes by either UVA light of 365 nm at 3 mW/cm<sup>2</sup> (SCHWIND CXL-365 vario system; SCHWIND Eye-Tech- Solutions, Kleinostheim, Germany) or NIR light of 753 nm at 10 mW/cm<sup>2</sup> (Cerelas PDT 753, CeramOptec GmbH, Bonn, Germany), respectively. During irradiation, every 5 minutes, a drop of distilled water was placed on the cornea to prevent dehydration.

## Sample evaluation

### *Central corneal and epithelial thickness measurements*

Corneas were imaged with a CASIA2 OCT (Tomey, Nagoya, Japan), prior to (patterned) de-epithelialization, directly after de-epithelialization and, when applicable, after photosensitizer impregnation and after irradiation (Figure 4). Central epithelial thickness (CET) was determined for each cornea individually. Following mechanical de-epithelialization, CET was determined by calculating the difference between CCT prior and directly after de-epithelialization. In the excimer laser ablation group, the residual epithelium did not allow similar subtraction, and thus, CET was determined by averaging five manual CET measurements in the central four millimeters of the pre-excimer laser ablation high-resolution OCT image.

### *Safety*

Described in detail below, treatment safety was assessed by absorbance spectrophotometry (total indicating stromal chromophore concentration and direct determining the de-epithelialization's scattering effect) and confocal fluorescence microscopy (imaging stromal chromophore penetration depth).

### *Absorbance spectrophotometry*

Corneas in the chromophore diffusion group (n = 100, Figure 3A) were consecutively placed in the beam of two UV-visible spectrophotometers: adapted with an integrative sphere (V-570, Jasco Inc., Mary's Court, MD, USA) or without (Evolution 220, Thermo Fischer Scientific Inc., Waltham, MA, USA). Total and direct absorbance was measured between 300 and 900 nm with a spectral bandwidth of 5 nm. Total spectroscopy, measuring all transmitted light independent of scattering, was used to assess stromal



chromophore concentration in the five subgroups (native/RF/RF-D/WST11/WST-D impregnated). Given the toxic nature of UVA light, sufficient stromal chromophore is needed to attenuate the UVA light. Stromal chromophore concentration serves as an indirect measure for treatment safety. Direct spectroscopy, excluding scattered light, was used to assess changes in transmittance induced by excimer laser ablation. A curve was fitted including a wavelength-dependent (Rayleigh) and wavelength-independent factors (Tryptophan; derived from Van de Kraats *et al.*).<sup>24</sup> The percentual decrease for both factors was calculated as a measure of changes in the cornea's optical properties.

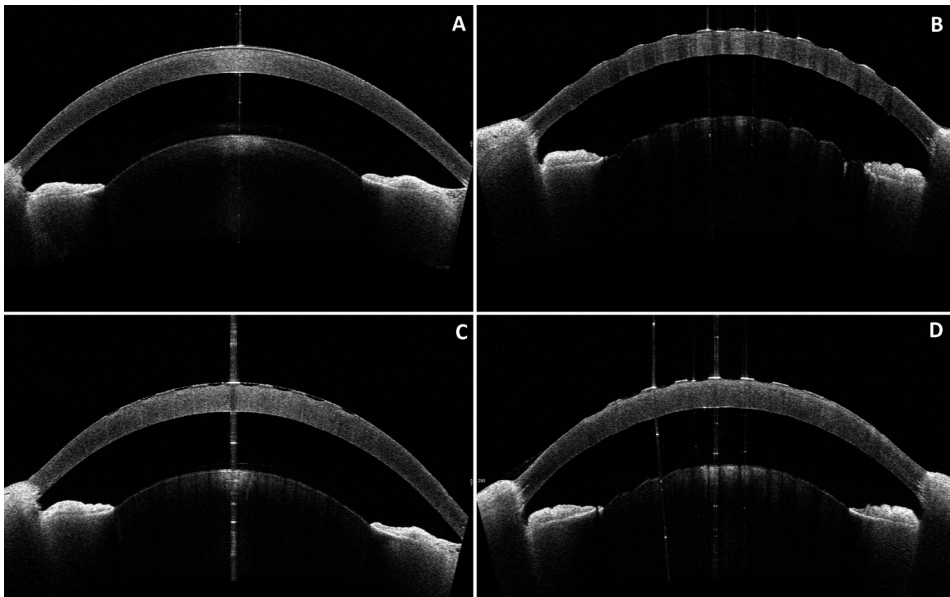


Figure 4. Ocular coherence tomography images of a porcine cornea, consecutively: (A) prior to procedure, (B) after excimer laser-assisted patterned de-epithelialization, (C) after water-soluble taurine (WST11) impregnation for 20 minutes, and (D) after near-infrared irradiation for 30 minutes.

#### *Confocal fluorescence microscopy*

After absorbance spectrophotometry, corneal chromophore diffusion was assessed using an inverted confocal fluorescence microscope (BX61 Olympus, Tokyo, Japan), with images taken at 10  $\mu\text{m}$  steps using a CCD camera (Cascade 512B, Roper Sci., New Jersey, USA). Samples were stained by 5  $\mu\text{M}$  propidium iodide (PI), allowing visualization of the sample's stromal borders. All samples were excited at 561 nm with fluorescence being recorded at 617 nm to image PI-stained cell nuclei. Additionally, samples were consecutively excited at 488 nm (RF-based impregnated corneas) or 755 nm (WST11-based impregnated corneas), or at both 488 nm and 755 nm (unimpregnated control

corneas). Fluorescence intensity was recorded above 525 nm and 760 nm using a filter, for RF and WST respectively. Per cornea, abovementioned images were taken at three (mechanically de-epithelialized samples) or six (excimer laser-assisted de-epithelialized samples) different areas. In the latter, three areas each were taken, manually centered at either an epithelial channel or a non-ablated area (Figure 1). Samples were measured from endothelium to epithelium, to avoid the influence of photobleaching and clear imaging of the chromophore's penetration front depth. Per image, the intensity in the central 100x100 pixels for both measured channels was averaged and plotted against the depth into the sample, using MATLAB (MATLAB R2018b; The MathWorks Inc., Natick, USA). The stromal border's position, visualized by the PI staining, was used to determine each frame's depth within that specific corneal sample. Intensity plots corresponding to RF and WST11 were baseline corrected. Penetration depth was determined to be the point where the intensity dropped below a predetermined threshold value of 30 A.U., below which the signal was considered noise. Supplemental Figure S2 shows a representative example of the output generated by above-mentioned method of a RF impregnated cornea after excimer laser ablation. Per cornea in the excimer laser-assisted group six such graphs were generated (following the sampled areas as shown in Figure 1), with three areas sampled in the manual de-epithelialization group.

### *Efficacy*

Treatment efficacy was measured by measuring the sample's increased stiffness after treatment by strip extensimetry.

### *Strip extensimetry*

In 60 pairs, one eye received full CXL treatment by RF-D, WST11 or WSTD, with the contralateral eye only undergoing similar de-epithelialization as the paired treated cornea (Figure 3B). Two 2 mm wide adjacent central strips were cut in superior-inferior direction, and the sample's Young's modulus was determined as described previously.<sup>25</sup> Strips were centered and mounted in the clamps of an extensometer with a 5 kN load cell (Instron 5965; Instron, Norwood, MA, USA) set 6 mm apart, to include treated tissue only. The average of both strips per cornea was used for analysis.

### **Statistical analysis**

Corneal pachymetry and chromophore penetration depth were analyzed using analysis of variance (ANOVA), while a repeated-measures ANOVA was used for strip extensimetry analysis, permitted by the paired study design. A linear regression model was used for the spectrometry data. Statistical calculations were done with SPSS statistical software (version 23; IBM Corp., Armonk, USA).



## RESULTS

### Baseline measurements

#### *Central corneal and epithelial thickness*

Mean CCT prior to treatment read  $919 \pm 69$  ( $n = 20$ ),  $927 \pm 103$  ( $n = 20$ ),  $919 \pm 81$  ( $n = 60$ ),  $893 \pm 64$  ( $n = 60$ ) and  $925 \pm 75$   $\mu\text{m}$  ( $n = 60$ ), for corneas receiving no impregnation, RF, RF-D, WST11 or WST-D impregnation, respectively ( $p = 0.147$ ). Epithelial thickness measured  $77 \pm 21$  ( $n = 20$ ),  $83 \pm 16$  ( $n = 20$ ),  $74 \pm 18$  ( $n = 60$ ),  $79 \pm 16$  ( $n = 60$ ) and  $75 \pm 20$   $\mu\text{m}$  ( $n = 60$ ) ( $p = 0.212$ ). Figure 4 shows representative consecutive OCT imaging of a porcine cornea at all stages of sample preparation.

### Safety

#### *Absorbance spectrophotometry*

Mean total transmittance at 365 nm for RF and RF-D, at 755 nm for WST11 and WST-D impregnated samples, and at both 365 nm and 755 nm for unimpregnated samples is shown in Figure 5. Total transmittance measurements (RF-based at 365 nm, WST11-based at 755 nm) for fully and patterned de-epithelialized corneas read  $14.4 \pm 3.2\%$  ( $n = 8$ ) versus  $31.1 \pm 6.7\%$  ( $n = 12$ ),  $47.4 \pm 6.9\%$  ( $n = 8$ ) versus  $48.7 \pm 5.5\%$  ( $n = 12$ ),  $0.1 \pm 0.0\%$  ( $n = 8$ ) versus  $2.7 \pm 1.0\%$  ( $n = 12$ ) and  $4.7 \pm 0.8\%$  ( $n = 8$ ) versus  $17.7 \pm 4.4\%$  ( $n = 12$ ), for RF, RF-D, WST11 and WST-D, respectively. For unimpregnated corneas, total transmittance measured  $76.8 \pm 10.8\%$  ( $n = 8$ ) versus  $65.5 \pm 5.3\%$  ( $n = 12$ ) and  $93.2 \pm 6.9\%$  ( $n = 8$ ) versus  $90.0 \pm 3.8\%$  ( $n = 12$ ) for fully and patterned de-epithelialized corneas at 365 nm and 755 nm, respectively. In chromophore impregnated corneas (RF, RF-D, WST11 and WST-D), total transmittance was significantly lower in fully de-epithelialized corneas compared with the patterned de-epithelialized corneas ( $p < 0.001$ ). Compared with hypotonic solutions (RF and WST11), the addition of 20% dextran (RF-D, WST-D) significantly increased the total transmittance ( $p < 0.001$ ). In native corneas, total transmittance was not significantly different between fully and patterned de-epithelialized corneas ( $p = 0.189$ ). Direct transmission spectrometry showed reduced transmission after excimer laser-patterned de-epithelialization, compared with full mechanical de-epithelialization. Figure 6 shows the average measured direct transmission of unimpregnated samples, with curve fittings as described in the methods section. Wavelength independent and dependent (Rayleigh scattering) scattering increased by 125% and 77%, respectively, indicating reduced optical clarity by excimer laser-assisted de-epithelialization alone.

#### *Confocal fluorescence microscopy*

In unimpregnated corneas, no chromophore fluorescence was detected in either full or patterned de-epithelialization groups. In the RF and RF-D subgroup, full chromophore penetration, regardless of full or patterned de-epithelialization was seen. In WST11 and

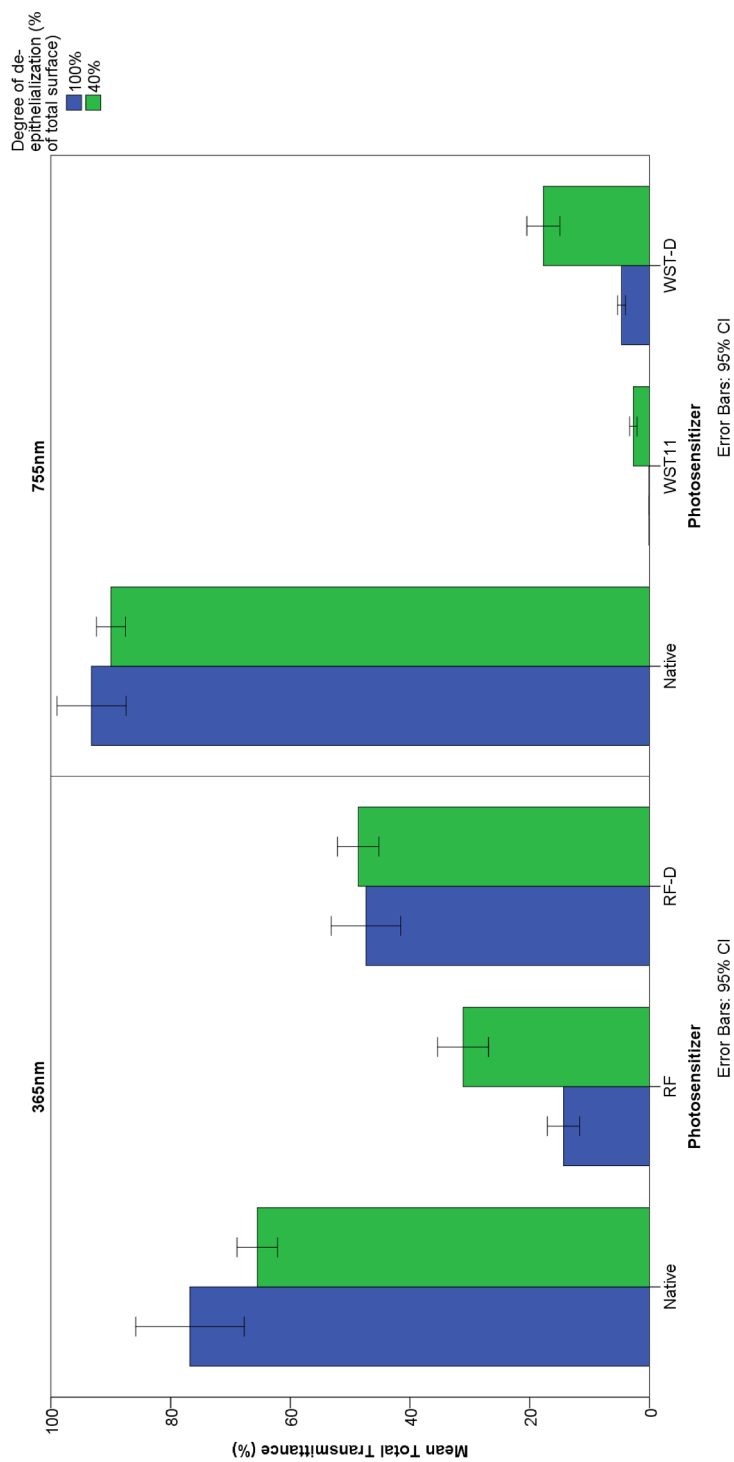


Figure 5. Mean total transmittance of light at 365 nm and 755 nm through porcine cornea, non-impregnated or impregnated with either of four chromophore formulations, after full (n = 8 per group) or patterned (n = 12 per group) de-epithelialization. Measured applying an integrated sphere. Transmission was significantly higher in patterned de-epithelialized corneas ( $p < 0.001$ ) and in dextran-enriched (RF-D and WST-D) formulations ( $p < 0.001$ ), indicating lower total stromal chromophore concentrations. Error bars represent 95% confidence interval.

WST-D impregnated samples, a clear chromophore penetration front was noted, with only partial stromal chromophore penetration. When comparing penetration depth in fully and patterned de-epithelialized corneas, no difference was seen for both WST11 ( $592 \pm 43$  versus  $593 \pm 64 \mu\text{m}$ ,  $p = 0.963$ ) and WSTD ( $504 \pm 43$  versus  $489 \pm 93 \mu\text{m}$ ,  $p = 0.669$ ) impregnated samples. Similarly, within the patterned de-epithelialized subgroup, no difference in penetration depth was seen between channels and intermediate areas for both WST11 ( $593 \pm 64$  versus  $575 \pm 62 \mu\text{m}$ ,  $p = 0.479$ ) and WST-D ( $489 \pm 93$  versus  $433 \pm 94 \mu\text{m}$ ,  $p = 0.160$ ) impregnated samples. The addition of dextran significantly reduced the stromal penetration depth, in both fully and patterned de-epithelialized corneas, and in both channels and intermediate areas in patterned de-epithelialized corneas (both  $p < 0.001$ ).

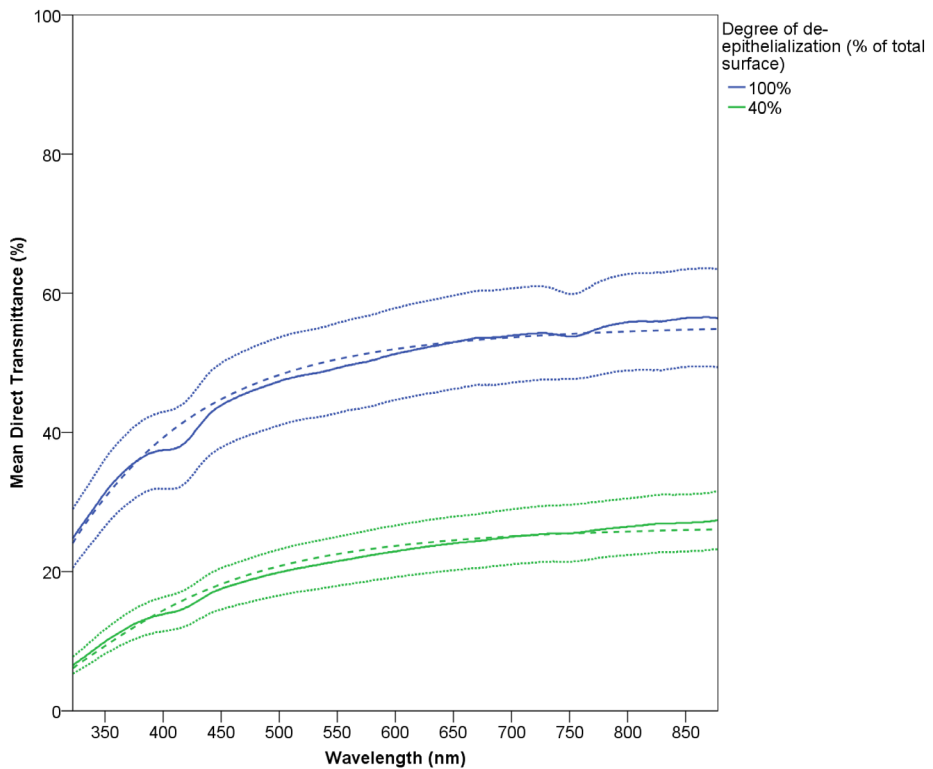


Figure 6. Mean direct transmittance of unimpregnated porcine corneas, fully mechanically de-epithelialized (100%,  $n = 8$ ) or excimer laser-assisted patterned de-epithelialized (40%,  $n = 12$ ). An overall reduced transmittance is seen after patterned de-epithelialization, which we hypothesize may be in part due to the irregular surface created. Dotted lines represent respective 95% confidence intervals of the means, and striped lines indicate best fitted curve.

## Efficacy

### *Strip extensiometry*

Out of 120 corneas, three samples were excluded from analysis, due to testing apparatus failure (two samples) and as a result of sample slippage during testing (one sample). A significant CXL treatment effect ( $p < 0.001$ ) was seen for all examined chromophores (RF-D, WST11 and WST-D). There was no difference in stiffening effect between chromophores ( $p = 0.601$ ) or between fully or patterned de-epithelialized groups ( $p = 0.564$ ). In the fully de-epithelialized samples, mean Young's Modulus for control versus treated corneas read  $145.7 \pm 21.4$  versus  $162.7 \pm 8.8$  kPa ( $n = 8$ ),  $144.2 \pm 12.0$  kPa versus  $168.9 \pm 14.4$  kPa ( $n = 8$ ) and  $139.5 \pm 8.0$  kPa versus  $160.3 \pm 10.0$  kPa ( $n = 7$ ), for RF-D, WST11 and WST-D groups, respectively. Similarly, the respective means in the patterned de-epithelialized group were  $169.8 \pm 30.3$  kPa versus  $183.7 \pm 28.8$  kPa ( $n = 11$ ),  $151.1 \pm 25.3$  kPa versus  $168.7 \pm 27.8$  kPa ( $n = 12$ ) and  $166.9 \pm 12.9$  kPa versus  $188.5 \pm 22.3$  kPa ( $n = 11$ ). Figure 7 shows a scatter plot of all treated samples per chromophore and degree of de-epithelialization. Points to the upper left of the dashed line indicate no treatment effect was seen.

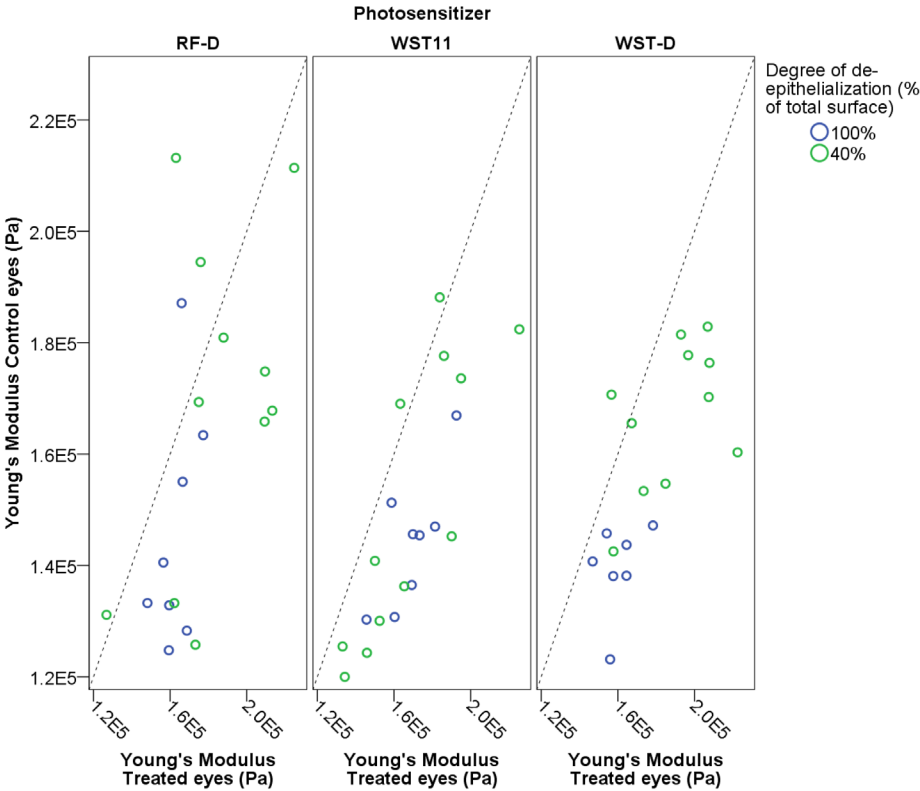


Figure 7. Scatter plot of all paired corneal samples tested by strip extensimetry. Shown is the Young's Modulus of control samples (vertical axis) versus the Young's Modulus of its paired treated sample (horizontal axis), per chromophore and degree of epithelial removal (full, 100%; patterned, 40%). Treatment induced significant stiffening for all three chromophores ( $p < 0.001$ ), without difference between chromophores ( $p = 0.601$ ) or degree of epithelial removal ( $p = 0.0564$ ). In Pascal. Dashed line indicates equality between control and treated samples.

## DISCUSSION

As Wollensak's seminal publication, the Dresden CXL protocol, involving central corneal epithelial removal, was first approved in Europe and recently in the United States.<sup>22</sup> Keeping the epithelium intact during CXL could reduce pain and complications, such as delayed re-epithelialization, haze formation and microbial keratitis. It is, therefore, that many studies have focused on delivering RF to the corneal stroma without the removal of the epithelium, known as 'epi-on' CXL, by addition of penetration enhancers, alteration of the RF formulation or by the use of iontophoresis.<sup>26,27</sup> Several studies show outcomes after epi-on treatment similar to the standard CXL procedures.<sup>11,28–31</sup> However, similarly multiple studies do show inferior results after epi-on CXL.<sup>12–14,32–34</sup> The role of epithelial removal, therefore, remains subject of debate.

Several authors attempted to partially remove the corneal epithelium, either selectively leaving 'epithelial islands' in situ or by only removing superficial layers of the epithelium. While published data are limited, several clinical studies have been performed. Rechichi *et al.*, Razmjoo *et al.*, Hashemi *et al.* and Galvis *et al.* all manually removed only part of the epithelium, by repeatedly puncturing the epithelium with a self-made device, leaving the central 3 mm of epithelium in situ, or removing several parallel strips of epithelium, respectively.<sup>7–10</sup> These studies not only show arrested progression and improved corrected distance visual acuity, but also indicate epi-off protocols provide superior improvement in topographic indices. Besides mechanical debridement, the application of alcohol (ALD) is now widely adopted, facilitating epithelial removal. While ALD was shown to result in a smoother surface, postoperative pain and epithelial healing time were shown to increase significantly.<sup>35,36</sup> In a recent study, Bradford *et al.* applied a femtosecond laser to create epithelial channels.<sup>37</sup> They show stromal RF concentrations of approximately 50% the concentration after regular epi-off protocols, but biomechanical effects are not reported on. While excimer lasers have been used to perform full epithelial debridement, to our knowledge, this is the first study to apply an excimer laser in order to create small epithelium penetrating channels.<sup>38,39</sup>

In corneal chromophore-based CXL, stromal chromophore distribution greatly determines the treatment's safety. For RF-based CXL, stromal RF is needed to sufficiently attenuate the applied toxic UVA light before reaching deeper ocular structures or inducing photochemical damage at the endothelial level.<sup>40,41</sup> Thus, stromal RF concentration is an important measure in determining the treatment's safety. In standard epi-off CXL, this has been an area of great concern, specifically in thin corneas, and several solutions have been suggested, such as covering the cornea with an additional layer of RF solution or by a RF soaked contact lens.<sup>23,42,43</sup>

In WST11-based CXL, safe NIR light is applied, omitting the need to obtain sufficient stromal chromophore concentration to attenuate the applied light. For WST11-based CXL, chromophore penetration depth provides a more important safety measure, as a damaging photochemical reaction may still occur if WST11 reaches the endothelium. In this study, total transmission spectrometry was used to assess stromal chromophore concentrations, and confocal fluorescence microscopy allowed visualization of the chromophores' penetration depth. Lower stromal chromophore concentrations were seen by total transmission spectrometry in the patterned de-epithelialization group. Whereas RF was shown to penetrate the full stroma, regardless of dextran addition or degree of de-epithelialization, confocal fluorescence microscopy showed that the addition of dextran limits the stromal penetration depth of WST11 to the anterior half of the stroma. Thus, while for WST-D/NIR standard CXL parameters may be used safely in conjunction with this novel excimer laser-patterned de-epithelialization, protocol adaptation may be needed for RF/UVA CXL to ensure endothelial safety.

While this study provides a proof of concept, several limitations should be addressed. First, although we show that patterned de-epithelialization achieves similar stiffening as the regular Dresden protocol *ex vivo*, further *in vivo* models should address the clinical safety and efficacy. Direct transmission spectrometry shows increased scattering after patterned de-epithelialization, which indicates inferior optical clarity. This may be due to light absorption by remaining epithelium, the periodic structure of the laser ablation pattern or the irregular surface after excimer laser pretreatment.<sup>44,45</sup> Resolution of this increased scattering after epithelial healing could, however, not be confirmed in this *ex vivo* model. Also, while clinical studies suggest faster epithelial recovery and reduced postoperative pain after partial de-epithelialization, this study cannot confirm or disprove these hypothesized benefits.<sup>7,9,46</sup> Thus, future *in vivo* studies should investigate the technique's effect on corneal transparency and posttreatment epithelial healing and pain. Second, it is most likely corneal hydration *ex vivo* differs from the *in vivo* situation, with rapid swelling occurring after enucleation. As corneal swelling occurs mainly within the stroma, limited influence on excimer laser epithelial ablation may be expected, but stromal chromophore diffusion could differ from the *in vivo* situation. Third, in this study, an average epithelial thickness was determined for each cornea to set the laser's ablation depth, aimed to prevent ablation beyond the Bowman layer. In healthy eyes, this may be sufficient, as chromophore penetration may not be influenced by a thin layer of remaining epithelium due to only few tight junction complexes in the posterior epithelium, allowing a safe distance from the stroma.<sup>47</sup> However, in KC eyes, the epithelium is known to be highly irregular and an average epithelial thickness would not suffice.<sup>48</sup> In order to prevent stromal ablation, excimer laser-assisted patterned ablation of diseased eyes should thus involve accurate epithelial mapping with corresponding

individualized and mapped ablation depth profiles. Given the fast-evolving imaging technology and increasing interest in personalized and targeted CXL, this limitation may soon be overcome. Last, while the total number of eyes in this study is high, the number of eyes per group as used for sub-analysis is relatively low.

In conclusion, the results of this study show the epithelium does not have to be removed completely to achieve effective corneal CXL but can be performed using an excimer laser to create epithelial channels, leaving approximately 60% of the epithelium in the treated area in situ. Stromal chromophore concentration, however, is found to be significantly lower when the epithelium is only partially removed and is influenced by the addition of dextran. This raises safety implications for RF-based CXL, while less relevant for WST11-based CXL due to its different safety mechanism. As interest in partial or selective de-epithelialization is growing along with customized CXL, and clinical studies applying partial mechanical de-epithelialization have already been partaken, these results may help to guide the development of a CXL technique reducing treatment burden, while guaranteeing patients' safety.



## REFERENCES

1. O'Brart DPS, Patel P, Lascaratos G, et al. Corneal Cross-linking to Halt the Progression of Keratoconus and Corneal Ectasia: Seven-Year Follow-up. *Am J Ophthalmol.* 2015;160(6):1154-1163.
2. Poli M, Lefevre A, Auxenfans C, Burillon C. Corneal Collagen Cross-linking for the Treatment of Progressive Corneal Ectasia: 6-Year Prospective Outcome in a French Population. *Am J Ophthalmol.* 2015;160(4):654-662.e1.
3. Raiskup F, Theuring A, Pillunat LE, Spoerl E. Corneal collagen crosslinking with riboflavin and ultraviolet-A light in progressive keratoconus: Ten-year results. *J Cataract Refract Surg.* 2015;41(1):41-46.
4. Koller T, Mrochen M, Seiler T. Complication and failure rates after corneal crosslinking. *J Cataract Refract Surg.* 2009;35(8):1358-1362.
5. Cagil N, Sarac O, Cakmak HB, Can G, Can E. Mechanical epithelial removal followed by corneal collagen crosslinking in progressive keratoconus: Short-term complications. *J Cataract Refract Surg.* 2015;41(8):1730-1737.
6. Maharana PK, Sahay P, Sujeeth M, et al. Microbial keratitis after accelerated corneal collagen cross-linking in keratoconus. *Cornea.* 2018;37(2):162-167.
7. Rechichi M, Daya S, Scorgia V, Meduri A, Scorgia G. Epithelial-disruption collagen crosslinking for keratoconus: One-year results. *J Cataract Refract Surg.* 2013;39(8):1171-1178.
8. Peyman A, Kharraji M, Koosha N, Razmjoo H, Rahimi B. Corneal haze and visual outcome after collagen crosslinking for keratoconus: A comparison between total epithelium off and partial epithelial removal methods. *Adv Biomed Res.* 2014;3(1):221.
9. Hashemi H, Miraftab M, Hafezi F, Asgari S. Matched comparison study of total and partial epithelium removal in corneal cross-linking. *J Refract Surg.* 2015;31(2):110-115.
10. Galvis V, Tello A, Carreño NI, et al. Corneal Cross-Linking (with a Partial Deepithelization) in Keratoconus with Five Years of Follow-Up. *Ophthalmol Eye Dis.* 2016;8:OED.S38364.
11. Stulting RD, Trattler WB, Woolfson JM, Rubinfeld RS. Corneal crosslinking without epithelial removal. *J Cataract Refract Surg.* 2018;44(11):1363-1370.
12. Lombardo M, Micali N, Villari V, et al. Ultraviolet A: Visible spectral absorbance of the human cornea after transepithelial soaking with dextran-enriched and dextran-free riboflavin 0.1% ophthalmic solutions. *J Cataract Refract Surg.* 2015;41(10):2283-2290.
13. Akbar B, Intisar-Ul-Haq R, Ishaq M, Fawad A, Arzoo S, Siddique K. Comparison of transepithelial corneal crosslinking with epithelium-off crosslinking (epithelium-off CXL) in adult Pakistani population with progressive keratoconus. *Taiwan J Ophthalmol.* 2017;7(4):185-190.
14. Godefrooij DA, El Kandoussi M, Soeters N, Wisse RPL. Higher order optical aberrations and visual acuity in a randomized controlled trial comparing transepithelial versus epithelium-off corneal crosslinking for progressive keratoconus. *Clin Ophthalmol.* 2017;11:1931-1936.
15. Marcovich AL, Brandis A, Daphna O, et al. Stiffening of rabbit corneas by the bacteriochlorophyll derivative WST11 using near infrared light. *Investig Ophthalmol Vis Sci.* 2012;53(10):6378-6388.
16. Cherfan D, Verter EE, Melki S, et al. Collagen cross-linking using rose bengal and green light to increase corneal stiffness. *Investig Ophthalmol Vis Sci.* 2013;54(5):3426-3433.
17. Alageel SA, Arafat SN, Salvador-Culla B, et al. Corneal Cross-Linking with Verteporfin and Nonthermal Laser Therapy. *Cornea.* 2018;37(3):362-368.

18. ICNIRP (International Commission on Non-ionizing Radiation Protection). Guidelines on limits of exposure to broad-band incoherent optical radiation (0.38 To 3  $\mu\text{M}$ ). *Health Phys.* 1997;73(3):539-554.
19. Jay L, Brocas A, Singh K, Kieffer JC, Brunette I, Ozaki T. Determination of porcine corneal layers with high spatial resolution by simultaneous second and third harmonic generation microscopy. *Opt Express.* 2008;16(21):16284.
20. Nibourg LM, Koopmans SA. Preservation of enucleated porcine eyes for use in a wet laboratory. *J Cataract Refract Surg.* 2014;40(4):644-651.
21. Stoddard JE, Marneris AG, Borr MJ, Keil ML. Optimization of femtosecond lasers using porcine and human donor corneas before in vivo use. *J Cataract Refract Surg.* 2018;44(8):1018-1022.
22. Wollensak G, Spoerl E, Seiler T. Riboflavin/ultraviolet-A-induced collagen crosslinking for the treatment of keratoconus. *Am J Ophthalmol.* 2003;135(5):620-627.
23. Wollensak G, Aurich H, Wirbelauer C, Sel S. Significance of the riboflavin film in corneal collagen crosslinking. *J Cataract Refract Surg.* 2010;36(1):114-120.
24. van de Kraats J, van Norren D. Optical density of the aging human ocular media in the visible and the UV. *J Opt Soc Am A.* 2007;24(7):1842.
25. Brekelmans J, Goz A, Dickman MM, et al. Long-term biomechanical and histologic results of WST-D/NIR corneal stiffening in rabbits, up to 8 months follow-up. *Investig Ophthalmol Vis Sci.* 2017;58(10):4089-4095.
26. Beckman KA, Gupta PK, Farid M, et al. Corneal crosslinking: Current protocols and clinical approach. *J Cataract Refract Surg.* 2019;45(11):1670-1679.
27. Henriquez MA, Hernandez-Sahagun G, Camargo J, Izquierdo L. Accelerated Epi-On Versus Standard Epi-Off Corneal Collagen Cross-Linking for Progressive Keratoconus in Pediatric Patients: Five Years of Follow-Up. *Cornea.* 2020;39(12):1493-1498.
28. Magli A, Forte R, Tortori A, Capasso L, Marsico G, Piozzi E. Epithelium-off corneal collagen cross-linking versus transepithelial cross-linking for pediatric keratoconus. *Cornea.* 2013;32(5):597-601.
29. Stojanovic A, Zhou W, Utheim TP. Corneal collagen cross-linking with and without epithelial removal: A contralateral study with 0.5% hypotonic riboflavin solution. *Biomed Res Int.* 2014;2014:619398.
30. Nawaz S, Gupta S, Gogia V, Sasikala N, Panda A. Trans-epithelial versus conventional corneal collagen crosslinking: A randomized trial in keratoconus. *Oman J Ophthalmol.* 2015;8(1):9-13.
31. Rossi S, Orrico A, Santamaria C, et al. Standard versus trans-epithelial collagen cross-linking in keratoconus patients suitable for standard collagen cross-linking. *Clin Ophthalmol.* 2015;9:503-509.
32. Wollensak G, Iomdina E. Biomechanical and histological changes after corneal crosslinking with and without epithelial debridement. *J Cataract Refract Surg.* 2009;35(3):540-546.
33. Çerman E, Toker E, Ozarslan Ozcan D. Transepithelial versus epithelium-off crosslinking in adults with progressive keratoconus. *J Cataract Refract Surg.* 2015;41(7):1416-1425.
34. Lombardo M, Serrao S, Lombardo G, Schiano-Lomoriello D. Two-year outcomes of a randomized controlled trial of transepithelial corneal crosslinking with iontophoresis for keratoconus. *J Cataract Refract Surg.* 2019;45(7):992-1000.
35. Katbab A, Owji SM, Eghtedari M. Morphologic changes of corneal epithelial flap: Ethanol-mediated versus mechanical removal. *Ultrastruct Pathol.* 2012;36(6):400-403.

36. Vingopoulos F, Kanellopoulos AJ. Epi-Bowman Blunt Keratectomy Versus Diluted EtOH Epithelial Removal in Myopic Photorefractive Keratectomy: A Prospective Contralateral Eye Study. *Cornea*. 2019;38(5):612-616.
37. Bradford S, Mikula E, Xie Y, Juhasz T, Brown DJ, Jester J V. Enhanced transepithelial riboflavin delivery using femtosecond laser-machined epithelial microchannels. *Transl Vis Sci Technol*. 2020;9(6):1.
38. Kanellopoulos AJ, Asimellis G. Keratoconus management: Long-term stability of topography-guided normalization combined with high-fluence CXL stabilization (the Athens Protocol). *J Refract Surg*. 2014;30(2):88-92.
39. Sarac O, Kosekahya P, Caglayan M, Tanriverdi B, Taslipinar Uzel AG, Cagil N. Mechanical versus transepithelial phototherapeutic keratectomy epithelial removal followed by accelerated corneal crosslinking for pediatric keratoconus: Long-term results. *J Cataract Refract Surg*. 2018;44(7):827-835.
40. Wollensak G, Spoerl E, Wilsch M, Seiler T. Endothelial cell damage after riboflavin-ultraviolet-A treatment in the rabbit. *J Cataract Refract Surg*. 2003;29(9):1786-1790.
41. Marcovich AL, Brekelmans J, Brandis A, et al. Decreased riboflavin impregnation time does not increase the risk for endothelial phototoxicity during corneal cross-linking. *Transl Vis Sci Technol*. 2020;9(6):4.
42. Jacob S, Kumar DA, Agarwal A, Basu S, Sinha P, Agarwal A. Contact lens-assisted collagen cross-linking (CACXL): A new technique for cross-linking thin corneas. *J Refract Surg*. 2014;30(6):366-372.
43. Hafezi F, Kling S, Gilardoni F, et al. Individualized Corneal Cross-linking With Riboflavin and UV-A in Ultrathin Corneas: The Sub400 Protocol. *Am J Ophthalmol*. 2021;224(December):133-142.
44. Pérez-Merino P, Martínez-García MC, Mar-Sardaña S, et al. Corneal light transmission and roughness after refractive surgery. *Optom Vis Sci*. 2010;87(7):E469-74.
45. Meek KM, Knupp C. Corneal structure and transparency. *Prog Retin Eye Res*. 2015;49:1-16.
46. Mazzotta C, Ramovecchi V. Customized epithelial debridement for thin ectatic corneas undergoing corneal cross-linking: Epithelial island cross-linking technique. *Clin Ophthalmol*. 2014;8:1337-1343.
47. Bakke EF, Stojanovic A, Chen X, Drolsum L. Penetration of riboflavin and postoperative pain in corneal collagen crosslinking. Excimer laser superficial versus mechanical full-thickness epithelial removal. *J Cataract Refract Surg*. 2009;35(8):1363-1366.
48. Franco J, White CA, Kruh JN. Analysis of Compensatory Corneal Epithelial Thickness Changes in Keratoconus Using Corneal Tomography. *Cornea*. 2020;39(3):298-302.

SUPPLEMENTARY MATERIAL

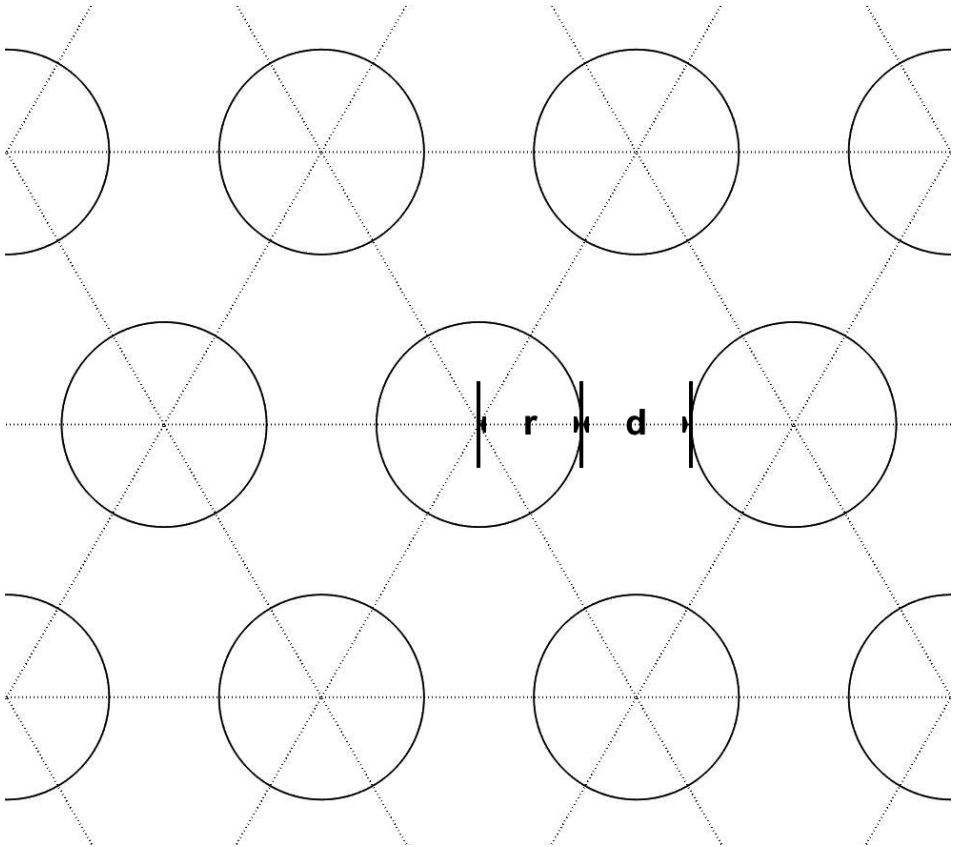
Supplementary Table S1. Paired sample allocation scheme to each applied chromophore or control (no chromophore applied) in the chromophore diffusion and penetration subgroup.

Pair	Eye 1	Eye 2
1-5	RF	RF-D
6-10	RF	WST
11-15	RF	WST-D
16-20	RF	Control
21-25	RF-D	WST
26-30	RF-D	WST-D
31-35	RF-D	Control
36-40	WST	WST-D
41-45	WST	Control
46-50	WST-D	Control

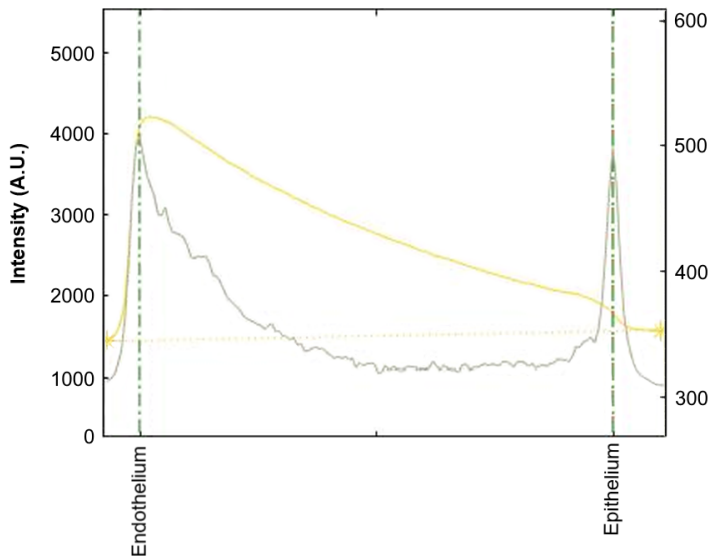
Percentage total surface ablation

$$\begin{aligned} &= \frac{(\text{cumulative surface of channels per equilateral triangle})}{(\text{surface of equilateral triangle})} \\ &= \frac{3 * 1/6 * \pi r^2}{\sqrt{3} * (d + 2r)^2/4} * 100\% \end{aligned}$$

Supplementary Equation S1. Applied equation to assess degree of de-epithelialization. The applied SCHWIND Amaris excimer laser has a spot size of 0.7 mm, allowing to ablate channels with a fixed radius (r) of 0.35 mm. In this study we set the distance between channels (d) at 0.375 mm, resulting in approximately 40% of the total epithelial surface to be ablated.



Supplementary Figure S1. Schematic representation of excimer laser assisted ablation patterns. Using a SCHWIND Amaris excimer laser, epithelial channels were ablated to allow for corneal chromophore penetration, whilst part of the epithelium was left untouched. A hexagonal pattern, with equal distances between channels was chosen, as illustrated in Figure 2 and Supplementary Figure S1. The percentage of total surface ablation can be calculated by following Supplementary Equation S1, when the ablation zone is considered to consist of connected triangles, indicated in by dashed lines.



Supplementary Figure S2. Fluorescence intensity (in arbitrary units; A.U.) measured by confocal fluorescence microscopy of a riboflavin (RF) impregnated cornea in the excimer laser assisted group, obtained from a non-ablated area. The yellow line is the fluorescence intensity recorded at 525 nm (corresponding to RF, left Y-axis), with the dashed yellow line representing its baseline. In grey, the fluorescence intensity measured at 617 nm is represented (corresponding to the propidium iodide staining, right Y-axis), from which two peaks were identified automatically using MATLAB (MATLAB R2018b, The MathWorks Inc., Natick, USA). The identified peaks correspond to the basement membranes of the endothelium and epithelium, which were used to identify the sample's borders, and chromophore penetration depth (in %). For samples in the excimer laser assisted group, six graphs were obtained (three from an epithelial channel and three from a non-ablated area) per cornea (also see Figure 1). For mechanical de-epithelialized samples three graphs were obtained. The data in this exemplary graph shows full RF penetration (100%) in an area between excimer laser assisted epithelial channels.







# Chapter 5

## **Corneal stiffening by a bacteriochlorophyll derivative with dextran and near-infrared light: effect of shortening irradiation time up to 1 minute**

Jurriaan Brekelmans, Alexandra Goz, Mor M. Dickman, Alexander Brandis,  
Xiaomeng Sui, H. Daniel Wagner, Rudy M.M.A. Nuijts,  
Avigdor Scherz, Arie L. Marcovich

*Cornea.* 2017 Nov;36(11):1395-1401



# ABSTRACT

Purpose: The aim of this study is to determine the effect of variation of the exposure time of near-infrared irradiation on corneal stiffening after a bacteriochlorophyll derivative (WST11) with dextran (WST-D) application.

Methods: One hundred four paired eyes of 3-month-old New Zealand White rabbits were included in this study. Fifty-two eyes (ex vivo  $n = 34$ , in vivo  $n = 18$ ) were mechanically deepithelialized, treated topically with WST-D, and irradiated at  $10 \text{ mW/cm}^2$  using a diode laser at  $755 \text{ nm}$  for 1, 5, or 30 minutes. Untreated fellow eyes served as controls. Corneoscleral rings were removed immediately after treatment (ex vivo), or 1 month after treatment (in vivo). Corneal strips were cut and underwent biomechanical stress-strain measurements.

Results: Ex vivo, the mean tangent elastic modulus was significantly higher in the treatment groups than in the control groups for 1, 5, and 30 minutes of irradiation, respectively,  $6.06 \text{ MPa}$ , 95% confidence interval (CI,  $4.5\text{--}7.6$ ) versus  $14.02 \text{ MPa}$ , 95% CI ( $10.2\text{--}17.8$ ),  $n = 11$ ,  $4.8 \text{ MPa}$ , 95% CI ( $3.9\text{--}5.7$ ) versus  $15.03 \text{ MPa}$ , 95% CI ( $12\text{--}18.1$ ),  $n = 11$ , and  $7.8 \text{ MPa}$ , 95% CI ( $5.6\text{--}10.02$ ) versus  $16.2 \text{ MPa}$ , 95% CI ( $13.6\text{--}18.9$ ),  $n = 11$ ;  $p < 0.001$  for all comparisons. In vivo, the mean elastic moduli in the treatment groups were significantly higher for 5 and 30 minutes of irradiation but not for 1 minute of irradiation, respectively,  $11.4 \text{ MPa}$ , 95% CI ( $8.5\text{--}14.2$ ), versus  $17.1 \text{ MPa}$ , 95% CI ( $14.5\text{--}19.7$ ),  $n = 5$ ;  $p < 0.001$ , and  $9.4 \text{ MPa}$ , 95% CI ( $5.1\text{--}13.8$ ) versus  $16.0 \text{ MPa}$ , 95% CI ( $13.1\text{--}19$ ),  $n = 5$ ;  $p < 0.01$ , and  $11.3 \text{ MPa}$ , 95% CI ( $6\text{--}16.6$ ) versus  $12.2 \text{ MPa}$ , 95% CI ( $7.5\text{--}16.8$ ),  $n = 5$ ;  $p = 0.7$ .

Conclusions: WST-D/near-infrared treatment using shortened irradiation time (1 minute ex vivo and 5 minutes in vivo) results in significant corneal stiffening, and this might provide an alternative to the currently applied riboflavin/ultra-violet A cross-linking.

## INTRODUCTION

Corneal collagen cross-linking (CXL) has become a widely accepted alternative for the treatment of progressive corneal ectasia in the last decade. The classic Dresden protocol involves corneal impregnation with the chromophore riboflavin (RF) for 30 minutes, followed by 30 minutes of photosensitization by ultra-violet A (UVA) irradiation, resulting in significant corneal stiffening.<sup>1,2</sup> In an attempt to reduce total treatment time and patient discomfort, several adaptations to the Dresden protocol have been suggested.<sup>3,4</sup> High-fluency cross-linking protocols reduce treatment time by increasing radiation intensity according to the Bunsen-Roscoe law, limiting cumulative delivered energy below 5.4 J/cm<sup>2</sup> to prevent endothelial cell damage.<sup>2,5</sup> However, controversy exists about the efficacy of such protocols, as the effect is variable and the treatment depth is reported to be lower than that of the classic Dresden protocol.<sup>6–10</sup>

Recently, our group described a novel method for corneal stiffening using the bacteriochlorophyll derivative WST11 in a dextran solution (WST-D) and near-infrared light (NIR), using parameters similar to the Dresden protocol.<sup>11</sup> Reduction of the total treatment time could benefit patients and reduce treatment costs. Therefore, in this study, we examined the efficacy of shortened protocols for WST-D/NIR corneal stiffening. We compared 30, 5, and 1 minute of NIR irradiation at a constant irradiance of 10 mW/cm<sup>2</sup>, in in vivo and ex vivo New Zealand White (NZW) rabbit models.

## METHODS

One hundred four corneas of NZW rabbits were included in this study and treated *ex vivo* ( $n = 34$ ) or *in vivo* ( $n = 18$ ). Treated corneas of eyes in both groups were deepithelialized mechanically, impregnated with WST11- dextran T500 (WST-D) for 20 minutes as described by Marcovich *et al.* and irradiated with NIR light at 10 mW/cm<sup>2</sup> using a diode laser at 755 nm for either 30, 5, or 1 minute (Figure 1).<sup>11</sup> Corneoscleral strips were cut from all eyes and used for biomechanical testing.

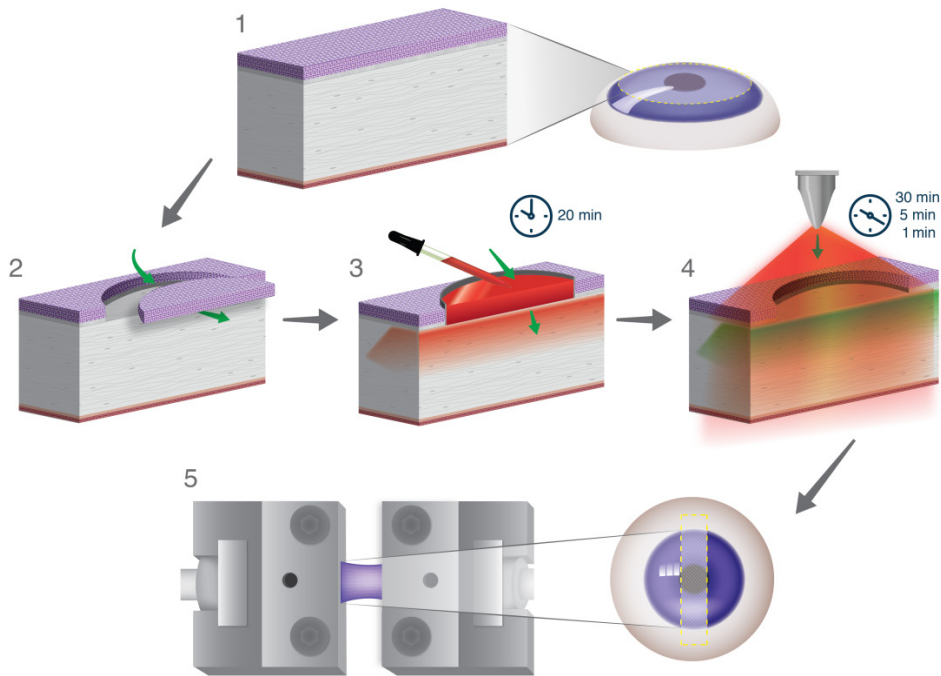


Figure 1. Flowchart of the applied method. (1, 2) Corneas in the WST-D/NIR treatment group are mechanically deepithelialized up to 2 to 3 mm of the limbus, (3) WST-D is applied for 20 minutes, and (4) the cornea is irradiated with NIR light for 1, 5, or 30 minutes. Of both treated and control corneas, (5) a 4 mm-wide corneoscleral strip is cut for extensimetry to determine its tangent elastic modulus by extensimetry.

### Ex vivo rabbit model

Paired whole globes of 3-month-old NZW rabbits were obtained from a local abattoir within hours after enucleation and transported on ice in a humid container until further processing. One eye of each pair was randomly chosen, and allocated to one of the 3 study groups. Full mechanical deepithelialization of corneas in the treatment

group, including the limbus, was manually performed and microscopically confirmed before impregnation with WST-D. Contralateral corneas, serving as controls, were left untouched until processing into strips and were not deepithelialized, similar to the methodology used in the in vivo model.

### **In vivo rabbit model**

NZW rabbits were housed with ad libitum access to food and water at the Core Animal Facility of the Weizmann Institute of Science (Rehovot, Israel). All experimental procedures were approved by the Institutional Animal Care and Use Committee, in adherence to the Association for Research in Vision and Ophthalmology (ARVO) Statement for the Use of Animals in Ophthalmic and Visual Research.<sup>12</sup> At the age of 3 months, rabbits were anesthetized by intramuscular injection of 5 mg/kg xylazine (Vitamed, Binyamina, Israel) and 35 mg/kg ketamine (Rhone Merieux, Lyon, France), topped off with additional ketamine if longer anesthesia was needed. Corneas of the left eyes, allocated to the treatment group, underwent mechanical deepithelialization up to ~2 mm of the limbus under microscopic confirmation. Right eyes, serving as paired controls, were left untouched except for eyelid closure during the entire procedure, in accordance with ARVO regulation.<sup>12</sup> After treatment, ophthalmic ointment containing dexamethasone 0.1%, neomycin and polymyxin B (Maxitrol; Alcon, Puurs, Belgium) was applied to the treated eyes once daily, until full epithelial closure was confirmed by fluorescent dye and slit-lamp examination. Four weeks after treatment, the rabbits were killed using intravenous injection of pentobarbital sodium (CTS Chemical Industries Ltd, Kiryat Malakhi, Israel).

### **Photosensitizer WST-D**

WST-D was prepared from WST11 (Steba Laboratories Ltd, Rehovot, Israel) at a concentration of 2.5 mg/mL in double-distilled water containing 20% 500-kDa dextran (*Leuconostoc* spp. Mr 450,000-650,000; Sigma-Aldrich, St. Louis) and 0.9% NaCl, with pH adjusted to 7.2-7.3 with sodium hydrogen carbonate (Merck, Darmstadt, Germany), if needed. Corneas in the treatment group were impregnated for 20 minutes using a cup filled with approximately 1 mL of WST-D placed on top of the deepithelialized cornea. After 20 minutes, remaining WST-D was removed, and the corneas were slightly rinsed with a few milliliters of Dulbecco's phosphate-buffered saline (Biological Industries, Beit Haemek, Israel).

### **Near-infrared light**

A NIR diode laser with tunable output of up to 1 W at 755 nm (CeramOptec, Bonn, Germany) was used to irradiate the impregnated corneas. Irradiance of 10 mW/cm<sup>2</sup> at the corneal apex was confirmed using a power meter (NOVEL; Ophir Optonics Ltd, Jerusalem, Israel). Directly after impregnation, corneas were placed under the NIR

laser for 30, 5, or 1 minute. In the 30-minute group, a drop of Dulbecco's phosphate-buffered saline (ex vivo) or Tears Naturale Free (Alcon, Fort Worth, TX) (in vivo) was applied every 5 minutes during irradiation, to maintain corneal hydration.

### **Biomechanical testing of corneal stiffness**

Central corneal thickness (CCT) was measured using an ultrasound pachymeter (Humphrey ultrasonic pachymeter, Humphrey Instruments, San Leandro, CA), before and after treatment. For strip extensimetry,  $4 \pm 0.2$  mm wide strips were cut from all corneas in the superior-inferior direction, with 2 to 3 mm of sclera on both ends. By placing the corneoscleral buttons on paraffin hemispheres matching the corneal curvature, and using a double-bladed cutter, the strips were cut without stretching the tissue. Samples were stored separately, for less than 3 hours, in humid Eppendorf containers on ice before extensimetry testing. All strips were placed horizontally between the clamps of a microcomputer-controlled extensimeter with a 200-N load cell (Minimat; Rheometric Scientific GmbH, Bensheim, Germany) at a gauge length of 6 mm, set at a deformation speed of 5 mm/min. The clamps were tightened with a controlled maximal force of 9 cN·m using a calibrated screwdriver (Torqueleader, Surrey, United Kingdom). Stress is the applied force normalized by the cross-sectional area before testing, and strain is the displacement normalized by the gauge length in percentage. The obtained stress-strain curves were considered to consist of 3 different regions as is common to biological tissue (Figure 2).<sup>13</sup> It was hypothesized that region 1 reflects elongation of the sample without stretching followed by uncrimping of collagen (toe region), region 2 represents load bearing of collagen fibers (linear region), and region 3 indicates breakage of interfibrillar bonds due to increased shear stress between collagen fibers, before complete rupture of the sample at the end of region 3 (failure region). Using a self-written MATLAB script and graphical user interface (MATLAB R2015b, MathWorks, Inc, Natick, MA), the borders of a linear section within region 2 were manually chosen 3 times, in a masked and random-sample order. A linear fit was applied, the slope of which represents the tangent elastic modulus, often called the Young's modulus in the ophthalmic literature. The average of 3 values obtained from each stress-strain curve was used for further statistical analysis.

### **Sample size and statistical analysis**

The sample size was chosen based on the previously published literature on WST-D/NIR corneal stiffening, indicating a mean difference between control and treated corneas of 13.9 and 20.3 MPa for an ex vivo and in vivo rabbit model, respectively, with a standard deviation of 8.3 MPa.<sup>11</sup> This yielded a sample size of 8 and 4 corneas for the ex vivo and in vivo models, respectively, with 90% power and 0.05 probability of a type I error. The sample size was increased by 50% to account for a possibly decreased treatment effect after shorter irradiation times.

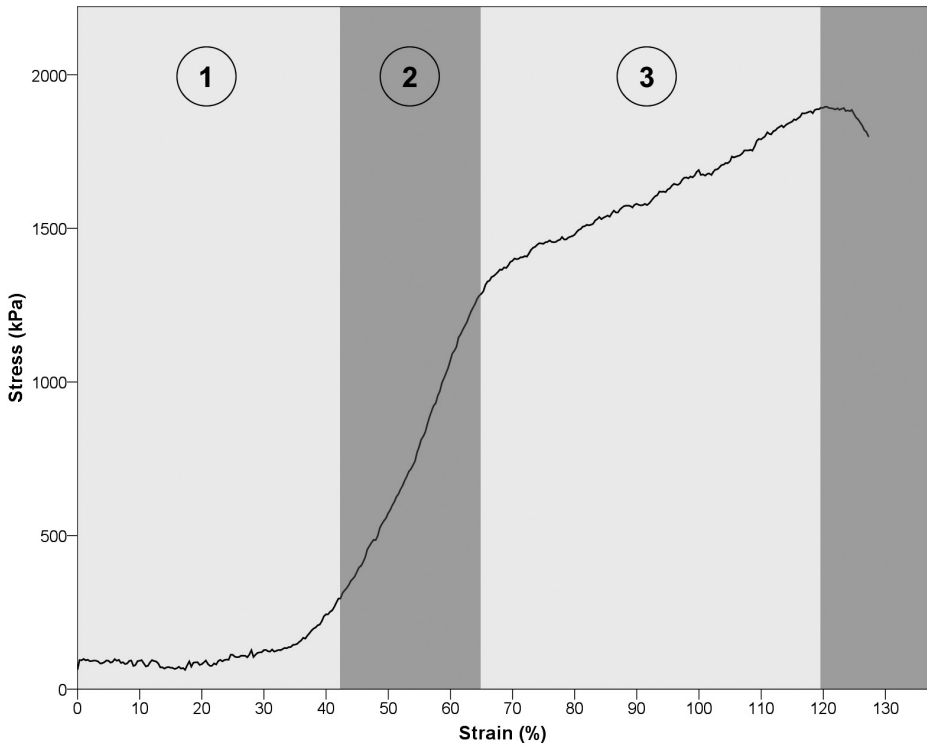


Figure 2. Example of the obtained stress–strain curve. It is hypothesized that the different regions represent (1) relaxing state and toe region, (2) load bearing on collagen fibers, and (3) breakage of interfibrillar bonds due to increased shear stress between collagen fibers.

Statistical analysis was performed by the Bioinformatics and Biological Computing department at the Weizmann Institute of Science, using Statistica, version 12 (StatSoft Inc, Tulsa, OK). Results of both *ex vivo* and *in vivo* biomechanical experiments and corneal pachymetry were analyzed using repeated-measures analysis of variance (ANOVA), with treatment (treatment versus control) as the within-subject effect, and irradiation time as the between-subject effect. The mean tangent elastic moduli and pachymetry data of control and treated corneas in each of the 3 irradiation time groups were compared using dependent Student *t* tests. The level of statistical significance was set at 0.05 for all analyses.

# RESULTS

## Ex vivo biomechanics

One pair in the 5-minute irradiation group was excluded from further analysis because of a software error during measurement of the control eye. The tangent elastic moduli for the ex vivo irradiation time groups are shown in Figure 3 and Table 1. The mean elastic moduli after WST-D/NIR treatment were significantly higher in all 3 groups. The mean difference between treated corneas and controls measured 8.46 (95% confidence interval; 95% CI [6.61-10.31],  $n = 11$ ), 10.25 (95% CI [7.58-12.91],  $n = 11$ ), and 7.95 (95% CI [4.40-11.51],  $n = 11$ ), in the 30-, 5-, and 1-minute groups, respectively ( $p < 0.001$  for all comparisons).

Factorial ANOVA showed a significant treatment effect ( $F_{1,30} = 152.26, p < 0.001$ ). The interaction between treatment and irradiation time was not significant ( $F_{2,30} = 0.93, p = 0.4$ ).

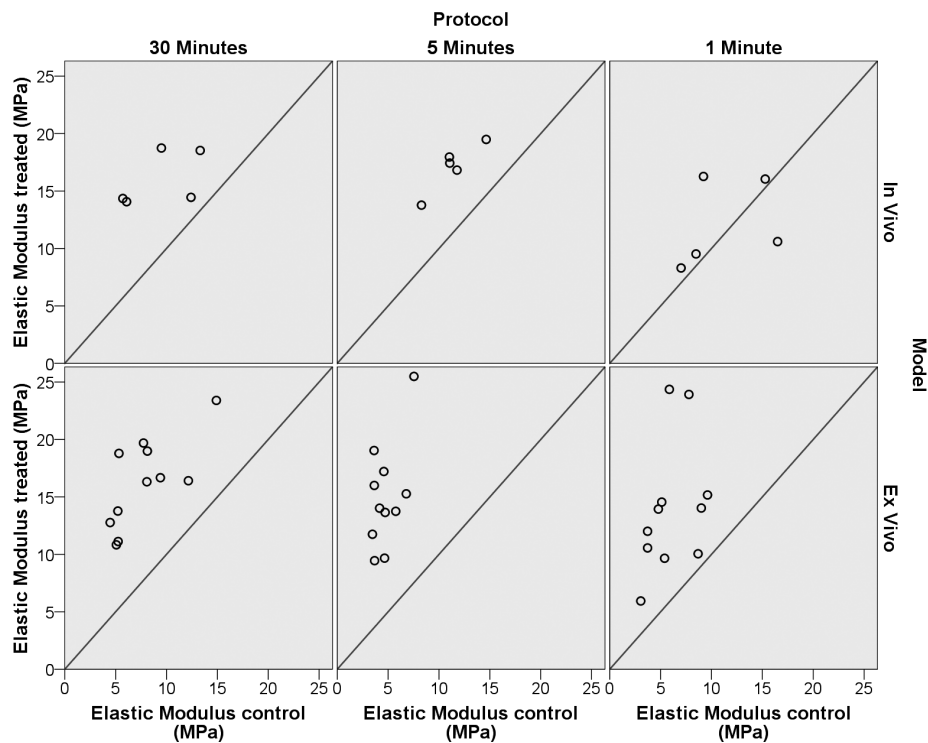


Figure 3. Scatter plot showing the elastic moduli (in mega Pascal; MPa) of control corneas (x axis) versus their paired WST-D/NIR-treated corneas (y axis), per irradiation time, and in vivo (upper row) or ex vivo (bottom row) model. The diagonal line represents the effect threshold.



Table 1. Tangent elastic moduli per irradiation time for ex vivo, paired, control and WST-D/NIR treated corneal strips.

	Elastic modulus 30 minutes irradiation (n = 11)	Elastic modulus 5 minutes irradiation (n = 11)	Elastic modulus 1 minute irradiation (n = 11)
<b>Untreated controls</b>	7.79 95% CI [5.56-10.02]	4.78 95% CI [3.86-5.70]	6.06 95% CI [4.50-7.63]
<b>WST-D/NIR treated</b>	16.25 95% CI [13.64-18.86]	15.03 95% CI [11.97-18.08]	14.02 95% CI [10.20-17.83]
<b>p-value</b>	<0.001	<0.001	<0.001

Mean and 95% confidence interval (95% CI), in MPa.

### In vivo biomechanics

Of the 18 pairs treated in vivo, three (one pair from each irradiation time group) were excluded from biomechanical testing, leaving five pairs in each group to be analyzed. Pairwise exclusion was due to problems with four different corneas: difficulties reading central corneal pachymetry (one control cornea in the 5-minute group) or failure to cut a 4-mm-wide parallel strip (paired control and treated corneas in the 1-minute group and one treated cornea in the 30-minute group). Figure 3 and Table 2 show the tangent elastic moduli for the in vivo groups. One month after WST-D/NIR treatment, the mean elastic moduli increased significantly in the 30- and 5-minute groups, with mean differences between treated and control corneas of 6.63 MPa (95% CI [2.9-10.3],  $n = 5$ ,  $p < 0.01$ ), and 5.74 MPa (95% CI [4.6-6.8],  $n = 5$ ,  $p < 0.001$ ), respectively. In the 1-minute group, the mean elastic modulus of the treated corneas was not significantly higher than that of the paired controls, with a mean difference of 0.85 MPa (95% CI [24.85-6.55],  $n = 5$ ,  $p = 0.7$ ).

Factorial ANOVA showed a significant treatment effect ( $F_{1,12} = 28.33$ ,  $p < 0.001$ ). The interaction between treatment effect and irradiation time was significant ( $F_{2,12} = 4.71$ ,  $p = 0.031$ ).

### Corneal pachymetry

No significant differences in CCT were seen between control and treated eyes before treatment ex vivo and in vivo and before biomechanical measurement in vivo (Table 3). Factorial ANOVA showed no significant difference in CCT between the irradiation time groups in vivo at baseline ( $F_{1,2} = 0.161$ ,  $p = 0.854$ ), whereas ex vivo, there was a significant difference ( $F_{1,2} = 86.23$ ,  $p < 0.001$ ).

Table 2. Tangent elastic moduli per irradiation time for in vivo, paired, control and WST-D/NIR treated corneal strips.

	Elastic modulus 30 minutes irradiation (n = 5)	Elastic modulus 5 minutes irradiation (n = 5)	Elastic modulus 1 minute irradiation (n = 5)
<b>Untreated controls</b>	9.40 95% CI [5.06-13.75]	11.35 95% CI [8.53-14.17]	11.30 95% CI [5.97-16.62]
<b>WST-D/NIR treated</b>	16.03 95% CI [13.07-18.99]	17.09 95% CI [14.48-19.71]	12.15 95% CI [7.49-16.80]
<b>p-value</b>	< 0.01	< 0.001	0.7

Mean and 95% confidence interval (95% CI), in MPa.

Table 3. Central corneal thickness (CCT) per model and per irradiation time group, before treatment and before extensimetry.

		CCT before treatment			CCT before extensimetry			
	Time	n	Control	Treated	p-value	Control	Treated	p-value
Ex vivo	1	11	466.5 95% CI [450.1-482.8]	465.9 95% CI [447.5-484.3]	0.865	<i>n.a.</i>	347.5 95% CI [320.9-374.0]	<i>n.a.</i>
	5	8	539.9 95% CI [518.7-561.0]	542.1 95% CI [523.2-561.0]	0.308	<i>n.a.</i>	383.9 95% CI [354.8-413.0]	<i>n.a.</i>
	30	11	410.7 95% CI [401.7-419.7]	412.3 95% CI [401.2-423.3]	0.726	<i>n.a.</i>	305.2 95% CI [287.4-323.0]	<i>n.a.</i>
In vivo	1	3	394.3 95% CI [302.2-486.4]	415.7 95% CI [308.2-523.1]	0.414	360.4 95% CI [351.4-369.3]	374.1 95% CI [318.0-430.3]	0.340
	5	5	395.8 95% CI [344.2-447.4]	398.0 95% CI [345.1-450.9]	0.794	387.4 95% CI [331.7-443.1]	370.6 95% CI [328.7-412.5]	0.375
	30	3	403.0 95% CI [312.5-493.5]	421.3 95% CI [341.0-501.7]	0.437	399.9 95% CI [285.6-514.2]	424.4 95% CI [329.8-519.1]	0.523

Extensimetry was performed either immediately (ex vivo) or one month (in vivo) after treatment. Ex vivo control eyes were only measured once as they remained untouched until extensimetry. N.a. = 'Not applicable'. Mean and 95% confidence interval (95% CI), in micrometer.

## DISCUSSION

This study shows that WST-D/NIR treatment provides significant corneal stiffening, even with a reduced irradiation time of only 1 minute ex vivo and 5 minutes in vivo, without increasing irradiance. A comparable and significant stiffening effect of WST-D/NIR treatment was observed in all but the 1-minute in vivo group (Figure 3). Shortening the irradiation time is not only beneficial in terms of patient comfort but also makes WST-D/NIR corneal stiffening more suitable for children and less cooperative patients.

When the stiffening effect is expressed percentually, as is common in the literature, a large difference will be noted between the ex vivo and in vivo models (mean increase ex vivo: 108.6%, 214.4%, 131.4%; in vivo: 70.5%, 50.6%, 7.5%, after 30, 5, or 1 minute of irradiation, respectively). We believe that the in vivo results are to be considered as true values, as treatment and measurement were performed under stable and physiological circumstances. Ex vivo eyes show a trend in stiffness after treatment, which is in line with the in vivo effect. The ex vivo treatment effect is most likely skewed because of variability that exists between abattoir rabbits, which are not bred and kept for research purposes. This emphasizes the importance of conducting in vivo experiments. Besides the differences between ex vivo and in vivo results, we observed a decrease in the elastic modulus after WST-D/NIR treatment in one cornea in the 1-minute irradiation in vivo group, compared with its paired control. After reviewing our records carefully, we do not have an explanation for this unexpected finding, which may be related to the inherent variability associated with strip extensimetry.

In agreement with the main objective of this study, namely to establish the efficacy of shortened WST-D/NIR treatment protocols, and to keep animal numbers to a minimum, in conjunction with ethical guidelines, we did not include an RF/UVA control group in this study. The NZW rabbit and extensimetry models are accepted in corneal CXL research, allowing indirect comparison with the literature. Wollensak *et al.* evaluated corneal stiffening in NZW rabbits after RF/CXL and reported a 79% increase in the elastic modulus at both one day and three months after treatment. However, the treatment effect at three months was compared with a control group measured immediately after treatment.<sup>14</sup> Such a comparison neglects age-related stiffening in the treatment group during follow-up, resulting in overestimation of the treatment effect. Taking into consideration variation in strip extensimetry readings and age-related corneal stiffening in the control group of our study, we conclude that the stiffening after WST-D/NIR treatment (30 and 5 minutes of NIR irradiation) is comparable to RF/UVA CXL after 30 minutes of UVA irradiation.

NIR light causes no intrinsic damage to cells by itself and is, within ranges, considered safe for patients and the environment by the International Commission of Non-Ionizing Radiation Protection (ICNIRP).<sup>15</sup> NIR can however cause thermal damage to ocular structures, in particular to the retina, at high irradiance and/or exposure time. The ICNIRP considers NIR irradiance at 10 mW/cm<sup>2</sup>, as used in this study, to be safe to the cornea and lens for a duration longer than 1000 seconds.<sup>15</sup> For shorter exposure times, the thermal effect decreases exponentially, and irradiance safety limits follow the formula  $1.8 t^{-3/4} \text{ W/cm}^2$  (t in seconds).<sup>16</sup> For 5 and 1 minute of irradiation, this would mean a safety threshold of 25 and 83 mW/cm<sup>2</sup>, respectively. The irradiance applied in our current protocols can thus be considered safe, without the need for absorbance of light before reaching the endothelium, as is the case with toxic UVA light.

In this study, NIR irradiation time was shortened, whereas irradiance remained constant at 10 mW/cm<sup>2</sup>, resulting in a decrease in irradiation dose from 18 to 3 J/cm<sup>2</sup> and 0.6 J/cm<sup>2</sup> in the 30-, 5-, and 1-minute groups, respectively. Our results show a nonlinear positive correlation between irradiation time and corneal stiffening with a nonproportional increase in stiffening, reaching a plateau phase as the irradiation time is increased, suggesting saturation of the effect (i.e., cross-linking bond formation). To our knowledge, RF/UVA CXL studies focusing on reducing irradiation time have only done so while proportionally increasing irradiance, to maintain the same total delivered energy of 5.4 J/cm<sup>2</sup>. This is suggested to be the maximal delivered energy that does not induce endothelial toxicity.<sup>2</sup> These so-called “high-fluency” protocols show a similar nonlinear positive correlation between the irradiation time and biomechanical effect.<sup>17,18</sup> Hammer *et al.* concluded that oxygen depletion is likely the limiting factor in the rate of cross-link formation with such protocols, and they stated that a higher irradiance accompanying a shorter irradiation time depletes oxygen faster, resulting in a decreased stiffening effect.<sup>17</sup> The current study shows that 5-minute irradiation at 10 mW/cm<sup>2</sup>, instead of an expected 60 mW/cm<sup>2</sup> according to RF/UVA high-fluency protocol logic, results in an elastic modulus of approximately 15 MPa, similar to the stiffening effect observed after 30 minutes of irradiance at 10 mW/cm<sup>2</sup>. Future studies are needed to determine whether shortened WST-D/NIR protocols with linearly increased irradiance can provide a greater stiffening effect compared with the shortened constant fluency protocol with 5 minutes of NIR irradiation presented in this study.

Clinically, WST-D/NIR treatment could provide a safe alternative to RF/UVA CXL, particularly for patients with a CCT below 400 µm, for whom RF/UVA is considered unsafe. The safe nature of NIR light and the ability to prevent WST from reaching the endothelium by controlling the dextran concentration in the WST-D solution ensure safe treatment regardless of corneal thickness. Theoretically, WST-D/NIR could even

allow targeted local treatment of selected (thin) regions in the cornea, which may prove sufficient or even preferable to arrest corneal ectasia.<sup>19</sup> In a previous study of our group, endothelial viability after WST-D/NIR treatment was shown by the TUNEL assay.<sup>11</sup> Also, edema was not observed in any of the WST-D/NIR treated corneas, at any time point, and the CCT before biomechanical testing was similar for treated and control eyes, indicating a functional corneal endothelium. Because of the safe nature of NIR light, WST-D/NIR treatment potentially has a superior safety profile for both patients and care providers compared with RF/UVA CXL.

Although a larger sample size may have resulted in a different overall effect in the 1-minute irradiation in vivo group, sample sizes were kept small in the in vivo groups in adherence to the ARVO statement for the Use of Animals in Ophthalmic and Vision Research.<sup>12</sup> Nonetheless, this study established a proof of concept for the efficacy of shortened WST-D/NIR protocols for corneal stiffening.

In summary, in this study, we have shown that WST-D/ NIR corneal stiffening can be effectively achieved using a significantly shortened protocol, both ex vivo and in vivo. Photoexcitation using safe NIR light overcomes the major limitations of RF/UVA CXL, related to the potential toxicity of UVA light. Importantly, corneas thinner than 400  $\mu\text{m}$ , as often is the case with progressive corneal ectasia, may benefit from WST-D/NIR treatment. A significantly shortened treatment protocol, as presented in this study, may reduce patient discomfort.

## REFERENCES

1. Wollensak G, Spoerl E, Seiler T. Riboflavin/ultraviolet-A-induced collagen crosslinking for the treatment of keratoconus. *Am J Ophthalmol*. 2003;135(5):620-627.
2. Wollensak G, Spoerl E, Wilsch M, Seiler T. Endothelial cell damage after riboflavin-ultraviolet-A treatment in the rabbit. *J Cataract Refract Surg*. 2003;29(9):1786-1790.
3. Krueger RR, Herekar S, Spoerl E. First proposed efficacy study of high versus standard irradiance and fractionated riboflavin/ultraviolet a cross-linking with equivalent energy exposure. *Eye Contact Lens*. 2014;40(6):353-357.
4. Lytle G. Advances in the technology of corneal cross-linking for keratoconus. *Eye Contact Lens*. 2014;40(6):358-364.
5. Bunsen RW, Roscoe HE. III. Photochemical researches.—Part V. On the measurement of the chemical action of direct and diffuse sunlight. *Proc R Soc London*. 1863;12(12):306-312.
6. Touboul D, Efron N, Smadja D, Praud D, Malet F, Colin J. Corneal confocal microscopy following conventional, transepithelial, and accelerated corneal collagen cross-linking procedures for keratoconus. *J Refract Surg*. 2012;28(11):769-775.
7. Ozgurhan EB, Sezgin Akcay BI, Yildirim Y, Karatas G, Kurt T, Demirok A. Evaluation of corneal stromal demarcation line after two different protocols of accelerated corneal collagen cross-linking procedures using anterior segment optical coherence tomography and confocal microscopy. *J Ophthalmol*. 2014;2014:1-5.
8. Cingü AK, Sogutlu-Sari E, Çinar Y, et al. Transient corneal endothelial changes following accelerated collagen cross-linking for the treatment of progressive keratoconus. *Cutan Ocul Toxicol*. 2014;33(2):127-131.
9. Kanellopoulos AJ. Long term results of a prospective randomized bilateral eye comparison trial of higher fluence, shorter duration ultraviolet A radiation, and riboflavin collagen cross linking for progressive keratoconus. *Clin Ophthalmol*. 2012;6(1):97-101.
10. Çinar Y, Cingü AK, Turkcu FM, et al. Accelerated corneal collagen cross-linking for progressive keratoconus. *Cutan Ocul Toxicol*. 2014;33(2):168-171.
11. Marcovich AL, Brandis A, Daphna O, et al. Stiffening of rabbit corneas by the bacteriochlorophyll derivative WST11 using near infrared light. *Investig Ophthalmol Vis Sci*. 2012;53(10):6378-6388.
12. ARVO. Statement for the Use of Animals in Ophthalmic and Visual Research. Published 2013
13. Fratzl P, Misof K, Zizak I, Rapp G, Amenitsch H, Bernstorff S. Fibrillar structure and mechanical properties of collagen. *J Struct Biol*. 1998;122(1-2):119-122.
14. Wollensak G, Iomdina E. Long-term biomechanical properties of rabbit cornea after photodynamic collagen crosslinking. *Acta Ophthalmol*. 2009;87(1):48-51.
15. ICNIRP (International Commission on Non-ionizing Radiation Protection). Guidelines on limits of exposure to broad-band incoherent optical radiation (0.38 To 3  $\mu$ M). *Health Phys*. 1997;73(3):539-554.
16. Kourkoumelis N, Tzaphlidou M. Eye safety related to near infrared radiation exposure to biometric devices. *ScientificWorldJournal*. 2011;11:520-528.
17. Hammer A, Richoz O, Mosquera SA, Tabibian D, Hoogewoud F, Hafezi F. Corneal biomechanical properties at different corneal cross-linking (CXL) irradiances. *Investig Ophthalmol Vis Sci*. 2014;55(5):2881-2884.

18. Wernli J, Schumacher S, Spoerl E, Mrochen M. The efficacy of corneal cross-linking shows a sudden decrease with very high intensity UV light and short treatment time. *Investig Ophthalmol Vis Sci*. 2013;54(2):1176-1180.
19. Scarcelli G, Besner S, Pineda R, Yun SH. Biomechanical characterization of keratoconus corneas ex vivo with brillouin microscopy. *Investig Ophthalmol Vis Sci*. 2014;55(7):4490-4495.





# Chapter 6

## **Long-term biomechanical and histologic results of WST-D/NIR corneal stiffening in rabbits, up to 8 months follow-up**

Jurriaan Brekelmans, Alexandra Goz, Mor M. Dickman, Alexander Brandis,  
Xiaomeng Sui, H. Daniel Wagner, Rudy M.M.A. Nuijts,  
Avigdor Scherz, and Arie L. Marcovich

*Invest. Ophthalmol. Vis. Sci.* 2017 Aug 1; 58(10):4089-4095



# ABSTRACT

Purpose: To determine the long-term safety and efficacy of WST-D/near-infrared (NIR) corneal stiffening.

Methods: One eye of 23 New Zealand White rabbits was de-epithelialized mechanically followed by topical application of 2.5 mg/mL WST11, combined with dextran-500 (WST-D) for 20 minutes. Subsequently, samples were irradiated with a NIR (755 nm) laser at 10 mW/cm<sup>2</sup> for 30 minutes. Untreated fellow eyes served as controls. One week (n = 4), 1 month (n = 6), 4 months (n = 9), or 8 months (n = 4) after treatment rabbits were euthanized. Corneal strips were cut in superior-inferior direction for extensimetry testing (1, 4, and 8 months), and histologic sections were prepared for evaluation of keratocyte distribution (1 week and 8 months).

Results: Elastic modulus after treatment was significantly higher than in paired controls (16.0 ± 2.3 MPa versus 9.6 ± 3.6 MPa,  $p = 0.008$ ; 18.1 ± 4.5 MPa versus 12.6 ± 2.3 MPa,  $p = 0.003$ ; and 18.6 ± 3.6 MPa versus 14.2 ± 3.6 MPa,  $p = 0.010$ ), at 1, 4, and 8 months, respectively). A significant decrease in keratocyte count at the anterior stroma was observed directly after treatment (1.5 ± 1.7 versus 19.0 ± 4.1,  $p = 0.002$ ). At 8 months keratocyte repopulation appeared completed, with similar distribution in treated and untreated corneas (15.9 ± 1.1 versus 14.5 ± 2.5,  $p = 0.562$ ). Corneal thickness was comparable between treated and untreated corneas at all time points.

Conclusions: WST-D/NIR treatment resulted in significant and persistent long-term increase in corneal stiffness. Initial keratocyte apoptosis in the anterior stroma is followed by repopulation to normal level at 8 months after treatment. The safe nature of NIR light allows treatment of corneas of any thickness without endangering corneal endothelium or deeper ocular structures, potentially benefiting patients deemed unsuitable for riboflavin/UVA cross-linking.

## INTRODUCTION

Keratoconus (KC), a bilateral progressive condition characterized by reduced corneal strength, progressive corneal thinning, and decreased visual acuity, is the leading cause of corneal transplantation at an early age, with high personal and societal costs.<sup>1,2</sup> Corneal collagen cross-linking (CXL) using riboflavin (RF) and ultra-violet A (UVA) irradiation is the first, and currently the only, clinically approved treatment capable of effectively arresting KC progression. RF/UVA CXL provides additional stiffening to the cornea, bridging the gap between disease onset and natural arrest of progression. Indeed, recent reports confirm a decrease in corneal transplantations for KC.<sup>3,4</sup>

Despite its promising long-term results, RF/UVA CXL has some disadvantages, mostly related to the toxic nature of UVA irradiation. Ocular exposure to high doses of UVA irradiance causes damage to deeper ocular structures, in particular the endothelium and the lens.<sup>5,6</sup> It is therefore of the utmost importance that enough UVA be absorbed by intrastromal RF, which can be achieved only in corneas with a minimal thickness of 400  $\mu\text{m}$ .<sup>7-9</sup> Keratoconus, an ectatic disorder, is characterized by progressive corneal thinning, rendering many patients unsuitable for RF/UVA CXL.<sup>10</sup>

The cascade of events triggered by RF upon UVA illumination, like that of many other photosensitizers, is initiated by generation of reactive oxygen species (ROS) that induce cross-links between collagen fibers.<sup>7</sup> Our group has recently reported on the safety and efficacy of corneal stiffening using near-infrared (NIR) light to activate the bacteriochlorophyll- derived photosensitizer WST-D.<sup>11</sup> NIR irradiation at a wavelength of 755 nm is safe to the eye and causes no discomfort by itself.<sup>12</sup> The ability to treat corneas of any thickness without endangering corneal endothelium or deeper ocular structures could potentially benefit patients deemed unsuitable for riboflavin/UVA cross-linking.

Keratoconus progression knows a relatively short lifespan, with a general onset at adolescence and natural regression during the third or fourth decade of life. Accumulation of nonenzymatic glycation end products, causing a stiffening effect of approximately 16% per decade, has been suggested to underlie age-related regression.<sup>13</sup> Therefore, to be successful, KC treatment has to provide sufficient corneal stiffening and maintain stability for an extended time to bridge the period between onset and natural stabilization. We have shown that WST-D/NIR treatment results in significant corneal stiffening 1 month after treatment in an *in vivo* and *ex vivo* rabbit animal model without toxic effect to corneal endothelial cells.<sup>11</sup>

Safety of systemic WST-D administration has also been established through its use in vascular-targeted photodynamic therapy of prostate cancer.<sup>14,15</sup> In the current study we set out to determine the long-term outcomes and histologic changes after WST-D/NIR treatment in an in vivo rabbit model, to evaluate the validity of this novel treatment for corneal CXL in a clinical setting.

# MATERIALS AND METHODS

## Animal model

One eye of twenty-three 3-month-old New Zealand White (NZW) rabbits was treated with WST-D/NIR according to standard protocol (Figure 1).<sup>11</sup> The rabbits had ad libitum access to food and water, and were housed at the Core Animal Facility of the Weizmann Institute of Science (Rehovot, Israel). All procedures were performed according to the Association for Research in Vision and Ophthalmology Statement for the Use of Animals in Ophthalmic and Visual Research, and following approval of the Institutional Animal Care and Use Committee of the Weizmann Institute of Science.<sup>16</sup>

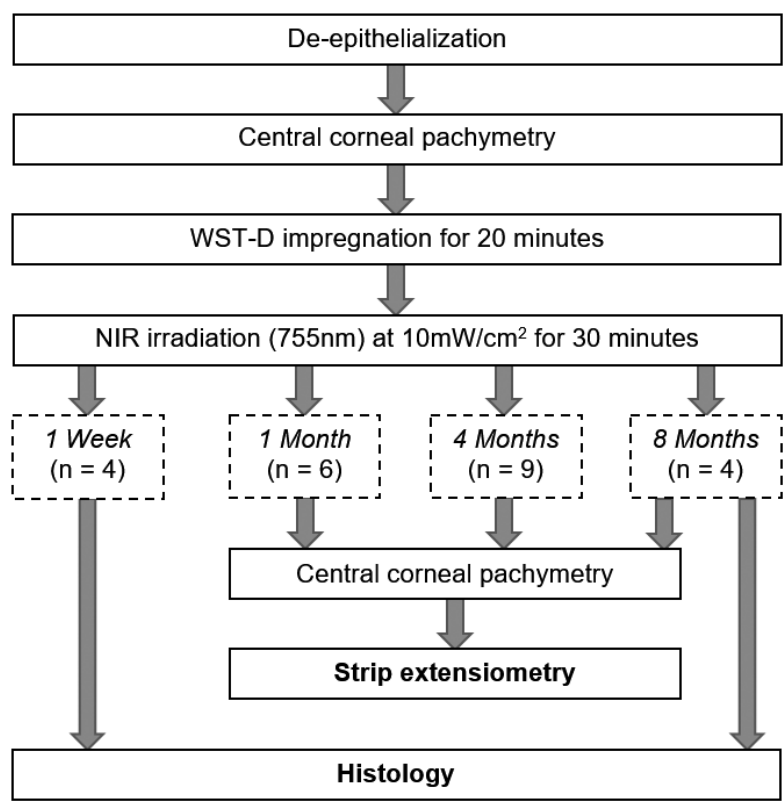


Figure 1. Flowchart of steps in current study. Left eye of each rabbit was (1) mechanically de-epithelialized, (2) its central corneal thickness was determined with ultrasound pachymetry, (3) WST-D solution was applied topically for 20 minutes, and (4) the cornea was irradiated with NIR for 30 minutes. (5) One week, 1 month, 4 months, or 8 months after treatment the rabbits were euthanized. The cornea's elastic modulus was determined by using strip extensimetry 1 month, 4 months, and 8 months after treatment. Histologic slides were prepared both 1 week and 8 months after treatment.

### Treatment procedure

Anesthesia was induced by intramuscular injections of 35 mg/kg ketamine (Rhône Merieux, Lyon, France) and 5 mg/kg xylazine (Vitamed, Benyamina, Israel). The epithelium of the left eyes was mechanically removed up to 2 to 3 mm of the limbus with a PRK spatula (Becton Dickinson, Franklin Lakes, NJ, USA). Treated corneas were impregnated for 20 minutes with 2.5 mg/mL WST11 (Steba Biotech, Luxembourg, France), in a 20% dextran 500-kDa (WST-D, Leuconostoc spp. Mr 450,000–650,000; Sigma-Aldrich Corp., St. Louis, MO, USA) and 0.9% saline solution corrected to a pH of 7.2 to 7.3. WST-D impregnated eyes were briefly rinsed with a few milliliters of artificial tears and irradiated for 30 minutes with a 755 nm NIR diode laser (CeramOptec, Bonn, Germany). Laser intensity at the corneal apex was confirmed to be 10 mW/cm<sup>2</sup> with a power meter (NOVEL; Ophir Optics, Jerusalem, Israel). Artificial tears (Tears Naturale Free; Alcon, Puurs, Belgium) were applied every 5 minutes during irradiation to prevent corneal dehydration. Immediately after treatment, Maxitrol ointment (Alcon) was applied and repeated once or twice daily until full re-epithelialization was confirmed by slit lamp evaluation with a fluorescent dye. The contralateral right eyes served as untouched controls and were kept closed during treatment. The rabbits were examined for corneal pathology by a trained cornea specialist (ALM) with a portable slit lamp, before treatment, regularly during epithelial healing, and directly before euthanization. Full epithelial regrowth was confirmed by fluorescent dye staining. One week (n = 4), 1 month (n = 6), 4 months (n = 9), or 8 months (n = 4) after treatment, rabbits were euthanized by intravenous injection of pentobarbital sodium (CTS Chemical Industries Ltd, Kiryat Malachi, Israel), and corneal samples were prepared for biomechanical or histologic evaluation. Corneal Pachymetry Central corneal thickness (CCT) was determined by ultrasound pachymetry (Humphrey ultrasonic pachymeters; Humphrey Instruments, San Leandro, CA, USA) before treatment (all rabbits) and before euthanasia (in the 1-, 4-, and 8-month follow-up groups). The last pachymetry measurement was used to determine the tissue elastic modulus.

### Biomechanical measurements

After enucleation, corneoscleral buttons were prepared in the 1-, 4-, and 8-month follow-up groups, and placed endothelial side down on paraffin hemispheres matching the corneal curvature. Corneas in the 1-week follow-up group were not tested for their biomechanical strength, as they might not have completely returned to physiological conditions. Central strips of  $4 \pm 0.2$  mm width with approximately 2 to 3 mm of sclera on both ends were cut in superior-inferior direction by using a self-constructed double-bladed cutter. Corneoscleral strips were kept on ice in closed humid Eppendorf containers pending biomechanical testing, approximately 2 hours after enucleation. The time between enucleation and biomechanical measurement was similar for all

strips. Strips were mounted horizontally between two clamps at a gauge length of 6 mm of a biomaterial tester loaded with a 200 N load cell (Minimat; Rheometric Scientific GmbH, Benzheim, Germany). Clamp tightening was controlled to be 9 cN·m by using a calibrated screwdriver (Torqueleader, Surrey, UK). Clamp distance was increased with a constant speed of 1 mm/min, while the applied force and corresponding displacement were measured constantly. Stress was calculated by normalizing the applied force by the cross-sectional area before testing, and strain by normalizing the displacement by the gauge length expressed percentually. Figure 2 shows the derived stress-strain curves of both a WST-D/NIR treated and control cornea, with their respective slopes representing the cornea's elastic modulus. Furthermore, in Figure 2 three distinguishable areas within the stress-strain curves are indicated. These areas represent different biomechanical properties: (1) a flat initial phase with nonlinear toe region, (2) a linear steep increase in the elastic region, and (3) a shallow increase during the plastic phase. Subsequently, a drop in force is seen, indicating breaking of the sample and end point of the measurement. The elastic modulus was determined in the linear region (2), as this is considered the true elastic modulus in which corneas exhibit only elastic properties under the physiological influence of intraocular pressure.<sup>17,18</sup> A blinded examiner (JB) determined the slope of the steep linear increase (i.e., the tissue's elastic modulus) three times for each sample to assure objective determination of the start and end of the linear region. The average was used in further analyses.<sup>17,18</sup>

### Histologic evaluation

One hemisphere of each cornea in the 1-week and 8-month follow-up groups was fixed in 4% formaldehyde. The fixed hemispheres were mounted in paraffin in anatomic configuration conserving the original corneal curvature, and 4 µm thick sagittal slices were cut. After staining with hematoxylin and eosin, five images of each sample were captured at x200 magnification (Eclipse 80i; Nikon, Tokyo, Japan) with a high-resolution charge-coupled device camera (DS-Fi1; Nikon). On each image, a 300 µm wide area in the center of the cornea was selected in which the coordinates of the stromal borders and keratocytes were manually determined by using the image-processing software Fiji and its Cell Counter plugin (Figure 3).<sup>19</sup> Keratocytes were counted in a random fashion, blinded from treatment procedure or follow-up time, according to a predetermined counting protocol developed together with a certified pathologist (Ori Brenner, PhD, Department of Veterinary Resources, Weizmann Institute of Science, Rehovot, Israel). In accordance with this protocol, a cell was counted if it showed a dark-stained and oval nucleus 10 to 20 µm wide in a horizontal orientation, and was at least 50 µm apart from other keratocytes in the same horizontal plane. All other cellular objects were considered to reside in a plane other than the section under evaluation and were therefore not included in the count. The corneal stroma was divided to anterior, middle,

and posterior thirds, and the relative position of keratocytes throughout the stroma was determined by using a self-written MATLAB script (MATLAB R2016b; The MathWorks, Inc., Natick, MA, USA). In the treated eyes one week after treatment the depth of CXL was assessed by determining the average depth of keratocyte loss. An average depth of the five most anterior keratocytes was calculated, to limit the influence of single remaining keratocytes in the cross-linked stroma, and expressed as percentage of total stromal thickness (Figure 3).

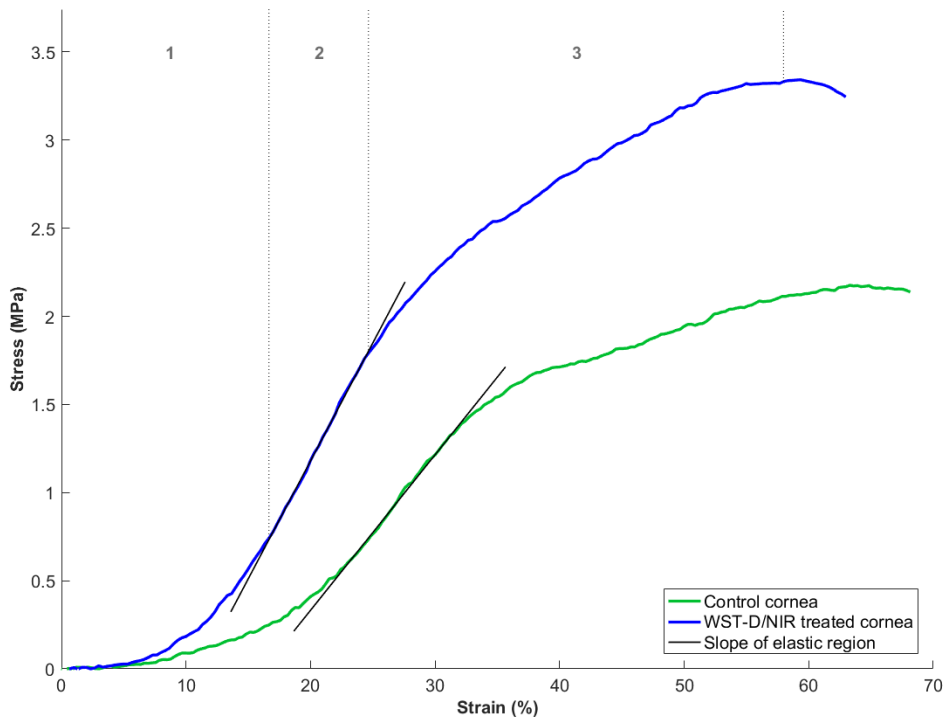


Figure 2. Stress-strain curves of untreated and WST-D/NIR-treated corneas, obtained by corneal strip extensimetry. For the WST-D/NIR-treated cornea, three regions, typically distinguishable in collagen-rich tissue, are indicated to illustrate the different biomechanical properties. These regions represent (1) a relaxing state and nonlinear toe region, (2) a linear elastic region showing collagen load bearing, and (3) a plastic region indicating breakage of interfibrillar bonds until complete rupture.



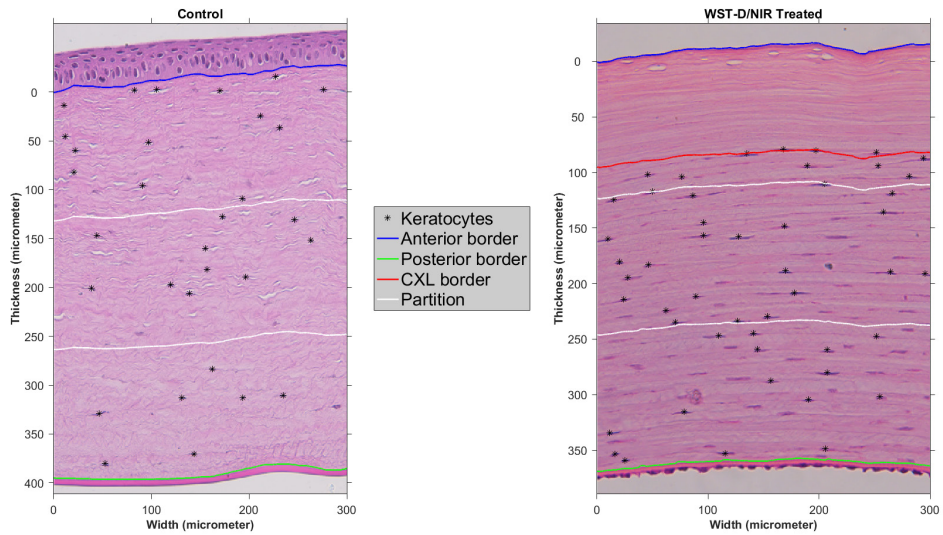


Figure 3. Representative histologic evaluation of a 300  $\mu\text{m}$  wide central area of a control (left) and WST-D/NIR-treated (right) cornea. Per cornea, five areas were analyzed, and the average keratocyte count and CXL depth was used for statistical testing. Lines indicate anterior stromal border (blue), posterior stromal border (green), derived partitioning lines dividing the stroma in three equal parts (white), and CXL depth (red). Keratocytes of 10 to 20  $\mu\text{m}$  width, with a horizontal distance of at least 50  $\mu\text{m}$ , and a clear visible nucleus, are marked (black cross).

### Statistical analyses

Elastic moduli and keratocyte counts were analyzed by using a repeated-measures analysis of variance (ANOVA), with treatment (treatment versus control) as within-subject effect and follow-up time as between-subject effect. A dependent Student's t-test was applied to the mean elastic moduli, central corneal pachymetry, and keratocyte counts of control and treated corneas. The level of statistical significance was set at 0.05 for all analyses. Statistical calculations were done with Statistica version 12 (StatSoft, Inc., Tulsa, OK, USA).

## RESULTS

### Corneal pachymetry

Table 1 shows the mean CCT for control and treated corneas, measured just before treatment (all corneas) and before extensimetry (1-, 4-, and 8-month groups). No significant differences were found between control and treated eyes before treatment and before extensimetry at all follow-up moments.

Table 1. Mean central corneal thickness (CCT) before treatment, and before extensimetry of treated and control eyes, per follow-up time.

		N	Central corneal thickness Control eyes	Central corneal thickness Treated eyes	<i>p</i> -value
1 Week	Pre-treatment	4	401.3 95% CI [375.8-426.7]	399.5 95% CI [373.6-425.4]	0.275
1 Month	Pre-treatment	6	387.2 95% CI [354.2-420.1]	395.5 95% CI [354.4-436.6]	0.436
	Pre-extensimetry	6	378.8 95% CI [354.6-403.1]	398.2 95% CI [354.9-441.4]	0.378
4 Months	Pre-treatment	9	411.7 95% CI [394.2-429.2]	411.9 95% CI [393.9-429.9]	0.842
	Pre-extensimetry	9	426.1 95% CI [409.9-442.4]	422.8 95% CI [400.8-444.7]	0.645
8 Months	Pre-treatment	4	355.5 95% CI [346.8-364.2]	363.8 95% CI [351.4-376.1]	0.133
	Pre-extensimetry	4	399.8 95% CI [366.8-432.7]	422.0 95% CI [382.9-461.1]	0.091

Mean and 95% confidence interval (95% CI) in  $\mu\text{m}$ . *p*-value for paired Student's *t*-test comparing treatment effect between control and treated eyes on the CCT.

### Elastic modulus

Four biomechanical measurements were excluded from analysis owing to accidental prestretching ( $n = 1$ , control group, 4 months), software error during measurement ( $n = 1$ , treatment group, 4 months), unequal strip preparation ( $n = 1$ , treatment group, 1 month), and slippage of the sample from the clamps during measurement ( $n = 1$ , treatment group, 8 months). Treatment was effective in all corneas compared to their paired untreated controls (Figure 4). Corneal stiffness was significantly higher in treated eyes than their paired controls by 6.4 MPa (16.0 MPa, 95% CI [13.2-18.8] versus 9.6 MPa, 95% CI

[5.1-14.0],  $n = 5$ ,  $p = 0.008$ ), 5.5 MPa (18.1 MPa, 95% CI [14.0-22.3] versus 12.6 MPa, 95% CI [10.5-14.7],  $n = 7$ ,  $p = 0.003$ ), and 4.4 MPa (18.6 MPa, 95% CI [9.5-27.6] versus 14.2 MPa, 95% CI [5.3-23.1],  $n = 3$ ,  $p = 0.010$ ) at 1, 4, and 8 months after treatment, respectively (Figure 5). A nonsignificant trend of gradual increase in corneal stiffness over time was noted in the control eyes, which might have reached significance given a larger sample size (factorial ANOVA;  $F_{2,12} = 2.620$ ,  $p = 0.114$ ).

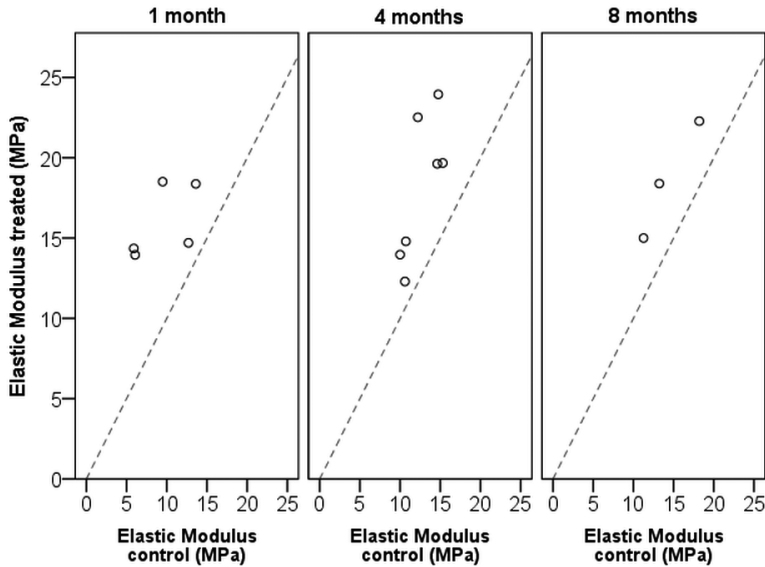


Figure 4. Elastic modulus of control relative to paired treated corneas, 1, 4, and 8 months after treatment. Dashed line indicates similar stiffness of control and treated corneas, with values left of the line indicating a stiffening effect after treatment. A significant treatment effect was seen in all pairs at all time points.

### Keratocyte count

One pair (8 months) was excluded from analysis owing to problems during fixation, resulting in respectively four and three pairs, with five different sections per cornea, to be included in histologic examination at 1-week and at 8-month follow-up. Table 2 shows the average number of keratocytes counted per 300  $\mu\text{m}$  wide region of the corneal stroma, 1 week or 8 months after treatment, for control and treated eyes. Compared with paired untreated eyes, a highly significant decrease in the number of keratocytes was measured in the anterior stroma 1 week after treatment ( $p = 0.002$ ), with an average CXL depth in treated eyes of 39.3% stromal thickness (95% CI [32.0-46.5]). Eight months after treatment, the number of keratocytes in the anterior stroma did not differ between treated and control eyes ( $p = 0.562$ ). Keratocyte count in the middle and posterior thirds

of the stroma did not differ between control and treated eyes at 1 week and at 8 months and between treatment groups at 1 week and at 8 months (factorial ANOVA;  $F_{1,5} = 0.263$ ,  $p = 0.630$  and  $F_{1,5} = 0.022$ ,  $p = 0.887$ , respectively).

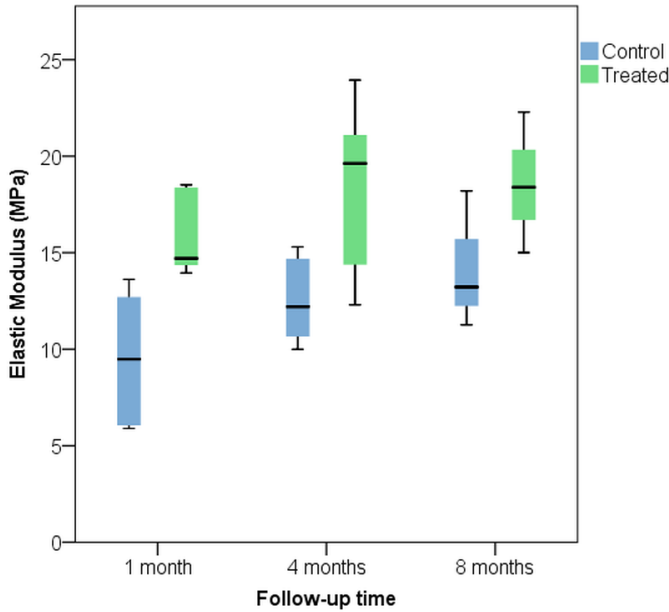


Figure 5. Boxplot of elastic moduli of treated and paired control eyes, per follow-up time. Elastic modulus increased significantly in the treated eyes compared to their paired control from  $9.6 \pm 3.6$  MPa to  $16.0 \pm 2.3$  MPa ( $p = 0.008$ ),  $12.6 \pm 2.3$  MPa to  $18.1 \pm 4.5$  MPa ( $p = 0.003$ ), and  $14.2 \pm 3.6$  MPa to  $18.6 \pm 3.6$  MPa ( $p = 0.010$ ) at 1, 4, and 8 months, respectively. In the control eyes a nonsignificant trend was seen of increasing corneal rigidity over time ( $F_{2,12} = 2.620$ ,  $p = 0.114$ ), which might have been significant given a larger sample size.

### Adverse effects

During this study no adverse effects, such as corneal edema, loss of transparency, haze formation, scarring, or corneal thinning, were observed after WST-D/NIR treatment. The applied WST-D slightly stains the cornea red during treatment, but this coloring disappeared within 1 to 2 days. Epithelial regrowth occurred within 5 to 7 days in all rabbits without complications, and no difference in thickness between control and treated eye, as a sign of corneal decompensation, was seen at any time point (Table 1). Although keratocyte loss was found in the anterior stroma 1 week after treatment, no related adverse effects were observed.

Table 2. Keratocyte count 1 week and 8 months after treatment, per stromal region for control and treated eyes.

	Region	n	Control	Treated	p-value
1 Week	Posterior	4x5	12.9	14.4	0.463
			95% CI [11.4-14.3]	95% CI [9.3-19.5]	
	Middle	4x5	12.8	12.1	0.640
			95% CI [10.2-15.4]	95% CI [8.8-15.3]	
	Anterior	4x5	19.0	1.5	0.002
			95% CI [12.5-25.5]	95% CI [-1.2-4.2]	
8 Months	Posterior	3x5	11.2	12.4	0.355
			95% CI [9.0-13.4]	95% CI [8.6-16.2]	
	Middle	3x5	11.2	12.1	0.810
			95% CI [6.8-15.6]	95% CI [1.9-22.3]	
	Anterior	3x5	14.5	15.9	0.562
			95% CI [8.3-20.6]	95% CI [13.1-18.6]	

Mean and 95% confidence interval (95% CI), in keratocytes per 300 µm wide histological section. For each corneal sample, the average keratocyte count of five different areas was used. *p*-value for paired Student's t-test comparing control and treated eyes per follow-up time.

## DISCUSSION

This study showed that WST-D/NIR achieves effective and sustained corneal stiffening over a period up to 8 months in an in vivo rabbit animal model. During this period, a trend toward natural age-related corneal stiffening was seen in the untreated fellow eyes. Keratoconus often presents during adolescence, progressing over time up to the third or fourth decade of life. During this period of approximately 20 years, nonenzymatic glycosylation occurs, stiffening the cornea to a degree such that progression is arrested.<sup>20,21</sup> To effectively prevent progression, the stiffening effect of CXL has to persist until natural corneal stiffening has occurred. The results of this study showed that the stiffening effect of WST-D/NIR persists up to 8 months when natural age-related stiffening reaches its highest values, in an in vivo NZW rabbit animal model.

Currently, RF/UVA is the only clinically approved CXL technique, with reported success rates between 90% to 100% and follow-up up to 10 years.<sup>22–24</sup> Despite excellent clinical outcomes, the classic Dresden protocol is unsuitable for corneas thinner than 400  $\mu\text{m}$ , owing to potential damage to the corneal endothelium and deep ocular structures.<sup>5–9</sup> WST-D has a peak excitation wavelength of approximately 755 nm in the NIR region, which provides deep tissue penetration, induces a low retinal response, and is safe to the eye for extended exposure at an irradiance of 10 mW/cm<sup>2</sup>.<sup>25</sup> Even higher irradiances are permitted for exposure times under approximately 16 minutes.<sup>25</sup> The applied irradiance in this study (10 mW/cm<sup>2</sup> for 30 minutes) is thus completely safe to the eye. In RF/UVA CXL a minimal corneal thickness of 400  $\mu\text{m}$ , fully impregnated with RF, is required to provide sufficient absorbance of toxic UVA irradiance to prevent damage to the endothelium. Alternatively, NIR light is nontoxic and thus does not have to be absorbed by WST-D to prevent endothelial damage, potentially permitting safe corneal stiffening regardless of corneal thickness.

In addition to measuring the biomechanical effect, histology at the last follow-up was compared to that obtained shortly after treatment as a measure for long-term safety of WST-D/NIR cross-linking. We found loss of keratocytes in the anterior stroma throughout, covering an average of 40% of stromal thickness 1 week after treatment, with full repopulation at 8 months. Full keratocyte repopulation suggests WST-D/NIR treatment does not compromise long-term corneal cellularity. The ability of activated keratocytes to migrate within the corneal stroma and repopulate after damage is well known.<sup>26</sup> Comparable keratocyte counts in the unaffected middle and posterior stroma of control and treated eyes, 1 week and 8 months after treatment, indicate that repopulation of the anterior stroma with keratocytes is independent of keratocyte counts in the middle and posterior stroma. Keratocyte repopulation may therefore begin from the periphery and follow the direction of the lamellae, rather than in posterior-anterior direction.

The underlying mechanism of keratocyte apoptosis is likely related to formation of ROS, superoxide and hydroxyl radicals, upon irradiation of WST-D by NIR light, similar to the reaction initiated by RF/UVA, whereby mainly singlet oxygen is generated and initiates CXL. A local excess in ROS, causing oxidative stress to the cornea, could potentially be detrimental to the corneal endothelium. To avoid such toxicity, RF/UVA applies light attenuation by a layer of RF that covers the cornea through treatment. Notably, RF penetration to the posterior cornea is not prevented by dextran. In contrast, the addition of high-molecular-weight dextran T-500 to the WST11 solution limits its penetration depth and speed, and prevents damage to the corneal endothelium from ROS.<sup>41</sup> This is in contrast to RF, where dextran maintains corneal dehydration, but does not influence RF penetration pattern. Dextran thus provides the possibility to control the penetration depth of WST-D and prevent localized damage to the endothelium by ROS formation, theoretically allowing safe treatment of patients with a thin cornea (CCT below 400  $\mu\text{m}$ ).

There is a limited understanding of the turnover of the corneal extracellular matrix and the exact biochemical changes during corneal CXL, limiting the prediction capability of the stiffening effect duration. The term (photosensitizer) 'corneal collagen cross-linking', such as used for RF/UVA and WST-D/NIR treatment, suggests that the stiffening effect is based on the formation of additional (covalent) bonds between, and within, the corneal extracellular matrix. The photochemical events and their kinetics are however still under debate and there is only limited evidence that covalent bonds are formed directly between collagen fibrils after RF/UVA CXL. Notably, the nontreated cornea in the aged rabbit approaches the stiffening of the treated cornea in the young rabbit. This finding suggests that 30-minute illumination after WST-D/NIR impregnation saturates the stiffening capability of the treated cornea. Indeed, in a very recent study we show that delivering a lower light dose, by reducing irradiation time with the same light fluency, can result in a similar stiffening effect.<sup>27</sup> A translation of this outcome to the clinical setting may significantly ease the treatment to the average patient.

To our knowledge, no studies have been performed comparing ageing of ocular tissue in rabbits to that in human, which is a limitation in the clinical translation of this study's results. In NZW rabbits, where sexual maturation occurs at the age of 6 months, corneal parameters such as keratometry and CCT are known to stabilize at approximately 8 months of age.<sup>28,29</sup> With measurements done at the age of 4, 7, and 11 months, data provided here, concerning corneal biomechanics, complement the preclinical landscape by addressing a relatively wide age range, with a premature, an intermediate, and a mature age included. Furthermore, a similar long-term follow-up study in rabbits treated by RF/UVA CXL shows results similar to this WST-D/NIR study.<sup>30</sup> Clinical data, with a follow-up of up to 10 years, available on RF/UVA CXL, show persistent stabilization of KC.<sup>22-24</sup>

In summary, WST-D/NIR treatment resulted in significant and long-lasting corneal stiffening that sustains for at least 8 months after treatment, bridging the period until natural age-related stiffening occurs. Treatment affected the anterior 40% of the corneal stroma, based on full keratocyte depletion 1 week after treatment. Eight months after treatment, full keratocyte repopulation was observed. The excellent safety characteristics of nontoxic NIR irradiance and the ability to control WST-D penetration suggest WST-D/NIR treatment could be a safe alternative for patients with advanced corneal thinning unsuited for RF/UVA CXL.



## REFERENCES

1. Kymes SM, Walline JJ, Zadnik K, Sterling J, Gordon MO. Changes in the Quality-of-Life of People with Keratoconus. *Am J Ophthalmol*. 2008;145(4):611-617.
2. Rebenitsch RL, Kymes SM, Walline JJ, Gordon MO. The lifetime economic burden of keratoconus: A decision analysis using a markov model. *Am J Ophthalmol*. 2011;151(5):768-773.e2.
3. Godefrooij DA, Gans R, Imhof SM, Wisse RPL. Nationwide reduction in the number of corneal transplantations for keratoconus following the implementation of cross-linking. *Acta Ophthalmol*. 2016;94(7):675-678.
4. Ghosheh FR, Cremona FA, Rapuano CJ, et al. Trends in penetrating keratoplasty in the United States 1980-2005. *Int Ophthalmol*. 2008;28(3):147-153.
5. Rogers CS, Chan LM, Sims YS, Byrd KD, Hinton DL, Twining SS. The effects of sub-solar levels of UV-A and UV-B on rabbit corneal and lens epithelial cells. *Exp Eye Res*. 2004;78(5):1007-1014.
6. Dong X, Löfgren S, Ayala M, Söderberg PG. Maximum tolerable dose for avoidance of cataract induced by ultraviolet radiation-B for 18 to 60 week old rats. *Exp Eye Res*. 2005;80(4):561-566.
7. Spoerl E, Mrochen M, Sliney D, Trokel S, Seiler T. Safety of UVA-riboflavin cross-linking of the cornea. *Cornea*. 2007;26(4):385-389.
8. Wollensak G, Spoerl E, Wilsch M, Seiler T. Endothelial cell damage after riboflavin-ultraviolet-A treatment in the rabbit. *J Cataract Refract Surg*. 2003;29(9):1786-1790.
9. Wollensak G, Spoerl E, Seiler T. Riboflavin/ultraviolet-A-induced collagen crosslinking for the treatment of keratoconus. *Am J Ophthalmol*. 2003;135(5):620-627.
10. Weed KH, MacEwen CJ, Giles T, Low J, McGhee CNJ. The Dundee University Scottish Keratoconus study: Demographics, corneal signs, associated diseases, and eye rubbing. *Eye*. 2008;22(4):534-541.
11. Marcovich AL, Brandis A, Daphna O, et al. Stiffening of rabbit corneas by the bacteriochlorophyll derivative WST11 using near infrared light. *Investig Ophthalmol Vis Sci*. 2012;53(10):6378-6388.
12. ICNIRP (International Commission on Non-ionizing Radiation Protection). Guidelines on limits of exposure to broad-band incoherent optical radiation (0.38 To 3  $\mu\text{m}$ ). *Health Phys*. 1997;73(3):539-554.
13. Elsheikh A, Wang D, Brown M, Rama P, Campanelli M, Pye D. Assessment of corneal biomechanical properties and their variation with age. *Curr Eye Res*. 2007;32(1):11-19.
14. Azzouzi AR, Barret E, Bennet J, et al. TOOKAD® Soluble focal therapy: pooled analysis of three phase II studies assessing the minimally invasive ablation of localized prostate cancer. *World J Urol*. 2015;33(7):945-953.
15. Azzouzi AR, Vincendeau S, Barret E, et al. Padeliporfin vascular-targeted photodynamic therapy versus active surveillance in men with low-risk prostate cancer (CLIN1001 PCM301): an open-label, phase 3, randomised controlled trial. *Lancet Oncol*. 2017;18(2):181-191.
16. ARVO. Statement for the Use of Animals in Ophthalmic and Visual Research. Published 2013
17. Liu X, Wang L, Ji J, et al. A Mechanical model of the cornea considering the crimping morphology of collagen fibrils. *Investig Ophthalmol Vis Sci*. 2014;55(4):2739-2746.
18. Elsheikh A, Anderson K. Comparative study of corneal strip extensometry and inflation tests. *J R Soc Interface*. 2005;2(3):177-185.
19. Schindelin J, Arganda-Carreras I, Frise E, et al. Fiji: An open-source platform for biological-image analysis. *Nat Methods*. 2012;9(7):676-682.

20. Cartwright NEK, Tyrer JR, Marshall J. Age-related differences in the elasticity of the human cornea. *Investig Ophthalmol Vis Sci*. 2011;52(7):4324-4329.
21. Elsheikh A, Geraghty B, Rama P, Campanelli M, Meek KM. Characterization of age-related variation in corneal biomechanical properties. *J R Soc Interface*. 2010;7(51):1475-1485.
22. O'Brart DPS, Patel P, Lascaratos G, et al. Corneal Cross-linking to Halt the Progression of Keratoconus and Corneal Ectasia: Seven-Year Follow-up. *Am J Ophthalmol*. 2015;160(6):1154-1163.
23. Poli M, Lefevre A, Auxenfans C, Burillon C. Corneal Collagen Cross-linking for the Treatment of Progressive Corneal Ectasia: 6-Year Prospective Outcome in a French Population. *Am J Ophthalmol*. 2015;160(4):654-662.e1.
24. Raiskup F, Theuring A, Pillunat LE, Spoerl E. Corneal collagen crosslinking with riboflavin and ultraviolet-A light in progressive keratoconus: Ten-year results. *J Cataract Refract Surg*. 2015;41(1):41-46.
25. Borchert M, Lambert J, Sliney D. Validation of ICNIRP estimates of toxicity thresholds for NIR (785 NM) light in the retinas of pigmented rabbits. *Health Phys*. 2006;90(1):3-10.
26. Torricelli AAM, Santhanam A, Wu J, Singh V, Wilson SE. The corneal fibrosis response to epithelial-Stromal injury. *Exp Eye Res*. 2016;142(4):110-118.
27. Brekelmans J, Goz A, Dickman MM, et al. Corneal Stiffening by a Bacteriochlorophyll Derivative with Dextran and Near-Infrared Light: Effect of Shortening Irradiation Time up to 1 Minute. *Cornea*. 2017;36(11):1395-1401.
28. Riau AK, Tan NYS, Angunawela RI, Htoon HM, Chaurasia SS, Mehta JS. Reproducibility and age-related changes of ocular parametric measurements in rabbits. *BMC Vet Res*. 2012;8(1):138.
29. Macari M, Machado CR. Sexual maturity in rabbits defined by the physical and chemical characteristics of the semen. *Lab Anim*. 1978;12(1):37-39.
30. Wollensak G, Iomdina E. Long-term biomechanical properties of rabbit cornea after photodynamic collagen crosslinking. *Acta Ophthalmol*. 2009;87(1):48-51.





# Chapter 7

## **Enzymatic digestion of porcine corneas cross-linked by hypo- and hyperosmolar formulations of riboflavin/ultra-violet A or WST11/ near-infrared light**

Jurriaan Brekelmans, Judith Veugen, Koen Rieff, Mor M. Dickman, Alexa Goz,  
Petra Wolffs, Alexander Brandis, Tos T.J.M. Berendschot, Rudy M.M.A. Nuijts,  
Avigdor Scherz, Arie L. Marcovich

*Transl. Vis. Sci. Technol.* 2020 Sep 3;9(10):4



# ABSTRACT

Purpose: To assess enzymatic digestion rate after Riboflavin (RF) and Water-Soluble-Taurine (WST11) based corneal cross-linking (CXL), with or without the addition of high molecular weight dextran (RF-D and WST-D).

Methods: Eighty-eight paired porcine corneas were cross-linked by either RF (n = 11) or RF-D (n = 11) and ultra-violet A (UVA) light, or WST11 (n = 11) or WST-D (n = 11) and near-infrared (NIR) light, or used as paired control (n = 44). Corneal buttons of treated and paired control eyes were placed in a 0.3% collagenase solution. Time to full digestion and remaining dry sample weight after six hours were compared.

Results: A strong treatment effect was seen with all four formulations, as all controls had been fully digested whilst all treated samples were still visible at the experiment's endpoint. After irradiation, central corneal thickness was significantly higher in samples treated with hypo-osmolar formulations, compared to dextran enriched formulations ( $p < 0.001$ ). Dry sample weight after digestion was non-significantly different between corneas treated by the four different formulations ( $p = 0.102$ ). Average dry sample weight was  $1.68 \pm 0.6$  (n = 10),  $2.19 \pm 0.50$  (n = 8),  $1.48 \pm 0.76$  (n = 11), and  $1.54 \pm 0.60$  (n = 9) mg, for RF, RF-D, WST11, and WST-D treated samples, respectively. Enzymatic resistance was similar for RF and WST based CXL ( $p = 0.61$ ) and was not affected by the addition of dextran ( $p = 0.221$ ).

Conclusions: Both RF and WST11 based CXL significantly increases resistance to enzymatic digestion, with similar effect for hypo-osmolar and hyperosmolar (dextran enriched) formulations.

## INTRODUCTION

After its introduction in 2003 by Wollensak *et al.*, Riboflavin/ultra-violet A (RF/UVA) cross-linking (CXL) has become a widely accepted treatment for keratoconus (KC), and multiple long-term clinical studies have shown its safety and efficacy.<sup>1-4</sup> The mechanism of action of RF/UVA CXL is thought to involve the formation of new bonds between the collagen bundles and surrounding proteoglycans within the corneal stroma.<sup>5</sup> Besides increasing corneal biomechanical properties, corneal CXL was also shown to increase resistance against enzymatic digestion (Table 1). Increased proteinase activity and reduced expression of proteinase inhibitors in keratoconic corneas play an important role in corneal thinning, a hallmark of progressive disease.<sup>6</sup> Increased resistance to keratolysis is therefore an important mechanism of action in arresting KC progression. Keratolysis is also a major complication of corneal infections, resulting in significant thinning and even corneal melting. RF/UVA CXL has therefore been suggested as a novel treatment modality for infectious keratitis (IK), with promising preliminary results.<sup>7</sup>

Despite the revolution introduced by RF/UVA CXL in the treatment of KC, there are still drawbacks to overcome, mainly related to the toxic nature of UVA irradiation.<sup>8</sup> To prevent irreversible endothelial damage and allow safe CXL treatment, corneal thickness has to be at least 400  $\mu\text{m}$ .<sup>9</sup> In corneal ectatic disorders such as KC and IK, this is often a problem because stromal thinning frequently progresses beyond this safety threshold. In the treatment of KC, several solutions have been suggested to overcome this problem, the most established of which is application of hypo-osmolar RF where dextran or other high molecular weight molecules are omitted from the formulation to induce corneal swelling above the 400  $\mu\text{m}$  safety threshold.<sup>10</sup>

In IK, progressive corneal melting with subsequent stromal thinning often occurs rapidly after onset of the disease, *a priori* rendering these patients unsuitable for currently available RF/UVA CXL treatment. Thus, patients suffering from IK may greatly benefit from a CXL modality that would allow treatment of thin corneas, postponing or preventing the need for invasive corneal transplantation.

To provide a safe alternative for patients with thin corneas, novel chromophores that can be excited at safer wavelengths have been investigated.<sup>11-13</sup> In 2012, our group established the stiffening capabilities of a water-soluble bacteriochlorophyll derivative, water-soluble-aurine (WST11), which is excited by near-infrared (NIR) light at 755 nm.<sup>13</sup> Because NIR light by itself in the applied intensities is nontoxic to the eye, corneal thickness may be reduced below the current threshold of 400  $\mu\text{m}$  without endangering the corneal endothelium or deeper ocular structures.<sup>14</sup> Although we have shown safe,

efficient, and long-term stiffening in rabbits, enzymatic resistance of WST11/NIR CXL had not yet been determined.<sup>15,16</sup> Moreover, in this study we compare for the first time corneal resistance to enzymatic digestion following application of hypo-osmolar and hyperosmolar (dextran enriched) RF, currently used in clinical practice.

Table 1. Studies reporting on enzymatic digestion after corneal cross-linking

Model	Essay	Treatment	Results	References
Porcine	Pepsin, trypsin, collagenase	RF/UVA	Slower digestion with higher irradiance	Spoerl <i>et al.</i> <sup>17</sup>
Porcine	Collagenase	RF/UVA	Increased resistance for both superficial and deeper crosslinked flaps	Schilde <i>et al.</i> <sup>18</sup>
Ox (fragmented)	Collagenase	SM+NM	Lower protein residue in controls	Naderi <i>et al.</i> <sup>19</sup>
Porcine (acellular)	Collagenase	Genipin	Highly reduced digestion after Genipin treatment	Liu <i>et al.</i> <sup>20</sup>
Porcine	Pepsin	RF/UVA	Highly reduced digestion after RF/UVA treatment	Hayes <i>et al.</i> <sup>5</sup>
Bovine	MMP's	RF/UVA	Resistance to cleavage by MMP's 1, 2, 9, and 13	Zhang <i>et al.</i> <sup>21</sup>
Human	Collagenase	RF/UVA	Increased resistance with longer irradiation up to 30 minutes	Arafat <i>et al.</i> <sup>22</sup>
Porcine	Collagenase	RB/GL	Reduced digestion after RB/GL treatment	Wang <i>et al.</i> <sup>23</sup>
Porcine	Pepsin	RF/UVA	Dresden protocol parameters most effective	Aldahlawi <i>et al.</i> <sup>24</sup>
Human (FS-LASIK)	Collagenase	RF/UVA	Increased resistance of deeper stroma after treatment	Kanellopoulos <i>et al.</i> <sup>25</sup>
Human	Collagenase	RF/UVA	Longer RF impregnation increases resistance	Laggner <i>et al.</i> <sup>26</sup>
Porcine	Pepsin	RF/UVA	Greater resistance with higher irradiation dose	Aldahlawi <i>et al.</i> <sup>27</sup>
Porcine (incl. epi-on)	Pepsin	RF/UVA	Hypo-osmolar RF less effective	Aldahlawi <i>et al.</i> <sup>28</sup>



Table 1. Continued

Model	Essay	Treatment	Results	References
Rabbit	Collagenase	RB/GL	RB/GL at high irradiance comparable to RF/UVA Dresden protocol	Fadlallah <i>et al.</i> <sup>29</sup>
Human	Collagenase	RF/UVA	Dresden achieves greatest resistance, compared to accelerated protocols	Kanellopoulos <i>et al.</i> <sup>30</sup>
Human	Collagenase	VP/RL	VP/RL comparable to RF/UVA	Alageel <i>et al.</i> <sup>12</sup>
Human (incl. trans-epi)	Collagenase	RF/UVA	Epi-on RF/UVA comparable to untreated controls	Cruzat <i>et al.</i> <sup>31</sup>
Mouse	Pepsin	RF/UVA	Digestion speed inversely correlated to biomechanical stiffness	Kling <i>et al.</i> <sup>32</sup>
Rat	Collagenase	RF/UVA	Threshold dose of 0.54 J/cm <sup>2</sup> to increase resistance	Zhu <i>et al.</i> <sup>33</sup>
Porcine	Pepsin	RF/UVA	Significant increase in resistance with higher RF concentrations	O'Brart <i>et al.</i> <sup>34</sup>

RF/UVA = Riboflavin/ultra-violet A, SM = sulfur mustard, NM = nitrogen mustard, MMP = matrix metalloproteinases, RB/GL = Rose Bengal/Green light, FS-LASIK = Femtosecond laser assisted in situ keratomileusis, epi-on = epithelium in situ, VP/RL = Verteporfin/Red laser, trans-epi = trans-epithelial

## METHODS

### Chromophore formulations

Four different chromophore formulations were prepared: (1) hypo-osmolar riboflavin (RF), (2) hyperosmolar riboflavin (RF-D), (3) hypo-osmolar WST11 (WST11), and (4) hyperosmolar WST11 (WST-D). Riboflavin formulations were prepared from 0.1% Riboflavin-5'-phosphate (F6750; Sigma-Aldrich, St. Louis, MO, USA) in 0.9% saline solution and used as is (RF) or enriched by 20% dextran 500 kD (RF-D; Leuconostoc spp. Mr 450,000-650,000, Sigma-Aldrich). Similarly, WST11 formulations were prepared from 0.25% WST11 (Steba Laboratories, Rehovot, Israel) in 0.9% saline solution, without (WST11) or with addition of 20% dextran 500 kD (WST-D). All solutions were corrected to a pH 7.2 to 7.3.

### Treatment procedure

Figure 1 shows a flow chart of the applied procedures. Eighty-eight porcine corneas were obtained in pairs from a local abattoir within two hours of enucleation, in accordance to the Association for Research in Vision and Ophthalmology Statement for the Use of Animals in Ophthalmic and Visual Research.<sup>35</sup> Per pair, one eye received full CXL treatment by either RF/UVA, RF-D/UVA, WST11/NIR, or WST-D/NIR ( $n = 11$  per group), the contralateral eye ( $n = 11$  per group) serving as paired control. Central corneal thickness (CCT) was determined for all corneas as an average of five consecutive measurements using an ultrasound pachymeter (Humphrey ultrasonic pachymeters; Humphrey Instruments, San Leandro, CA, USA) at four different time points: (1) before and (2) after de-epithelialization, (3) after chromophore impregnation, and (4) irradiation, if applicable. The corneal epithelium of all corneas, both treated and control, was removed mechanically up to the limbus using a blunt hockey knife. After de-epithelialization, a corneoscleral button was cut from the control eyes, tightly wrapped in clingfilm and aluminum foil, and frozen at  $-80^{\circ}\text{C}$  until further processing. Eyes in the treatment group were treated according to established protocols.<sup>1,13</sup> In short, eyes were impregnated through one of the aforementioned chromophore formulations by placing a chromophore filled plastic cup on top of the cornea for 30 (RF/RF-D) or 20 (WST11/WST-D) minutes. The corneas were then placed under UVA LED (RF/RF-D) or NIR laser light source (WST11/WST-D), calibrated to deliver  $3 \text{ mW}/\text{cm}^2$  or  $10 \text{ mW}/\text{cm}^2$ , respectively, to the corneal surface for 30 minutes. During irradiation the corneas were topically rehydrated in five-minute intervals to avoid dehydration. Corneoscleral buttons were then cut and frozen, similarly to the control group, until further testing.

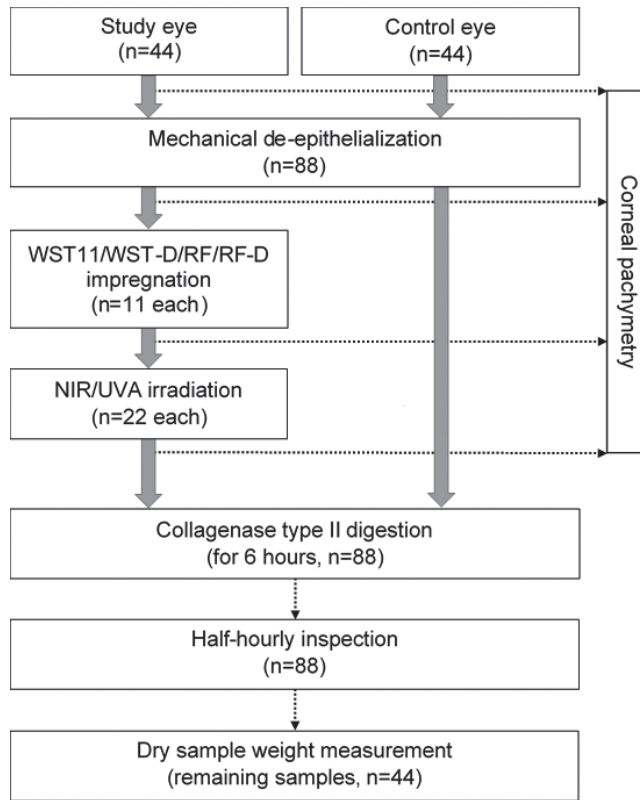


Figure 1. Study flowchart. Eighty-eight paired porcine eyes were mechanically de-epithelialized. One eye of each pair served as control ( $n = 44$ ), whereas the contralateral eye was treated by one of the following: WST11 ( $n = 11$ ) or WST-D (dextran enriched,  $n = 11$ ) impregnation with consecutive NIR irradiation, or RF ( $n = 11$ ) or RF-D ( $n = 11$ ) impregnation with UVA irradiation. Between steps, if applicable, central corneal thickness was measured by ultrasound pachymetry. After treatment, samples were subjected to a collagenase type II digestion assay, during which samples were inspected half-hourly. After six hours dry sample weight of remaining samples ( $n = 44$ ) was measured to quantify the degree of digestion.

### Enzymatic assay

After defrosting, the corneoscleral buttons were unwrapped and a central 8 mm button was punched and transferred to 12-well plates. Each well contained 2 mL of freshly prepared and cooled 0.3% collagenase of the same batch (420 u/mg; Type 2, Worthington Biochemical Corporation, Lakewood, USA) and Dulbecco's phosphate buffered saline solution (Biological Industries, Kibbutz Beit-Haemek, Israel) solution. The solution was measured to ensure a stable pH of 7.38, which allows for collagenase's optimal activity. Samples were covered in aluminum foil to prevent light exposure and transferred to a shaker rotating at 170 rpm in an incubator set at 37°C. A collagenase

digestion assay that is most commonly used in studies on corneal enzymatic digestion was applied (Table 1). Testing parameters were calibrated to achieve full digestion of native corneal samples in approximately five hours. Pilot studies showed this timeframe allowed for optimal differentiation between treatment groups, without the need to renew the collagenase solution as it loses its activity over time, deemed undesirable because fluid exchange may disrupt the remaining corneal tissue.

### **Quantification of digestion**

Pilot studies showed initial swelling in anterior-posterior direction, after which the posterior stroma detached and completely dissolved, leaving a thin lamella of anterior stroma behind. The dimensions of this remaining lamella appeared to remain quite stable over time in the CXL treated groups, thus measuring the samples' surface dimensions provided incomplete data. Therefore we adopted the approach established by O'Brart *et al.* to measure the samples' dry weight.<sup>34</sup> During a six hours digestion phase in the collagenase solution, sample appearance (n = 88) was assessed every 30 minutes by a blinded observer (JB) and time to full digestion was noted if no tissue was seen anymore. After six hours, the visibly remaining samples (n = 44) were transferred to Eppendorf containers and placed in a lyophilizer (Gamma 2-16 LSCplus; Martin Christ Gefriertrocknungsanlagen GmbH, Osterode am Harz, Germany) set at 0.2 mbar for 72 hours to fully dry the remaining corneal samples. Consecutively, the dry sample weight was determined. All measurements were done blinded from the received treatment.

### **Statistical analyses**

Baseline CCT characteristic were analyzed for control and treated groups, and for hypo-osmolar and hyperosmolar formulations using a one-way analysis of variance (ANOVA). Similarly, the sample's dry weight of treated corneas amongst chromophore groups and dextran addition was analyzed using a one-way ANOVA. The level of statistical significance was set at 0.05 for all analyses. Statistical calculations were done with SPSS software (version 25; IBM Corp., Armonk, NY, USA).

## RESULTS

### Baseline characteristics

Figure 2 shows the CCT per chromophore and treatment group before de-epithelialization, after de-epithelialization, and for the treated eyes after chromophore impregnation and irradiation. CCT at baseline was comparable between chromophore groups for both control ( $p = 0.148$ ) and treated ( $p = 0.124$ ) eyes. Samples were significantly ( $p < 0.001$ ) thicker after impregnation by hypo-osmolar chromophore formulations, compared to impregnation by hyper-osmolar formulations.

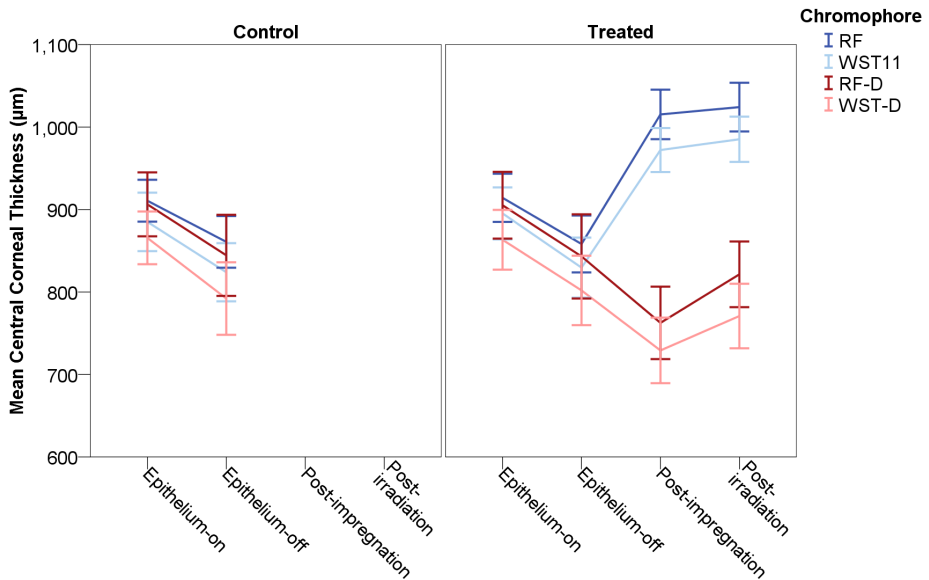


Figure 2. Mean central corneal thickness (CCT) for control ( $n = 44$ ) and treated ( $n = 44$ ,  $n = 11$  per chromophore) corneas. CCT was determined for each sample as the average of five consecutive measurements, and was repeated at different timepoints: (1) epithelium on, (2) epithelium off, (3) post-chromophore impregnation (treated group only), and (4) post-irradiation (treated group only). At baseline, no significant difference in CCT was seen between chromophore groups for both control ( $p = 0.148$ ) or treated ( $p = 0.124$ ) corneas. Hypo-osmolar chromophore impregnation induced significant swelling compared to impregnation by hyperosmolar formulations ( $p < 0.001$ ). CCT in  $\mu\text{m}$ , error bars indicate 95% confidence interval.

### Residual sample weight

All control samples ( $n = 44$ ) had been completely digested. In the treated group ( $n = 44$ ), average dry sample weight measurements read  $1.68 \pm 0.6$  ( $n = 10$ ),  $2.19 \pm 0.50$  ( $n = 8$ ),  $1.48 \pm 0.76$  ( $n = 11$ ), and  $1.54 \pm 0.60$  ( $n = 9$ ) mg, for RF, RF-D, WST11, and WST-D treated

samples, respectively. Six samples were excluded from analysis, as after 72 hours in the lyophilizer the Eppendorf containers of these samples still contained clearly visible liquid due to blockage of the venting holes. No significant difference in dry weight was seen between the four chromophore formulations (between-subject effect,  $p = 0.102$ ). Similarly, no significant differences were seen between RF-based (RF and RF-D) and WST11-based (WST11 and WST-D) formulations (between-subject effect,  $p = 0.061$ ), between hypo-osmolar (RF and WST11) and hyper-osmolar (RF-D and WST-D) solutions (between-subject effect,  $p = 0.221$ ).

### **Time to full digestion**

All treated samples remained after six hours of digestion, while all control samples had been completely digested. For the control samples, average time to digestion was  $5.4 \pm 0.2$ ,  $5.4 \pm 0.4$ ,  $5.5 \pm 0.3$ , and  $5.5 \pm 0.4$  hours in the RF, RF-D, WST11, and WST-D subgroups ( $n = 11$  each) respectively. No difference in time to full digestion was seen between the four chromophore groups ( $p = 0.864$ ).

## DISCUSSION

RF/UVA corneal CXL has been shown to effectively arrest KC progression, revolutionizing the treatment of KC.<sup>2–4</sup> The induced CXL by RF/UVA application relies on the formation of new bonds within the collagenous stroma, shown to increase corneal stiffness and resistance against enzymatic digestion.<sup>5</sup> Its success and limitations have led to the investigation of new drug formulations or chromophores and light combinations like WST-D/NIR for preventing potential toxicity induced by the RF/UVA application.<sup>11,13</sup> The bacteriochlorophyll derivative-WST11 is a novel drug, developed as photogenerator of hydroxyl and superoxide radicals. Although approved as first-line treatment for localized prostate cancer in the setting of intravenous infusion, we have looked at the possible utilization of WST11 in the setting of topical application for the treatment of KC. We showed significant and persistent stiffening of the cornea *in vivo*, with X-ray diffraction and electron microscopy studies showing unaltered corneal microstructure and transparency.<sup>13,36</sup> Increased proteolytic activity is believed to be a major driver of disease progression in KC and corneal melting in IK.<sup>37</sup> Thus, after establishing biomechanical and structural effects of WST11/NIR treatment, in this study we assess its effect on resistance against enzymatic digestion.

This study shows highly increased resistance against enzymatic digestion by both RF and WST11 based corneal collagen CXL in both treatment types. Several studies evaluated the keratolytic resistance of different CXL protocols (Table 1), mainly focusing on RF/UVA. Although the time lag for full digestion of untreated control samples in our study is in line with previous publications, direct comparison should consider differences in treatment protocols and available information regarding study parameters, in particular the enzymatic activity of the applied assay.<sup>12,22,29</sup> Therefore we chose to directly compare WST/NIR and RF/UVA CXL. All four formulations showed a very strong reduced rate of enzymatic digestion after treatment, indicating the keratolytic resistance of both RF/UVA and WST/NIR derived corneal stiffening. This may be in part the mechanism of action in arresting keratoconic progression and makes CXL techniques interesting in the treatment of IK.

To maintain physiological corneal thickness, clinically applied RF contains dextran, which can be omitted or reduced in thin corneas to induce corneal swelling. If corneal swelling can increase corneal thickness above the threshold of 400  $\mu\text{m}$  CXL safety can be guaranteed. If this threshold cannot be achieved, patients may require transplantation surgery. This safety mechanism relies on achieving a minimal stromal RF concentration, such that sufficient UVA is attenuated before it reaches deeper ocular structures, so as not to induce a photochemical response near the fragile endothelium. In contrast, WST-D is

activated by NIR light at an intensity that it is safe to ocular structures.<sup>38</sup> Thus WST-D/NIR safety profile can rely on the diffusion profile of WST11 within the cornea, rather than light attenuation, as no endothelial damage will occur without WST11 present at the endothelial level. WST11 penetration depth can be controlled by the addition of high molecular weight dextran at different concentrations, as dextran concentration is inversely related to WST11 penetration.<sup>13</sup> It is this control on penetration depth, combined with the application of safe NIR light, which may give WST-D/NIR CXL clinical relevance because it may allow for safe corneal CXL on thin corneas when RF/UVA CXL cannot be applied.

Besides the treatment effect of both chromophores, our results indicate no statistically significant difference in resistance to enzymatic digestion between the four formulations tested or between dextran-free and dextran-enriched formulations. Although not statistically significant, a notable higher residual dry weight is seen in favor of RF-D. Considering the dry weight of a nontreated porcine cornea is  $9.1 \pm 0.5$  mg, 18.5%, 24.1%, 16.3%, and 16.9% stromal tissue remained in this study for RF, RF-D, WST11, and WST-D treated corneas, respectively.<sup>39</sup> Although RF-D may result in more residual stromal tissue (5.6%-7.8% compared to the other three formulations), the other formulations provide greater safety due to induced swelling and utilization of nontoxic irradiation, as described above. This is of particular importance in the treatment of IK, as IK is often associated with corneal thinning rendering corneal thickness below the safety threshold of 400  $\mu$ m for RF-based CXL. This balance between efficacy and safety may present a clinical dilemma.

As with previous studies investigating the enzymatic resistance of CXL methods, the in vitro model has limitations in mimicking the in vivo situation. Although it provides a good comparison between techniques, the clinical relevance remains to be determined and residual dry sample weight may not correlate directly to the clinical effect or relevance. In vivo studies are needed to further assess treatment efficacy in IK. Most in vivo studies have proven to be challenging, as the degree of infection is hard to control and the time point for performing CXL is debated. Current available studies on PACK-CXL were mainly conducted in a relatively advanced stage, with deep infectious penetration, often as a last resort.<sup>40,41</sup> Early CXL treatment may result in better effect as the treatment is predominantly effective in the anterior stroma. For deeper infections, potential benefits of WST-D/NIR CXL should be investigated, given its earlier described safety profile allowing to treat thinner corneas, and deep tissue penetration of NIR.

In conclusion, this study shows that both WST11 and RF based CXL have a strong anti-keratolytic effect, which may underlie the mechanism of action in both arresting KC progression and preventing stromal melting in IK. Reducing dextran concentration is



used clinically to allow for CXL in severely affected corneas, but its effect on the anti-keratolytic effect of CXL had not been investigated previously. Our results show that the addition of 20% high molecular weight dextran does not affect keratolytic resistance. This finding is important in CXL of thin corneas, as often seen in progressed KC and IK. WST-D/NIR CXL may provide a safe alternative in thin corneas due to the differences in safety profile. Although RF/UVA CXL has shown great results in arresting KC, studies investigating other CXL techniques should be encouraged to better personalize and broaden the application of CXL treatment.

## REFERENCES

1. Wollensak G, Spoerl E, Seiler T. Riboflavin/ultraviolet-A-induced collagen crosslinking for the treatment of keratoconus. *Am J Ophthalmol*. 2003;135(5):620-627.
2. O'Brart DPS, Patel P, Lascaratos G, et al. Corneal Cross-linking to Halt the Progression of Keratoconus and Corneal Ectasia: Seven-Year Follow-up. *Am J Ophthalmol*. 2015;160(6):1154-1163.
3. Poli M, Lefevre A, Auxenfans C, Burillon C. Corneal Collagen Cross-linking for the Treatment of Progressive Corneal Ectasia: 6-Year Prospective Outcome in a French Population. *Am J Ophthalmol*. 2015;160(4):654-662.e1.
4. Raiskup F, Theuring A, Pillunat LE, Spoerl E. Corneal collagen crosslinking with riboflavin and ultraviolet-A light in progressive keratoconus: Ten-year results. *J Cataract Refract Surg*. 2015;41(1):41-46.
5. Hayes S, Kamma-Lorger CS, Boote C, et al. The Effect of Riboflavin/UVA Collagen Cross-linking Therapy on the Structure and Hydrodynamic Behaviour of the Ungulate and Rabbit Corneal Stroma. *PLoS One*. 2013;8(1):e52860.
6. Zhou L, Sawaguchi S, Twining SS, Sugar J, Feder RS, Yue BYJT. Expression of degradative enzymes and protease inhibitors in corneas with keratoconus. *Investig Ophthalmol Vis Sci*. 1998;39(7):1117-1124.
7. Tabibian D, Mazzotta C, Hafezi F. PACK-CXL: Corneal cross-linking in infectious keratitis. *Eye Vis*. 2016;3(1):11.
8. Ivanov I V., Mappes T, Schaupp P, Lappe C, Wahl S. Ultraviolet radiation oxidative stress affects eye health. *J Biophotonics*. 2018;11(7):e201700377.
9. Spoerl E, Mrochen M, Sliney D, Trokel S, Seiler T. Safety of UVA-riboflavin cross-linking of the cornea. *Cornea*. 2007;26(4):385-389.
10. Raiskup F, Spoerl E. Corneal cross-linking with hypo-osmolar riboflavin solution in thin keratoconic corneas. *Am J Ophthalmol*. 2011;152(1):28-32.e1.
11. Cherfan D, Verter EE, Melki S, et al. Collagen cross-linking using rose bengal and green light to increase corneal stiffness. *Investig Ophthalmol Vis Sci*. 2013;54(5):3426-3433.
12. Alageel SA, Arafat SN, Salvador-Culla B, et al. Corneal Cross-Linking with Verteporfin and Nonthermal Laser Therapy. *Cornea*. 2018;37(3):362-368.
13. Marcovich AL, Brandis A, Daphna O, et al. Stiffening of rabbit corneas by the bacteriochlorophyll derivative WST11 using near infrared light. *Investig Ophthalmol Vis Sci*. 2012;53(10):6378-6388.
14. Borchert M, Lambert J, Sliney D. Validation of ICNIRP estimates of toxicity thresholds for NIR (785 NM) light in the retinas of pigmented rabbits. *Health Phys*. 2006;90(1):3-10.
15. Brekelmans J, Goz A, Dickman MM, et al. Corneal Stiffening by a Bacteriochlorophyll Derivative with Dextran and Near-Infrared Light: Effect of Shortening Irradiation Time up to 1 Minute. *Cornea*. 2017;36(11):1395-1401.
16. Brekelmans J, Goz A, Dickman MM, et al. Long-term biomechanical and histologic results of WST-D/NIR corneal stiffening in rabbits, up to 8 months follow-up. *Investig Ophthalmol Vis Sci*. 2017;58(10):4089-4095.
17. Spoerl E, Wollensak G, Seiler T. Increased resistance of crosslinked cornea against enzymatic digestion. *Curr Eye Res*. 2004;29(1):35-40.
18. Schilde T, Kohlhaas M, Spoerl E, Pillunat LE. Enzymatic evidence of the depth dependence of stiffening on riboflavin/UVA treated corneas. *Ophthalmologe*. 2008;105(2):165-169.

19. Naderi M, Jadidi K, Falahati F, Alavi SA. The effect of sulfur mustard and nitrogen mustard on corneal collagen degradation induced by the enzyme collagenase. *Cutan Ocul Toxicol.* 2010;29(4):234-240.
20. Liu Z, Zhou Q, Zhu J, et al. Using genipin-crosslinked acellular porcine corneal stroma for cosmetic corneal lens implants. *Biomaterials.* 2012;33(30):7336-7346.
21. Zhang Y, Mao X, Schwend T, Littlechild S, Conrad GW. Resistance of corneal RFUVA-cross-linked collagens and small leucine-rich proteoglycans to degradation by matrix metalloproteinases. *Investig Ophthalmol Vis Sci.* 2013;54(2):1014-1025.
22. Arafat SN, Robert MC, Shukla AN, Dohlman CH, Chodosh J, Ciolino JB. UV cross-linking of donor corneas confers resistance to Keratolysis. *Cornea.* 2014;33(9):955-959.
23. Wang T, Peng Y, Shen N, Yu Y, Yao M, Zhu J. Photochemical activation increases the porcine corneal stiffness and resistance to collagenase digestion. *Exp Eye Res.* 2014;123:97-104.
24. Aldahlawi NH, Hayes S, O'Brart DPS, Meek KM. Standard versus accelerated riboflavin-ultraviolet corneal collagen crosslinking: Resistance against enzymatic digestion. *J Cataract Refract Surg.* 2015;41(9):1989-1996.
25. Kanellopoulos AJ, Asimellis G, Salvador-Culla B, Chodosh J, Ciolino JB. High-irradiance CXL combined with myopic LASIK: Flap and residual stroma biomechanical properties studied ex-vivo. *Br J Ophthalmol.* 2015;99(6):870-874.
26. Laggner M, Pollreisz A, Schmidinger G, et al. Correlation between multimodal microscopy, tissue morphology, and enzymatic resistance in riboflavin-UVA cross-linked human corneas. *Investig Ophthalmol Vis Sci.* 2015;56(6):3584-3592.
27. Aldahlawi NH, Hayes S, O'Brart DPS, Akhbanbetova A, Littlechild SL, Meek KM. Enzymatic resistance of corneas crosslinked using riboflavin in conjunction with low energy, high energy, and pulsed UVA irradiation modes. *Investig Ophthalmol Vis Sci.* 2016;57(4):1547-1552.
28. Aldahlawi NH, Hayes S, O'Brart DPS, O'Brart ND, Meek KM. An investigation into corneal enzymatic resistance following epithelium-off and epithelium-on corneal cross-linking protocols. *Exp Eye Res.* 2016;153:141-151.
29. Fadlallah A, Zhu H, Arafat S, Kochevar I, Melki S, Ciolino JB. Corneal resistance to keratolysis after collagen crosslinking with rose bengal and green light. *Investig Ophthalmol Vis Sci.* 2016;57(15):6610-6614.
30. Kanellopoulos AJ, Loukas YL, Asimellis G. Cross-linking biomechanical effect in human corneas by same energy, different UV-A fluence: An enzymatic digestion comparative evaluation. *Cornea.* 2016;35(4):557-561.
31. Cruzat A, Shukla AN, Arafat SN, et al. Ex vivo study of transepithelial corneal cross-linking. *J Refract Surg.* 2017;33(3):171-177.
32. Kling S, Hammer A, Conti A, Hafezi F. Corneal cross-linking with riboflavin and UV-A in the mouse cornea in vivo: Morphological, biochemical, and physiological analysis. *Transl Vis Sci Technol.* 2017;6(1):7.
33. Zhu Y, Reinach PS, Zhu H, et al. High-intensity corneal collagen crosslinking with riboflavin and UVA in rat cornea. *PLoS One.* 2017;12(6):e0179580.
34. O'Brart NAL, O'Brart DPS, Aldahlawi NH, Hayes S, Meek KM. An investigation of the effects of riboflavin concentration on the efficacy of corneal cross-linking using an enzymatic resistance model in porcine corneas. *Investig Ophthalmol Vis Sci.* 2018;59(2):1058-1065.
35. ARVO. Statement for the Use of Animals in Ophthalmic and Visual Research. Published 2013

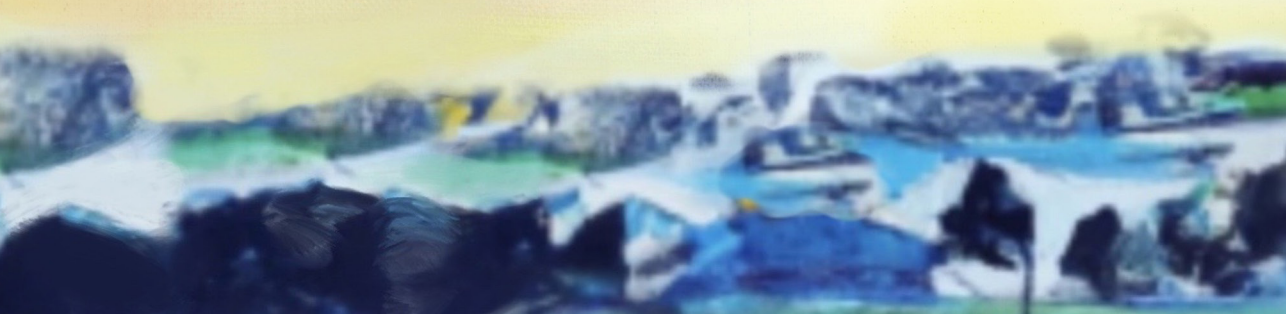
36. Hayes S, Aldahlawi N, Marcovich AL, et al. The effect of bacteriochlorophyll derivative WST-D and near infrared light on the molecular and fibrillar architecture of the corneal stroma. *Sci Rep.* 2020;10(1):9836.
37. Balasubramanian SA, Pye DC, Willcox MDP. Are proteinases the reason for keratoconus. *Curr Eye Res.* 2010;35(3):185-191.
38. ICNIRP (International Commission on Non-ionizing Radiation Protection). Guidelines on limits of exposure to broad-band incoherent optical radiation (0.38 To 3  $\mu$ M). *Health Phys.* 1997;73(3):539-554.
39. S ndergaard AP, Ivarsen A, Hjortdal J. Reduction of stromal swelling pressure after UVA-riboflavin cross-linking. *Investig Ophthalmol Vis Sci.* 2013;54(3):1625-1634.
40. Idrus EA, Utti EM, Mattila JS, Krootila K. Photoactivated chromophore corneal cross-linking (PACK-CXL) for treatment of severe keratitis. *Acta Ophthalmol.* 2019;97(7):721-726.
41. Hsia YC, Moe CA, Lietman TM, Keenan JD, Rose-Nussbaumer J. Expert practice patterns and opinions on corneal cross-linking for infectious keratitis. *BMJ Open Ophthalmol.* 2018;3(1):e000112.





# Chapter 8

## General discussion







## GENERAL DISCUSSION

Collagen cross-linking (CXL) bridged a century-long gap in keratoconus (KC) management between symptomatic treatment using contact lenses and highly invasive corneal transplantation. Therefore, it is not unexpected that adoption into clinical practice was rapid. While the U.S. Food and Drug Administration (FDA) only approved corneal CXL in 2016; off-label use in other parts of the world has provided almost two decades of valuable data since the clinical introduction of Riboflavin (RF) and ultra-violet A (UVA) CXL by Wollensak in 2003.<sup>1</sup> Meanwhile, CXL's success in arresting KC progression has been confirmed in multiple long-term follow-up studies in over 90% of adolescent patients.<sup>2,3</sup> In line with these studies, we demonstrate a 90.7% success rate for RF/UVA CXL in our clinic's long-term follow-up retrospective study in **Chapter 2**.<sup>4</sup> Due to its promising results, early adaptation, and many studies, RF/UVA CXL became a synonym for corneal CXL. However, this thesis shows there is more to CXL than RF/UVA only.

### Why investigate alternatives?

If treatment success rates are as high as 90%, why investigate alternatives to RF/UVA CXL? First, UVA is intrinsically toxic to ocular structures. Thus the safety of corneal RF/UVA CXL relies on sufficient attenuation by RF.<sup>5</sup> While its safety has been established under certain conditions, irradiation applying other wavelengths could highly benefit CXL safety. Several groups attempted to excite RF by either blue light or nonlinear optical (NLO) CXL, circumventing the need for UVA while still using RF.<sup>6-9</sup> Second, derived from this safety implication, is the minimal required corneal thickness. Although controversial, with reports on safe CXL of thinner corneas, a corneal thickness of 400  $\mu\text{m}$  is often still considered the minimum to allow safe RF/UVA CXL.<sup>10</sup> Given the progressive thinning nature of KC, this excludes a significant number of patients from CXL treatment. Third, although 90% is a high success percentage, still 10% of patients (often children, pregnancy-related ectasia, or thin corneas) show progression at some point in life after RF/UVA CXL treatment.<sup>11,12</sup> Repeated RF/UVA CXL was shown *ex vivo* not to result in additional stiffening and clinical reports on the efficacy of repeated RF/UVA CXL procedures after primary treatment failure are few and inconclusive.<sup>13-15</sup> Alternative CXL modalities may provide a solution in cases unresponsive to RF/UVA CXL. Fourth, the need for de-epithelialization remains a significant downside of RF/UVA CXL. Alternative modalities with lower molecular weights or more hydrophilic characteristics potentially allow CXL while leaving the epithelium (partially) *in situ*. Fifth, while established for corneal application, CXL may be interesting for other ocular indications, such as scleral CXL in treating progressive myopia. However, the intrinsic toxic nature of UVA proves a limiting

factor for application to deeper ocular structures. Sixth, in general, competing products stimulate free market forces that can reduce treatment costs. Especially in the United States, where FDA approval was granted only to a single platform, this may benefit patients and society.

## ASSESSING CORNEAL CROSS-LINKING EFFICACY

### How to evaluate a corneal cross-linking modality in a pre-clinical setting

In ex vivo (animal) studies, destructive testing modalities provide direct options to assess CXL efficacy. Biomechanical testing and determining keratolytic resistance are frequently used to assess CXL efficacy. Measuring the cornea's elastic modulus (often referred to as Young's Modulus) through strip extensimetry or inflation tests is a well-established model, with strip extensimetry, either mono- or biaxial, probably being the most frequent applied.<sup>16–22</sup> While its principle is relatively straightforward (i.e., measuring deformation while applying a known force), its interpretation can be challenging due to the heterogeneity and viscoelastic properties of the cornea. Heterogeneity exists both in-plane (the peripheral cornea is stiffer compared to the center) and in-depth (the anterior cornea is more rigid than the posterior cornea), between individuals (with increased stiffness in older subjects), and under different testing conditions (e.g., differences in hydration).<sup>18,20,23</sup> Thus, to obtain reliable and repeatable measurements, it is pertinent to be consistent in the methodology with particular attention to the sample's orientation and hydration during testing, the sample's age at testing, and the analysis method of the acquired data.

#### *Strip extensimetry*

Extensimetry testing yields a stress-strain curve (**Chapter 5**, Figure 2), as a strip of tissue is stretched at a known rate while the force applied is measured (**Chapter 5**, Figure 1). From this curve, a single value (the elastic modulus) can be derived for comparison. However, since the cornea is a viscoelastic tissue, as addressed in **Chapter 1**, stress-strain curves show a response with three distinctive regions rather than a single linear response, as seen in pure elastic tissue.<sup>24,25</sup> The first ('toe region') and third ('heel region') are non-elastic, while the second does show an elastic response.<sup>26</sup> Studies on corneal biomechanics applying strip extensimetry often report on a 'Young's modulus' at a strain between 6–12%. While this terminology is incorrect (Young's modulus represents an elastic modulus, while 6–12% strain is still within the range of non-elastic behavior), it also introduced a widespread misapprehension in the current literature on corneal CXL. The toe region represents uncrimping of collagen helices, as excised strips are in a relaxed state due to cessation of the force exerted by the physiologic intraocular pressure. The second region shows an elastic response that allows calculation of the elastic modulus (i.e., Young's Modulus), as applied in **Chapters 4, 5, and 6**, which correspond to physiological conditions.<sup>26–28</sup> Thus, while studies reporting on a modulus at 6–12% can establish a treatment effect (given similar conditions and analysis within a single study), great caution is advised when comparing between studies or when inferring potential clinical application if a modulus is calculated outside of the elastic region.

### *Enzymatic digestion*

Keratolytic activity is known to be elevated in KC-affected corneas, the culprit of the observed corneal thinning.<sup>29,30</sup> Corneal CXL is hypothesized to reduce enzymatic digestion by:

1. Increased biomechanical stability.
2. Reduced number of cleavage sites due to the additionally formed cross-links within the extracellular matrix.
3. CXL treatment may also reduce the rate of enzyme penetration through the stroma.

Measuring resistance against enzymatic digestion after CXL treatment thus became a second method to assess CXL efficacy in an ex vivo setting.<sup>31–46</sup> This method became even more relevant after the introduction of corneal CXL in treating infectious keratitis, in which enzymatic digestion plays a prominent role. Several protocols have been applied to assess enzymatic digestion, mainly including collagenase or pepsin (**Chapter 7**, Table 1).<sup>38</sup> In **Chapter 7**, we show in an ex vivo porcine model that both RF/UVA CXL and CXL using water-soluble-aurine (WST11) and near-infrared (NIR) light significantly increase the resistance against collagenase digestion.<sup>38</sup>

### **How to evaluate a corneal cross-linking modality in a clinical setting**

#### *Corneal topography, anterior segment optical coherence tomography and visual acuity*

The primary goal of clinical corneal CXL treatment for KC is to arrest corneal ectatic progression long-term and, ideally, induce corneal flattening. While the latter is frequently seen with the current RF/UVA CXL and is related to the improvement of uncorrected visual acuity, the main goal of corneal CXL is to prevent further visual impairment. Clinically, outcome measures on CXL effectivity are often based on corneal topographic indices, refraction and visual acuity. Using optical coherence tomography (OCT) a demarcation line can be seen after CXL, suggested to be the boundary between treated and untreated corneal stroma.<sup>47</sup> Safety parameters include endothelial cell counts and adverse events. In **Chapter 2**, we report on corneal topography indices, refraction and visual acuity, endothelial cell damage, adverse events, and treatment failure in a retrospective long-term follow-up clinical study of 265 eyes treated by RF/UVA CXL in our clinic. In this retrospective five-year follow-up study, we found significantly decreased keratometry values, and improved and stable visual acuity, while no endothelial cell loss or persistent complications were seen. However, 9.3% of the eyes continued progressing (defined as  $\geq 1$  diopter increase in mean keratometry) one year after treatment.<sup>4</sup>

### *Corneal biomechanics and collagen fibril organization*

The effectiveness of CXL in arresting KC progression is believed to result from increased biomechanical stiffness. Therefore, clinical biomechanical measurements in diagnosing KC and assessing CXL efficacy remain topics of investigation. Over the years, two clinical systems have been applied to measure corneal biomechanics in vivo: the Ocular Response Analyzer (Reichert Ophthalmic Instruments, NY, USA) and the CorVis ST (Oculus, Wetzlar, Germany).<sup>48–50</sup> While both measure the degree of deformation inflicted by a metered air puff, each provides its indices, and thus, outcomes can not be directly compared. In addition, while KC-affected corneas are significantly different from healthy corneas, sensitivity and specificity in diagnosing KC are low, and the clinical applicability of such devices remains under discussion.<sup>24,51,52</sup> Another non-invasive and more recently developed method to measure corneal biomechanics is Brillouin spectroscopy, which allows for highly detailed and mapped imaging of the corneal elastic modulus.<sup>53</sup> Brillouin measurements are still very time-consuming, and the technique is not readily available in the clinic (yet), currently rendering it applicable to research settings only. Altered collagen fibril organization is known to influence corneal biomechanical properties, and has thus been topic of interest in both KC diagnosis and assessing CXL treatment effect. Clinically, polarization-sensitive optical coherence tomography (PS-OCT) can be applied to image corneal collagen fibril organization and identify alterations in KC affected corneas.<sup>54</sup> Similarly, PS-OCT was shown capable of objectifying changes after CXL, potentially providing a novel clinical tool to assess CXL efficacy and risk of KC progression.<sup>55</sup>

## INNOVATIONS IN CORNEAL CROSS-LINKING

The original corneal CXL protocol introduced by Wollensak (i.e., the ‘Dresden protocol’) includes full epithelial debridement of the central cornea, RF impregnation for 30 minutes, and consecutive UVA irradiation at three mW/cm<sup>2</sup> for an additional 30 minutes.<sup>1</sup> To date, this is the gold standard of corneal CXL and has been applied in many ophthalmological clinics, including ours (**Chapter 2**). In an attempt to overcome the aforementioned limitations, several groups have suggested alternative CXL modalities (addressed further below). Still, many more have introduced adaptations to the existing RF/UVA CXL Dresden protocol. These alterations generally include changes to three main parameters of RF/UVA CXL:

- Epithelial debridement (total, none, or partial)
- RF impregnation (RF formulation and impregnation duration)
- UVA irradiation (intensity, time, and location)

### Innovations in Riboflavin and ultra-violet A cross-linking

#### *Epithelial debridement*

The epithelium is a barrier to the extracorporeal environment, preventing pathogens from intruding and infecting the underlying tissue. However, the epithelium and its tight junctions prevent RF or other chromophores from penetrating the corneal stroma, which drives the need to entirely remove the epithelium (‘epi-off’ protocols) before RF is instilled. Multiple methods have been investigated to increase the stromal RF concentration without epithelial debridement (‘epi-on’ or ‘transepithelial’ protocols). A widely studied epi-on protocol aims to increase the diffusion of RF into the stroma by using iontophoresis, in which a voltage gradient over the cornea is created to facilitate the transport of charged RF molecules.<sup>56</sup> A recent meta-analysis from 2020 by Nath *et al.*, including approximately 1000 eyes, showed that epi-on CXL’s efficacy remains inferior to epi-off protocols.<sup>57</sup> While this may be partly due to lower stromal RF concentrations, there is also evidence that an intact epithelium limits the amount of available stromal oxygen needed in the photochemical reaction forming cross-links, thus reducing the efficacy of treatments. This has led to the introduction of goggles supporting the delivery of supplemental oxygen during CXL treatment, but the CXL effect is still lower compared to epi-off protocols.<sup>58,59</sup> Not included in the meta-analysis by Nath *et al.*, is the approach to only partially remove the epithelium. Partial disruption of the epithelium was previously attempted using specially designed disruptors or grid-pattern de-epithelialization, and more recently using laser by Bradford *et al.*, and our group.<sup>60–64</sup> In **Chapter 4**, we applied a clinically approved excimer laser platform to selectively ablate only 40% of the epithelium by creating evenly spaced epithelial channels. Similar to

the abovementioned studies on partial disruption, the total stromal RF concentration was reduced compared to full de-epithelialization. However, in contrast to earlier studies, we showed significant and comparable stiffening for partial and complete de-epithelialization. Clinical safety, efficacy, and feasibility should be further investigated, but this study provides a proof-of-concept for laser-assisted partial de-epithelialization and may provide, in part, an answer to the de-epithelialization problem.

### *Riboflavin impregnation*

Riboflavin, the water-soluble vitamin B<sub>2</sub>, was first described a century ago.<sup>65</sup> Its main form is as a component of the coenzyme flavin mononucleotide (or riboflavin-5'-phosphate) or flavin adenine dinucleotide. In RF/UVA corneal CXL, following Wollensak's Dresden protocol, riboflavin-5'-phosphate is applied in a 0.1% solution, enriched with 20% high molecular weight Dextran (T500) to maintain corneal hydration during the procedure. Several changes to the RF formulation have been investigated to increase epithelial permeability and stromal concentrations: RF concentration and osmolarity have been altered, or substances such as topical anaesthetics, sodium ethylenediaminetetraacetic acid, trometamol, benzalkonium chloride, and sodium chloride were added to increase epithelial permeability.<sup>66–69</sup> As said these epi-on approaches are considered to achieve inferior results compared to epi-off CXL.<sup>57</sup>

In current protocols, RF formulation and impregnation play an important role in addressing safety issues regarding the CXL of thin corneas. Besides being a supplier of reactive oxygen species (ROS) that induce cross-links, stromal RF also attenuates UVA light before it can reach the endothelium and cause cellular damage. Early in vitro experiments on corneal endothelial cells by Wollensak *et al.*, have shown a cytotoxic threshold dose for UVA (in the presence of RF) of 0.63 J/cm<sup>2</sup>.<sup>70</sup> Given the original Dresden protocol applies UVA light at a surface dose of 5.4 J/cm<sup>2</sup> (i.e., 30 [minutes] x 60 seconds x 3 mW/cm<sup>2</sup> = 5.4 J/cm<sup>2</sup>) and with the absorption coefficient of RF known, it was calculated that the RF-soaked cornea has to be at least 400 µm thick to sufficiently attenuate the UVA light below the toxic endothelial threshold of 0.63 J/cm<sup>2</sup>.<sup>70,71</sup> Current clinical practice in corneas with a thickness below this 400 µm safety limit, is to apply hypo-osmolar RF formulations to induce stromal swelling, or add an RF-soaked contact lens or continuous thin RF film on top of the corneal surface during irradiation to account for the lower stromal RF concentration.<sup>72,73</sup>

Another adaptation lies in RF application duration before UVA irradiation is initiated. Initially, Wollensak *et al.*, instilled RF for 5 minutes, after which staining of the aqueous was observed. Thus, full stromal RF penetration was assumed, adhering to the abovementioned requisite that sufficient stromal RF has to be present. However, in further developing RF/

UVA CXL, protocols with impregnation times ranging from two minutes to 35 minutes have been applied.<sup>74</sup> Eventually, thirty minutes became the standard in the 'Dresden protocol', as the theoretical stromal RF concentration after 30 minutes is high enough to attenuate sufficient UVA light before reaching the endothelium.<sup>71</sup> In **Chapter 2**, however, we showed, with a theoretical and experimental basis through ex vivo, in vivo, and in vitro experiments, that the duration of RF impregnation can be safely reduced from 30 minutes to 10 minutes. Although the total stromal RF concentration (and thus UVA attenuation) is higher after 30 minutes, 10 minutes of RF impregnation decreases the risk for endothelial cell damage. In a 10-minute protocol, more UVA light will reach the endothelium, but also less RF is available at the endothelial level, reducing the total photochemical reaction inducing damage at the endothelium.<sup>75</sup> This means RF/UVA CXL treatment time can safely be reduced by 20 minutes by reducing RF impregnation time from 30 minutes to 10 minutes.

#### *Ultra-violet A irradiation*

While in clinical practice, RF is uniformly irradiated with UVA light, RF has three notable absorption peaks:

1. In the ultra-violet C range (around 265 nm)
2. In the UVA range (about 370 nm)
3. Within the visible spectrum (blue light, about 445 nm)

The first can induce DNA damage, while the third may cause retinal damage, rendering both unsuitable for corneal CXL.<sup>76</sup> The second, UVA light, is mostly applied in current RF based CXL protocols, and while also potentially toxic to the endothelium, this toxicity greatly depends on the applied intensity and presence of RF. In the absence of RF, high endothelial doses of over 7.2 J/cm<sup>2</sup> must be reached before damage occurs.<sup>77</sup> In combination with RF present, endothelial toxicity however drastically increases and cytotoxic thresholds are reached at an endothelial UVA dose of only 0.63 J/cm<sup>2</sup>.<sup>70</sup> As discussed before, increasing stromal RF concentrations decrease the amount of UVA light reaching the endothelium by attenuation. Two more parameters influence the UVA dose delivered to the endothelium: (1) the applied surface UVA irradiance, and (2) the duration of the UVA irradiance. While influencing the stromal RF concentration and corneal thickness proves challenging, UVA irradiance and duration allow for more leeway. This has resulted in several alternative RF/UVA CXL protocols, so-called accelerated CXL (A-CXL) protocols, applying higher irradiances while reducing irradiation time.<sup>78</sup> The scientific knowledge and popularity of A-CXL are growing, and multiple different protocols are applied clinically, significantly reducing the total treatment time.<sup>78</sup> Equally adapting irradiance and duration, these protocols generally adhere to the maximal corneal surface dose of 5.4 J/cm<sup>2</sup>. More recently, individualized



CXL was introduced. The protocol considers the patient's pachymetry values and lowers the delivered corneal surface dose below the 5.4 J/cm<sup>2</sup> threshold by reducing UVA irradiance duration.<sup>79</sup> Another upcoming trend in altering UVA irradiation is customized CXL, in which the delivered UVA irradiance is not homogenous, with higher irradiance targeted at more affected areas (i.e., the cone).<sup>80</sup> Preliminary results of individualized and customized CXL appear promising, and future RF/UVA CXL is most likely to steer in this direction. Additional studies, alike the randomized controlled trial currently undertaken in our clinic (ClinicalTrials.gov identifier NCT04532788), are however still needed to show the benefits of customized CXL over conventional CXL in both efficacy and cost-efficiency.

### **Innovations in alternative corneal cross-linking modalities**

While relatively new to the field of ophthalmology, collagen CXL is a well-known process in bio-engineering and industry, with applications in the pharmaceutical, cosmetic and food industries. A cross-link is a covalent bond linking polymers, such as collagen, increasing its rigidity and resistance against external factors like applied forces and enzymes. Its fast rise in ophthalmic research made RF/UVA CXL for ophthalmologists seemingly the only CXL modality. However, multiple other modalities exist. Broadly, two methods of CXL can be distinguished: chemical (direct) and physical (indirect).

#### *Direct corneal cross-linking*

In chemical CXL, chemical agents interact with collagen through functional (amino- and carboxyl-) groups, resulting in cross-links between collagen molecules. Various chemical cross-linkers have been investigated for corneal application in animal models (**Chapter 1**, Table 1), including Genipin, aldehydes (often formaldehyde releasers), nitro-alcohols, decorin, and Acai extract.<sup>6,81–103</sup> Benefits of direct corneal cross-linking lie in the fact that no external factor (i.e., heat or irradiation) is needed and that chemical CXL agents are generally much smaller molecules. Omitting an external energy source can improve safety, as these often present potential damaging effects. In addition, a smaller molecule size may prove beneficial for application without removal of the epithelium, as it may pass the tight junctions of the epithelial cells. On the other hand, a significant downside of chemical CXL is the reduced control over the site of activity with topical application, without an external factor that can selectively activate the compound. Potentially, unintended CXL of other tissues may occur.

#### *Indirect corneal cross-linking*

Physical CXL comprises applying a pharmacological compound and consecutive application of an external factor (irradiation in corneal CXL). This combination induces a chemical reaction, often generating ROS. The ROSs formed generally include

hydroxide, superoxide anions, and singlet oxygen, which can induce covalent bonds amongst collagen polymers, and surrounding proteoglycans. In the case of corneal CXL, methods rely on the exposure of a chromophore (e.g., RF) to light at its respective excitation wavelength (e.g., UVA). Either the chromophore or irradiation alone causes no or nihil additional bonds. To date, for corneal CXL, five different chromophores have been suggested: RF, Rose Bengal (RB), WST11, Eosin Y (EY), and verteporfin (VP).<sup>32,38,104-117</sup> While these chromophores have multiple excitation wavelength peaks, the most applied are UVA, green (GL), red (RL), and NIR light. The benefit of the drug and light combination is that it allows for a more targeted approach and thereby increases control of the area treated. The irradiation, however, often poses a risk to deeper ocular structures. The benefits of indirect CXL modalities thus greatly depend on the applied light source. The downsides of the UVA used in RF/UVA CXL are discussed above and result in additional measures that need to be taken to allow safe application. Green light (for RB and EY) and RL (for VP) may be harmless. However, the intensities needed to induce sufficient cross-links can cause retinal damage. Although NIR light may cause thermal damage at high intensities, the irradiance in WST/NIR CXL was shown to be completely safe, which may thus provide an effective and safe alternative.

## WST11 AND NEAR-INFRARED CORNEAL CROSS-LINKING

This thesis is devoted to investigating the safety, efficacy, and applicability of the alternative physical CXL modality WST11/NIR. It builds on the previous work of Marcovich *et al.*<sup>115</sup> WST11 is a water-soluble palladium bacteriochlorin 13'-(2-sulfonyl)amide dipotassium salt and is one of the compounds of a group of synthesized chemical derivatives of photosynthetic pigments (chlorophylls and bacteriochlorophylls) developed by the lab of prof. dr. Avigdor Scherz at the Weizmann Institute of Science, Israel. Directed initially to serve in the treatment of prostate cancer by tumor ablation via vascular targeted photodynamic therapy, its potential for corneal application soon became apparent.<sup>115,118</sup> When WST11 is excited by NIR irradiation, superoxide and hydroxide radicals are generated (in contrast to RF/UVA, no singlet oxygen is formed), capable of inducing cross-links within collagenous tissue such as the cornea.<sup>119–121</sup>

Hypothesized benefits of WST11/NIR CXL lie in the non-toxic nature of NIR light. Near-infrared light is non-toxic to ocular structures at intensities needed to achieve sufficient corneal stiffening.<sup>122,123</sup> Although the combination of WST11 and NIR is toxic, similar to RF/UVA, this results in a different safety profile. As NIR light does not have to be attenuated by WST11 before reaching deeper ocular structures, not the total stromal WST11 concentration but the availability of WST11 determines the safety of WST11/NIR CXL. Marcovich *et al.*, previously showed that the addition of high molecular weight Dextran to WST11 (WST-D) and the duration of WST11 application directly relate to its penetration depth.<sup>124</sup> Adjusting the concentration of added Dextran or WST11 application time thus allows individualization and treatment of corneas below the 400 µm threshold as is set for RF/UVA CXL.<sup>70,71,125</sup> Similarly, due to its safe nature and good tissue penetration, NIR irradiation may allow treatment of deeper ocular tissue such as the sclera, which is an area of interest for myopia control. WST-D/NIR CXL may thus provide a safe alternative in treating thin ectatic corneas and offer new opportunities for other ocular tissues.

This thesis contributes to developing WST11/NIR corneal CXL by optimizing treatment protocols, determining its long-term effect, and resistance against enzymatic digestion. In **Chapter 3**, we show in an ex vivo and in vivo rabbit model that WST-D/NIR corneal CXL results in increased stiffening, even if irradiation time is reduced up to 5 minutes in vivo, reducing irradiation duration by six-fold. A shorter treatment time benefits patients and clinicians by reducing treatment burden and expensive operating theatre time and improving patient comfort. As KC is often diagnosed at a young age, CXL treatment has to provide long-term biomechanical

stability. Therefore, **Chapter 4** determined the long-term effect of WST-D/NIR corneal CXL. In an in vivo rabbit model, we have shown a significant long-term stiffening. In **Chapter 5**, we also show significantly increased resistance against enzymatic digestion after WST-D/NIR CXL, similar to RF/UVA CXL.

## FUTURE DIRECTIVES

### Corneal cross-linking for ectatic disorders

Current research on corneal CXL for ectasia can be divided into two branches: (1) optimization of current RF/UVA CXL techniques and protocols, mainly in a clinical setting, and (2) the development of novel CXL modalities, to date only in a pre-clinical environment. While this occurs in parallel, there is a high degree of cross-fertilization and mutual benefits, as most CXL modalities rely on similar principles.

#### *Future of RF/UVA corneal cross-linking*

Research on the clinical application of RF/UVA corneal CXL is currently directed towards individualizing RF/UVA parameters based on patient's characteristics, such as age (e.g., more often epi-on in children), corneal pachymetry (e.g., reducing UVA intensity over thinner areas), and corneal topography (e.g., customized CXL aiming at the cone of the protrusion). Although the number of new concepts introduced exceeds clinical validation studies, preliminary results are promising, making personalized CXL the future of RF/UVA corneal CXL.

As mentioned earlier, in an attempt to overcome the limitations related to UVA light in RF/UVA CXL, anecdotal reports are available of exciting RF with two-photon excitation at 760 nm, termed nonlinear optical (NLO) CXL.<sup>6-9</sup> While it has not yet made it into clinical practice, and new reports are scarce, NLO appears promising. NLO benefits from the two-photon approach, determining the exact depth of excitation within the cornea and increasing safety, particularly in thin corneas. However, the application of an excimer laser makes the treatment rather costly, likely rendering it unsuitable for broad implementation. It may, however, find a place in specialized tertiary referral hospitals for a selected patient population (i.e., patients with thin corneas, unsuitable for safe regular RF/UVA corneal CXL).

#### *Future of alternative corneal cross-linking modalities*

While novel treatment modalities may still help overcome the abovementioned limitations of RF/UVA CXL, it is more likely efforts in their development will mainly focus on pathologies other than KC. Current research on alternative CXL modalities intensely focuses on infectious keratitis and scleral CXL for myopia control. Regarding the method of CXL, physical (indirect) CXL still appears to maintain the upper hand, although, in particular, Genipin and decorin have shown promising results in chemical (direct) corneal CXL. However, to date, no reports on the clinical application are available, and it is questionable if these new modalities could keep up with the rapid developments currently made in RF/UVA CXL.

### **Alternative indications for cross-linking**

Although outside the scope of this thesis, it is worth mentioning the application of CXL in ophthalmology reaches further than ectatic disorders. Other investigated corneal indications of (mainly RF/UVA or RB/GL) CXL include pellucid marginal degeneration<sup>126–134</sup>, Terrien's marginal degeneration<sup>135,136</sup>, bullous keratopathy<sup>137–155</sup>, chemical burns<sup>156–160</sup>, melting keratoprosthesis<sup>161–163</sup>, corneal lacerations<sup>164–166</sup> and radial keratotomy<sup>167,168</sup>, brittle cornea syndrome<sup>169</sup>, as pre-treatment for corneal donor tissue<sup>170–174</sup>, or as stand-alone or adjuvant to corneal refractive surgery<sup>142,145,175–186</sup>. Beyond the cornea, CXL has also been applied to other ocular structures, sometimes anecdotal, sometimes with great potential. For example, anecdotal reports of RF/UVA or RB/GL CXL of tarsus<sup>187–190</sup>, during glaucoma surgery<sup>191–196</sup>, and of amniotic grafts<sup>165,197–202</sup> exist. While most have been abandoned, these studies have contributed to a better overall understanding of CXL. A much greater effort is directed towards CXL-induced scleral stiffening in treating progressive myopia.

#### *Future of cross-linking for alternative corneal indications*

Another corneal application for CXL, currently widely investigated, is in treating infectious keratitis, with several randomized controlled trials showing promising results.<sup>203–208</sup> Based on the preliminary studies, corneal CXL for infectious keratitis may become an (adjuvant) treatment modality.

#### *Future of cross-linking of non-corneal ocular tissue*

The prevalence of myopia, nearsightedness, is rapidly growing worldwide, currently exceeding 28% globally.<sup>209</sup> Current projections show that by 2050 approximately half of the world's population will have some degree of myopia.<sup>210</sup> Individuals with myopia are at risk of retinal detachment, macular degeneration, glaucoma, amblyopia, and early-onset cataract. This results in up to one third of myopes to become visually impaired, making myopia the leading cause of blindness among young adults. The development of high myopia (≥6 Diopter or more) is associated with scleral thinning, especially in the posterior sclera, and changes in the diameter of collagen fibrils.<sup>211</sup> Given the similar nature of the collagen matrix in corneal and scleral tissue, CXL has been suggested as a treatment to arrest myopia progression. Multiple CXL modalities, both chemical and physical, are currently being investigated for their capability to arrest axial elongation to prevent the development of (high) myopia.<sup>85–87,212–264</sup> Due to the toxic nature of UVA light, RF/UVA seems less suitable for scleral CXL, and it is, therefore, that the greatest number of alternative CXL modalities can be found in this area of research. Nevertheless, while still in the pre-clinical phase, results are encouraging that scleral CXL may eventually provide a treatment modality to arrest progressive myopia.

## REFERENCES

1. Wollensak G, Spoerl E, Seiler T. Riboflavin/ultraviolet-A-induced collagen crosslinking for the treatment of keratoconus. *Am J Ophthalmol*. 2003;135(5):620-627.
2. Raiskup F, Theuring A, Pillunat LE, Spoerl E. Corneal collagen crosslinking with riboflavin and ultraviolet-A light in progressive keratoconus: Ten-year results. *J Cataract Refract Surg*. 2015;41(1):41-46.
3. O'Brart DPS, Kwong TQ, Patel P, McDonald RJ, O'Brart NA. Long-term follow-up of riboflavin/ultraviolet A (370 nm) corneal collagen cross-linking to halt the progression of keratoconus. *Br J Ophthalmol*. 2013;97(4):433-437.
4. Ayvaz A, Brekelmans J, Berendschot T, et al. Five years outcomes after corneal cross-linking for keratoconus. *J EuCornea*. 2020;6(February 2019):9-12.
5. Ivanov I V., Mappes T, Schaupp P, Lappe C, Wahl S. Ultraviolet radiation oxidative stress affects eye health. *J Biophotonics*. 2018;11(7):e201700377.
6. Spoerl E, Seiler T. Techniques for stiffening the cornea. *J Refract Surg*. 1999;15(6):711-713.
7. Spoerl E, Huhle M, Seiler T. Induction of cross-links in corneal tissue. *Exp Eye Res*. 1998;66(1):97-103.
8. Bradford SM, Brown DJ, Juhasz T, Mikula E, Jester J V. Nonlinear optical corneal collagen crosslinking of ex vivo rabbit eyes. *J Cataract Refract Surg*. 2016;42(11):1660-1665.
9. Bradford SM, Mikula ER, Chai D, Brown DJ, Juhasz T, Jester J V. Custom built nonlinear optical crosslinking (NLO CXL) device capable of producing mechanical stiffening in ex vivo rabbit corneas. *Biomed Opt Express*. 2017;8(10):4788.
10. Chen X, Stojanovic A, Eidet JR, Uttheim TP. Corneal collagen cross-linking (CXL) in thin corneas. *Eye Vis*. 2015;2(1):15.
11. Hafezi F, Iseli HP. Pregnancy-related exacerbation of iatrogenic keratectasia despite corneal collagen crosslinking. *J Cataract Refract Surg*. 2008;34(7):1219-1221.
12. Hafezi F. Limitation of collagen cross-Linking with hypoosmolar riboflavin solution: Failure in an extremely thin cornea. *Cornea*. 2011;30(8):917-919.
13. Beshtawi IM, Akhtar R, Hillarby MC, et al. Biomechanical changes after repeated collagen cross-linking on human corneas assessed in vitro using scanning acoustic microscopy. *Investig Ophthalmol Vis Sci*. 2014;55(3):1549-1554.
14. Hafezi F, Tabibian D, Richoz O. Additive effect of repeated corneal collagen cross-linking in keratoconus. *J Refract Surg*. 2014;30(10):716-718.
15. Tabibian D, Kling S, Hammer A, Richoz O, Hafezi F. Repeated cross-linking after a short time does not provide any additional biomechanical stiffness in the mouse cornea in vivo. *J Refract Surg*. 2017;33(1):56-60.
16. Boyce BL, Jones RE, Nguyen TD, Grazier JM. Stress-controlled viscoelastic tensile response of bovine cornea. *J Biomech*. 2007;40(11):2367-2376.
17. Wollensak G, Spoerl E, Seiler T. Stress-strain measurements of human and porcine corneas after riboflavin-ultraviolet-A-induced cross-linking. *J Cataract Refract Surg*. 2003;29(9):1780-1785.
18. Ruberti JW, Sinha Roy A, Roberts CJ. Corneal biomechanics and biomaterials. *Annu Rev Biomed Eng*. 2011;13(1):269-295.
19. Boyce BL, Grazier JM, Jones RE, Nguyen TD. Full-field deformation of bovine cornea under constrained inflation conditions. *Biomaterials*. 2008;29(28):3896-3904.

20. Hatami-Marbini H, Rahimi A. Stiffening effects of riboflavin/UVA corneal collagen cross-linking is hydration dependent. *J Biomech.* 2015;48(6):1052-1057.
21. Kling S, Ginis H, Marcos S. Corneal biomechanical properties from two-dimensional corneal flap extensometry: Application to UV-Riboflavin cross-linking. *Investig Ophthalmol Vis Sci.* 2012;53(8):5010-5015.
22. Elsheikh A, Wang D, Brown M, Rama P, Campanelli M, Pye D. Assessment of corneal biomechanical properties and their variation with age. *Curr Eye Res.* 2007;32(1):11-19.
23. Hatami-Marbini H, Rahimi A. The relation between hydration and mechanical behavior of bovine cornea in tension. *J Mech Behav Biomed Mater.* 2014;36:90-97.
24. Vellara HR, Patel D V. Biomechanical properties of the keratoconic cornea: A review. *Clin Exp Optom.* 2015;98(1):31-38.
25. Dupps WJ, Wilson SE. Biomechanics and wound healing in the cornea. *Exp Eye Res.* 2006;83(4):709-720.
26. Liu X, Wang L, Ji J, et al. A Mechanical model of the cornea considering the crimping morphology of collagen fibrils. *Investig Ophthalmol Vis Sci.* 2014;55(4):2739-2746.
27. Elsheikh A, Kassem W, Jones SW. Strain-rate sensitivity of porcine and ovine corneas. *Acta Bioeng Biomech.* 2011;13(2):25-36.
28. Elsheikh A, Anderson K. Comparative study of corneal strip extensometry and inflation tests. *J R Soc Interface.* 2005;2(3):177-185.
29. Balasubramanian SA, Pye DC, Willcox MDP. Are proteinases the reason for keratoconus. *Curr Eye Res.* 2010;35(3):185-191.
30. Zhou L, Sawaguchi S, Twining SS, Sugar J, Feder RS, Yue BYJT. Expression of degradative enzymes and protease inhibitors in corneas with keratoconus. *Investig Ophthalmol Vis Sci.* 1998;39(7):1117-1124.
31. O'Brart NAL, O'Brart DPS, Aldahlawi NH, Hayes S, Meek KM. An investigation of the effects of riboflavin concentration on the efficacy of corneal cross-linking using an enzymatic resistance model in porcine corneas. *Investig Ophthalmol Vis Sci.* 2018;59(2):1058-1065.
32. Fadlallah A, Zhu H, Arafat S, Kochevar I, Melki S, Ciolino JB. Corneal resistance to keratolysis after collagen crosslinking with rose bengal and green light. *Investig Ophthalmol Vis Sci.* 2016;57(15):6610-6614.
33. Aldahlawi NH, Hayes S, O'Brart DPS, Akhbanbetova A, Littlechild SL, Meek KM. Enzymatic resistance of corneas crosslinked using riboflavin in conjunction with low energy, high energy, and pulsed UVA irradiation modes. *Investig Ophthalmol Vis Sci.* 2016;57(4):1547-1552.
34. Aldahlawi NH, Hayes S, O'Brart DPS, O'Brart ND, Meek KM. An investigation into corneal enzymatic resistance following epithelium-off and epithelium-on corneal cross-linking protocols. *Exp Eye Res.* 2016;153:141-151.
35. Kanellopoulos AJ, Loukas YL, Asimellis G. Cross-linking biomechanical effect in human corneas by same energy, different UV-A fluence: An enzymatic digestion comparative evaluation. *Cornea.* 2016;35(4):557-561.
36. Cruzat A, Shukla AN, Arafat SN, et al. Ex vivo study of transepithelial corneal cross-linking. *J Refract Surg.* 2017;33(3):171-177.
37. Kling S, Hammer A, Conti A, Hafezi F. Corneal cross-linking with riboflavin and UV-A in the mouse cornea in vivo: Morphological, biochemical, and physiological analysis. *Transl Vis Sci Technol.* 2017;6(1):7.



38. Brekelmans J, Veugen J, Rieff K, et al. Enzymatic digestion of porcine corneas cross-linked by hypo- and hyperosmolar formulations of riboflavin/ultraviolet A or WST11/near-infrared light. *Transl Vis Sci Technol.* 2020;9(10):1-9.
39. Spoerl E, Wollensak G, Seiler T. Increased resistance of crosslinked cornea against enzymatic digestion. *Curr Eye Res.* 2004;29(1):35-40.
40. Schilde T, Kohlhaas M, Spoerl E, Pillunat LE. Enzymatic evidence of the depth dependence of stiffening on riboflavin/UVA treated corneas. *Ophthalmologe.* 2008;105(2):165-169.
41. Naderi M, Jadidi K, Falahati F, Alavi SA. The effect of sulfur mustard and nitrogen mustard on corneal collagen degradation induced by the enzyme collagenase. *Cutan Ocul Toxicol.* 2010;29(4):234-240.
42. Liu Z, Zhou Q, Zhu J, et al. Using genipin-crosslinked acellular porcine corneal stroma for cosmetic corneal lens implants. *Biomaterials.* 2012;33(30):7336-7346.
43. Wang T, Peng Y, Shen N, Yu Y, Yao M, Zhu J. Photochemical activation increases the porcine corneal stiffness and resistance to collagenase digestion. *Exp Eye Res.* 2014;123:97-104.
44. Aldahlawi NH, Hayes S, O'Brart DPS, Meek KM. Standard versus accelerated riboflavin-ultraviolet corneal collagen crosslinking: Resistance against enzymatic digestion. *J Cataract Refract Surg.* 2015;41(9):1989-1996.
45. Kanellopoulos AJ, Asimellis G, Salvador-Culla B, Chodosh J, Ciolino JB. High-irradiance CXL combined with myopic LASIK: Flap and residual stroma biomechanical properties studied ex-vivo. *Br J Ophthalmol.* 2015;99(6):870-874.
46. Laggner M, Pollreis A, Schmidinger G, et al. Correlation between multimodal microscopy, tissue morphology, and enzymatic resistance in riboflavin-UVA cross-linked human corneas. *Investig Ophthalmol Vis Sci.* 2015;56(6):3584-3592.
47. Doors M, Tahzib NG, Eggink FA, Berendschot TTJM, Webers CAB, Nuijts RMMA. Use of Anterior Segment Optical Coherence Tomography to Study Corneal Changes After Collagen Cross-linking. *Am J Ophthalmol.* 2009;148(6):844-851.e2.
48. Luce DA. Determining in vivo biomechanical properties of the cornea with an ocular response analyzer. *J Cataract Refract Surg.* 2005;31(1):156-162.
49. Shah S, Laiquzzaman M, Bhojwani R, Mantry S, Cunliffe I. Assessment of the biomechanical properties of the cornea with the ocular response analyzer in normal and keratoconic eyes. *Investig Ophthalmol Vis Sci.* 2007;48(7):3026-3031.
50. Tian L, Huang YF, Wang LQ, et al. Corneal biomechanical assessment using corneal visualization scheimpflug technology in keratoconic and normal eyes. *J Ophthalmol.* 2014;2014:147516.
51. Saad A, Lteif Y, Azan E, Gatineau D. Biomechanical properties of keratoconus suspect eyes. *Investig Ophthalmol Vis Sci.* 2010;51(6):2912-2916.
52. Ali NQ, Patel DV., McGhee CNJ. Biomechanical responses of healthy and keratoconic corneas measured using a noncontact scheimpflug-based tonometer. *Investig Ophthalmol Vis Sci.* 2014;55(6):3651-3659.
53. Seiler TG, Shao P, Eltony A, Seiler T, Yun SH. Brillouin Spectroscopy of Normal and Keratoconus Corneas. *Am J Ophthalmol.* 2019;202:118-125.
54. Götzinger E, Pircher M, Dejaco-Ruhswurm I, Kaminski S, Skorpik C, Hitznberger CK. Imaging of birefringent properties of keratoconus corneas by polarization-sensitive optical coherence tomography. *Invest Ophthalmol Vis Sci.* 2007;48(8):3551-3558.
55. Ju MJ, Tang S. Usage of polarization-sensitive optical coherence tomography for investigation of collagen cross-linking Usage of polarization-sensitive optical coherence tomography for investigation of collagen. *J Biomed Opt.* 2015;20(4):046001-1.

56. Vinciguerra P, Montericcio A, Catania F, et al. New perspectives in keratoconus treatment: an update on iontophoresis-assisted corneal collagen crosslinking. *Int Ophthalmol*. 2021;41(5):1909-1916.
57. Nath S, Shen C, Koziarz A, et al. Transepithelial versus Epithelium-off Corneal Collagen Cross-linking for Corneal Ectasia: A Systematic Review and Meta-analysis. *Ophthalmology*. 2021;128(8):1150-1160.
58. Matthys A, Cassagne M, Galiacy SD, El Hout S, Fournié P, Maleceze F. Transepithelial corneal cross-linking with supplemental oxygen in keratoconus: 1-year clinical results. *J Refract Surg*. 2021;37(1):42-48.
59. Kamaev P, Friedman MD, Sherr E, Muller D. Photochemical kinetics of corneal cross-linking with riboflavin. *Investig Ophthalmol Vis Sci*. 2012;53(4):2360-2367.
60. Bradford S, Mikula E, Xie Y, Juhasz T, Brown DJ, Jester J V. Enhanced transepithelial riboflavin delivery using femtosecond laser-machined epithelial microchannels. *Transl Vis Sci Technol*. 2020;9(6):1.
61. Rechichi M, Daya S, Scorgia V, Meduri A, Scorgia G. Epithelial-disruption collagen crosslinking for keratoconus: One-year results. *J Cataract Refract Surg*. 2013;39(8):1171-1178.
62. Galvis V, Tello A, Carreño NI, et al. Corneal Cross-Linking (with a Partial Deepithelization) in Keratoconus with Five Years of Follow-Up. *Ophthalmol Eye Dis*. 2016;8:OED.S38364.
63. Peyman A, Kharraji M, Koosha N, Razmjoo H, Rahimi B. Corneal haze and visual outcome after collagen crosslinking for keratoconus: A comparison between total epithelium off and partial epithelial removal methods. *Adv Biomed Res*. 2014;3(1):221.
64. Hashemi H, Miraftab M, Hafezi F, Asgari S. Matched comparison study of total and partial epithelium removal in corneal cross-linking. *J Refract Surg*. 2015;31(2):110-115.
65. Northrop-Clewes CA, Thurnham DI. The discovery and characterization of riboflavin. *Ann Nutr Metab*. 2012;61(3):224-230.
66. Filippello M, Stagni E, O'Brart D. Transepithelial corneal collagen crosslinking: Bilateral study. *J Cataract Refract Surg*. 2012;38(2):283-291.
67. Kissner A, Spoerl E, Jung R, Spekl K, Pillunat LE, Raiskup F. Pharmacological modification of the epithelial permeability by benzalkonium chloride in UVA/Riboflavin corneal collagen cross-linking. *Curr Eye Res*. 2010;35(8):715-721.
68. Raiskup F, Pinelli R, Spoerl E. Riboflavin osmolar modification for transepithelial corneal cross-linking. *Curr Eye Res*. 2012;37(3):234-238.
69. Alhamad TA, O'Brart DPS, O'Brart NAL, Meek KM. Evaluation of transepithelial stromal riboflavin absorption with enhanced riboflavin solution using spectrophotometry. *J Cataract Refract Surg*. 2012;38(5):884-889.
70. Wollensak G, Spörl E, Reber F, Pillunat L, Funk R. Corneal endothelial cytotoxicity of riboflavin/UVA treatment in vitro. *Ophthalmic Res*. 2003;35(6):324-328.
71. Wollensak G, Spoerl E, Wilsch M, Seiler T. Endothelial cell damage after riboflavin-ultraviolet-A treatment in the rabbit. *J Cataract Refract Surg*. 2003;29(9):1786-1790.
72. Wollensak G, Aurich H, Wirbelauer C, Sel S. Significance of the riboflavin film in corneal collagen crosslinking. *J Cataract Refract Surg*. 2010;36(1):114-120.
73. Srivatsa S, Jacob S, Agarwal A. Contact lens assisted corneal cross linking in thin ectatic corneas - A review. *Indian J Ophthalmol*. 2020;68(12):2773-2778.
74. Hayes S, O'Brart DP, Lamdin LS, et al. Effect of complete epithelial debridement before riboflavin-ultraviolet-A corneal collagen crosslinking therapy. *J Cataract Refract Surg*. 2008;34(4):657-661.

75. Marcovich AL, Brekelmans J, Brandis A, et al. Decreased riboflavin impregnation time does not increase the risk for endothelial phototoxicity during corneal cross-linking. *Transl Vis Sci Technol.* 2020;9(6):4.
76. Zhao ZC, Zhou Y, Tan G, Li J. Research progress about the effect and prevention of blue light on eyes. *Int J Ophthalmol.* 2018;11(12):1999-2003.
77. Pitts DG, Cullen AP, Hacker PD. Ocular effects of ultraviolet radiation from 295 to 365 nm. *Investig Ophthalmol Vis Sci.* 1977;16(10):932-939.
78. Shajari M, Kolb CM, Agha B, et al. Comparison of standard and accelerated corneal cross-linking for the treatment of keratoconus: a meta-analysis. *Acta Ophthalmol.* 2019;97(1):e22-e35.
79. Hafezi F, Kling S, Gilardoni F, et al. Individualized Corneal Cross-linking With Riboflavin and UV-A in Ultrathin Corneas: The Sub400 Protocol. *Am J Ophthalmol.* 2021;224(December):133-142.
80. Sachdev GS, Ramamurthy S, B S, Dandapani R. Comparative Analysis of Safety and Efficacy of Topography-Guided Customized Cross-linking and Standard Cross-linking in the Treatment of Progressive Keratoconus. *Cornea.* 2021;40(2):188-193.
81. Paik DC, Wen Q, Braunstein RE, Airiani S, Trokel SL. Initial studies using aliphatic  $\beta$ -nitro alcohols for therapeutic corneal cross-linking. *Investig Ophthalmol Vis Sci.* 2009;50(3):1098-1105.
82. Tang Y, Song W, Qiao J, Rong B, Wu Y, Yan X. A study of corneal structure and biomechanical properties after collagen crosslinking with genipin in rabbit corneas. *Mol Vis.* 2019;25(8):574-582.
83. Wu Y, Song W, Tang Y, Elsheikh A, Shao Y, Yan X. Efficacy and safety of transglutaminase-induced corneal stiffening in rabbits. *Transl Vis Sci Technol.* 2019;8(6):27.
84. Wu Y, Song W, Tang Y, Yan X. Biomechanical Changes after in vivo Enzyme-Induced Corneal Crosslinking in Rabbits. *Ophthalmic Res.* 2020;63(5):501-506.
85. Takaoka A, Cao K, Oste EM, Nagasaki T, Paik DC. Topical therapeutic corneal and scleral tissue cross-linking solutions: In vitro formaldehyde release studies using cosmetic preservatives. *Biosci Rep.* 2019;39(5):BSR20182392.
86. Mehta J, Takaoka A, Zyablitskaya M, Nagasaki T, Paik DC. Development of a topical tissue cross-linking solution using sodium hydroxymethylglycinate (SMG): Viscosity effect. *Biosci Rep.* 2020;40(1):BSR20191941.
87. Babar N, Kim M, Cao K, et al. Cosmetic preservatives as therapeutic corneal and scleral tissue cross-linking agents. *Investig Ophthalmol Vis Sci.* 2015;56(2):1274-1282.
88. Zyablitskaya M, Jayyosi C, Takaoka A, et al. Topical corneal cross-linking solution delivered via corneal reservoir in Dutch-belted rabbits. *Transl Vis Sci Technol.* 2020;9(9):1-12.
89. Wen Q, Trokel SL, Kim MJ, Paik DC. Aliphatic  $\beta$ -nitroalcohols for therapeutic corneal cross-linking: Corneal permeability considerations. *Cornea.* 2013;32(2):179-184.
90. Kim SYY, Babar N, Munteanu EL, et al. Evaluating the Toxicity/Fixation Balance for Corneal Cross-Linking With Sodium Hydroxymethylglycinate (SMG) and Riboflavin-UVA (CXL) in an Ex Vivo Rabbit Model Using Confocal Laser Scanning Fluorescence Microscopy. *Cornea.* 2016;35(4):550-556.
91. Paik DC, Wen Q, Braunstein RE, Trokel SL. Short chain aliphatic  $\beta$ -nitro alcohols for corneal cross-linking: Corneal endothelial toxicity studies. *J Refract Surg.* 2008;24(7):S741-7.
92. Bersanetti PA, Bueno TLN, Morandim-Giannetti A de A, Nogueira RF, Matos JR, Schor P. Characterization of Rabbit Corneas Subjected to Stromal Stiffening by the Açai Extract (Euterpe oleracea). *Curr Eye Res.* 2017;42(4):528-533.

93. Metzler KM, Roberts CJ, Mahmoud AM, Agarwal G, Liu J. Ex vivo transepithelial collagen cross-linking in porcine and human corneas using human decorin core protein. *J Refract Surg.* 2016;32(6):410-417.
94. Kim MJ, Takaoka A, Hoang Q V., Trokel SL, Paik DC. Pharmacologic alternatives to riboflavin photochemical corneal cross-linking: A comparison study of cell toxicity thresholds. *Investig Ophthalmol Vis Sci.* 2014;55(5):3247-3257.
95. Song W, Tang Y, Qiao J, et al. The comparative safety of genipin versus UVA-riboflavin crosslinking of rabbit corneas. *Mol Vis.* 2017;23:504-513.
96. Avila MY, Narvaez M, Castañeda JP, Castaneda JP. Effects of genipin corneal crosslinking in rabbit corneas. *J Cataract Refract Surg.* 2016;42(7):1073-1077.
97. Labate C, De Santo MP, Lombardo G, Lombardo M. Understanding of the viscoelastic response of the human corneal stroma induced by riboflavin/UV-A cross-linking at the nano level. *PLoS One.* 2015;10(4):e0122868.
98. Wang X, Majumdar S, Ma G, et al. Chondroitin sulfate-based biocompatible crosslinker restores corneal mechanics and collagen alignment. *Investig Ophthalmol Vis Sci.* 2017;58(10):3887-3895.
99. Zeitoune AA, Bersanetti PA, Schor P, Erbes LA, Cesar CL, Adur J. Comparison of morphological changes of corneal collagen fibers treated with collagen crosslinking agents using second harmonic generation images. *Int J Biol Macromol.* 2020;165(Pt A):346-353.
100. Avila MY, Gerena VA, Navia JL. Corneal crosslinking with genipin, comparison with UV-riboflavin in ex-vivo model. *Mol Vis.* 2012;18(April):1068-1073.
101. Gharaibeh AM, Saez V, Garcia N, Bataille L, Alió JL. Optimizing genipin concentration for corneal collagen cross-linking: An ex vivo study. *Ophthalmic Res.* 2018;60(2):100-108.
102. Avila MY, Navia JL. Effect of genipin collagen crosslinking on porcine corneas. *J Cataract Refract Surg.* 2010;36(4):659-664.
103. Song W, Tang Y, Qiao J, et al. The Short-Term Safety Evaluation of Corneal Crosslinking Agent-Genipin. *Ophthalmic Res.* 2019;62(3):141-149.
104. Singh M, Li J, Han Z, et al. Evaluating the effects of riboflavin/UV-a and rose-bengal/green light cross-linking of the rabbit cornea by noncontact optical coherence elastography. *Investig Ophthalmol Vis Sci.* 2016;57(9):OCT112-OCT120.
105. Zhu H, Alt C, Webb RH, Melki S, Kochevar IE. Corneal crosslinking with rose bengal and green light: Efficacy and safety evaluation. *Cornea.* 2016;35(9):1234-1241.
106. Bekesi N, Gallego-Muñoz P, Ibarés-Frias L, et al. Biomechanical changes after in vivo collagen cross-linking with rose bengal-green light and riboflavin-UVA. *Investig Ophthalmol Vis Sci.* 2017;58(3):1612-1620.
107. Wertheimer CM, Elhardt C, Kaminsky SM, et al. Enhancing rose bengal-photosensitized protein crosslinking in the cornea. *Investig Ophthalmol Vis Sci.* 2019;60(6):1845-1852.
108. Germann JA, Martínez-Enríquez E, Carmen Martínez-García M, Kochevar IE, Marcos S. Corneal collagen ordering after in vivo Rose Bengal and riboflavin cross-linking. *Investig Ophthalmol Vis Sci.* 2020;61(3):28.
109. Yildiz E, Anwaar Nazeer M, Bayraktutar B, Zibandeh N, Kizilel S, Sahin A. Novel corneal crosslinking technique with eosin-Y and visible light. *Acta Ophthalmol.* 2019;97(S263):j.1755-3768.2019.5148.
110. Wertheimer CM, Mendes B, Pei Q, Brandt K, Kochevar IE. Arginine as an enhancer in rose bengal photosensitized corneal crosslinking. *Transl Vis Sci Technol.* 2020;9(8):24.
111. Alageel SA, Arafat SN, Salvador-Culla B, et al. Corneal Cross-Linking with Verteporfin and Nonthermal Laser Therapy. *Cornea.* 2018;37(3):362-368.

112. Hayes S, Aldahlawi N, Marcovich AL, et al. The effect of bacteriochlorophyll derivative WST-D and near infrared light on the molecular and fibrillar architecture of the corneal stroma. *Sci Rep*. 2020;10(1):9836.
113. Brekelmans J, Goz A, Dickman MM, et al. Corneal Stiffening by a Bacteriochlorophyll Derivative with Dextran and Near-Infrared Light: Effect of Shortening Irradiation Time up to 1 Minute. *Cornea*. 2017;36(11):1395-1401.
114. Brekelmans J, Goz A, Dickman MM, et al. Long-term biomechanical and histologic results of WST-D/NIR corneal stiffening in rabbits, up to 8 months follow-up. *Investig Ophthalmol Vis Sci*. 2017;58(10):4089-4095.
115. Marcovich AL, Brandis A, Daphna O, et al. Stiffening of rabbit corneas by the bacteriochlorophyll derivative WST11 using near infrared light. *Investig Ophthalmol Vis Sci*. 2012;53(10):6378-6388.
116. Cherfan D, Verter EE, Melki S, et al. Collagen cross-linking using rose bengal and green light to increase corneal stiffness. *Investig Ophthalmol Vis Sci*. 2013;54(5):3426-3433.
117. N. B. C. D. Biomechanical properties and IOP reconstruction from air-puff corneal deformation imaging: Validations in model and porcine eyes. *Investig Ophthalmol Vis Sci*. 2016;57(12):2398.
118. Azzouzi AR, Barret E, Bennet J, et al. TOOKAD® Soluble focal therapy: pooled analysis of three phase II studies assessing the minimally invasive ablation of localized prostate cancer. *World J Urol*. 2015;33(7):945-953.
119. Vakrat-Haglili Y, Weiner L, Brumfeld V, et al. The microenvironment effect on the generation of reactive oxygen species by Pd-bacteriopheophorbide. *J Am Chem Soc*. 2005;127(17):6487-6497.
120. Ashur I, Goldschmidt R, Pinkas I, et al. Photocatalytic generation of oxygen radicals by the water-soluble bacteriochlorophyll derivative WST11, noncovalently bound to serum albumin. *J Phys Chem A*. 2009;113(28):8027-8037.
121. Brandis A, Mazor O, Neumark E, Rosenbach-Belkin V, Salomon Y, Scherz A. Novel water-soluble bacteriochlorophyll derivatives for vascular-targeted photodynamic therapy: synthesis, solubility, phototoxicity, and the effect of serum proteins. *Photochem Photobiol*. 2005;81(4):983-993.
122. ICNIRP (International Commission on Non-ionizing Radiation Protection). Guidelines on limits of exposure to broad-band incoherent optical radiation (0.38 To 3  $\mu$ M). *Health Phys*. 1997;73(3):539-554.
123. Borchert M, Lambert J, Sloney D. Validation of ICNIRP estimates of toxicity thresholds for NIR (785 NM) light in the retinas of pigmented rabbits. *Health Phys*. 2006;90(1):3-10.
124. Marcovich A. Light activated stiffening of collagen in the cornea and sclera by bacteriochlorophyll derivatives - mechanism and therapeutic implications. Published online 2013.
125. Wollensak G, Spoerl E, Wilsch M, Seiler T. Keratocyte Apoptosis after Corneal Collagen Cross-linking Using Riboflavin/UVA Treatment. *Cornea*. 2004;23(1):43-49.
126. Kymionis G, Voulgari N, Samutelela E, Kontadakis G, Tabibian D. Combined corneal wedge resection and corneal cross-linking for pellucid marginal degeneration: A first report. *Ther Clin Risk Manag*. 2019;15:1319-1324.
127. Pircher N, Lammer J, Holzer S, Gschließer A, Schmidinger G. Corneal crosslinking for pellucid marginal degeneration. *J Cataract Refract Surg*. 2019;45(8):1163-1167.
128. Kymionis GD, Grentzelos MA, Plaka AD, et al. Simultaneous conventional photorefractive keratectomy and corneal collagen cross-linking for pellucid marginal corneal degeneration. *J Refract Surg*. 2014;30(4):272-276.

129. Spadea L, Maraone G, Cagini C. Sliding keratoplasty followed by transepithelial iontophoresis collagen cross-linking for pellucid marginal degeneration. *J Refract Surg.* 2016;32(1):47-50.
130. Cagil N, Sarac O, Yesilirmak N, Caglayan M, Uysal BS, Tanriverdi B. Transepithelial Phototherapeutic Keratectomy Followed by Corneal Collagen Crosslinking for the Treatment of Pellucid Marginal Degeneration: Long-term Results. *Cornea.* 2019;38(8):980-985.
131. Mamoosa B, Razmjoo H, Peyman A, Ashtari A, Ghafouri I, Moghaddam A. Short-term result of collagen crosslinking in pellucid marginal degeneration. *Adv Biomed Res.* 2016;5(1):194.
132. de Almeida Ferreira G, Coral Ghanem V, Coral Ghanem R. Late progressive corneal flattening, haze and visual loss after eccentric crosslinking for Pellucid marginal degeneration. *Am J Ophthalmol Case Reports.* 2020;18(June 2019):100621.
133. Kymionis GD, Karavitaki AE, Kounis GA, Portaliou DM, Yoo SH, Pallikaris IG. Management of pellucid marginal corneal degeneration with simultaneous customized photorefractive keratectomy and collagen crosslinking. *J Cataract Refract Surg.* 2009;35(7):1298-1301.
134. Spadea L. Corneal collagen cross-linking with riboflavin and UVA irradiation in pellucid marginal degeneration. *J Refract Surg.* 2010;26(5):375-377.
135. Hafezi F, Gatziofufas Z, Seiler TG, Seiler T. Corneal collagen cross-linking for Terrien marginal degeneration. *J Refract Surg.* 2014;30(7):498-500.
136. Lamarca J, Salvador-Culla B, Fernández-Vega C, Barraquer RI. Long-term results of corneal cross-linking for terrien's marginal degeneration. *J Refract Surg.* 2018;34(6):424-429.
137. Krueger RR, Ramos-Esteban JC, Kanellopoulos AJ. Staged intrastromal delivery of riboflavin with UVA cross-linking in advanced bullous keratopathy: Laboratory investigation and first clinical case. *J Refract Surg.* 2008;24(7):S730-S736.
138. Choy BNK, Ng ALK, Zhu MM, Liu CC, Xu S, Lai JSM. Randomized Control Trial on the Effectiveness of Collagen Cross-linking on Bullous Keratopathy. *Cornea.* 2020;39(11):1341-1347.
139. Wollensak G, Aurich H, Wirbelauer C, Pham DT. Potential use of riboflavin/UVA cross-linking in bullous keratopathy. *Ophthalmic Res.* 2009;41(2):114-117.
140. Søndergaard AP, Ivarsen A, Hjortdal J. Reduction of stromal swelling pressure after UVA-riboflavin cross-linking. *Investig Ophthalmol Vis Sci.* 2013;54(3):1625-1634.
141. Cordeiro Barbosa MMV, Barbosa JB, Hirai FE, Hofling-Lima AL. Effect of cross-linking on corneal thickness in patients with corneal edema. *Cornea.* 2010;29(6):613-617.
142. Saim Khan M, Basit I, Ishaq M, Shakoor T, Yaqub A, Intisar R. Corneal collagen cross linking (CXL) in treatment of pseudophakic bullous keratopathy. *Pakistan J Med Sci.* 2016;32(4):965-968.
143. Arora R, Manudhane A, Saran RK, Goyal J, Goyal G, Gupta D. Role of corneal collagen cross-linking in pseudophakic bullous keratopathy: A clinicopathological study. *Ophthalmology.* 2013;120(12):2413-2418.
144. Ucakhan OO, Saglik A. Outcome of two corneal collagen crosslinking methods in bullous keratopathy due to Fuchs' endothelial dystrophy. *Case Rep Med.* 2014;2014:463905.
145. Gharaee H, Ansari-Astaneh MR, Armanfar F. The effects of riboflavin/ultraviolet: A corneal cross-linking on the signs and symptoms of bullous keratopathy. *Middle East Afr J Ophthalmol.* 2011;18(1):58-60.
146. Ehlers N, Hjortdal J. Riboflavin-ultraviolet light induced cross-linking in endothelial decompensation. *Acta Ophthalmol.* 2008;86(5):549-551.
147. Kim J, Ji DB, Takiyama N, Bae J, Kim MS. Corneal collagen cross-linking following superficial keratectomy as treatment for corneal endothelial cell dystrophy in dogs: Preliminary clinical study. *Vet Ophthalmol.* 2019;22(4):440-447.

148. Wang M. Effect of Glyceraldehyde Cross-Linking on a Rabbit Bullous Keratopathy Model. *J Ophthalmol.* 2015;2015:171690.
149. Ghanem RC, Santhiago MR, Berti TBTB, Thomaz S, Netto M V. Collagen crosslinking with riboflavin and ultraviolet-A in eyes with pseudophakic bullous keratopathy. *J Cataract Refract Surg.* 2010;36(2):273-276.
150. Bottós KM, Hofling-Lima AL, Barbosa MC, et al. Effect of collagen cross-linking in stromal fibril organization in edematous human corneas. *Cornea.* 2010;29(7):789-793.
151. Sharma N, Roy S, Maharana PK, et al. Outcomes of corneal collagen crosslinking in pseudophakic bullous keratopathy. *Cornea.* 2014;33(3):243-246.
152. Kasai K, Kato N, Den S, Konomi K, Shinzawa M, Shimazaki J. A prospective, randomized clinical study comparing accelerated corneal collagen crosslinking with 5% NaCl hypertonic saline for bullous keratopathy in Asian eyes. *Med (United States).* 2019;98(51):e18256.
153. Szigiato AA, Bujak M. Focal cross-linking: description of a novel technique for localizing collagen cross-linking. *Can J Ophthalmol.* 2016;51(1):e19-e21.
154. Pot SA, Gallhöfer NS, Walser-Reinhardt L, Hafezi F, Spiess BM. Treatment of bullous keratopathy with corneal collagen cross-linking in two dogs. *Vet Ophthalmol.* 2015;18(2):168-173.
155. Hafezi F, Dejica P, Majo F. Modified corneal collagen crosslinking reduces corneal oedema and diurnal visual fluctuations in Fuchs dystrophy. *Br J Ophthalmol.* 2010;94(5):660-661.
156. Colombo-Barboza M, Colombo-Barboza G, Felberg S, Dantas PEC, Sato EH. Induction of corneal collagen cross-linking in experimental corneal alkali burns in rabbits. *Arq Bras Oftalmol.* 2014;77(5):310-314.
157. Gao XW, Zhao XD, Li WJ, Zhou X, Liu Y. Experimental study on the treatment of rabbit corneal melting after alkali burn with Collagen cross-linking. *Int J Ophthalmol.* 2012;5(2):147-150.
158. Subasi S, Altintas O, Yardimoglu M, et al. Comparison of Collagen Cross-Linking and Amniotic Membrane Transplantation in an Experimental Alkali Burn Rabbit Model. *Cornea.* 2017;36(9):1106-1115.
159. Subasi S, Altintas O, Kasap M, Guzel N, Akpınar G, Karaman S. Comparative proteomic analysis of amnion membrane transplantation and cross-linking treatments in an experimental alkali injury model. *Int Ophthalmol.* 2018;38(6):2563-2574.
160. Karti O, Zengin MO, Cinar E, et al. Effect of 1- and 6-hour-delayed corneal collagen cross-linking on corneal healing in a rabbit alkali-burn model: Clinical and histological observations. *Cornea.* 2016;35(12):1644-1649.
161. Arafat SN, Robert MC, Shukla AN, Dohlman CH, Chodosh J, Ciolino JB. UV cross-linking of donor corneas confers resistance to Keratolysis. *Cornea.* 2014;33(9):955-959.
162. Kanellopoulos AJ, Asimellis G. Long-term safety and efficacy of high-fluence collagen crosslinking of the vehicle cornea in boston keratoprosthesis type 1. *Cornea.* 2014;33(9):914-918.
163. Tóth G, Bucher F, Siebelmann S, et al. In situ corneal cross-linking for recurrent corneal melting after boston type 1 keratoprosthesis. *Cornea.* 2016;35(6):884-887.
164. Wang T, Zhu L, Peng Y, et al. Photochemical Cross-Linking for Penetrating Corneal Wound Closure in Enucleated Porcine Eyes. *Curr Eye Res.* 2017;42(11):1413-1419.
165. Soeken TA, Zhu H, DeMartelaere S, et al. Sealing of corneal lacerations using photoactivated rose bengal dye and amniotic membrane. *Cornea.* 2018;37(2):211-217.
166. Ratzlaff T, Wei D, Wang Y, Xu M, Johnson D. Collagen cross-linking as an adjunct for repair of corneal lacerations: a cadaveric study. *Can J Ophthalmol.* 2017;52(5):508-512.



167. Fuentes-Páez G, Castanera F, Salazar-Martinez RG De, Salas JF, Izquierdo E, Pinalla B. Corneal cross-linking in patients with radial keratotomy: Short-term follow-up. *Cornea*. 2012;31(3):232-235.
168. Elbaz U, Yeung SN, Ziai S, et al. Collagen crosslinking after radial keratotomy. *Cornea*. 2014;33(2):131-136.
169. Kaufmann C, Schubiger G, Thiel MA. Corneal cross-linking for brittle cornea syndrome. *Cornea*. 2015;34(10):1326-1328.
170. Ziaei M, Gokul A, Vellara H, Patel D, McGhee CNJ. Peripheral cornea crosslinking before deep anterior lamellar Keratoplasty. *Med Hypothesis, Discov Innov Ophthalmol*. 2020;9(2):127-134.
171. Titiyal JS, Karunakaran A, Kaur M, Rath A, Agarwal T, Sharma N. Collagen Cross-Linked Therapeutic Grafts in Fungal Keratitis. *Ophthalmology*. 2018;125(9):1471-1473.
172. Mukherjee A, Hayes S, Aslanides I, Lanchares E, Meek KM. Donor cross-linking for keratoplasty: a laboratory evaluation. *Graefe's Arch Clin Exp Ophthalmol*. 2015;253(12):2223-2228.
173. Kymionis GD, Plaka AD, Diakonou VF, et al. Cross-Linking as an Adjuvant Treatment for Tectonic Corneal Lamellar Graft Preparation. *Open Ophthalmol J*. 2013;7(1):79-81.
174. Lammer J, Laggner M, Pircher N, Fischinger I, Hofmann C, Schmidinger G. Endothelial Safety and Efficacy of Ex Vivo Collagen Cross-linking of Human Corneal Transplants. *Am J Ophthalmol*. 2020;214:127-133.
175. Kornilovskiy IM, Kasimov EM, Sultanova AI, Burtsev AA. Laser-induced corneal cross-linking upon photorefractive ablation with riboflavin. *Clin Ophthalmol*. 2016;10:587-592.
176. Kanellopoulos AJ. Very high fluence collagen cross-linking as a refractive enhancement of a regressed previous astigmatic keratotomy. *J Refract Surg*. 2013;29(7):504-505.
177. Fredriksson A, Näslund S, Behndig A. A prospective evaluation of photorefractive intrastromal cross-linking for the treatment of low-grade myopia. *Acta Ophthalmol*. 2020;98(2):201-206.
178. Sachdev G, Ramamurthy S. Clinical presentation following photorefractive intrastromal cross-linking for myopic correction. *Indian J Ophthalmol*. 2018;66(7):993-994.
179. Elling M, Kersten-Gomez I, Dick HB. Photorefractive intrastromal corneal crosslinking for the treatment of myopic refractive errors: Six-month interim findings. *J Cataract Refract Surg*. 2017;43(6):789-795.
180. Lim WK, Da Soh Z, Choi HKY, Theng JTS. Epithelium-on photorefractive intrastromal cross-linking (PiXL) for reduction of low myopia. *Clin Ophthalmol*. 2017;11:1205-1211.
181. Stodulka P, Halasova Z, Slovak M, Sramka M, Liska K, Polisensky J. Photorefractive intrastromal crosslinking for correction of hyperopia: 12-month results. *J Cataract Refract Surg*. 2020;46(3):434-440.
182. El Hout S, Cassagne M, Sales de Gauzy T, Galiacy S, Malecaze F, Fournié P. Transepithelial photorefractive intrastromal corneal crosslinking versus photorefractive keratectomy in low myopia. *J Cataract Refract Surg*. 2019;45(4):427-436.
183. Bradford S, Mikula E, Kim SW, et al. Nonlinear optical corneal crosslinking, mechanical stiffening, and corneal flattening using amplified femtosecond pulses. *Transl Vis Sci Technol*. 2019;8(6):35.
184. Kang DSY, Kim SW. Effect of corneal cross-linking on epithelial hyperplasia and myopia regression after transepithelial photorefractive keratectomy. *J Refract Surg*. 2019;35(6):354-361.
185. Sachdev GS, Ramamurthy S, Dandapani R. Photorefractive intrastromal corneal crosslinking for treatment of low myopia: Clinical outcomes using the transepithelial approach with supplemental oxygen. *J Cataract Refract Surg*. 2020;46(3):428-433.



186. Elling M, Kersten-Gomez I, Dick HB. Photorefractive intrastromal corneal crosslinking for treatment of myopic refractive error: Findings from 12-month prospective study using an epithelium-off protocol. *J Cataract Refract Surg*. 2018;44(4):487-495.
187. Deparis SW, Zhu AY, Majumdar S, et al. Effects of collagen crosslinking on porcine and human tarsal plate. *BMC Ophthalmol*. 2019;19(1):255.
188. Smith TM, Suzuki S, Sabat N, Rayner CL, Harkin DG, Chirila T V. Further Investigations on the Crosslinking of Tarsal Collagen as a Treatment for Eyelid Laxity: Optimizing the Procedure in Animal Tissue. *Ophthalmic Plast Reconstr Surg*. 2019;35(6):600-603.
189. Ugradar S, Le A, Lesgart M, Goldberg RA, Rootman D, Demer JL. Biomechanical and morphologic effects of collagen cross-linking in human tarsus. *Transl Vis Sci Technol*. 2019;8(6):25.
190. Smith TM, Suzuki S, Cronin BG, et al. Photochemically Induced Crosslinking of Tarsal Collagen as a Treatment for Eyelid Laxity: Assessing Potentiality in Animal Tissue. *Ophthal Plast Reconstr Surg*. 2018;34(5):477-482.
191. Chan HMH, Choy BNK, Lai JSM. Effects of riboflavin and ultraviolet illumination on the biomechanical properties of conjunctiva. *Ophthalmic Res*. 2018;60(2):87-93.
192. Romanic Bubalo N, Loscos Arenas J, Romera Romero P, Moll Udina A, Grixolli Mazzon S, Diaz Aljaro P. Management of the hyper-filtrating ischaemic bleb: crosslinking with riboflavin and UV radiation versus a conjunctival sliding flap and conjunctival autologous graft. *Arch Soc Esp Oftalmol*. 2020;95(2):64-70.
193. Cai Y, Choy BNK, Zhu MM, et al. Prospective study on a novel treatment for leaking cystic bleb: Efficacy and safety of collagen crosslinking. *Clin Exp Ophthalmol*. 2019;47(6):749-756.
194. Choy BNK, Zhu MM, Shum JWH, et al. Collagen crosslinking in the management of leaking cystic blebs: a prospective study. *Graefe's Arch Clin Exp Ophthalmol*. 2016;254(3):529-533.
195. Wang Q, Harasymowycz P, Qianqian W, Harasymowycz P. Collagen Cross-linking for Late-onset Bleb Leakage: 1-Year Results. *J Glaucoma*. 2016;25(3):e273-6.
196. Stone DU, Craven ER, Ahmad SI, Albeshri A, Owaidhah OA. Glaucoma patch graft surgery utilizing corneas augmented with collagen cross-linking. *Middle East Afr J Ophthalmol*. 2019;26(3):148-152.
197. Spoerl E, Wollensak G, Reber F, Pillunat L. Cross-linking of human amniotic membrane by glutaraldehyde. *Ophthalmic Res*. 2004;36(2):71-77.
198. Verter EE, Gisel TE, Yang P, et al. Light-initiated bonding of amniotic membrane to cornea. *Invest Ophthalmol Vis Sci*. 2011;52(13):9470-9477.
199. Zhang C, Du T, Mu G, et al. Evaluation and ultrastructural changes of amniotic membrane fragility after UVA/riboflavin cross-linking and its effects on biodegradation. *Med (United States)*. 2020;99(20):e20091.
200. Yi S, Huh MI, Hong H, et al. Development of contact lens-shaped crosslinked amniotic membranes for sutureless fixation in the treatment of ocular surface diseases. *Transl Vis Sci Technol*. 2020;9(6):12.
201. Wang Y, Zhu L, Zhu J, Shen N, Yao M, Yu Y. Comparison of Photochemical Crosslinking Versus Sutures for Bonding Conjunctival Grafts. *Lasers Surg Med*. 2020;52(6):543-551.
202. Kitagawa K, Okabe M, Yanagisawa S, Zhang XY, Nikaido T, Hayashi A. Use of a hyperdried cross-linked amniotic membrane as initial therapy for corneal perforations. *Jpn J Ophthalmol*. 2011;55(1):16-21.
203. Bonzano C, Di Zazzo A, Barabino S, Coco G, Traverso CE. Collagen Cross-Linking in the Management of Microbial Keratitis. *Ocul Immunol Inflamm*. 2019;27(3):507-512.

204. Austin A, Lietman T, Rose-Nussbaumer J. Update on the Management of Infectious Keratitis. *Ophthalmology*. 2017;124(11):1678-1689.
205. Hsia YC, Moe CA, Lietman TM, Keenan JD, Rose-Nussbaumer J. Expert practice patterns and opinions on corneal cross-linking for infectious keratitis. *BMJ Open Ophthalmol*. 2018;3(1):e000112.
206. Tabibian D, Mazzotta C, Hafezi F. PACK-CXL: Corneal cross-linking in infectious keratitis. *Eye Vis*. 2016;3(1):11.
207. Price MO, Price FW. Corneal cross-linking in the treatment of corneal ulcers. *Curr Opin Ophthalmol*. 2016;27(3):250-255.
208. Chan TCY, Agarwal T, Vajpayee RB, Jhanji V. Cross-linking for microbial keratitis. *Curr Opin Ophthalmol*. 2016;27(4):348-352.
209. Landreneau JR, Hesemann NP, Cardonell MA. Review on the Myopia Pandemic: Epidemiology, Risk Factors, and Prevention. *Mo Med*. 2021;118(2):156-163.
210. Holden BA, Fricke TR, Wilson DA, et al. Global Prevalence of Myopia and High Myopia and Temporal Trends from 2000 through 2050. *Ophthalmology*. 2016;123(5):1036-1042.
211. McBrien NA, Cornell LM, Gentle A. Structural and ultrastructural changes to the sclera in a mammalian model of high myopia. *Invest Ophthalmol Vis Sci*. 2001;42(10):2179-2187.
212. Sun M, Zhang F, Ouyang B, et al. Study of retina and choroid biological parameters of rhesus monkeys eyes on scleral collagen cross-linking by riboflavin and ultraviolet A. *PLoS One*. 2018;13(2):1-14.
213. Ou-Yang B wen, Sun MS, Wang MM, Zhang FJ. Early changes of ocular biological parameters in rhesus monkeys after scleral cross-linking with riboflavin/ultraviolet-A. *J Refract Surg*. 2019;35(5):333-339.
214. Campbell IC, Hannon BG, Read AT, Sherwood JM, Schwaner SA, Ethier CR. Quantification of the efficacy of collagen cross-linking agents to induce stiffening of rat sclera. *J R Soc Interface*. 2017;14(129):20170014.
215. Kwok SJJ, Forward S, Wertheimer CM, et al. Selective equatorial sclera crosslinking in the orbit using a metal-coated polymer waveguide. *Investig Ophthalmol Vis Sci*. 2019;60(7):2563-2570.
216. Chu Y, Cheng Z, Liu J, Wang Y, Guo H, Han Q. The Effects of Scleral Collagen Cross-Linking Using Glyceraldehyde on the Progression of Form-Deprived Myopia in Guinea Pigs. *J Ophthalmol*. 2016;2016:3526153.
217. Zyablitskaya M, Munteanu EL, Nagasaki T, Paik DC. Second harmonic generation signals in rabbit sclera as a tool for evaluation of therapeutic tissue cross-linking (TXL) for myopia. *J Vis Exp*. 2018;2018(131):1-11.
218. Wollensak G. Thermomechanical stability of sclera after glyceraldehyde crosslinking. *Graefe's Arch Clin Exp Ophthalmol*. 2011;249(3):399-406.
219. Hannon BG, Schwaner SA, Boazak EM, et al. Sustained scleral stiffening in rats after a single genipin treatment. *J R Soc Interface*. 2019;16(159):20190427.
220. Iseli HP, Körber N, Koch C, et al. Scleral cross-linking by riboflavin and blue light application in young rabbits: damage threshold and eye growth inhibition. *Graefes Arch Clin Exp Ophthalmol*. 2016;254(1):109-122.
221. Li Y, Liu C, Sun M, et al. Ocular safety evaluation of blue light scleral cross-linking in vivo in rhesus macaques. *Graefe's Arch Clin Exp Ophthalmol*. 2019;257(7):1435-1442.
222. Choi S, Lee SC, Lee HJ, et al. Structural response of human corneal and scleral tissues to collagen cross-linking treatment with riboflavin and ultraviolet A light. *Lasers Med Sci*. 2013;28(5):1289-1296.

223. Sun X, Chen D, Liu X, Yan X, Wu Y. Effect of enzyme-induced collagen crosslinking on porcine sclera. *Biochem Biophys Res Commun.* 2020;528(1):134-139.
224. Hannon BG, Luna C, Feola AJ, et al. Assessment of visual and retinal function following in vivo genipin-induced scleral crosslinking. *Transl Vis Sci Technol.* 2020;9(10):1-11.
225. Krasselt K, Frommelt C, Brunner R, Rauscher FG, Francke M, Körber N. Various cross-linking methods inhibit the collagenase I degradation of rabbit scleral tissue. *BMC Ophthalmol.* 2020;20(1):488.
226. Guo P, Miao Y, Jing Y, et al. Changes in collagen structure and permeability of rat and human sclera after crosslinking. *Transl Vis Sci Technol.* 2020;9(9):1-10.
227. Wollensak G, Spoerl E. Collagen crosslinking of human and porcine sclera. *J Cataract Refract Surg.* 2004;30(3):689-695.
228. Paik DC, Wen Q, Airiani S, Braunstein RE, Trokel SL. Aliphatic beta-nitro alcohols for non-enzymatic collagen cross-linking of scleral tissue. *Exp Eye Res.* 2008;87(3):279-285.
229. Iseli HP, Spoerl E, Wiedemann P, Krueger RR, Seiler T. Efficacy and safety of blue-light scleral cross-linking. *J Refract Surg.* 2008;24(7):S752-5.
230. Thornton IL, Dupps WJ, Roy AS, Krueger RR. Biomechanical effects of intraocular pressure elevation on optic nerve/lamina cribrosa before and after peripapillary scleral collagen cross-linking. *Investig Ophthalmol Vis Sci.* 2009;50(3):1227-1233.
231. Zhang Y, Li Z, Liu L, Han X, Zhao X, Mu G. Comparison of riboflavin/ultraviolet-A cross-linking in porcine, rabbit, and human sclera. *Biomed Res Int.* 2014;2014:194204.
232. Stewart JM, Schultz DS, Lee OT, Trinidad ML. Exogenous collagen cross-linking reduces scleral permeability: Modeling the effects of age-related cross-link accumulation. *Investig Ophthalmol Vis Sci.* 2009;50(1):352-357.
233. Li Y, Zhang F, Sun M, et al. Safety and Long-term Scleral Biomechanical Stability of Rhesus Eyes after Scleral Cross-linking by Blue Light. *Curr Eye Res.* 2021;46(7):1061-1070.
234. Rong S, Wang C, Han B, et al. Iontophoresis-assisted accelerated riboflavin/ultraviolet A scleral cross-linking: A potential treatment for pathologic myopia. *Exp Eye Res.* 2017;162:37-47.
235. Wollensak G, Iomdina E. Crosslinking of scleral collagen in the rabbit using glyceraldehyde. *J Cataract Refract Surg.* 2008;34(4):651-656.
236. Wang M, Zhang F, Qian X, Zhao X. Regional biomechanical properties of human sclera after cross-linking by riboflavin/ultraviolet A. *J Refract Surg.* 2012;28(10):723-728.
237. Iseli HP, Körber N, Karl A, et al. Damage threshold in adult rabbit eyes after scleral cross-linking by riboflavin/blue light application. *Exp Eye Res.* 2015;139:37-47.
238. Jung GB, Lee HJ, Kim JH, et al. Effect of cross-linking with riboflavin and ultraviolet A on the chemical bonds and ultrastructure of human sclera. *J Biomed Opt.* 2011;16(12):125004.
239. Choi S, Moon SW, Jin KH, Shin JH. Microfluidic-based non-enzymatic glycation enhances cross-linking of human scleral tissue compared to conventional soaking. *Scanning.* 2016;38(5):421-426.
240. Dotan A, Kremer I, Livnat T, Zigler A, Weinberger D, Bourla D. Scleral cross-linking using riboflavin and ultraviolet-A radiation for prevention of progressive myopia in a rabbit model. *Exp Eye Res.* 2014;127:190-195.
241. Wang M, Corpuz CCC. Effects of scleral cross-linking using genipin on the process of form-deprivation myopia in the guinea pig: A randomized controlled experimental study. *BMC Ophthalmol.* 2015;15(1):89.

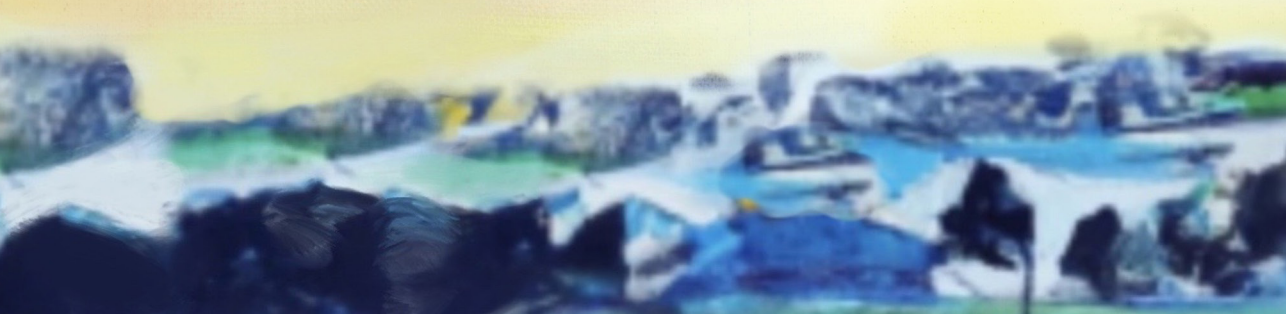
242. Zyablitskaya M, Takaoka A, Munteanu EL, Nagasaki T, Trokel SL, Paik DC. Evaluation of therapeutic tissue crosslinking (TXL) for myopia using second harmonic generation signal microscopy in rabbit sclera. *Investig Ophthalmol Vis Sci*. 2017;58(1):21-29.
243. Danilov NA, Ignatieva NY, Iomdina EN, et al. Stabilization of scleral collagen by glycerol aldehyde cross-linking. *Biochim Biophys Acta - Gen Subj*. 2008;1780(5):764-772.
244. Wollensak G, Iomdina E. Long-term biomechanical properties after collagen crosslinking of sclera using glycerinaldehyde. *Acta Ophthalmol*. 2008;86(8):887-893.
245. Wollensak G, Iomdina E. Long-term biomechanical properties of rabbit sclera after collagen crosslinking using riboflavin and ultraviolet A (UVA). *Acta Ophthalmol*. 2009;87(2):193-198.
246. Wollensak G, Iomdina E, Dittert DD, Salamatina O, Stoltz G. Cross-linking of scleral collagen in the rabbit using riboflavin and UVA. *Acta Ophthalmol Scand*. 2005;83(4):477-482.
247. Wong FF, Lari DR, Schultz DS, Stewart JM. Whole globe inflation testing of exogenously crosslinked sclera using genipin and methylglyoxal. *Exp Eye Res*. 2012;103:17-21.
248. Liu TX, Wang Z. Collagen crosslinking of porcine sclera using genipin. *Acta Ophthalmol*. 2013;91(4):e253-7.
249. Xiao B, Chu Y, Wang H, Han Q. Minimally Invasive Repetitive UVA Irradiation along with Riboflavin Treatment Increased the Strength of Sclera Collagen Cross-Linking. *J Ophthalmol*. 2017;2017:1324012.
250. Wang M, Zhang F, Liu K, Zhao X. Safety evaluation of rabbit eyes on scleral collagen cross-linking by riboflavin and ultraviolet A. *Clin Exp Ophthalmol*. 2015;43(2):156-163.
251. Zhang Y, Zou C, Liu L, et al. Effect of irradiation time on riboflavin-ultraviolet-A collagen crosslinking in rabbit sclera. *J Cataract Refract Surg*. 2013;39(8):1184-1189.
252. Schuldt C, Karl A, K??rber N, et al. Dose-dependent collagen cross-linking of rabbit scleral tissue by blue light and riboflavin treatment probed by dynamic shear rheology. *Acta Ophthalmol*. 2015;93(5):e328-36.
253. Kimball EC, Nguyen C, Steinhart MR, et al. Experimental scleral cross-linking increases glaucoma damage in a mouse model. *Exp Eye Res*. 2014;128(13):129-140.
254. Boubriak OA, Urban JPG, Akhtar S, Meek KM, Bron AJ. The effect of hydration and matrix composition on solute diffusion in rabbit sclera. *Exp Eye Res*. 2000;71(5):503-514.
255. Lin X, Naidu RK, Dai J, Zhou X, Qu X, Zhou H. Scleral Cross-Linking Using Glycerinaldehyde for the Prevention of Axial Elongation in the Rabbit: Blocked Axial Elongation and Altered Scleral Microstructure. *Curr Eye Res*. 2019;44(2):162-171.
256. Levy AM, Fazio MA, Grytz R. Experimental myopia increases and scleral crosslinking using genipin inhibits cyclic softening in the tree shrew sclera. *Ophthalmic Physiol Opt*. 2018;38(3):246-256.
257. Karl A, Makarov FN, Koch C, et al. The ultrastructure of rabbit sclera after scleral crosslinking with riboflavin and blue light of different intensities. *Graefes Arch Clin Exp Ophthalmol*. 2016;254(8):1567-1577.
258. Dotan A, Kremer I, Gal-Or O, et al. Scleral cross-linking using riboflavin and ultraviolet-A radiation for prevention of axial myopia in a rabbit model. *J Vis Exp*. 2016;2016(110):e53201.
259. Zhang M, Zou Y, Zhang F, Zhang X, Wang M. Efficacy of blue-light cross-linking on human scleral reinforcement. *Optom Vis Sci*. 2015;92(8):873-878.
260. Gawargious BA, Le A, Lesgart M, Ugradar S, Demer JL. Differential Regional Stiffening of Sclera by Collagen Cross-linking. *Curr Eye Res*. 2020;45(6):718-725.

261. Liu S, Li S, Wang B, et al. Scleral cross-linking using riboflavin UVA irradiation for the prevention of myopia progression in a guinea pig model: Blocked axial extension and altered scleral microstructure. *PLoS One*. 2016;11(11):e0165792.
262. Kim TG, Kim W, Choi S, Jin KH. Effects of scleral collagen crosslinking with different carbohydrate on chemical bond and ultrastructure of rabbit sclera: Future treatment for myopia progression. *PLoS One*. 2019;14(5):e0216425.
263. Xue A, Zheng L, Tan G, et al. Genipin-crosslinked donor sclera for posterior scleral contraction/reinforcement to fight progressive myopia. *Investig Ophthalmol Vis Sci*. 2018;59(8):3564-3573.
264. Sun M, Zhang F, Li Y, et al. Evaluation of the safety and long-term scleral biomechanical stability of UVA cross-linking on scleral collagen in rhesus monkeys. *J Refract Surg*. 2020;36(10):696-702



# Addendum

## Summary









## SUMMARY

Keratoconus (KC) is a bilateral corneal disease causing progressive corneal thinning and irregular deformation of the ocular surface, drastically decreasing visual acuity if left untreated. Progression often starts during the teenage years, presenting a high lifetime burden if visual impairment occurs. Up to 20 years ago, treatment options included symptomatic relief by spectacles or contact lenses or curative but highly invasive corneal transplantation surgery. Recently, a new treatment modality was developed: corneal collagen cross-linking (CXL) by application of Riboflavin (RF; i.e., vitamin B<sub>2</sub>) and consecutive ultra-violet A (UVA) irradiation. Cross-linking induces new bonds within the corneal extracellular matrix, thereby increasing its stability and arresting the progressive deformation seen in KC. While RF/UVA CXL revolutionized KC management, effectively halting KC progression in over 90% of patients treated, it has limitations. To allow for sufficient RF uptake in the cornea, the epithelium has to be removed, exposing the cornea to the risk of infection, haze formation, and causing pain and discomfort to the patient.

Furthermore, especially in the presence of RF, UVA can cause cellular damage, limiting its application to corneas of at least 400 µm thickness. As KC is associated with progressive thinning, many patients are thus excluded from RF/UVA CXL. To overcome (part) of these limitations, protocol adaptations and alternative CXL modalities have been investigated over the years. One of these alternative CXL modalities is water-soluble-taurine (WST11) which can be photo-activated by intrinsically safe near-infrared (NIR) light. This thesis sets out to assess the clinical effectiveness of currently applied RF/UVA CXL, optimize its treatment protocol, and further develop the new WST11/NIR CXL treatment modality.

In **Chapter 2**, we report a retrospective clinical study on RF/UVA CXL, with a 5-year follow-up in our clinic, at the University Eye Clinic Maastricht, the Netherlands. Keratoconus progression was arrested in over 90% of the patients, and pre-operative corneal astigmatism and corrected distance visual acuity were shown to provide predictive indices for post-CXL outcomes.

The most widely applied RF/UVA CXL protocol includes installing RF for 30 minutes before UVA irradiation. In **Chapter 3**, we provide theoretical and experimental evidence that reducing this time from 30 minutes to 10 minutes may increase treatment safety. In addition, this 20-minute reduction in total treatment time will reduce treatment costs and patient burden.

A proof-of-concept of a new corneal de-epithelialization method is presented in **Chapter 4**. An excimer laser creates small epithelial penetrating channels, allowing corneal RF and WST11 uptake while leaving approximately 60% of the epithelium intact. Although corneal RF and WST11 concentrations are reduced, corneal stiffening is significantly increased, similar to CXL following total epithelial removal. We hypothesize that this partial de-epithelialization may reduce epithelial healing time and cause less pain and discomfort to the patient.

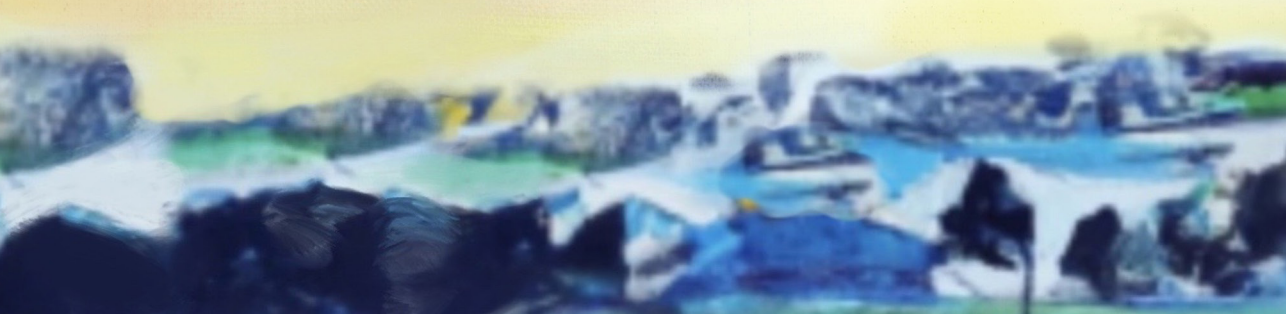
**Chapters 5, 6, and 7** continue to investigate WST11/NIR CXL, as previous work showed the corneal stiffening capabilities of this novel CXL modality. In **Chapter 5**, we show NIR irradiation time can be reduced from 20 minutes to 5 minutes in vivo and to even 1 minute ex vivo while still achieving significant corneal stiffening. The long-term effect of WST11/NIR CXL is studied in **Chapter 6**. Keratoconus is known to progress over time before natural stabilization occurs with ageing, usually in the fourth decade. In an in vivo rabbit model, we show WST11/NIR CXL achieves significant stiffening until full maturation, and natural age-related stiffening occurs. In **Chapter 7**, we show CXL using different RF, and WST11 formulations significantly increase the resistance against enzymatic digestion. The latter occurs in infectious diseases of the cornea, and preliminary clinical reports in the literature show encouraging results of several CXL modalities in treating corneal infections. Adding WST11/NIR to this treatment spectrum may provide a safer alternative to currently available CXL modalities.





# Addendum

**Samenvatting**





## SAMENVATTING

Keratoconus (KC) is een bilaterale hoornvliesandoening, waarbij progressieve verdunning en irregulaire vervorming van het hoornvliesoppervlak optreedt, met een drastische daling van het zicht tot gevolg. De achteruitgang begint vaak al tijdens de tienerjaren, waardoor de levenslange impact groot is als de aandoening niet wordt behandeld. Tot 20 jaar geleden bestonden de behandelmogelijkheden uit symptomatische behandeling met een bril of contactlenzen, of curatief door zeer invasieve corneale transplantatiechirurgie. Recent is een nieuwe behandelmethode ontwikkeld: collageen crosslinking (CXL) waarbij riboflavine (RF; vitamine B2) op het hoornvlies wordt aangebracht en vervolgens wordt belicht met ultraviolet A (UVA) licht. Crosslinking zorgt voor nieuwe verbindingen tussen de extracellulaire matrix van het hoornvlies, waardoor de stabiliteit wordt vergroot en de progressieve vervorming door KC wordt tegengegaan. Crosslinking met RF/UVA heeft gezorgd voor een revolutie in de behandeling van KC, met een succespercentage van ruim 90%, maar kent desondanks ook tekortkomingen. Allereerst, om voldoende opname van RF in het hoornvlies te krijgen, moet de epitheel cellaag aan de buitenzijde van het hoornvlies verwijderd worden. Dit stelt het hoornvlies bloot aan mogelijke infecties, kan vertroebeling van het hoornvlies veroorzaken en zorgt voor pijn en ongemak bij de patiënt. Daarnaast kan UVA, met name in de aanwezigheid van RF, celschade veroorzaken en kan RF/UVA CXL als gevolg daarvan alleen toegepast worden op hoornvliezen met een minimale dikte van 400 µm. Aangezien KC gekenmerkt wordt door progressieve verdunning van het hoornvlies, is RF/UVA CXL daarmee ongeschikt voor een deel van de KC-patiënten. In een poging om oplossingen voor deze tekortkomingen te vinden, zijn er over de jaren heen meerdere aanpassingen aan de behandelprotocollen gedaan en alternatieve CXL-methodes onderzocht. Een alternatieve crosslinker is water-soluble-aurine (WST11) dat geactiveerd kan worden met veilig nabij infrarood (NIR) licht. Dit proefschrift beoordeelt de klinische effecten van RF/UVA CXL, beschrijft optimalisatie van het hierbij toegepaste protocol en bouwt verder aan de ontwikkeling van WST11/NIR CXL.

In **hoofdstuk 2** worden de uitkomsten van een retrospectieve klinische studie naar RF/UVA CXL met een opvolging van 5 jaar gepresenteerd, uitgevoerd in onze eigen kliniek, de Universiteitskliniek voor Oogheelkunde Maastricht. We vonden dat KC-progressie werd gestopt in ruim 90,7% van de patiënten en dat preoperatief gemeten astigmatisme en gecorrigeerde visus voorspellende waardes zijn voor de postoperatieve resultaten.

Het meest toegepaste protocol voor RF/UVA CXL past RF gedurende 30 minuten toe op het hoornvlies voordat wordt gestart met UVA-belichting. In **hoofdstuk 3** tonen we aan, zowel theoretisch als experimenteel, dat het terugbrengen van deze stap

van 30 minuten naar 10 minuten de veiligheid van RF/UVA CXL zelfs kan vergroten. De tijdsbesparing van 20 minuten op de totale behandelingsduur resulteert in een kostenbesparing en afgenomen belasting voor de patiënt.

In **hoofdstuk 4** wordt een nieuwe methode geïntroduceerd om het hoornvlies epitheel te verwijderen. Een excimer laser wordt gebruikt om kleine kanalen door het epitheel te maken, waardoor RF en WST11 het hoornvlies binnen kunnen dringen, terwijl ca. 60% van het epitheel behouden blijft. We laten zien dat, ondanks een lagere concentratie van RF en WST11 in het hoornvlies, het hoornvlies significant verstevigt en niet significant minder in vergelijking met CXL waarbij het gehele epitheel wordt verwijderd. We veronderstellen dat het slechts gedeeltelijk verwijderen van het epitheel de herstelduur kan verkorten en zorgt voor minder pijn en ongemak voor de patiënt.

**Hoofdstukken 5, 6 en 7** bouwen verder op het onderzoek naar WST11/NIR CXL, waarvan eerder onderzoek het verstevigende effect op het hoornvlies heeft aangetoond. In **hoofdstuk 5**, laten we zien dat de duur van de NIR-belichting teruggebracht kan worden van 20 minuten naar 5 minuten in vivo en tot zelfs 1 minuut ex vivo, terwijl nog steeds significante versteviging wordt bereikt. Het lange termijneffect van WST11/NIR CXL wordt bestudeerd in **hoofdstuk 6**. Keratoconus kan lange tijd progressief zijn, totdat er met de veroudering een natuurlijke stabilisatie optreedt, meestal tussen het 30<sup>e</sup> en 40<sup>e</sup> levensjaar. In een in vivo konijnmodel laten we zien dat WST11/NIR CXL lange tijd significante versteviging blijft geven totdat natuurlijke leeftijdsgebonden versteviging optreedt. In **hoofdstuk 7** tonen we aan dat CXL door middel van verschillende RF en WST11 formuleringen de weerstand tegen enzymatische vertering vergroot. Dit laatste kan optreden bij infecties van het hoornvlies en voorlopige klinische studies elders laten bemoedigende resultaten zien van verschillende CXL-methodes in de behandeling van hoornvliesinfecties. De toevoeging van WST11/NIR CXL aan dit behandelspectrum, kan mogelijk een veiliger alternatief bieden.







# Addendum

**Impact paragraph**





## IMPACT PARAGRAPH

Developing a new treatment modality takes approximately 17 years from bench to bedside.<sup>1</sup> During this period, many experiments will fail, only a few will be successful, and about half of the successful products will eventually find their way into clinical practice.<sup>1</sup> The unmet need of keratoconus (KC) patients allowed for faster corneal collagen cross-linking (CXL) adoption within six years of the proof-of-concept and its first clinical application.<sup>2,3</sup> However, there was still much to learn and challenges to overcome along the way. Corneal CXL has evolved into a booming scientific field with many different research groups and as many perspectives, and a variety in success of implementing innovative ideas into clinical practice. The work presented in this thesis occupies a small niche in this academic field and focuses on:

- Improving existing protocols, increasing CXL safety and decreasing patients' burden (**Chapters 2, 3, and 4**). **Chapter 2** endorses the excellent success rate of current Riboflavin (RF) and ultra-violet A (UVA) CXL, found in our clinical study to be approximately 90%. For this 90% of patients, we suggest increasing safety in **Chapter 3**, as we show it is safer to reduce RF impregnation time. **Chapter 4** introduces a proof-of-concept for a novel treatment protocol that potentially reduces patients' burden.
- Developing a new CXL treatment modality to overcome the limitations of current options (**Chapters 5, 6, and 7**). Despite the great success rate, **Chapter 2** shows that 10% of patients exhibit a progression of KC despite CXL treatment. It is this 10% that warrants further investigation towards alternative treatment modalities. **Chapter 5** shows the stiffening capabilities of the alternative CXL method WST11 and near-infrared (NIR) CXL. **Chapter 6** demonstrates its long-term capabilities, and **Chapter 7** its resistance to enzymatic digestion.

In 2020, the Dutch National Institute for Public Health and Environment ('RIVM') predicted healthcare expenditures would increase by 2.8% annually until at least 2060.<sup>4</sup> About one-third of this increase can be attributed to population ageing. The other two-thirds are due to increasing healthcare accessibility, better and more frequent diagnosis, and new treatment options. As this growth in healthcare expenditures is not sustainable, political and societal solutions are sought. This prediction levies a responsibility on the medical and scientific communities to increase awareness of costs and pay more attention to cost-effectiveness. Riboflavin/UVA CXL is cost-effective, with rising effect rates as long-term results on CXL become available.<sup>5,6</sup> Godefrooij *et al.* calculated personnel costs account for 88.1% of the total costs.<sup>7</sup> Thus, reducing treatment time would directly minimize treatment costs. **Chapter 3** shows treatment time can be safely

reduced by 20 minutes, resulting in an approximately 15% reduction in treatment costs in a Dutch tertiary setting.<sup>7</sup> In **Chapter 5**, we show in an animal model that WST11/NIR CXL may further decrease treatment time to 1 minute only. Reducing treatment time also allows to treat more patients. Especially within the developing world, where KC prevalence is high while access to healthcare is scarce, this could result in a greater number of patients receiving adequate treatment. Furthermore, although RF costs only account for 3.4% of the total treatment costs, competing CXL modalities may also reduce material costs through free market forces.

Riboflavin/UVA CXL has been shown to effectively arrest KC progression, as illustrated by the significant reduction in corneal transplantations for KC since its introduction into clinical practice.<sup>8</sup> Where in 2003, RF/UVA CXL was first applied for KC, it has expanded over the years to photoactivated chromophore for infectious keratitis CXL (PACK-CXL), scleral CXL for myopia control, and other indications as discussed in **Chapter 8**. In traditional corneal CXL, WST11/NIR CXL may offer a solution to a select number of KC patients unfit for or unresponsive (i.e., 9.3% of patients, following **Chapter 2**) to RF/UVA CXL. However, current research heads towards individualized and targeted CXL, which aims to maximize treatment effect in the most affected regions of the cornea. Due to its favorable safety profile as compared to RF/UVA CXL, WST11/NIR CXL is more suited for such targeted approaches. Similarly, the safety profile of WST11/NIR may prove beneficial for emerging research areas such as PACK-CXL and scleral CXL for myopia. Two fellow PhD-researcher in our group, Judith Veugen and Demi Vogels, continue to research WST11/NIR CXL on these respective topics.

Patients may directly benefit from the protocol adaptations for RF/UVA CXL suggested in **Chapter 3**. **Chapters 5, 6, and 7** contribute to the general understanding of CXL and have broadened the scope by adding WST11 and NIR to the crosslinking armamentarium. While RF/UVA CXL was rapidly incorporated in KC management due to the absence of alternative treatment options, novel CXL modalities will have to meet the outcome of RF/UVA CXL. **Chapters 5, 6, and 7** are a scientific contribution to the rapidly evolving field of CXL, with **Chapters 5, and 6** showing practical advantages of WST11/NIR over current RF/UVA CXL protocols, and **Chapter 7** providing a direct comparison between RF/UVA and WST11/NIR CXL, with similar outcomes. Next, randomized controlled trials will have to show whether clinical outcomes of WST11/NIR CXL can equal or exceed that of RF/UVA CXL.

## REFERENCES

1. Kirchner Jo Ann E, Smith Jeffrey L, Powell Byron J, Waltz Thomas J, Proctor Enola K. Getting a clinical innovation into practice: An introduction to implementation strategies. *Psychiatry Res.* 2020;283(June 2019):112467. <https://doi.org/10.1016/j.psychres.2019.06.042>
2. Spörl Eberhard, Huhle Michael, Kasper Michael, Seiler Theo. Erhöhung der festigkeit der hornhaut durch vernetzung. *Ophthalmologe.* 1997;94(12):902-906. <http://www.ncbi.nlm.nih.gov/pubmed/9487761>
3. Wollensak Gregor, Spoerl Eberhard, Seiler Theo. Riboflavin/ultraviolet-A-induced collagen crosslinking for the treatment of keratoconus. *Am J Ophthalmol.* 2003;135(5):620-627. <http://ovidsp.ovid.com/ovidweb.cgi?T=JS&PAGE=reference&D=emedg&NEWS=N&AN=36457967>
4. Vonk RAA, Hilderink HBM, Plasmans MHD, Kommer GJ, Polder JJ. Toekomstverkenning zorguitgaven 2015-2060 : Kwantitatief vooronderzoek in opdracht van de Wetenschappelijke Raad voor het Regeringsbeleid (WRR). Deel 1: toekomstprojecties. *Health care Expend foresight 2015-2060 Quant Prelim study Req Sci Coun Gov Policy (WRR) Part 1 Futur Proj.* Published online 2020. <https://rivm.openrepository.com/bitstream/10029/623734/1/2020-0059.pdf%0Ahttp://hdl.handle.net/10029/623734>
5. Godefrooij Daniel A, Mangen Marie Josee J, Chan Elsie, et al. Cost-Effectiveness Analysis of Corneal Collagen Crosslinking for Progressive Keratoconus. *Ophthalmology.* 2017;124(10):1485-1495. <http://www.elsevier.com/locate/ophtla>
6. Salmon HA, Chalk D, Stein K, Frost NA. Cost effectiveness of collagen crosslinking for progressive keratoconus in the UK NHS. *Eye.* 2015;29(11):1504-1511. <http://dx.doi.org/10.1038/eye.2015.151>
7. Godefrooij Daniel A, Van Geuns Pepijn, De Wit G Ardine, Wisse Robert PL. What are the costs of corneal cross-linking for the treatment of progressive keratoconus? *J Refract Surg.* 2016;32(5):355. <http://www.ncbi.nlm.nih.gov/pubmed/27163622>
8. Godefrooij Daniel A, Gans Renze, Imhof Saskia M, Wisse Robert PL. Nationwide reduction in the number of corneal transplantations for keratoconus following the implementation of cross-linking. *Acta Ophthalmol.* 2016;94(7):675-678. <http://www.ncbi.nlm.nih.gov/pubmed/27213687>





# Addendum

## Acknowledgements





## ACKNOWLEDGEMENTS

Dit proefschrift is het werk van velen, van wie ik enkelen graag specifiek wil bedanken. Voor hun hulp en steun, zowel direct als indirect.

Prof. Rudy Nuijts, dank voor de mogelijkheden die u geboden hebt en voor het vertrouwen om mij op afstand mijn gang te laten gaan. Mijn promotie en verblijf in Israël is een tijd die ik nooit zal vergeten. Uw kritische blik heeft mij geleerd dat het geheim in de details zit en heeft dit proefschrift naar een hoger niveau getild. Zonder u was dit niet mogelijk geweest.

Dr. Mor Dickman, dankzij jou zal mijn promotie een onvergetelijke periode in mijn leven zijn. In 2013 begon ik onder jouw leiding bij de oogheelkunde. Een jaar waarin ik veel van je heb mogen leren; van basale zaken die bij onderzoek komen kijken, tot het aanvragen van financiering voor mijn eigen onderzoek. Door je eindeloze geduld in lezen, herschrijven en becommentariëren (van het eerste manuscript heb ik 7 versies van je gekregen) weet ik nu wat wetenschappelijk schrijven inhoudt. Toen ik je vertelde dat ik na het afronden van mijn master graag een tijdje in het buitenland door zou willen brengen, had je binnen no-time een prachtige plek geregeld. Wat begon als een half jaar, werden er uiteindelijk drie. Dit bood niet alleen een kijk in een andere keuken, maar bleek ook een schat aan levenservaring op te leveren, waar ik je altijd dankbaar voor zal blijven.

Prof. Arie Marcovich, thank you for your incredible kindness. You are the perfect mixture of a skilled clinician and a resourceful scientist. From the moment I arrived in Israel, you and your family did your very best to make me feel at home, which you succeeded at. Many more memories come to mind, but you inviting me to your home, taking me out on my birthday, and bringing La Chouffe to our lunch breaks really made me feel welcome. Your creativity, combined with all the resources available at the Weizmann Institute made nothing felt impossible. I greatly admire how you manage to combine your demanding jobs in both private and public clinics with outstanding research, while still keeping your family and friends in the first place.

Prof. Avigdor Scherz and dr. Alex Brandis, you are probably two of the most brilliant people I have ever met. Not only due to the amazing work you do, but also your ability to make it understandable to someone without a background in biochemistry. Dr. Alexa Goz, thank you for all the experiments we've run together. Dear Anwar, Asher, Danielle, Dina, Iddo, Ilan, Keren, Lilach, Natasha, Nicole, Oksana, Olga, Racheli, Ronen, Ronny, Ruth, Tami, Tianqi, Varda, there are too many memories to state here. Thank you all very much.

Prof. Tilman Hackeng, prof. Anders Behndig, prof. René Van der Hulst, dr. Ruth Lapid-Gortzak, and prof. Chris Reutelingsperger, thank you for taking the time to read and comment on my work as members of the assessment committee.

Dr. Tos Berendschot, in specific, and all other co-authors, thank you for your insights and contributions. This thesis would not have been possible without you.

Felix, Dorien, Mira, Mareike, Agnes, Miguel, Kim, Ciara, Vishu, Lisha, Aditya, Bidyut, thank you for all the games of Catan, the drinks at ha faculta, and the imported Dutch cheese. Without you the Weizmann Institute would not have been as much fun as it has been.

Laura, Rob, Natalia, Ilona, Eline, Palwasha, Suryan, Christian, Shuo, Soraya, Lindsay, Lotte, mijn mede-onderzoekers, eerst op afstand en later ook in Maastricht. Dank voor jullie samenwerking, gedachtes, gedeelde smart en gezelschap op congressen. Dank ook aan mijn mede AIOS die iedere keer het rooster weer rond kregen, ondanks dat ik een onderzoeksdag had.

Eefje, waarschijnlijk ben jij degene die de meeste verhalen over het reilen en zeilen van mijn onderzoek heeft moeten aanhoren. Gelukkig kan je het nu delen met Rick. Dank voor je geduld, je relativierungsvermogen en het feit dat je tot het einde (letterlijk) achter me blijft staan als paranimf.

Lieve familie, de inhoud is niet altijd het belangrijkste in promotieonderzoek. Dank voor de eindeloze interesse in saaie onderwerpen en steun bij frustraties. Ik prijs mij gelukkig met de warmte onderling. Koen, het was heel speciaal om met je samen te mogen werken en ook te publiceren. Hopelijk kom je nog tot inkeer en kies je ook voor de oogheekunde. Een extra gedachte aan Ad en Jopie, die wel het begin, maar niet het einde van dit proefschrift mee hebben gemaakt.

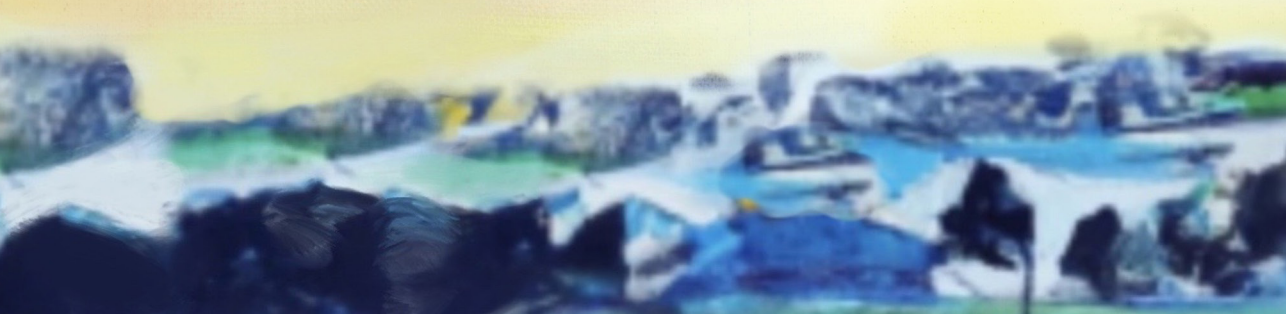
Lieve mam, zo lang ik mij kan heugen heb je achter me gestaan, of ik nou links of rechts ging. Af en toe een duwtje in de rug, maar altijd een veilig valnet om op terug te vallen. Dank voor je onvoorwaardelijke vertrouwen. Lieve broer, je nuchtere kijk op zaken helpt relativeren. Ik hoop dat men ons uit elkaar weet te houden als deze bul uitgereikt wordt, zo niet dan zou ik je hem direct gunnen.





# Addendum

## Curriculum Vitae







## CURRICULUM VITAE

Jurriaan Brekelmans was born on December 13<sup>th</sup> 1988 in Amsterdam, the Netherlands. In 2007, he graduated with honors from secondary school (Sint Maartenscollege, Maastricht, the Netherlands). In the same year he started his medical study at Maastricht University (Maastricht, the Netherlands). In 2008-2009 he was treasurer of the International Federation of Medical Students' Associations in Maastricht (IFMSA Maastricht) and a year later for the Netherlands (IFMSA-NL). In his last year of medical school, he was an intern at the University Eye Clinic Maastricht under the supervision of dr. Mor Dickman. After graduating in 2014, he started his PhD under the supervision of prof. dr. Rudy Nuijts, dr. Mor Dickman, and prof. dr. Arie Marcovich. As part of an academic cooperation, he worked in the lab of prof. dr. Avigdor Scherz at the Weizmann Institute of Science (Rehovot, Israel), under the supervision of prof. dr. Arie Marcovich, between 2014 and 2017. This research led to this thesis, and was presented at multiple international congresses of the European Society of Cataract and Refractive Surgeons, the Association for Research in Vision and Ophthalmology, and national meetings in both Israel and the Netherlands. From October 2017 until March 2022, he was an ophthalmology resident at the University Eye Clinic Maastricht (the Netherlands), headed by prof. dr. Carroll Webers. Currently, Jurriaan works as an ophthalmologist at Eyescan Zuyderland (Sittard, the Netherlands).



# Addendum

## List of publications





## LIST OF PUBLICATIONS

1. **Brekelmans J\***, Goz A\*, Dickman MM, Brandis A, Sui X, Wagner HD, Nuijts RMMA, Scherz A, Marcovich AL. Corneal Stiffening by a Bacteriochlorophyll Derivative With Dextran and Near-Infrared Light: Effect of Shortening Irradiation Time up to 1 Minute. *Cornea* 2017 May; 0:1–7. \*Equal contribution.
2. **Brekelmans J**, Goz A, Dickman MM, Brandis A, Sui X, Wagner HD, Nuijts RMMA, Scherz A, Marcovich AL. Long-Term Biomechanical and Histologic Results of WST-D/NIR Corneal Stiffening in Rabbits, Up to 8 Months Follow-up. *Invest. Ophthalmol. Vis. Sci.* 2017 Jul; 58:4089–4095.
3. Ayvaz A, **Brekelmans J**, Berendschot TTJM, Dickman MM, Visser N, Nuijts RMMA, Saelens IEY. Five years outcomes after corneal cross-linking for keratoconus. *J of EuCornea* 2019 Dec; 6:9–12.
4. Hayes S, Aldahlawi N, Marcovich AL, **Brekelmans J**, Goz A, Scherz A, Young RD, Bell JS, O'Bart DP, Nuijts RMMA, Meek KM. The effect of bacteriochlorophyll derivative WST-D and near infrared light on the molecular and fibrillar architecture of the corneal stroma. *Sci. Rep.* 2020 Jun; 17:10(1):9836.
5. Marcovich AL\*, **Brekelmans J\***, Brandis A, Samish I, Pinkas I, Preise D, Sasson K, Feine I, Goz A, Dickman MMA, Nuijts RMMA, Scherz A. Decreased Riboflavin Impregnation Time Does Not Increase the Risk for Endothelial Phototoxicity During Corneal Cross-Linking. *Trans. Vis. Sci. Tech.* 2020 May; 9(6):4. \*Equal contribution.
6. **Brekelmans J**, Veugen J, Rieff K, Dickman MM, Goz A, Wolffs P, Brandis A, Berendschot TTJM, Nuijts RMMA, Scherz A, Marcovich AL. Enzymatic Digestion of Porcine Corneas Cross-linked by Hypo- and Hyperosmolar Formulations of Riboflavin/ultraviolet A or WST11/Near-Infrared Light. *Trans. Vis. Sci. Tech.* 2020 Aug; 9(10):4.
7. **Brekelmans J**, Dickman MM, Verma S, Arba-Mosquera S, Goldschmidt R, Goz A, Brandis A, Berendschot TTJM, Saelens IEY, Marcovich AL, Scherz A, Nuijts RMMA. Excimer laser-assisted corneal epithelial pattern ablation for corneal cross-linking. *Acta Ophthalmol.* 2022 Jun;100(4):422-430.

\* These authors contributed equally





